MULTI-COMPONENT CRYSTAL STRUCTURES OF NETWORK SOLIDS AND PHARMACEUTICAL SALTS

**A Thesis Submitted during 2006-2011 to the
University of Hyderabad in partial fulfillment of the award of a
Ph.D. degree in Chemistry**

By

RANJIT THAKURIA

**School of Chemistry
University of Hyderabad
Central University P.O., Gachibowli
Hyderabad 500 046
Andhra Pradesh
India**

উৎসর্গিত

শ্রদ্ধাৰ মা–দেউতা আৰু ছাৰ

লৈ

CERTIFICATE

This is to certify that the thesis entitled **"Multi-Component Crystal Structures of Network Solids and Pharmaceutical Salts"** submitted by **Ranjit Thakuria** bearing Regd. No. CH05PH27 in partial fulfillment of the requirements for the award of Doctor of Philosophy in Chemistry is a bonafide work carried out by him under my supervision and guidance.

The thesis has not been submitted previously in part or in full to this or any other University or Institution for the award of any degree or diploma.

Dean

School of Chemistry

Prof. Ashwini Nangia

Thesis Supervisor

DECLARATION

I **Ranjit Thakuria** hereby declare that this thesis entitled **"Multi-Component Crystal Structures of Network Solids and Pharmaceutical Salts"** submitted by me under the guidance and supervision of **Professor Ashwini Nangia** is a bonafide research work. I also declare that it has not been submitted previously in part or in full to this University or any other University of Institution for the award of any degree or diploma.

Name: **Ranjit Thakuria**

Date:

February 2011

Hyderabad

Signature of the Student

Regd. No. CH05PH27

ACKNOWLEDGEMENT

It gives me immense pleasure to express my profound gratitude and deep respect to my supervisor, **Prof. Ashwini Nangia** for teaching me research methodology and introducing me to the fascinating field of research. He has inspired me with thought provoking discussions and invaluable lectures.

I thank Prof. D. Basavaiah, Dean, School of Chemistry, former Deans, and all faculty members of the School for their cooperation.

I would like to thank Barooah sir, for his constant guidance throughout my life. I also like to thank Diganta sir for his support, Jaykanta sir, Dhruba sir, Bijoy sir, Shymal sir, Ajay Das sir, Dinesh Nath sir, Bordoloi sir and all other teachers who taught me throughout my career from my primary school to University for their constant encouragement. Special thanks to the institution, B. Borooah College where I spent my golden days with my friends like Sanjeev, Ganesh, Naba, Sanjay, Dhruba, Prem, Samiran, Anupam, Dipankar, Nabanita and Mouchumi.

I am grateful to Prof. Jubaraj Bikash Baruah sir, O. K. Medhi sir, Pradeep Phukan sir, P. J. Das sir, Rupam da and all other faculty members of Gauhati University.

I wish to record my thanks to UGC for fellowship support. I also would like to record my thanks to DST-PURSE programme for funding my visit to NTU, Singapore.

I thank all the non-teaching staff of the School of Chemistry, CIL and Department of Nano Science for their assistance on various occasions.

I wish to thank my friendly and cooperative labmates Drs. Anthony Addlagatta, Ram Jetti, P. Vishweshwar, S. Aitipamula, Bala Krishna Reddy, B. K. Saha, V. R. Vangala, S. Basavoju, Dinabandhu Das, Rahul Banerjee, C. Malla Reddy, L. S. Reddy, A. Dey, V. Aparna, S. Panigrahi, S. Roy, P. M. Bhatt, T. Thakur, N. J. Babu, Y. Azim, Bipul Ch. Sarma and Mr. Sreekanth. Naba K. Nath, Palash, Suryanarayan, Rajesh, Kalyan, Kanishka, Maddileti, Sudalai, Geetha, Suresh, Sumanth, Swarupa, Uday, Srinu, Kishore, Satyanarayana and Moumita for creating a cheerful working atmosphere in the lab.

SYNOPSIS

This thesis entitled **"Multi-Component Crystal Structures of Network Solids and Pharmaceutical Salts"** consists of seven chapters.

CHAPTER ONE

Introduction

Solid-state chemistry deals with the synthesis, structure, and properties of solid phase materials. The focus is on the synthesis of novel compounds to discover new phenomena or enhanced properties, and also to understand the bonding interactions present in the crystal structures. The relationship between structure and property is a central theme in solid-state chemistry.

Several network solids and porous coordination polymers synthesized in the last two decades have provided a variety of exotic architectures with properties ranging from gas storage, isomers separation, targeted drug delivery, exchange of guests, magnetism, conductivity and catalysis by the framework solids. A topological analysis gives an idea of packing trends that will allow for the rational design of functional materials. For example, interpenetrating nets have been considered as potential super-hard materials, and peculiar magnetic and electrical properties have been attributed to extended systems as a consequence of their interpenetration. Moreover, interpenetration can also, unexpectedly, enhance the porosity of a network and can produce flexible hosts with high selectivity for guest inclusion.

Chemists and engineers in the pharmaceutical industry generally seek to deliver crystalline forms of the active drug compounds, mainly due to the inherent stability of crystalline materials and the well-established impact of crystallization processes on purification and isolation of chemical substances. Poor dissolution rate, low solubility, chemical instability and moisture uptake influence the therapeutic efficacy of many pharmaceuticals, and significantly lower the market value of a drug. Multi-component crystals, e.g. hydrates, solvates, salts, cocrystals play an important role in the design of new solids, notably for the pharmaceutical industry with improved physico-chemical

properties. Almost half of the drugs present in the market are delivered as salts. Cocrystallization for pharmaceutical solids provides inherent benefits as compared to salt formation in at least two ways. Firstly, all types of molecules can form cocrystals, including weakly ionizable and non-ionizable active pharmaceutical ingredients (APIs), which are traditionally considered to present a higher risk in terms of physical property optimization because they have either limited or no capabilities for salt formation. Secondly, for toxicological reasons only 12 or so acidic or basic counterions are explored in a typical API salt screen, there are many potential coformer molecules that may be used in cocrystal assembly. In the recent literature nutraceuticals are also used as coformers to give extension to the list of potential molecules accessible to the pharmaceutical industry as well as provide additional physiological benefits to the patient.

CHAPTER TWO
H-Shaped Molecules and Network Solids

The use of crystal engineering concepts has produced a variety of coordination networks, many of which exhibit novel and fascinating types of entanglements of individual motifs. The 'network approach' or topological approach to crystal chemistry is an important achievement and a useful tool for the analysis, comparison and design of network structures which simplifies complex species to schematized reference nets. Network architectures are common in inorganic structures, minerals, metal–organic compounds and coordination polymers. In general, the classification of organic crystal structures as nets is over a decade old now. The fact that hydrogen bonds are weaker and less directional than metal–heteroatom and metal–ligand bonds means that the geometry of organic structures is not as clearly definable as that at the metal center of coordination compounds and polymers. Even though hydrogen bond directionality has an angular spread, organic crystal structures can be topologically classified akin to inorganic and coordination network structures. Here, new examples of rare network topologies and interpenetration/ catenation modes of organic supramolecular architectures will be presented built from a H-shaped tecton.

1,4-Di[bis(4'-hydroxyphenyl)methyl]benzene **A** and its methoxy and methyl derivatives **B–D** were prepared by the acid-catalyzed condensation of terephthaldehyde with the requisite phenol (4 equiv.). These H-shaped molecules **A–D** forms numerous solvates and cocrystals that results in diverse network structures from the same starting tecton (Figure 1). 1D ladder and polyrotaxanes, 2D honeycomb and Catalan nets, as well as their interpenetrated/ catenated structures were the main network structures that resulted from different guest or co-formers. The most novel and remarkable results were the Catalan ($5,_4^3$) nets in **A**•(CH$_3$NO$_2$)$_2$ and **D**•(CHCl$_3$)$_2$ solvates, the two-component polyrotaxane of **A**•(Quinox)$_2$ cocrystal, and the interpenetrated ladders in the **A**•(Phez)$_{1.5}$ cocrystal and its guest-free form.
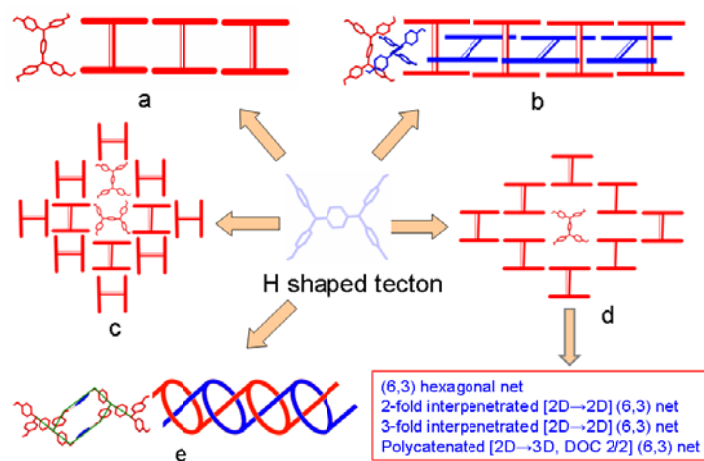
Figure 1 Supramolecular networks in host-guest compounds and cocrystals of H-shaped molecules. (a) 1D ladder, (b) interpenetrated ladders, (c) Catalan or ($5,_4^3$) net, (d) common (6,3) hexagonal or 2D brick wall motif, and (e) polyrotaxane or polythreading.

A reason for guest- or co-former induced supramolecular diversity is that the H-shaped molecule is flexible at three points — the phenol OH group orientation, the tetrahedral V-shaped bis(phenol), and the para-phenyl connector. The presence of a second aromatic component gives interplay between hydrogen bonding and π-stacking motifs. The rational construction of newer network architectures from H-shaped molecules should be possible based on a better understanding of the network diversity of these structures.

CHAPTER THREE

Cocrystals of Pyrogallol and Catechol with N-Heterocycle Bases

Cocrystal is defined as "a crystalline structure made up of two or more components in a definite stoichiometric ratio". They are historical compounds in solid-state chemistry. The multi-component crystal structure is held together through hydrogen bonds and non-covalent interactions which influence the crystal packing in modifying physical and chemical properties due to which the cocrystal has wide application in pharmaceutical industry, chemical processing, etc. Inspite of their diverse applications, cocrystals represent only 0.5 % of the total crystal structures archived in the Cambridge Structural Database (CSD).

Pyrogallol or benzene-1,2,3-triol is a white crystalline powder and a powerful reducing agent. It was first prepared by Scheele in 1786 by heating gallic acid. In alkaline solution it is an active reducing agent, absorbs water readily, turning purple from a colorless solution. It can also absorb oxygen and is used to calculate the amount of oxygen in air, in photography as developing agent, hair dying, dying of suturing materials, etc. Apart from the other laboratory uses, it is reported recently that pyrogallol generates reactive oxygen species (ROS) and results in apoptosis (cell death) and thus can be developed as a promising anti-lung cancer drug for non-small cell lung cancer. Surprisingly there is no 3D structure in the CSD for this historic molecule. The guest-free form and 0.25-hydrate of pyrogallol and in addition some cocrystals of pyrogallol and catechol were prepared with N-aromatic heterocycles (Scheme 1).

16: Pyro-guest free
17: Pyro.H$_2$O (1:0.25)
18: Pyro.Pza (1:1)
19: Pyro.Isonico (2:1)
20: Pyro.Isonico (2:4)
21: Pyro.Nico (2:1)
22: Pyro.Quin (3:5)
23: Pyro.Quin (2:3)
24: Pyro.2-Hqui (1:2)
25: Pyro.Bipy.H$_2$O (2:3:2)
26: Cate.Bipy.H$_2$O (1:1:1)
27: Cate.Nico (2:1)
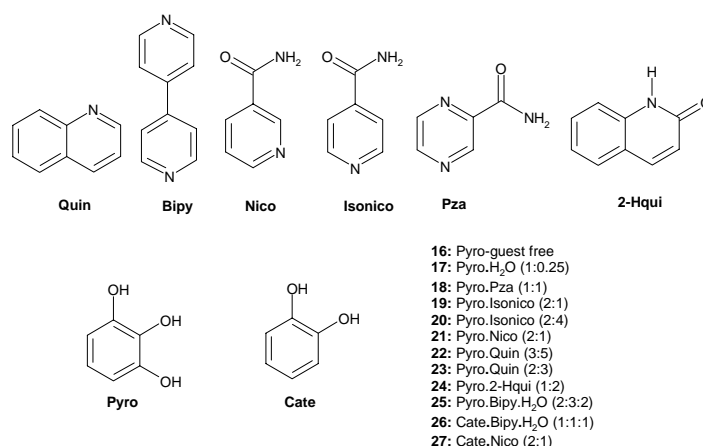
Scheme 1 Cocrystals of Pyrogallol and Catechol with N-heterocycle bases.

Crystal packing and hydrogen bonding synthons in the cocrystal structures of pyrogallol and catechol are discussed. The solubility and dissolution behaviour of a few cocrystals were studied.

CHAPTER FOUR

Olanzapinium Salts/ Solvates

Crystal engineering principles are now being actively considered for pharmaceutical applications in order to modulate the properties of drugs. Because the physical properties that influence the performance of pharmaceutical solids are well appreciated, there is a unique opportunity to apply crystal engineering techniques and the appropriate follow-up studies to solve real world problems, such as poor physical and chemical stability or inadequate solubility/ dissolution for appropriate biopharmaceutical performance of a drug. In this regard apart from polymorphism, salt preparation and cocrystallization are the most widely used strategies in pharmaceutical industry. An estimated half of all drug molecules used in medicine are administered as salts, and salt selection is recognized as an essential step in the preclinical phase of modern drug development. Salt forms of a pharmaceutical can have many benefits, such as improved stability, characteristics, optimal bioavailability and aqueous solubility for an injectable formulation.

2-methyl-4-(4-methylpiperazin-1-yl)-10H-thieno[2,3-b][1,5]benzodiazepine, commonly known as Olanzapine is a blockbuster psychotropic agent marketed by Eli Lilly under the brand name ZYPREXA. According to the Biopharmaceutics Classification System (BCS), Olanzapine belongs to Class II category, namely a drug with low solubility (43 mg/L) and high permeability. To improve the solubility and dissolution behaviour of the drug some salts with malonic acid, maleic acid, fumaric acid, nicotinic acid, p-amino benzoic acid and salicylic acid were synthesized along with some solvated structures of the parent API. The solubility and dissolution of the corresponding salts (Figure 2) were studied and found improvement in the properties to a considerable extent. The hydrogen bonding and structural analysis of the salts and solvates are discussed.
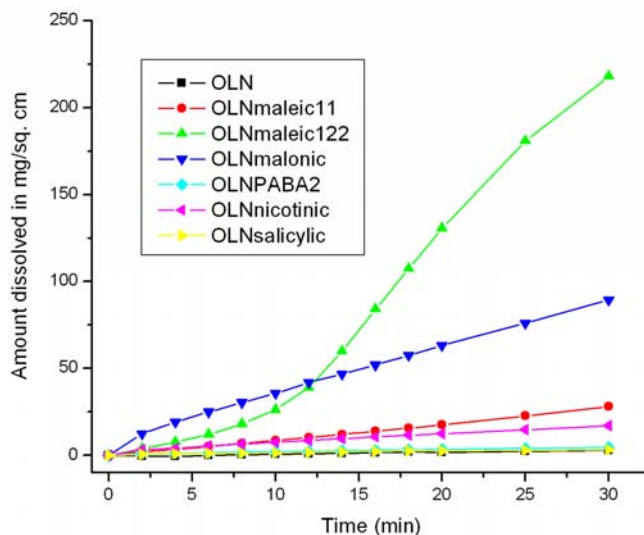
Figure 2 Dissolution profile of Olanzapinium salts

CHAPTER FIVE

Olanzapinium Maleate Salts

As discussed in the chapter 4, polymorphism, salt preparation and cocrystallization are widely used methods to improve the physico-chemical properties of an API. Another phase of interest in pharmaceutical systems is the amorphous formulation of a drug. In the past decade, there has been a high level of interest and investigation on the use of amorphous solids of small molecule active pharmaceutical ingredients (APIs) as attractive means of improving the oral bioavailability of poorly soluble drugs. Compared to the crystalline form the amorphous form has excess entropy, enthalpy and free energy which accounts for its improved solubility. However due to the excess thermodynamic properties amorphous state is relatively unstable and crystallization may occur. The glass transition temperature (T_g) plays a crucial role in the stability of an amorphous material. To prepare the amorphous solids generally the following methods are used namely (1) melting followed by quench cooling, (2) spray-drying or freeze-drying of the solution, (3) precipitation by the addition of anti-solvents, (4) mechanical activation, e.g., milling, cryomilling, or by a combination of the

aforementioned techniques, such as melt extrusion, and (5) desolvation of the crystalline hydrate/ solvate form.

For Olanzapine with very low solubility (43 mg/L), two stoichiometric salts of 1:1 and 1:2 with maleic acid, both in amorphous and crystalline states, were prepared. Amorphous materials were prepared by neat grinding and crystalline materials using liquid-assisted grinding; the reason of formation of the amorphous material on neat grinding is explained and the mechanism for crystallization of the salt is discussed.
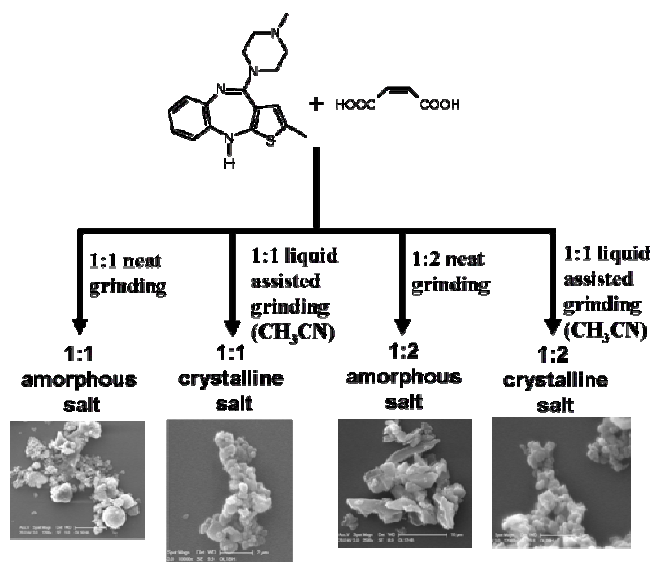
Figure 3 Olanzapinium monomaleate and olanzapinium dimaleate salts in amorphous and crystalline forms were prepared using the above mentioned conditions. Scanning electron microscopy images of the amorphous and crystalline forms are shown.

Dissolution and solubility of the mono and dimaleate salts were studied and the higher dissolution rate of dimaleate was explained through the crystal structure analysis and hydrogen bonding sites of the maleate anion.

CHAPTER SIX

Molecular Salts of an Anti-Depressant Drug Mirtazapine

(±)-1,2,3,4,10,14b-hexahydro-2-methylpyrazino[2,1-a]pyrido[2,3-c]benzazepine commonly known as Mirtazapine with empirical formula $C_{17}H_{19}N_3$ has a tetracyclic

skeleton belonging to the piperazino-azepine group of compounds. It is used in the treatment of depression and anxiety, and as a hypnotic, antiemetic, appetite stimulant and antihistamine. Mirtazapine is the most popular anti-depressant among the top 12 SNRI and SSRI drugs according to a recent survey.

It is a white to creamy white crystalline powder belongs to the class I drug category according to the Biopharmaceutical Classification System (BCS). It used to sublime at ambient temperature and this poses stability problem for tablet formulation. Generally salt pre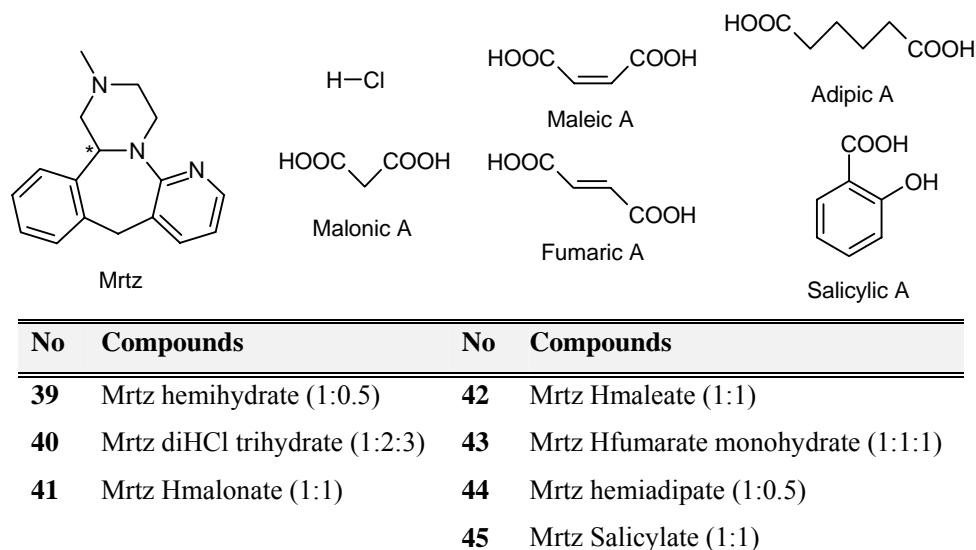paration and cocrystallization are the common crystal engineering approach to improve the physico-chemical properties of an API. The N-methyl basic site of the piperazine group of Mirtazapine has a pK_a of 7.1, therefore based on the ΔpK_a rule it should form salts with organic acids having pK_a < 4. Some molecular salts of Mirtazapine with HCl, malonic acid, maleic acid, fumaric acid, adipic acid, salicylic acid and hemihydrate of the free base (Scheme 2) were synthesized to understand the hydrogen bonding, molecular packing and hydration states.

No	Compounds	No	Compounds
39	Mrtz hemihydrate (1:0.5)	42	Mrtz Hmaleate (1:1)
40	Mrtz diHCl trihydrate (1:2:3)	43	Mrtz Hfumarate monohydrate (1:1:1)
41	Mrtz Hmalonate (1:1)	44	Mrtz hemiadipate (1:0.5)
		45	Mrtz Salicylate (1:1)

Scheme 2 Structures described in Chapter 6.

Except the dihydrochloride and fumarate salts, all other Mirtazapinium salts were non-hygroscopic in nature. Whereas the free base undergoes sublimation at near above ambient temperature, the maleate, salicylate and fumarate salts did not sublime even at elevated temperatures.

CHAPTER SEVEN

Conclusion and Future Prospects

Based on crystal engineering principles some novel materials were synthesized and studied the alteration of the physico-chemical properties of some APIs. An organic phenol host 1,4-di[bis(hydroxyphenyl)methyl]benzene and its methyl and methoxy derivatives were synthesized having a H-shaped geometry and used to generate different network topology like ladder, honeycomb, calatan, polyrotaxane, polycatenane and different interpenetration based on the guest hydrogen bonding, π-stacking and host molecular conformation. Some novel cocrystals of pyrogallol and catechol were synthesized with some of the N-heterocycle bases in order to study crystal structures from a hydrogen bonding point of view. Salt preparation and cocrystallization for some APIs was undertaken to improve their physico-chemical properties. Salts/ solvates of the psychotropic drug Olanzapine were synthesized and the solubility and dissolution behavior of the drug was improved to a large extent in maleate salts, for which structure-solubility relationship was studied. Similarly some non-subliming and non-hygroscopic salts of an anti-depressant drug Mirtazapine were synthesized to improve the stability and studied the synthon and hydrogen bonding patterns.

The role of crystal engineering in pharmaceutical science will open new opportunities to solve the current challenges in human health.

CONTENTS

CHAPTER SIX

MOLECULAR SALTS OF AN ANTI-DEPRESSANT DRUG   167-192

MIRTAZAPINE

CHAPTER SEVEN

CONCLUSIONS AND FUTURE PROSPECTS   193-196

APPENDIX   197-206

CHAPTER ONE

INTRODUCTION

1.1 SOLID-STATE CHEMISTRY

Solid-state chemistry deals with the synthesis, structure, and properties of solid phase materials.[1] It focuses on the design and synthesis of new solid materials to discover new phenomena or enhanced properties, and to understand the bonding interactions present in the crystal structures. The properties of a material depend not only on the constituent's identity but also on their intermolecular interactions. If a crystalline solid contains more than one component then its properties differ from the individual ones. The relationship between structure and property of a solid is the central theme in solid-state chemistry. Therefore it has a strong overlap with solid-state physics, crystallography, ceramics, material science, electronics, etc. in the synthesis and characterization of novel materials.[2]

Solids can show differences externally or internally. External differences are referred to as shapes, habits or morphology and the internal structure that make the solid substance remains the same.[3] With respect to the internal structure based on the degree of long range order or periodicity, solids can be divided into three categories. They are – amorphous, liquid crystalline and crystalline solids.

Amorphous phases are those solids that do not exhibit long range order but usually have short range order.[4] It is difficult to study the short range order of amorphous materials. Spectroscopic techniques such as IR and Raman spectroscopy can provide information on the molecular assembly and hydrogen bonding patterns and X-ray, neutron and to some extent electron scattering provide details about the average separation of molecular species in amorphous materials. If the material is having long range order in one or two dimensions they are referred to as liquid crystalline materials. Liquid crystalline materials are further categorized based on the number of components. The vast majority of solid-state materials belong to the category of crystalline solids. They exhibit both short and long range order in all three directions.[5] Based on the number of component present crystalline and amorphous materials can be further categorized into

single component, binary, ternary adducts and so on. Polymorphism is possible for all categories of solids;[6] for crystalline solids it is referred as polymorph and for amorphous material as polyamorph. The classification of chemical compounds in various solid-state categories is shown in Figure 1.
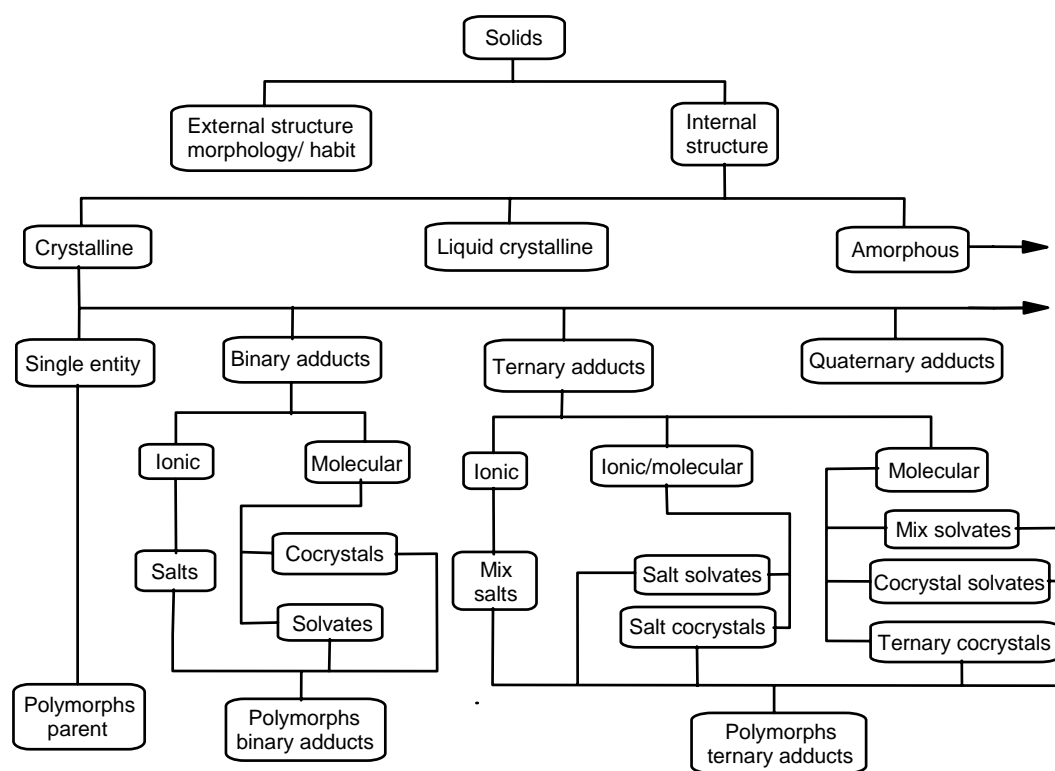
Figure 1 Schematic diagram showing the classification of chemical compounds in various solid state categories. Adapted from the book *Developing Solid Oral Dosage Forms: Pharmaceutical Theory and Practice*, published by Elsevier (reference 7g).

Solid-state chemistry is a very important aspect in pharmaceutical research,[7] because a majority of small and big molecule drugs in the market are available as solid oral dosage forms, primarily including tablets, capsules, and powders. Many of the parental products are formulated as lyophiles and reconstructed before administration, and dry powder inhalers are popular for respiratory products. As solid materials show different properties and small modifications affect their solubility, dissolution, stability,

flowability, compressibility and hygroscopicity which have prime importance in drug development. The role of solid-state chemistry in the pharmaceutical world is summarized in Figure 2.
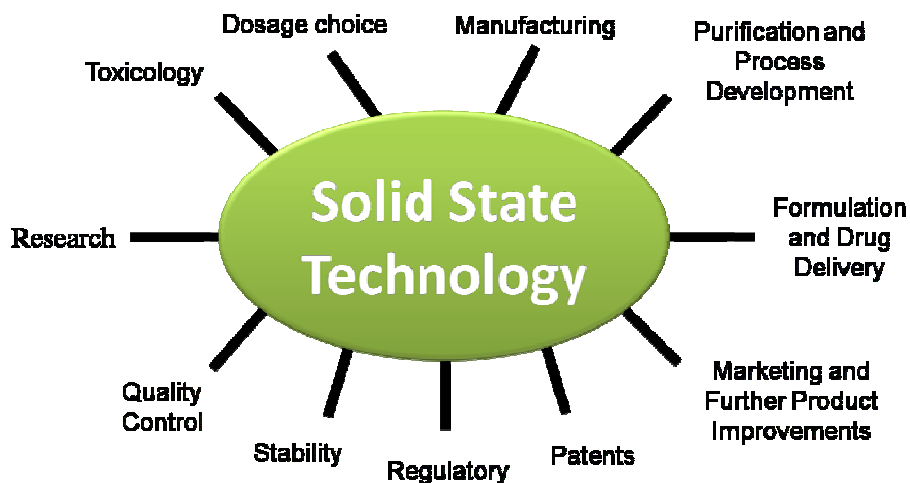
Figure 2 Role of solid-state chemistry in pharmaceutical research and development. This diagram is culled from *J. Pharm. Sci.*, John Wiley & Sons (reference 7e).

The application of solid-state chemistry gained importance after the accidental appearance of the more stable and less soluble Ritonavir form II from a liquid formulation of metastable form I,[8a] the pet food crisis incident,[8b,c] etc. A recent report of green tea extract in preventing large kidney stones shows the application of crystal engineering in human health. Xudong Li[9] and co-workers studied that generally calcium oxalate, the key component of kidney stone, tends to form a monohydrate structure which is thermodynamically stable and can lead to the formation kidney stones. But in presence of green tea the dihydrated form use to crystallize which is less stable and so less likely to grow into problematic sizes before being extracted in urine (Figure 3).
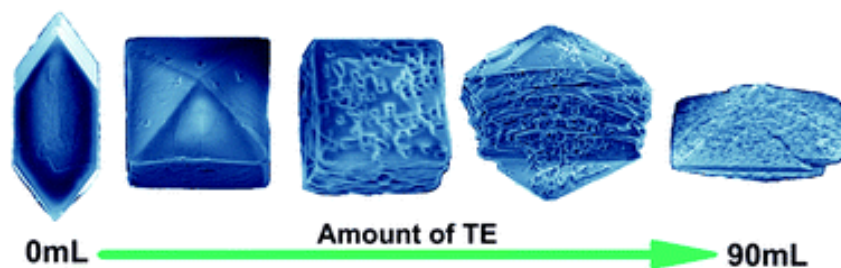
Figure 3 The shape of calcium oxalate crystals from SEM image in presence of 0–90 mL of green tea extract. This figure is taken from *CrystEngComm*, RSC publication (reference 9).

1.2 CRYSTALLINE PHASE

Crystals are made up of molecules arranged in a periodic fashion; this periodic arrangement of molecules determines the physical properties of the substance and in turn affects its property.[7] The infinite periodic arrangement of a crystal can be defined in terms of the smallest repeating unit which is called the unit cell, which contains all the structural features and the symmetry elements to generate the whole crystal. When only one type of molecules are present it is referred to as a single component system, but crystals may also contain more than one type of atom, ionic compound, or molecule, i.e., a broad category multi-component system. The components in the crystal lattice are held together by non-covalent interactions like ionic, hydrogen bond and van der Waal forces. A crystalline material can be arranged in more than one way, the phenomenon is known as polymorphism. McCrone defined polymorphism as "a solid crystalline phase of a given compound resulting from possibility of at least two different arrangements of the molecules of that compound in solid state".[6a]

1.3 FORCES RESPONSIBLE FOR CRYSTAL PACKING

INTERIONIC INTERACTIONS

These interactions are generally observed in ionic crystals and are of magnitude around 30 kcal mol^{-1}.

HYDROGEN BONDS

According to the recent IUPAC committee "*a typical hydrogen bond may be depicted as X–H···Y–Z, where the three dots denote the bond. X–H represents the hydrogen-bond donor. The acceptor may be an atom or an anion Y, or a fragment or a molecule Y–Z, where Y is bonded to Z. In specific cases X and Y can be the same with both X–H and Y– H bonds being equal. In any event, the acceptor is an electron-rich region such as, but not limited to, a lone pair in Y or a π-bonded pair in Y–Z*".[10] Based on the strength of hydrogen bond, they can be classified into three categories as very strong, strong and weak (Table 1).[11] O–H…O, N–H…O, O–H…N and N–H…N are some well-studied and commonly observed strong hydrogen bonds.

Table 1 Some properties of very strong, strong and weak H-bonds.

Properties	Very strong	Strong	Weak
Bond energy ($-kcal\ mol^{-1}$)	15–40	4–15	<4
Examples	$[F···H···F]^-$	O–H···O=C	C–H···O
	$[N···H···N]^+$	O–H···O=C	O–H···π
	P–OH···O=P	O–H···O–H	Os–H···O
Red shift in IR	>25%	5–25%	<5%
$D(X···A)$ (Å)	2.2–2.5	2.5–3.2	3.0–4.0
$d(H···A)$ (Å)	1.2–1.5	1.5–2.2	2.0–3.0
$\theta(X–H···A)$ (°)	175–180	130–180	90–180
Covalency	Pronounced	Weak	Vanishing
Electrostatic	Significant	Dominant	Moderate

VAN DER WAALS INTERACTIONS

It is the sum of the attractive or repulsive forces between molecules (or between parts of the same molecule) other than those due to covalent bonds or the electrostatic interaction of ions with one another or with neutral molecules. The van der Waals forces include those between two permanent dipoles, between a dipole and an induced dipole and between two instantaneous induced dipoles. The structure of organic compound in which

the van der Waals forces operate are characterised by close packing.[12] They are very weak in magnitude but numerous. Therefore, their overall importance is significant.

1.4 NETWORK SOLIDS

The 'network approach' or topological approach to crystal chemistry is an important achievement and a useful tool for the design, comparison and analysis of network structures which simplifies complex species to schematized reference nets.[13] Based on the crystal engineering approach in the reverse direction specific network topologies with definite properties are built by manipulating molecules and/ or functional moiety in the building blocks. Network architectures are common in inorganic structures, minerals, metal–organic compounds and coordination polymers.[14] The inorganic network structures or metal organic frameworks commonly known as MOFs have wide applications in gas absorption and separation, catalysts for organic and inorganic synthesis, sorption of organic molecules, enantiomeric separation, selective detection of organic and inorganic compounds, targeted drug delivery, etc.[15] In general, the classification of organic crystal structures as nets is over a decade old now.[16] The fact that hydrogen bonds are weaker and less directional than metal–heteroatom and metal–ligand bonds means that the geometry of organic structures is not as clearly definable as that at the metal center in coordination compounds and polymers. Even though hydrogen bond directionality has an angular spread, organic crystal structures can be topologically classified akin to inorganic and coordination network structures. New examples of rare network topologies, interpenetration/ catenation modes of organic supramolecular architectures and network diversity of H-shaped phenol host[17] in presence of coformers (guest) are discussed.

1.5 MULTI-COMPONENT SYSTEM

HOST-GUEST COMPOUNDS, SALTS AND COCRYSTALS

Multi-component system can be divided into host-guest compounds, molecular salts and cocrystals. The inclusion of small guest molecules in the open framework of a host molecule constitutes a host-guest compound. Host-guest compounds are mainly divided

into Cavitands and Clathrands based on the nature of the host.[18] Cavitands consists of intra-molecular cavities and clathrands are the hosts with extra-molecular cavities that result from aggregation of more than one molecule. Some common host molecules are cyclodextrins,[19a,b,c] calixarenes,[19d] cucurbiturils,[19e,f] porphyrins,[19g,h] metallacrowns,[19i,j] crown ethers,[19k] cryptophanes,[19l,m] bisphenols[19n] and zeolites,[19o] etc. The difference between a host-guest adduct H•G and a binary molecular complex A•B is that, in a host guest adduct there are either no H···H and G···G interactions, or H···H interactions along with weak H···G association stabilizing the structure. But in case of binary molecular complex A•B, there is a definite A···B interaction comparable in strength to A···A/ or B···B aggregation. When the guest molecule is a solvent of crystallization, the structure is referred to as solvate or pseudopolymorph. When the guest molecule present in the crystal structure is water, it is designated as hydrate.

Solvates, hydrates and pseudopolymorphs are of great importance in the pharmaceutical industry.[20] The drug development process exposes active pharmaceutical ingredients (APIs) to various organic and aqueous solvents during crystallization, wet granulation, storage and dissolution and can lead to the formation of solvated crystals by design or by accident. The most important point is that some APIs form solvates while others do not. The propensity of an API molecule to form solvates has been related to molecular structural features, hydrogen bond patterns, and crystal packing. Some important drugs which are marketed as solvates[21] are Indinavir sulphate ethanolate (Crixivan), Darunavir ethanolate, Doxycycline HCl ethanolate, Mirtazapine hemihydrate (Remeron), Paroxetine HCl hemihydrate (Paxil), Atorvastatin calcium trihydrate (Lipitor) and Cephradine dihydrate (Velosef).

A cocrystal can be defined as "*compounds constructed from discrete neutral molecular species, made from reactants that are solids at ambient conditions and structurally homogeneous crystalline material and contains two or more neutral building blocks that are present in definite stoichiometric amounts*".[22] Salts and cocrystals are the extreme cases of proton position between an acid and a base in multi-component crystals. At the salt end the proton transfer is complete, and on the opposite end proton transfer is

absent in cocrystals where the acid ionization constant (pK_a) governs the formation of a salt or cocrystal.[23] Both of them are very useful for alteration of physico-chemical properties of an API. Salts of API are used in pharmaceutical industry for the past many decades but pharmaceutical cocrystals are still in the pipeline and much widely studied in the past few years.[24]

1.6 PHARMACEUTICAL SALTS

Salt formation is a useful method for isolation and purification of substances. The formation of a pharmaceutical salt can modify the physicochemical as well as the biological properties of an ionizable drug, which cannot be predicted from the properties of the parent drug and of the counter ion. Salt formation is an acid base reaction and a compound having an acidic or basic group can participate in salt formation. Improvement of solubility and dissolution rate of weakly acidic or basic drug having poor water solubility is the primary reason for preparation of pharmaceutical salt forms.[25] In addition to this, salt formation also influences many other properties like melting point, hygroscopicity, chemical stability, solution pH, crystal form, and mechanical properties. An estimated half of the drugs in the market are administered in the salt form. It is easier to select a salt forming agent by knowing the acid ionization constant (pK_a) value of each ionizable group present in API. It is generally accepted that reaction of an acid with a base will be expected to form a salt if the ΔpK_a (ΔpK_a = pK_a(conjugate acid of base) – pK_a(acid)) is greater than 3.[23] Nangia[23b] and coworkers noted that a smaller ΔpK_a (less than 0) will almost exclusively result in cocrystal formation, the parameter is inappropriate for accurately predicting salt formation in the solid state when ΔpK_a is between 0 and 3, as some examples are there where partial proton transfer is the case. Salt former selection is an important aspect in preparing pharmaceutical salts from toxicological and pharmacological point of view. Salt formers can be subdivided into a number of categories, depending upon their functionality and purpose. Some of the most frequently used examples are listed in Table 2.

Table 2 Classification of some common pharmaceutical salts. This table is adapted from *Org. Proc. Res. Dev.*, ACS publication (reference 25h).

Salt Class	Examples
Anions	
Inorganic acids	hydrochloride, hydrobromide, sulfate, nitrate, phosphate
Sulfonic acids	mesylate, esylate, isethionate, tosylate, napsylate, besylate
Carboxylic acids	acetate, propionate, maleate, benzoate, salicylate, fumarate
Anionic amino acids	glutamate, aspartate
Hydroxyacids	citrate, lactate, succinate, tartrate, glycollate
Fatty acids	hexanoate, octanoate, decanoate, oleate, stearate
Insoluble salts	paemoate (embonate), polystyrene sulfonate (resinate)
Cations	
Organic amines	triethylamine, ethanolamine, triethanolamine, meglumine, ethylenediamine, choline
Insoluble salts	procaine, benzathine
Metallic	sodium, potassium, calcium, magnesium, zinc
Cationic amino acids	arginine, lysine, histidine

1.7 PHARMACEUTICAL COCRYSTALS

Generally for low soluble active pharmaceutical ingredients (APIs), salt preparation is the preferred solution to improve the physico-chemical properties. But for the APIs which lack an ionization site, salt preparation is either unsuccessful or impossible. In comparison cocrystals offer a different pathway where an API regardless of an ionizable or nonionizable group can form hydrogen bond with coformers to generate cocrystals with modified physico-chemical properties.[22g,24] Pharmaceutical cocrystals are crystalline molecular complexes of an Active Pharmaceutical Ingredient (API) with another pharmaceutically acceptable molecule or Generally Regarded As Safe (GRAS) chemicals. Combining an API with a pharmaceutically acceptable agent in this guest/ host like manner has become an increasingly attractive route for developing pharmaceutical products. Furthermore, exploring the co-crystallization potential around an API increases the intellectual property protection of a particular drug product; thus,

reducing the risk of costly litigation and market erosion.[24h,26] The application of co-crystal technologies has been recognised within the last decades as a way to enhance solubility, stability and the Intellectual Property (IP) position with respect to the development of APIs. In the last few years more than 90 case studies by various groups, e.g. Childs,[24b] Jones,[24d] Nangia,[24e] Zaworotko,[22g,24a,j] Almarsson,[24a] Rodríguez,[24e,j,k,l] Remenar[7f,24c,25g] and several others were reported in the literature which describe the importance of the field of pharmaceutical cocrystals.

1.8 AMORPHOUS SOLIDS

The amorphous state is important in pharmaceutical development in order to improve the physicochemical properties of an active pharmaceutical ingredient (API), apart from that it exists in many industrial products such as ceramics, polymers, metals, optical materials (glass and fiber), and foods, etc. The importance in pharmaceutical industry is because of the three main characteristic properties, namely

1. Useful properties: Amorphous solids have high solubility, dissolution rate and sometimes better compressibility than corresponding crystalline phase.

2. Instability: Because of the high thermodynamic properties they are highly metastable physically and chemically than their corresponding crystalline counterpart.

3. Common occurrence: They can be prepared by standard pharmaceutical processes and are the common forms of certain materials like proteins, peptides, some sugars and polymers.

   Amorphous state is characterized by solidification in a disordered, random manner, structurally similar to a liquid. Generally an amorphous form has short range order but it lacks any long range interaction like the crystalline phase.[27] When a crystalline solid is heated beyond its melting point and quenched cool to its original temperature, without allowing nucleation to occur, an amorphous material results. It lacks a proper melting point. An amorphous solid is characterized by its glass transition temperature (T_g). The glass transition temperature is the temperature at which the glassy material (plastic) is converted to a rubbery phase having some of the properties of liquid.

Amorphous materials have higher entropy, enthalpy and free energy than the crystalline phase. Due to the excess thermodynamic properties (Figure 4) amorphous materials are generally hygroscopic in nature and readily undergo crystallization.
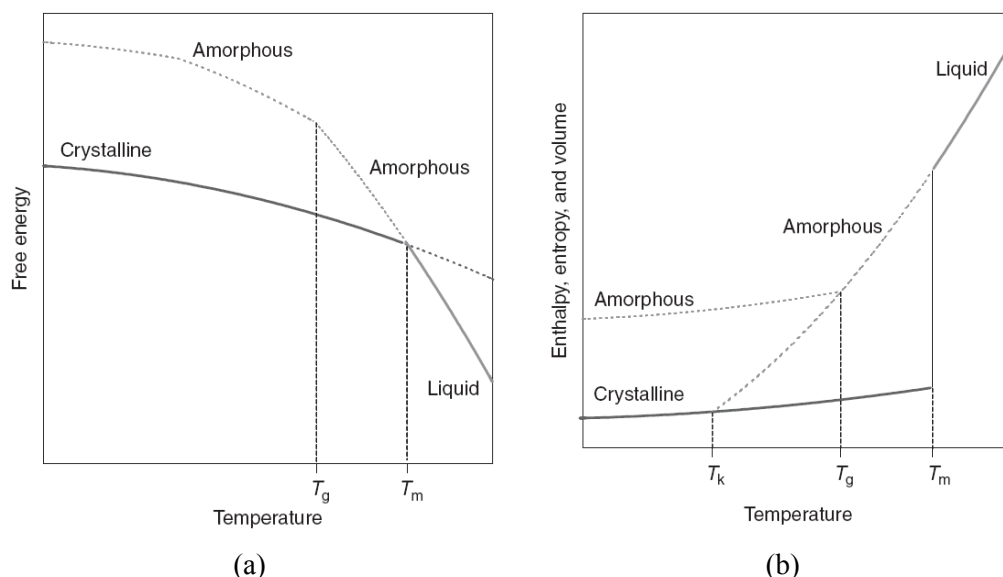
Figure 4 Phase diagram of amorphous and crystalline solids. (a) Free energy, (b) Enthalpy, entropy and volume. This diagram is adapted from the book *Developing Solid Oral Dosage Forms: Pharmaceutical Theory and Practice,* published by Elsevier (reference 7g).

KAUZMANN'S PARADOX

As a liquid is supercooled, the difference in entropy between the liquid and solid phase decreases. The temperature at which this entropy difference becomes zero is referred to as Kauzmann temperature (T_K).[28] On extrapolating temperature below T_K leads to a unphysical situation where the entropy of disordered liquid is lower than that of the ordered crystal, which results in the violation of the third law of thermodynamics. This is known as the Kauzmann's paradox under the name of Walter Kauzmann who put forward this concept. There are three types of approaches to resolve the Kauzmann's paradox – (1) **Ideal glass-transition approach**: In this case, a supercooled liquid is supposed to transform into an ideal glass state at T_0, which is the second-order phase

transition. Accordingly, the structural relaxation time diverges at T_0. (2) **Smooth extrapolation scenario**: In this scenario, the excess entropy smoothly goes to zero toward $T = 0$ K. Thus, there is no divergence of the structural relaxation time at T_0. This is the singularity-free scenario, and (3) **Crystallization scenario**: This is the original approach of Kauzmann where a supercooled liquid becomes unstable against crystallization and thus it transforms into a crystalline state as a result of the first-order phase transition (crystallization) before the excess entropy becomes zero. These three different approaches are shown in the Figure 5.
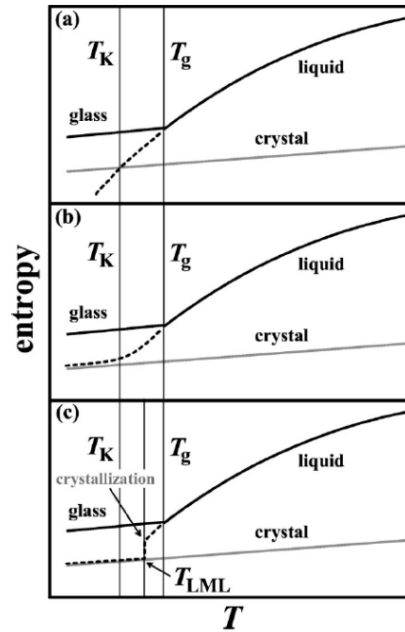
Figure 5 Three scenarios to resolve the Kauzmann paradox. (a) ideal glass transition approach. (b) Smooth extrapolation scenario and (c) crystallization scenario. The diagram is taken from *Physical Rev.*, APS publication (reference 28c).

The glass transition temperature is further lowered by water or other solvents, facilitating conversion to the rubbery state and hence facilitating crystallization. In order to stabilize amorphous form generally the amorphous material is dispersed in a polymer matrix (stabilizer) with very high glass transition temperature. The effect of additives on T_g can be described by modified Gordon-Taylor equation.[29] The equation is written as

$$T_{g12} = (w_1 T_{g1} + K w_2 T_{g2})/(w_1 + K w_2) \qquad \text{where } K = \rho_1 \Delta \alpha_1 / \rho_2 \Delta \alpha_2$$

Here T_{gi} indicating the glass transition temperature of component i, w_i indicating the weight fraction of component i in the mixture, ρ_i indicating the true density of the component i and $\Delta \alpha_i$ the change in thermal expansivity for component i.

As values for $\Delta \alpha_i$ are not readily available for many materials, K is often approximated using the Simha-Boyer rule presented as

$$K \cong \rho_1 T_{g1} / \rho_2 T_{g2}$$

Now correlating the theoretical and experimental T_g value the miscibility of the system can be assessed.

The amorphous material may be prepared from a single component or multi-component system using the processes shown in the Figure 6.
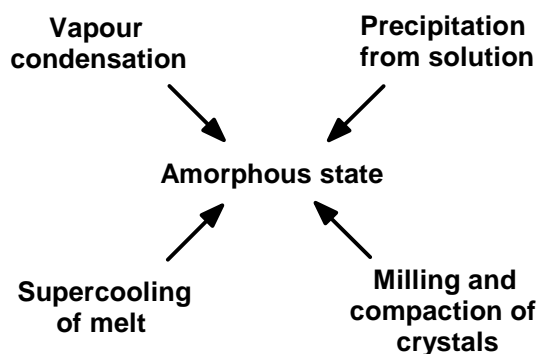
Figure 6 Different methods to prepare amorphous phase. The diagram is adapted from *J. Pharm. Sci.*, John Wiley & Sons (reference 4a).

POLYAMORPHISM

Polymorphism is also applicable to amorphous material. Like the crystalline materials amorphous materials can also have more than one local packing arrangement. The phenomenon of different local packing arrangement of amorphous material is termed as polyamorphism.[30] The different polyamorphous phases possess different glass transition temperature (T_g). Generally for amorphous materials slow cooling delays the glass

transition of many organic molecules and cooling 10 times more slowly lowers T_g by 3–5 K. As amorphous material do not contain any Bragg lines therefore it is very difficult to characterize different polyamorphous phases. For example polyamorphism in H_2O is extensively studied, but the interpretation of data remains controversial.[31]

1.9 SOLUBILITY AND DISSOLUTION

A true solution is a homogeneous mixture of two or more components at a molecular level. In a two component system, the component present in large amount is referred as solvent, and the other component is defined as solute. The solubility of a drug is one of the most important physico-chemical properties.[25] The determination of solubility and the way to alter if necessary by amorphisation, salt formation, cocrystallization, etc. are vital steps in pharmaceutical development programs. The bioavailability of an orally administered drug depends on its solubility in the gastrointestinal tract and its permeability across the cell membranes. This solubility and permeability are the basis for the Biopharmaceutics Classification System (BCS) of drugs.[32] Based on the three dimensionless parameters ― absorption number (A_n), dissolution number (D_n), and dose number (D_o), Amidon *et. al.* divided all drugs into four categories (Figure 7). They are

Class I – High solubility, High permeability	Class II – Low solubility, High permeability
Propranolol, Metoprolol, Diltiazem, Verapamil, Theophyline, Paracetamol, Pseudoephedrine sulfate, Motformin hydrochloride	Danazol, Ketoconazole, Mefanimic acid, Nisoldipine, Nifedipine, Nicardipine, Felodipine, Atovaquone, Griseofulvin, Troglitrazone, Glibenclamade, Carbamazepine
Class III – High solubility, Low permeability	Class IV – Low solubility, Low permeability
Acyclovir, Neomycin, Captopril, Enalprilate, Alendronate, Atenolol, Cimetidine, Ranitidine	Chlorothiazine, Furosemide, Tobramycin, Cefuroxime, Itraconazole, Cyclosporin

Figure 7 The Biopharmaceutics Classification System.

Class I – High **Permeability**, High **Solubility**

These compounds are well absorbed and their absorption rate is usually higher than excretion.

Class II – High **Permeability**, Low **Solubility**

The bioavailability of these products is limited by their solvation rate.

Class III – Low **Permeability**, High **Solubility**

The absorption is limited by the permeation rate but the drug is solvated very fast.

Class IV – Low **Permeability**, Low **Solubility**

These compounds have a poor bioavailability. Usually they are not well absorbed over the intestinal mucosa and a high variability is expected.

The three dimensionless parameters, the basis for Biopharmaceutics Classification System can be defined as ―

The ***dose number*** (D_o) is the ratio of the dose to the amount of drug that will dissolve in 250 mL of test solution at the lowest solubility within the pH range 1 to 8. Ideally, this ratio should be below 1 if full dissolution is to be possible in principle. Obviously, higher doses will raise the ratio and make good absorption less likely.

The ***absorption number*** (A_n) is the ratio of the transit time to the absorption time (1/absorption rate constant). Ideally, this should exceed 1. Longer absorption times resulting from lower permeability will reduce this ratio.

The ***dissolution number*** (D_n) is the ratio of the transit time to the dissolution time (1/dissolution rate constant). Ideally, it should exceed 1. In case of solid dosage forms, a combination of inadequate solubility or diffusivity, or excessive particle size or density can increase the time needed for full dissolution and reduce this ratio.

The solubility and dissolution are related to each other. The concentration of the solute in the solvent, at which the rate of molecules leaving the bulk solute surface becomes equal to the rate of redeposition, is the thermodynamic solubility. The rate at

which this equilibrium is achieved is defined as the dissolution rate. Therefore solubility is an equilibrium process while dissolution is a kinetic phenomenon. According to Noyes–Whitney,[33] dissolution rate of a solute in a solvent is directly proportional to its solubility described by the equation

$$\text{Dissolution rate} = \frac{dQ}{dt} = \frac{DA}{h}(C_s - C_b)$$

where,

dQ/ dt is the rate of mass transfer

D is the diffusion coefficient ($cm^2/$ sec)

A is the surface area of the drug (cm^2)

h is the diffusion layer thickness (cm)

C_s is the saturation solubility of the drug

C_b is bulk solution concentration.

The solid dissolution process generally involves two sequential steps – the first step is the interaction between solid and solvent molecules to form solvated molecules, which take place at solid-liquid interface and is governed by regular chemical reaction. The second step is the mass transport of solvated molecules from the solid-liquid interface to the bulk solution which involves a large distance movement compared to molecular dimensions (1st step) and usually much slower. Hence the second step is the rate determining step for two-step dissolution process.

To describe the dissolution phenomenon various models are being proposed. They are ―

1.9.1 DISSOLUTION BY PURE DIFFUSION

For solid dissolution processes, the dissolved molecules are transported by convection. Dissolution through pure diffusion without any contribution from some form of convection is rare. Even without mixing, density gradient caused by concentration difference or thermal effects due to heat of solvation leads to natural convection.

When a particle dissolves by pure diffusion, the concentration at every point away from the solid-liquid interface increases, but the concentration gradient decreases

with time. Therefore overall dissolution rate decreases and becomes constant with time and a pseudo-steady state is reached.

1.9.2 DIFFUSION LAYER MODEL

Noyes and Whitney proposed the diffusion layer model.[33a] They stated that when surface area is constant, the dissolution rate is proportional to the difference between solubility and the bulk solution concentration.

$$\text{Dissolution rate} = k(C_s - C_b)$$

where, k is a constant (mass transfer coefficient)

Nernst[34] and Brunner[35] suggested that rapid equilibrium (i.e., saturation) is achieved at the solid-liquid interface during dissolution. Diffusion occurs across a thin layer of stagnant solution, called as diffusion layer, to the bulk solution. Diffusion across the diffusion layer is the rate limiting step in most cases.

$$\text{Dissolution rate} = \frac{dQ}{dt} = \frac{DA}{h}(C_s - C_b)$$

This model is shown in the Figure 8.
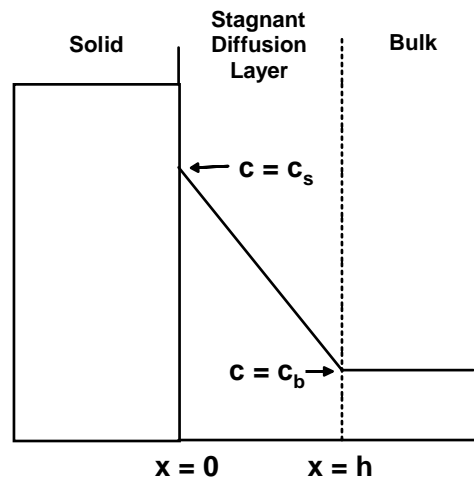
Figure 8 Diffusion layer model of drug dissolution. This diagram is adapted from the book *Developing Solid Oral Dosage Forms: Pharmaceutical Theory and Practice*, published by Elsevier (reference 7g).

In the Nersnst and Brunner's concept it is assumed that the diffusion layer is stagnant or unstirred layer attached to the solid surface is hydrodynamically unrealistic. This is one of the major limitations of the diffusion layer model. One more limitation is that the diffusion layer thickness cannot be calculated independently based on hydrodynamics and can be calculated only by fitting equations to experimental data.

1.9.3 CONVECTIVE DIFFUSION MODEL

The limitation of the diffusion layer model is the basis for the convective diffusion model,[36] where there are two mechanisms for transport of solute molecules from a solid in a moving liquid. Firstly, the molecular diffusion is due to concentration gradient and secondly, solute molecules are carried along by moving solvent (convection).

$$\frac{\partial C}{\partial t} = D\left(\frac{\partial^2 C}{\partial x^2} + \frac{\partial^2 C}{\partial y^2} + \frac{\partial^2 C}{\partial z^2}\right) - v_x\frac{\partial C}{\partial x} - v_y\frac{\partial C}{\partial y} - v_z\frac{\partial C}{\partial z}$$

v_x, v_y and v_z are liquid velocities in the x, y and z directions in Cartesian coordinates.

This equation is an extension of Fick's second law of diffusion with a convection term. It is different from the Nernst's model by having a velocity gradient of the diffusion layer, mass transport by convection and diffusion both across and along the diffusion layer and no definite boundary of the diffusion layer.

1.10 TYPES OF DISSOLUTION

There are two different types of experimental dissolution methods (1) Planar surface dissolution and (2) Particulate dissolution.

1.10.1 PLANAR SURFACE DISSOLUTION

For experimental determination of dissolution rate the planar surface model is the simplest one having simple mathematics for calculation. For calculating dissolution rate both the Noyes-Whitney equation and convective methods can be used. Generally for

pharmaceutical solids measuring dissolution rate from a well defined surface is a popular way, for that intrinsic dissolution rate (IDR) determination is one example.

INTRINSIC DISSOLUTION RATE

When agitation intensity and surface area are fixed, dissolution rate can be considered as a property of solid. This loosely defined property is called the Intrinsic Dissolution Rate (IDR). Due to the close relation between IDR and solubility, it can be used as a method of solubility estimation, when equilibrium solubility cannot be obtained experimentally. For the intrinsic model the container shape, agitation intensity (rotation per minute, rpm), bulk solvent volume, etc. are kept constant to calculate the dissolution rate. The rotating disk apparatus for measuring IDR and the liquid flow are shown in the Figure 9.[37]

(a)   (b)

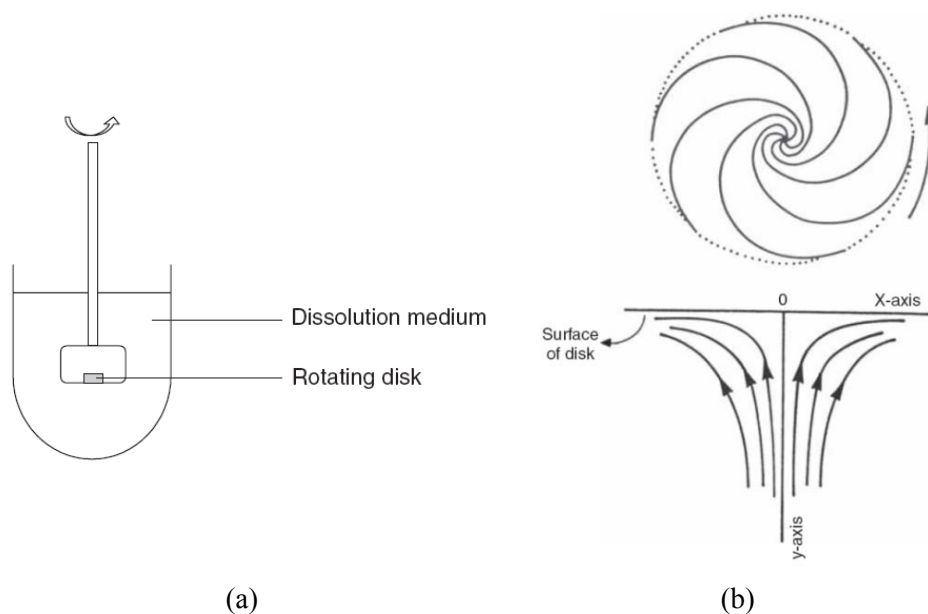**Figure 9** (a) Rotating disk apparatus for measuring IDR. (b) Liquid flow pattern around the rotating disk apparatus. This diagram is adapted from the book *Developing Solid Oral Dosage Forms: Pharmaceutical Theory and Practice*, published by Elsevier (reference 7g).

1.10.2 PARTICULATE DISSOLUTION

For calculating dissolution rate experimentally the planar surface model is useful but in a real sense the drug dissolution involves solid particles and is very complicated process as the total surface area changes during dissolution. Particulate dissolution[38] is based on the real dissolution phenomenon occurs inside the body. It can be explained with both the diffusion layer model and convective diffusion-based particulate model. In this model the effect of particle size and shape play a crucial role.

1.11 REFERENCES

1. (a) M. Jansen, *Angew Chem Int Ed.*, 41, **2002**, 3746. (b) F. J. Disalvo, *Pure Appl Chem.*, 72, **2000**, 1799. (c) J.-M. Lehn, *Supramolecular Chemistry: Concepts and Perspectives*, VCH: Weinheim, **1995**. (d) R. Bishop, F. Toda, D. D. MacNicol, *Solid-State Supramolecular Chemistry: Crystal Engineering* Vol.6, in *Comprehensive Supramolecular Chemistry*, Pergamon, Chichester (UK), **1996**. (e) A. Nangia and G. R. Desiraju, *Acta Cryst.*, A54, **1998**, 934. (f) C. B. Aakeröy, N. R. Champness and C. Janiak, *CrystEngComm*, 12, **2010**, 22.

2. M. G. Kanatzidis and K. R. Poeppelmeier (Organizers), *Prog. in Solid State Chem.*, 36, **2007**, 1.

3. J. K. Haleblian, *J. Pharm. Sci.*, 64, **1975**, 1269.

4. (a) B. C. Hancock and G. Zografi, *J. Pharm. Sci.*, 86, **1997**, 1. (b) L. Yu, *Adv. Drug Deliv. Rev.*, 48, **2001**, 27.

5. (a) S. R. Vippagunta, H. G. Brittain and D. J. W. Grant, *Adv. Drug Deliv. Rev.*, 48, **2001**, 3. (b) D. Braga, F. Grepioni and L. Maini, *Chem. Commun.*, 46, **2010**, 6232.

6. (a) W. C. McCrone, *Polymorphism in Physics and Chemistry of the Organic Solid-State*, Vol 2 Ed., D. Fox, M. M. Labes, A. Weisemberg, Interscience, New York, **1965**, p. 725-767. (b) J. Haleblian and W. McCrone, *J. Pharm. Sci.*, 58, **1969**, 911. (c) A. Nangia, *Acc. Chem. Res.*, 41, **2008**, 595. (d) N. J. Babu, L. S. Reddy, S. Aitipamula and A. Nangia, *Chem. Asian J.*, 3, **2008**, 1122. (e) S. K.

Chandran, N. K. Nath, S. Roy and A. Nangia, *Cryst. Growth Des.*, 8, **2008**, 140. (f) G. P. Stahly, *Cryst. Growth Des.*, 7, **2007**, 1007.

7. (a) S. Dutta and D. J. W. Grant, *Nat. Rev. Drug Discovery*, 3, **2004**, 42. (b) C. R. Gardner, C. T. Walsh and Ö. Almarsson, *Nat. Rev. Drug Discovery*, 3, **2004**, 926. (c) S. R. Byrn, R. R. Pfeiffer and J. G. Stowell, *Solid-State Chemistry of Drugs*, 2nd Ed., SSCI, West Lafayette, Indiana, **1999**. (d) A. Zakrzewski and M. Zakrzewski (Eds.), *Solid state characterization of pharmaceuticals*, Assa international Inc., Danbury, Connecticut, USA, **2006**. (e) S. R. Byrn, G. Zografi, X. (Sean) Chen, *J. Pharm. Sci.*, 99, **2010**, 3665. (f) S. L. Morissette, Ö. Almarsson, M. L. Peterson, J. F. Remenar, M. J. Read, A. V. Lemmo, S. Ellis, M. J. Cima and C. R. Gardner, *Adv. Drug Deliv. Rev.*, 56, **2004**, 275. (g) Y. Qiu, Y. Chen, G. G. Z. Zhang, L. Liu and W. R. Porter (Eds.), *Developing Solid Oral Dosage Forms: Pharmaceutical Theory and Practice*, 1st Ed., Elsevier, **2009**.

8. (a) S. R. Chemburkar, J. Bauer, K. Deming, H. Spiwek, K. Patel, J. Morris, R. Henry, S. Spanton, W. Dziki, W. Porter, J. Quick, P. Bauer, J. Donaubauer, B. A. Narayanan, M. Soldani, D. Riley and K. McFarland, *Org. Process Res. Dev.* 4, **2000**, 413. (b) C. T. Seto, G. M. Whitesides, *J. Am. Chem. Soc.*, 112, **1990**, 6409. (c) N. Shan and M. J. Zaworotko, *Drug. Disc. Today*, 13, **2008**, 440.

9. Z. Chen, C. Wang, H. Zhou, L. Sang and X. Li, *CrystEngComm*, 12, **2010**, 845.

10. G. R. Desiraju, *Angew. Chem. Int. Ed.*, 50, **2011**, 52.

11. (a) G. A. Jeffrey and W. Saenger, *Hydrogen Bonding in Biological Structures*, Springer: Berlin, **1991**. (b) D. Hadzi, *Theoretical Treatments of Hydrogen Bonding*, Wiley: Chichester, **1997**. (c) G. A. Jeffrey, *An Introduction to Hydrogen Bonding*, Oxford University Press: Oxford, **1997**. (d) G. R. Desiraju and T. Steiner, *The Weak Hydrogen Bond in Structural Chemistry and Biology*, Oxford University Press: Oxford, **1999**. (e) T. Steiner, *Angew. Chem. Int. Ed. Engl.*, 41, **2002**, 48. (f) G. R. Desiraju, *Acc. Chem. Res.*, 35, **2002**, 565. (g) B. K. Saha, A. Nangia and M. Jaskólski, *CrystEngComm*, 7, **2005**, 355. (h) P.

Vishweshwar, N. J. Babu, A. Nangia, S. A. Mason, H. Puschmann, R. Mondal and J. A. K. Howard, *J. Phys. Chem. A*, 108, **2004**, 9406.

12. A. I. Kitaigorodsky, *Molecular crystals and molecules*, Academic press, New York, **1973**.

13. (a) A. F. Wells, *Three-Dimensional Nets and Polyhedra,* Wiley, New York, **1977**. (b) M. O'Keeffe and B. G. Hyde, *Philos. Trans. R. Soc. London, Ser. A,* 295, **1980**, 553. (c) L. Öhrström and K. Larsson, *Molecule-Based Materials*, Elsevier, **2005**. (d) R. Robson, *J. Chem. Soc., Dalton Trans.*, **2000**, 3735. (e) B. Moulton and M. J. Zaworotko, *Chem. Rev.*, 101, **2001**, 1629. (f) L. Carlucci, G. Ciani and D. M. Proserpio, *Coord. Chem. Rev.*, 246, **2003**, 247. (g) S. R. Batten and R. Robson, *Angew. Chem. Int. Ed.*, 37, **1998**, 1460. (h) G. R. Desiraju, *Chem. Commun.*, **1997**, 1475.

14. (a) S. C. Jones, V. Coropceanu, S. Barlow, T. Kinnibrugh, T. Timofeeva, J.-L. Brédas and S. R. Marder, *J. Am. Chem. Soc.*, 126, **2004**, 11782. (b) X. Shi, G. Zhu, X. Wang, G. Li, Q. Fang, G. Wu, G. Tian, M. Xue, X. Zhao, R. Wang and S. Qiu, *Cryst. Growth Des.*, 5, **2005**, 207; 341. (c) V. Madhu and S. K. Das, *Inorg. Chem.*, 45, **2006**, 10037. (d) Q.-G. Zhai, C.-Z. Lu, X.-Y. Wu and S. R. Batten, *Cryst. Growth Des.*, 7, **2007**, 2332. (e) Y. Qi, Y. Che, F. Luo, S. R. Batten, Y. Liu and J. Zheng, *Cryst. Growth Des.*, 8 , **2008**, 1654. (f) L.-F. Ma, L.-Y. Wang, D.-H. Lu, S. R. Batten and J.-G. Wang, *Cryst. Growth Des.*, 9, **2009**, 1741.

15. (a) O. M. Yaghi, G. Li and H. Li, *Nature*, 378, **1995**, 703. (b) S. L. James, *Chem. Soc. Rev.*, 32, **2003**, 276. (c) N. L. Rosi, M. Eddaoudi, J. Kim, M. O'Keeffe and O. M. Yaghi, *Angew. Chem. Int. Ed.*, 41, **2002**, 284. (d) C. N. R. Rao, S. Natarajan, A. Choudhury, S. Neeraj and A. A. Ayi, *Acc. Chem. Res.*, 34, **2001**, 80. (e) P. Ryan, L. J. Broadbelt and R. Q. Snurr, *Chem. Commun.*, **2008**, 4132. (f) D. Braga, L. Brammer and N. R. Champness, *CrystEngComm*, 7, **2005**, 1.

16. (a) S. Basavoju, S. Aitipamula and G. R. Desiraju, *CrystEngComm*, 6, **2004**, 120. (b) B. R. Bhogala, P. Vishweshwar and A. Nangia, *Cryst. Growth Des.*, 5, **2005**,

1271. (c) L. S. Reddy, B. R. Bhogala and A. Nangia, *CrystEngComm*, 7, **2005**, 206. (d) B. K. Saha, S. Aitipamula, R. Banerjee, A. Nangia, R. K. R. Jetti, R. Boese, C.-K. Lam and T. C. W. Mak, *Mol. Cryst. Liq. Cryst.*, 440, **2005**, 295. (e) B. R. Bhogala and A. Nangia, *Cryst. Growth Des.*, 6, **2006**, 32. (f) N. J. Babu and A. Nangia, *Cryst. Growth Des.*, 6, **2006**, 1995. (g) K. Endo, T. Sawaki, M. Koyanagi, K. Kobayashi, H. Masuda and Y. Aoyama, *J. Am. Chem. Soc.*, 117, **1995**, 8341. (h) T. Tanaka, T. Tasaki and Y. Aoyama, *J. Am. Chem. Soc.*, 124, **2002**, 12453. (i) K. Endo, T. Koike, T. Sawaki, O. Hayashida, H. Masuda and Y. Aoyama, *J. Am. Chem. Soc.*, 119, **1997**, 4117. (j) B. R. Bhogala, S. K. Chandran, L. S. Reddy, R. Thakuria and A. Nangia, *CrystEngComm*, 10, **2008**, 1735.

17. (a) R. Thakuria, B. Sarma and A. Nangia, *Cryst. Growth Des.*, 8, **2008**, 1471. (b) R. Thakuria, B. Sarma and A. Nangia, *New J. Chem.*, 34, **2010**, 623. (c) S. Aitipamula and A. Nangia, *Supramol. Chem.*, 17, **2005**, 17.

18. (a) A. Nangia, *Nanoporous Materials: Science and Engineering,* Eds. G. Q. Lu, X. S. Zhao, Imperial College Press, London, 2004, p. 165. (b) A. Nangia, *Curr. Opin. Solid State Mater. Sci.*, 5, **2001**, 115.

19. (a) W. Saenger and T. Steiner, *Acta Cryst.*, A54, **1998**, 798. (b) W. M. Nau and X. Zhang, *J. Am. Chem. Soc.*, 121, **1999**, 8022. (c) M. L. Singleton, J. H. Reibenspies and M. Y. Darensbourg, *J. Am. Chem. Soc.*, 132, **2010**, 8870. (d) S. Shinkai, *Pure Appl. Chem.*, 58, **1986**, 1523. (e) J. W. Lee, S. Samal, N. Selvapalam, H.-J. Kim and K. Kim, *Acc. Chem. Res.*, 36, **2003**, 621. (f) C. Márquez, R. R. Hudgins and W. M. Nau, *J. Am. Chem. Soc.*, 126, **2004**, 5806. (g) D. Sun, F. S. Tham, C. A. Reed, L. Chaker, M. Burgess and P. D. W. Boyd, *J. Am. Chem. Soc.*, 122, **2000**, 10704. (h) A. M. Beatty, *Coord. Chem. Rev.*, 246, **2003**, 131. (i) A. A. Zinn, Z. Zheng, C. B. Knobler and M. F. Hawthorne, *J. Am. Chem. Soc.*, 118, **1996**, 70. (j) S. K. Mandal, V. G. Young Jr. and L. Que Jr., *Inorg. Chem.*, 39, **2000**, 1831. (k) J. W. Steed and J. L. Atwood, *Supramolecular Chemistry*, 2nd Ed., John Wiley & Sons, Ltd., **2009**. (l) A. Coilet, J.-P. Dutasta, B. Lozach and J. Canceill, *Topics in Cur. Chem.*, 165, **1993**, 103. (m) P. D.

Kirchhoff, M. B. Bass, B. A. Hanks, J. M. Briggs, A. Collet and J. A. McCammon, *J. Am. Chem. Soc.*, 118, **1996**, 3237. (n) S. Aitipamula, G. R. Desiraju, M. Jaskólski, A. Nangia and R. Thaimattam, *CrystEngComm*, 5, **2003**, 447. (o) C. Janiak, *Angew. Chem. Int. Ed.*, 36, **1997**, 1431.

20. (a) T. L. Threlfall, *Org. Proc. Res. Dev.*, 4, **2000**, 384. (b) S. Garnier, S. Petit and G. Coquerel, *J. Thermal Anal. & Calorimetry,* 68, **2002**, 489. (c) Y.-S. Kim and R. W. Rousseau, *Cryst. Growth Des.*, 4, **2004**, 1211. (d) T. Hosokawa, S. Datta, A. R. Sheth, N. R. Brooks, V. G. Young and D. J. W. Grant, *Cryst. Growth Des.*, 4, **2004**, 1195. (e) M. R. Caira, T. le-Roex, L. R. Nassimbeni, J. A. Ripmeester and E. Weber, *Org. Biomol. Chem.*, 2, **2004**, 2299. (f) S. Roy, N. R. Goud, N. J. Babu, J. Iqbal, A. K. Kruthiventi and A. Nangia, *Cryst. Growth Des.*, 8, **2008**, 4343. (g) A. Nangia, *Cryst. Growth Des.*, 8, **2008**, 1079.

21. E. Tiekink, J. Vittal and M. Zaworotko (Eds.), *Organic crystal engineering: Frontiers in Crystal Engineering*, 1st Ed., John Wiley & Sons, Ltd., **2010**.

22. (a) M. C. Etter, *J. Phys. Chem.*, 95, **1991**, 4601. (b) J. D. Dunitz, *CrystEngComm*, 4, **2003**, 506. (c) G. R. Desiraju, *CrystEngComm*, 5, **2003**, 466. (d) B. R. Bhogala and A. Nangia, *New J. Chem.*, 32, **2008**, 800. (e) S. L. Childs and K. I. Hardcastle, *Cryst. Growth Des.*, 7, **2007**, 1291. (f) W. Jones, W. D. Motherwell and A. V. Trask, *MRS Bull.*, 341, **2006**, 875. (g) P. Vishweshwar, J. A. McMahon, J. A. Bis and M. J. Zaworotko, *J. Pharm. Sci.*, 95, **2006**, 499. (h) C. B. Aakeröy and D. J. Salmon, *CrystEngComm*, 7, **2005**, 439. (i) C. B. Aakeröy, J. Desper, M. Fasulo, I. Hussain, B. Levin and N. Schultheiss, *CrystEngComm*, 10, **2008**, 1816.

23. (a) S. L. Johnson and K. A. Rumon, *J. Phys. Chem.*, 69, **1965**, 74. (b) B. Sarma, N. K. Nath, B. R. Bhogala and A. Nangia, *Cryst. Growth Des.*, 9, **2009**, 1546. (c) C. B. Aakeröy, M. E. Fasulo and J. Desper, *Mol. Pharm.*, 4, **2007**, 317. (d) C. B. Aakeröy, A. Rajbanshi, Z. J. Li and J. Desper, *CrystEngComm*, 12, **2010**, 4231. (e) S. L. Childs, G. P. Stahly and A. Park, *Mol. Pharm.*, 4, **2007**, 323. (f) S.

Mohamed, D. A. Tocher, M. Vickers, P. G. Karamertzanis and S. L. Price, *Cryst. Growth Des.*, 9, **2009**, 2881.

24. (a) Ö. Almarsson and M. J. Zaworotko, *Chem. Commun.*, **2004**, 1889. (b) S. L. Childs, L. J. Chyall, J. T. Dunlap, V. N. Smolenskaya, B. C. Stahly, G. P. Stahly, *J. Am. Chem. Soc.*, 126, **2004**, 13335. (c) M. B. Hickey, M. L. Peterson, L. A. Scoppettuolo, S. L. Morrisette, A. Vetter, H. Guzmán, J. F. Remenar, Z. Zhang, M. D. Tawa, S. Haley, M. J. Zaworotko and Ö. Almarsson, *Eur. J. Pharm. Biopharm.*, 67, **2007**, 112. (d) A. V. Trask, W. D. S. Motherwell and W. Jones, *Cryst. Growth Des.*, 5, **2005**, 1013. (e) A. Nangia, N. Rodríguez-Hornedo, *Cryst. Growth Des.,* 9, **2009**, 3339. (f) M. L. Cheney, D. R. Weyna, N. Shan, M. Hanna, L. Wojtas and M. J. Zaworotko, *J. Pharm. Sci.*, DOI 10.1002/jps.22434. (g) N. Schultheiss, S. Bethune and J.-O. Henck, *CrystEngComm*, 12, **2010**, 2436. (h) N. Schultheiss and A. Newman, *Cryst. Growth Des.,* 9, **2009**, 2950. (i) C. B. Aakeröy, S. Forbes and J. Desper, *J. Am. Chem. Soc.*, 131, **2009**, 17048. (j) R. D. B. Walsh, M. W. Bradner, S. Fleischman, L. A. Morales, B. Moulton, N. Rodríguez-Hornedo and M. J. Zaworotko, *Chem. Commun.*, **2003**, 186. (k) N. Rodríguez-Hornedo, *Mol. Pharm.*, 4, **2007**, 299. (l) C. Maheshwari, A. Jayasankar, N. A. Khan, G. E. Amidon and N. Rodríguez-Hornedo, *CrystEngComm*, 11, **2009**, 493.

25. (a) P. H. Stahl and C. G. Wermuth (Eds.), *Handbook of Pharmaceutical Salts: Properties, Selection, and Use*; Wiley-VCH, **2002**. (b) S. M. Berge, L. D. Bighley and D. C. Monkhouse, *J. Pharm. Sci.*, 66, **1977**, 1. (c) L. D. Bighley, S. M. Berge and D. C. Monkhouse, *Salt forms of drugs and absorption*, in: J. Swarbrick, J. Boylan (Eds.), *Encyclopaedia of Pharmaceutical Technology*, vol. 13, Dekker, New York, **1996**, p 453–499. (d) A. T. M. Serajuddin, *Adv. Drug Deliv. Rev.*, 59, **2007**, 603. (e) A. V. Trask, D. A. Haynes, W. D. S. Motherwell and W. Jones, *Chem. Commun.*, **2006**, 51. (f) D. A. Haynes, W. Jones and W. D. S. Motherwell, *CrystEngComm*, 7, **2005**, 538. (g) J. F. Remenar, J. M. MacPhee, B. K. Larson, V. A. Tyagi, J. H. Ho, D. A. McIlroy, M. B. Hickey, P. B. Shaw

and Ö. Almarsson, *Org. Proc. Res. Dev.*, 7, **2003**, 990. (h) R. J. Bastin, M. J. Bowker and B. J. Slater, *Org. Proc. Res. Dev.*, 4, **2000**, 427. (i) N. Blagden, M. de Matas, P. T. Gavan and P. York, *Adv. Drug Deliv. Rev.*, 59, **2007**, 617.

26. (a) A. V. Trask, *Mol. Pharm.*, 4, **2007**, 301. (b) M. L. Peterson, M. B. Hickey, M. J. Zaworotko and Ö. Almarsson, *J. Pharm. Pharmaceut. Sci.*, 9, **2006**, 317. (c) F. Lara-Ochoa and G. Espinosa-Pérez, *Cryst. Growth Des.*, 7, **2007**, 1213. (d) M. K. Stanton and A. Bak, *Cryst. Growth Des.*, 8, **2008**, 3856. (e) H. G. Brittain, *J. Pharm. Sci.*, 99, **2010**, 3648; DOI 10.1002/jps.22386.

27. (a) J. F. Willart and M. Descamps, *Mol. Pharm.*, 5, **2008**, 905. (b) H. G. Brittain, *Polymorphism in Pharmaceutical Solids*, 2nd Ed., Inc. New York, **2009**, Chapter 16, p 587–629. (c) J. E. Patterson, M. B. James, A. H. Forster, R. W. Lancaster, J. M. Butler and T. Rades, *Int. J. Pharm.*, 336, **2007**, 22. (d) J. P. Lakshman, Y. Cao, J. Kowalski and A. T. M. Serajuddin, *Mol. Pharm.*, 5, **2008**, 994. (e) Z. Wojnarowska, K. Grzybowska, K. Adrjanowicz, K. Kaminski, M. Paluch, L. Hawelek, R. Wrzalik, M. Dulski, W. Sawicki, J. Mazgalski, A. Tukalska and T. Bieg, *Mol. Pharm.*, 7, **2010**, 1692.

28. (a) W. Kauzmann, *Chem. Rev.*, 43, **1948**, 219. (b) S. F. Swallen, K. L. Kearns, M. K. Mapes, Y. S. Kim, R. J. McMahon, M. D. Ediger, T. Wu, L. Yu and S. Satija, *Science*, 315, **2007**, 353. (c) H. Tanaka, *Physical Rev.*, E68, **2003**, 011505–1.

29. (a) T. G. Fox, *Bull. Am. Phys. Soc. Ser.*, II, 1, **1956**, 123. (b) P. R. Couchman, *Polymer Eng. Sci.*, 24, **1984**, 135. (c) M. Gordon and J. S. Taylor, *J. Appl. Chem.*, 2, **1952**, 493.

30. (a) P. H. Poole, T. Grande, C. A. Angell and P. F. McMillan, *Science*, 275, **1997**, 322. (b) J. Kieffer, *J. Phys. Chem.*, B 103, **1999**, 4153. (c) J. Wiedersich, A. Kudlik, J. Gottwald, G. Benini, I. Roggatz and E. Rössler, *J. Phys. Chem.*, B 101, **1997**, 5800. (d) K. L. Kearns, S. F. Swallen, M. D. Ediger, Y. Sun and L. Yu, *J. Phys. Chem.*, B 113, **2009,** 1579. (e) H. Zhou, H. Dang, J.-H. Yi, A. Nanci, A. Rochefort and J. D. Wuest, *J. Am. Chem. Soc.*, 129, **2007**, 13774. (f) I. Cohen, A.

Ha, X. Zhao, M. Lee, T. Fischer, M. J. Strouse and D. Kivelson, *J. Phys. Chem.* 100, **1996**, 8518.

31. (a) D. Mishima, L. E. Calvert and E. Whalley, *Nature*, 319, **1984**, 393; 314, **1985**, 76. (b) J. P. Johari, A. Hallbrucker and E. Mayer, *Nature*, 330, **1987**, 552.

32. (a) G. L. Amidon, H. Lennernäs, V. P. Shah and J. R. Crison, *Pharm. Res.*, 12, **1995**, 413. (b) A. Dahan, J. M. Miller and G. L. Amidon, *The AAPS Journal*, 11, **2009**, 740. (c) N. A. Kasim, M. Whitehouse, C. Ramachandran, M. Bermejo, H. Lennernäs, A. S. Hussain, H. E. Junginger, S. A. Stavchansky, K. K. Midha, V. P. Shah and G. L. Amidon, *Mol. Pharm.*, 1, **2004**, 85. (d) B. A. Hendriksen, M. V. S. Felix and M. B. Bolger, *AAPS PharmSci.*, 5, **2003**, 1.

33. (a) A. A. Noyes and W. R. Whitney, *J. Am. Chem. Soc.*, 19, **1897**, 930. (b) W. E. Hamlin, J. I. Northam and J. G. Wagner, *J. Pharm. Sci.*, 54 , **1965**, 1651.

34. W. Nernst, *Zeitschrift für Physikalische Chemie*, 47, **1904**, 52.

35. E. Bruner, *Zeitschrift für Physikalische Chemie*, 47, **1904**, 56.

36. (a) V. G. Levich, *Physicochemical Hydrodynamics*, 2nd Ed., Prentice-Hall, Englewood Cliffs, New Jersey, **1962**, p 57–60. (b) D. P. McNamara and G. L. Amidon, *J. Pharm. Sci.*, 75, **1986**, 858. (c) K. G. Nelson and A. C. Shah, *J. Pharm. Sci.*, 76, **1987**, 799.

37. (a) V. G. Levich, *Physicochemical Hydrodynamics*, 2nd Ed., Prentice-Hall, Englewood Cliffs, New Jersey, **1962**, p 61–72. (b) D. J. W. Grant and H. G. Brittain, *Physical Characterization of Pharmaceutical Solids*, H. G. Brittain. (Ed.), Marcel Dekker, Inc, New York, p. 359.

38. (a) P. J. Niebergall, G. Milosovich and J. E. Goyan, *J. Pharm. Sci.*, 52, **1963**, 236. (b) W. I. Higuchi, E. L. Rowe and E. N. Hiestand, *J. Pharm. Sci.*, 52 , **1963**, 162.

CHAPTER TWO

H-SHAPED MOLECULES AND NETWORK SOLIDS

2.1 INTRODUCTION

Molecular materials can be designed and built up from one or several molecules with specific properties to give a bulk solid with desired properties such as magnetism, porosity, catalytic activity, zeolite type activity, etc.[1] In order to achieve some of these properties, there may be a specific three-dimensional arrangement required by the molecular building blocks. To acquire the three-dimensional arrangement the molecule or molecular building blocks use directional intermolecular or coordination bonds. If the pattern extends in all three directions then the final structure is regarded as three-dimensional net. It may be 1D or 2D net depending upon the pattern of hydrogen bond/coordination bond. The crystal engineering approach can be used in the reverse direction to build a specific network topology with definite properties by manipulating molecules and/or functional moiety in the building blocks. The 'network approach' or topological approach to crystal chemistry is an important advancement and a useful tool for the design, comparison and analysis of network structures which simplifies complex architectures to schematized reference nets.[2] Network architectures are common in inorganic structures, minerals, metal–organic compounds and coordination polymers. A. F. Wells through his famous book '*Three Dimensional Nets and Polyhedra*' published in 1977 contributed immensely to the chemistry of network structures and defined some of the networks before they were actually discovered in real structures, most of them are of inorganic origin.[2a] In general, the classification of organic crystal structures as nets is a decade old now.[3] The fact that hydrogen bonds are weaker and less directional than metal–heteroatom and metal–ligand bonds means that the geometry of organic structures is not clearly definable in contrast to coordination compounds and polymers. Even though hydrogen bond directionality has an angular spread, still the organic crystal structures can be topologically classified akin to inorganic and coordination network structures.

For the construction of a network structure, the monomeric units that used are called building blocks or sometimes tectons. Tecton is derived from a Greek word "tekton" meaning "builder" and therefore synonymous to building block. The word tecton was first used in early 1990's and is popular among network solids.[4] The network approach is practically useful in crystal engineering for both design and analysis, and also reduces complicated structures to simple networks. Thus if a relatively small number of 3D nets can be understood, since most of the structures belong to the 10-15 most common nets, it will be easier to rationalize multiple molecular arrangements in the solid state and will help in understanding structural similarity between them. The analysis of nets and the interactions within them provide information that can be utilized in projecting the exact position of molecular building blocks to give the solid compounds with predefined properties.

PROPERTIES AND APPLICATIONS

The properties of a solid are guided by the molecular structure and packing in the solid state. Thus the properties of a molecule can be controlled by manipulating the packing of the molecule through network approach. The intrinsic properties possessed by a 3D network solid are (1) strong interactions in three dimensions, (2) non close-packing structure because the framework is built through coordination bond and thus have potentially large voids and channels, (3) exact positioning of molecules and coordination complexes as building blocks. Network architecture may be used to create multi-component systems with exact ordering, non-centrosymmetric nets with non-linear optical properties,[5] chiral nets to separate enantiomers and enantioselective synthesis and catalysis, to obtain conglomerates (or spontaneous resolution) from racemic mixtures.[6] The inorganic network structures or metal organic frameworks commonly known as MOF have wide applications in – hydrogen gas storage, gas absorption and separation, catalysts for organic and inorganic synthesis, sorption of organic molecules, enantiomeric separation, selective detection of organic and inorganic compounds, targeted drug delivery, etc.[7]

DEFINITIONS OF SOME DESCRIPTORS

Before going into the details of network structure and classification some basic descriptors used in network chemistry are described below.

NODES OR VERTICES AND EDGES

A Network may be represented as a collection of nodes, some of which are connected by links. A 'node' is a molecular or supramolecular point which is connected by lines to construct a network structure. It may be an atom, a molecule, a cluster or a supramolecular entity and the lines that connect the node or vertex is called 'edge' or '–gon'. The network topology is represented by (n,p) which represents a network with n number of '–gons' and 'p' number of nodes or vertices.[2a,b,c]

(a) (4,4)   (b) (6,3)
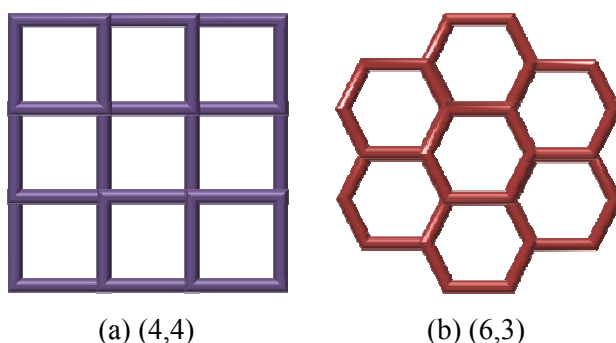
Figure 1 (a) Square grid and (b) Honeycomb net.

HOPF LINK

Hopf link is a two-component link of two unknots that no isotopy can separate, such that there are two non-intersecting spheres that can isolate each component. In mathematical knot theory, the Hopf link is the simplest nontrivial link with more than one component. It consists of two circles linked together exactly once. For a concrete model take the unit circle in the xy-plane centered at the origin and another unit circle in the yz-plane centered at (010). The Hopf link is also referred to as [2]-catenane.[8]

Figure 2 Hopf link

INTERPENETRATION VERSUS POLYCATENATION

"Nature abhors a vacuum" the quote attributed to the Greek philosopher Aristotle is a necessary requirement in crystalline solids. The origin of interpenetration and polycatenation can be ascribed to the presence of large free voids in a single network. However interpenetration does not prevent the possibility of obtaining open porous materials. Interpenetration is a well known phenomenon in the network chemistry of inorganic, organic and mineral world. Wells introduced the theme of interpenetrating net by stating that the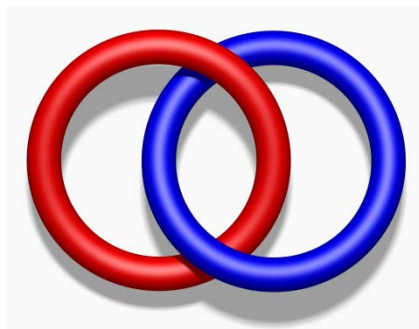y "*cannot be separated without breaking links*".[2a] At that time in 1977 only few examples were available which showed interpenetration mode like – the mineral neptunite, a 2-fold interpenetrating net with the α–ThSi$_2$ topology [10^3–b, ($10_2 \cdot 10_4 \cdot 10_4$)], cuprite Cu$_2$O (one of the first crystal structures determined), some borates and Ice VII, all containing two-fold interpenetrating diamondoid nets.[9] Thereafter numerous structures with interpenetration mode were reported every year[10] from the highly cited paper in *Crystal Growth and Design* journal of 3-fold interpenetrated cocrystals of 1,3,5-Cyclohexanetricarboxylic acid with 4,4'–Bipyridine reported by Nangia[10f] to the world record of 18-fold 2:3 co-crystal of trimesic acid and 1,2-bis(4-pyridyl)ethane by Zaworotko.[10e]

According to Batten and Robson interpenetrating structures are characterized by the presence of infinite structurally regular motifs that must contain rings through which independent components are inextricably entangled and can be disentangled only by

breaking internal connections.[11] Thus they have not differentiated between the interpenetration and polycatenation mode and defined them under the same topology as inclined interpenetration of 1D or 2D nets through one another.

However Carlucci, Ciani and Proserpio[12] differentiated them into two subclasses of 'interpenetration' and 'polycatenation'. They considered that all the constituent motifs in polycatenated structures have lower dimensionality than that of the resulting architecture. The common feature between polycatenated and interpenetrated species is that in both cases the individual motifs cannot be separated "without breaking rings". According to the concepts of chemical topology applied to the study of molecular knots and links (catenanes), both these subclasses give nontrivial entanglements, in the sense that the whole arrays can be considered 'topological isomers' of their component motifs (like an *n*-catenane versus the separated *n* rings). Both the subclasses are differentiated by the features in Table 1.

Table 1 Difference between interpenetration and polycatenation according to Carlucci, Ciani and Proserpio, reference 12a.

Interpenetration	Polycatenation
The component motifs are infinitely extended 2D or 3D nets	The motifs can be 0D and 1D (with closed circuits) or 2D, of the same or of different types
The individual motifs have an identical topology[a]	The resulting entangled array is infinite periodic
The number of the entangled motifs is finite	Finite or infinite number of entangled motifs
The resulting dimensionality is the same as the component motifs	The resulting dimensionality is increased
Each motif is interlaced with all the other ones forming the array	Each motif is never interlaced with all the other ones of the array

[a] This is an arbitrary choice and not a strictly necessary condition. Rare examples are known of interpenetrating 3D nets with different topology.[13]

Some well known interpenetrated and polycatenated networks are shown in Figure 3.

Interpenetration
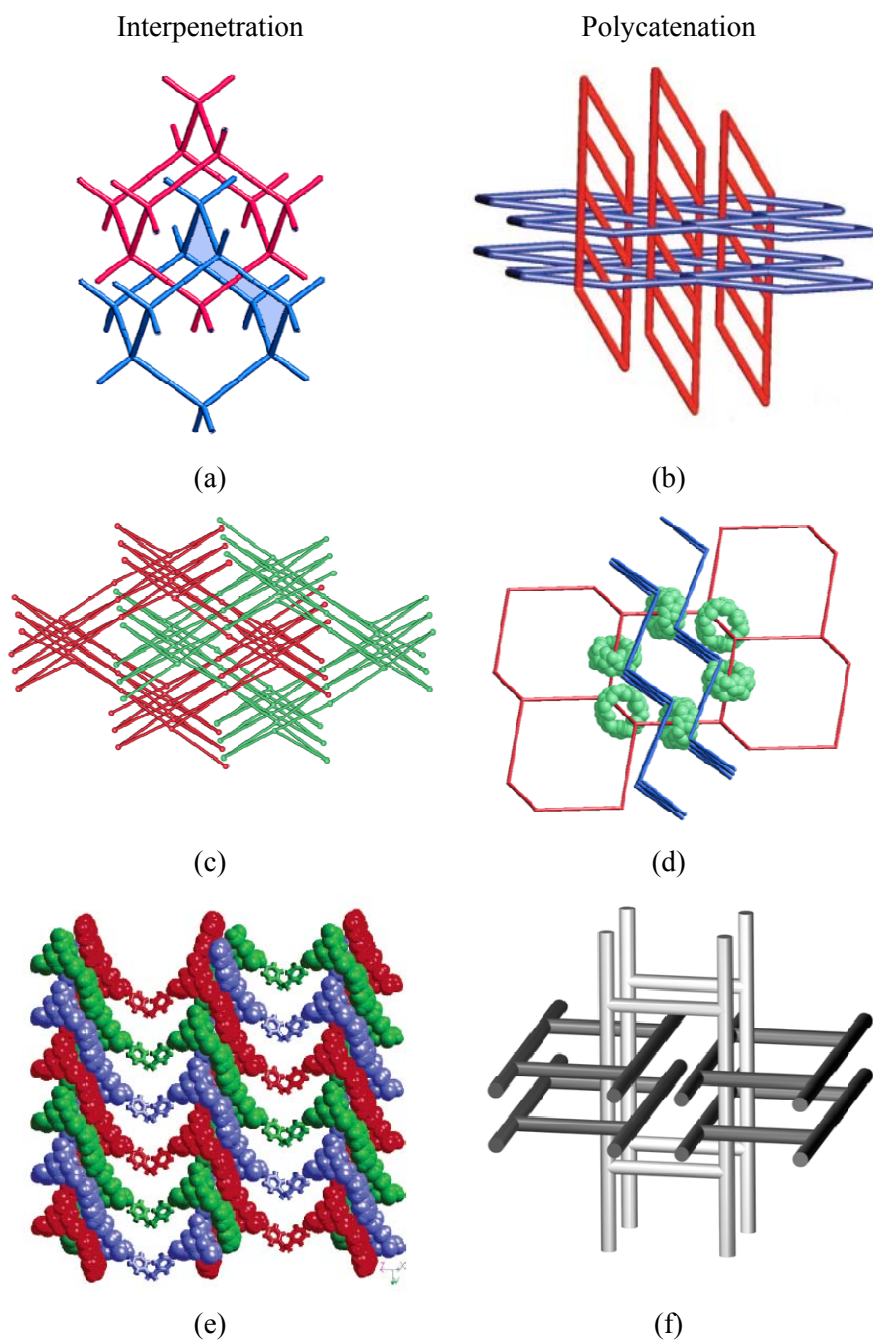
Polycatenation

(a)

(b)

(c)

(d)

(e)

(f)

Figure 3 A few common interpenetration and polycatenation network topology encountered in literature. Figure adapted from *Cryst. Growth Des.*, and *J. Am. Chem. Soc.*, of ACS publication, *Angew. Chem.*, John Wiley & Sons, *J. Solid State Chem.*, Elsevier, *Dalton Trans.*, RSC publication (references 12d, 14a-e).

POLYROTAXANE

Polyrotaxane or polythreading[14d,15] is a special kind of network structure that belongs to the Euclidean network. A rotaxane is a mechanically-interlocked molecular architecture consisting of a "dumbbell shaped molecules" which is threaded through rings or macrocycles. However pseudo-rotaxanes are architectures consisting of rods threaded through rings, thus both of them are closely related to each other and the boundary to differentiate is not well defined. Rotaxane and pseudo-rotaxane are of great importance because of their wide applicability in the design of molecular shuttles, molecular machines, and switches. Polythreading or polyrotaxane can be considered as extended periodic analogue of the molecular rotaxane or pseudo-rotaxane. Polyrotaxane consists of loops and the elements that thread the loops. These two units may belong to the same unit or may be supplied separately by motifs having different structures. The constituent motifs can be, 0D species, 1D polymers or arrays of higher dimensionality. Stang[15b] and Puddephatt[15c] reported same type of polyrotaxane structure of organometallic compounds comprised of 1D chains of alternating rings and rods sustained by concomitant coordination and hydrogen bonds.
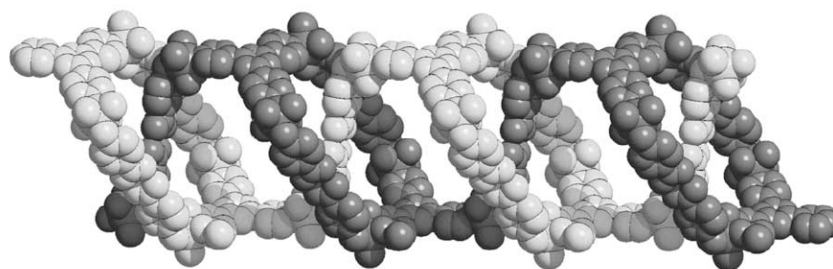
Figure 4 1D Polyrotaxane network. Figure culled from *Chem. Commun.*, RSC publication (reference 15c).

Robson,[15h] Suslick and coworkers[15i] also reported a 1D → 2D polyrotaxane formed by 1D chains of rings and rods shown in Figure 5.

<center>(a)   (b)</center>
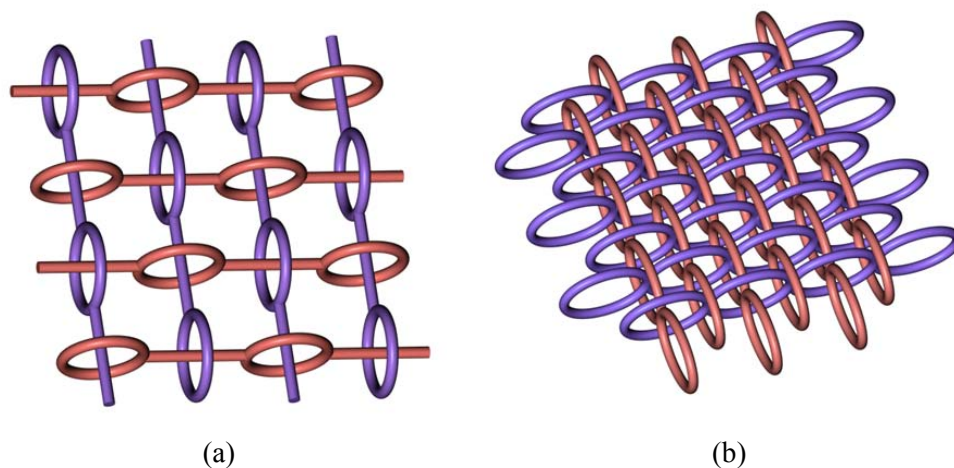
Figure 5 1D → 2D polyrotaxane net. The figures are adapted from *J. Am. Chem. Soc.*, ACS publication and *J. Porph. Phthal.*, Society of Porphyrins & Phthalocyanines (references 15h-i).

POLYKNOTTING (SELF-PENETRATING NETWORKS)

Polyknotting entanglement is a fascinating entanglement also known as self-penetrating network[12a,16] which itself defines the name. It is also known as "intrapenetrating network" or network having trefoil link (Figure 6). In 1989, Dietrich-Buchecker and Sauvage[16c] reported the first case. Batten[10b,16d,e] has also mentioned the structure of Ice IV as an example of self-penetrating net.
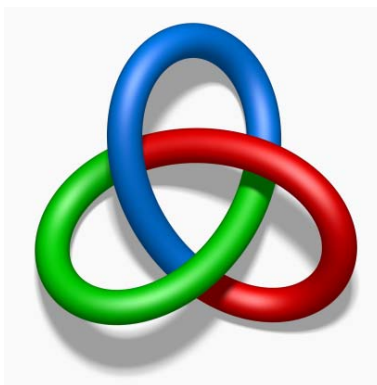
<center>**Figure 6** Trefoil link</center>

BORROMEAN AND TORUS LINK

For a network entanglement the presence of hopf link is not mandatory, one alternative way involving at least three closed circuits at a time is represented by the Borromean links.[17] Borromean link can be defined as a non-trivial link in which three rings are entangled in such a way that any two component rings form a trivial link, i.e. if one ring is cut the other two are free to separate. For example the two isomorphous polymeric silver(I) complexes reported by Chen and coworkers,[17d,12b] namely $[Ag_2(H_2L)_3](NO_3)_2$ and $[Ag_2(H_2L)_3](ClO_4)_2$ [H_2L = N,N'-bis(salicylidene)-1,4-di-aminobutane] form the Borromean network connected through the Borromean links (Figure 7).

(a)   (b)
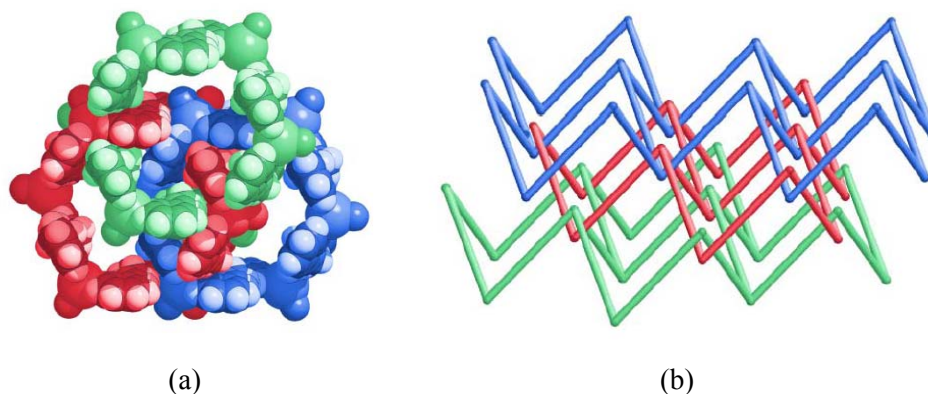
Figure 7 Borromean links of three 6-membered rings of different adjacent layers in $[Ag_2(H_2L)_3](NO_3)_2$. (a) space fill model. (b) Infinite stacking of Borromean links. The diagrams are adapted from *CrystEngComm*, RSC publication (reference 12b).

The Torus link[18] is a non-trivial link of three rings where at least one hopf link will be present and to separate all the three rings two bonds have to be cut (Figure 8b).
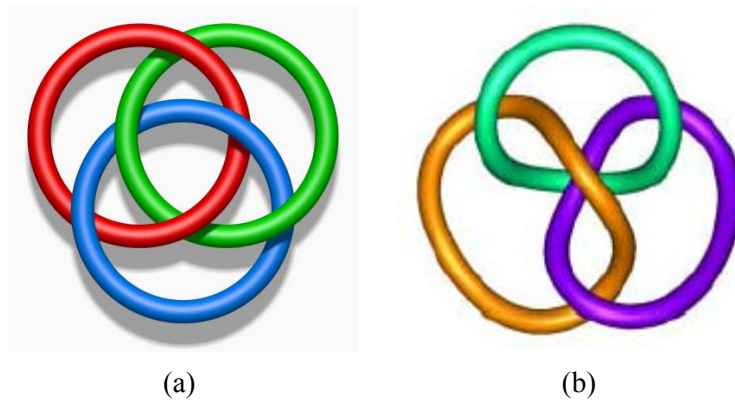
Figure 8 (a) Borromean link. (b) Torus link

CLASSIFICATION OF NETWORK STRUCTURE

Network architecture is divided into two classes;[2a] Uniform net and Non-uniform[3c,f] net. A uniform net can be defined as a network with one type of regular 'polygon', while non-uniform networks consists of shortest circuits of more than one kind of regular 'polygons'. They can be further classified as shown below, adapted from the book *Three-Dimensional Nets and Polyhedra,* published by Wiley (reference 2a).

Uniform (n,p) nets
{
Platonic {
all shortest circuits n-gons
all points p-connected
}
Catalan {
all shortest circuits n-gons
points p-, q-, and so on, connected
}
}

Non-uniform net or Archimedean {
shortest circuits of more than one kind
all points p-connected
}

Some network structures of the above classes are shown in the Figure 9.

(a) Platonic (6,3) (b) Catalan $(5,^3_4)$ (c) Archimedean $(^4_8, 3)$
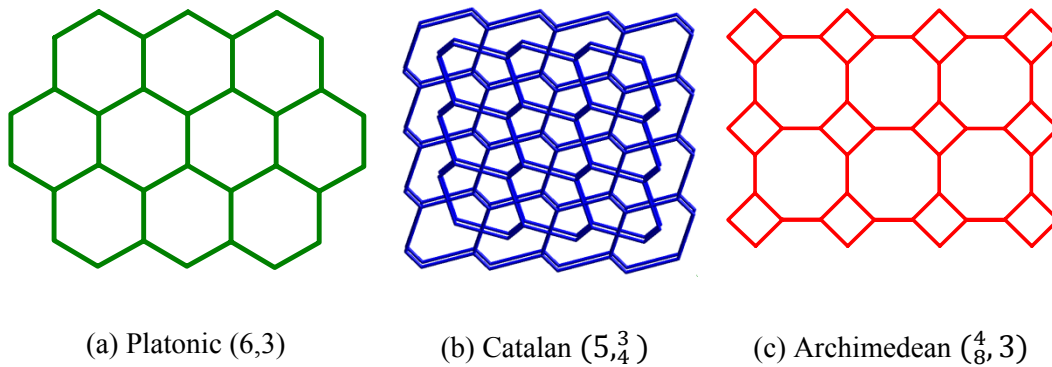
Figure 9 Topological networks of various kind.

NOMENCLATURE

The nomenclature of network architecture is most important in order to classify or describe a net. In order to define a net, two systems of network nomenclature are used, (1) Wellsian nomenclature[2a] and (2) Schläfli symbol.[2b]

In Wellsian nomenclature system generally the network is designated by numbers separated by "comma" in a "small bracket" like (n,p), where 'n' refers to type of polygon and 'p' refers to the nodal type. For example the regular honeycomb net Figure 9a is defined as (6,3) net, a square grid Figure 1(a) as (4,4) net. For Catalan net or Archimedean net, the two different nodes or polygons are written with the "smaller number" above and the "larger number" below in the same position. E.g., The Catalan net in Figure 9b is written as $(5,^3_4)$ and Archimedean net of Figure 9c as $(^4_8, 3)$.

In Schläfli symbol, generally for a regular net the symbol of the vertex figure also serve as the symbol for the tessellation, where the vertex symbol is given by a "regular number" followed by "superfix". The regular number defines the type of "polygon" and the "superfix" the repeating unit. For e.g., (6,3) net can be defined as 6^3, (3,6) net as 3^6 and (4,4) net as 4^4. For semi-regular or other complicated net separating the vertex symbol by "comma" revolving round the whole polygon and each vertex symbol by "·" for different polygons. E.g., $(5,^3_4)$ net is fully described as $[(5^3)^2, 5^4, 5^3, 5^4]$; and $(^4_8, 3)$ net as (4.8^2).

2.2 RESULTS AND DISCUSSION

1,4-Di[bis(4'-hydroxyphenyl)methyl]benzene **A** and its methoxy and methyl derivatives **B–D** were prepared by the acid catalyzed condensation of terephthaldehyde with the requisite phenol (4 equiv).[19] All compounds were purified and characterized by NMR and IR spectra. These molecules may be viewed as having a *p*-substituted phenyl linker that connects bis(hydroxylphenyl)methyl groups on the two sides for directed self-assembly (Figure 10a). The peripheral O atoms that engaged in hydrogen bonding and their connectivity to the carbon core via tetrahedral C atoms are considered to define the H-shape of prototype molecule **A**. The fact that the connecting carbon centers are sp^2 or sp^3 hybridized and has angles that are far from the idealized 180º and 90º is not relevant. The important point is that the mean plane of the phenol O and the *p*-phenyl linker C atoms (marked # in Figure 10b) are nearly coplanar (Figure 10c, deviation from the mean plane < 1 Å) and make an idealized H-shape.

(a)

H-shaped of A-D defined by # atoms

(b)

(c)
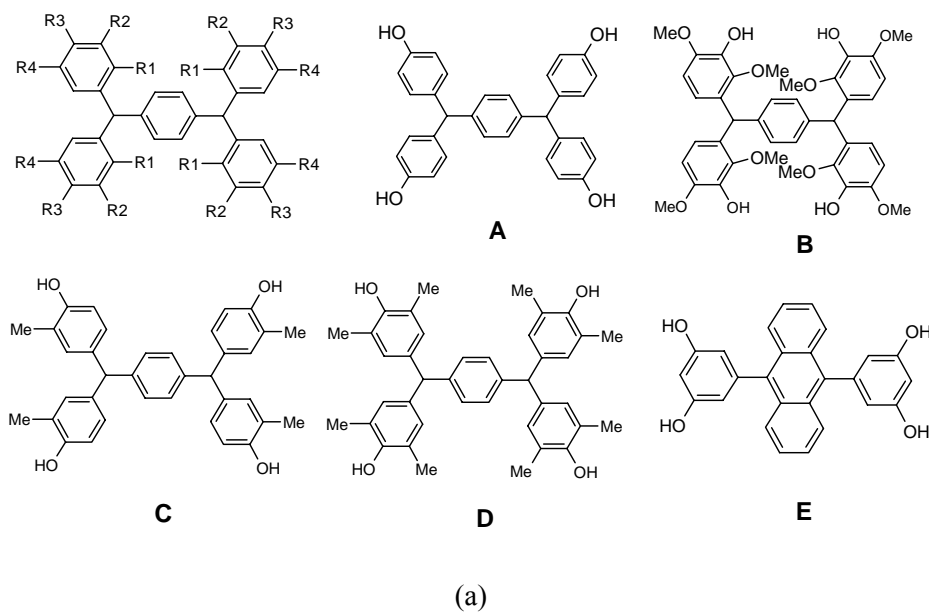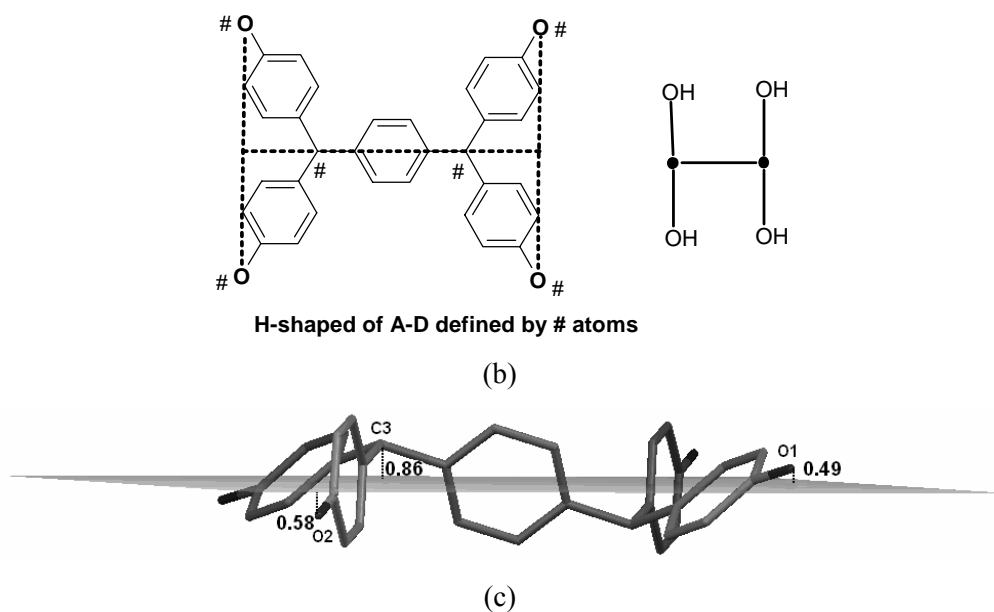
Figure 10 Molecules **A-D** described for network construction in this Chapter. The phenol OH groups are oriented outward to make hydrogen bond networks. (b) The H-shape of molecular core of **A** is realized by connecting the phenol O atoms and the central *p*-phenyl linker C atoms. (c) The # atoms that make up the H-shape are nearly coplanar, deviating from the mean plane by 0.49, 0.58 and 0.86 Å. Molecule **A** is extracted from its MeOH solvate structure (reference 19).

The importance of tetraphenol hosts was emphasized by Aoyama's group as a new class of organic zeolites in inclusion structures of **E** and its derivatives.[20] H-shaped organic molecular tectons are rare, even as there are examples of Y- and T-shaped organic tectons,[1d,12e,21] and L-shaped[22] molecules, and V-shaped[23] molecular tweezers. H-shaped organic pentiptycene functional molecules[24a] and a Mo–Au phosphinidene complex[24b] are known but these structures are not in the host–guest or cocrystals network category. H-shaped tetraphenol host **A** is a new tecton in organic nets reported by Nangia.[19,25] Network diversity in solvates and cocrystals of **A-D** are presented in this Chapter. Network structures are described in the order of 1D ladder[20a,26] to interpenetrated ladders to 2D hexagonal[27] sheets to polycatenated 3D framework to Catalan $(5,\frac{3}{4})$[25] and polyrotaxane nets.

2.3 STRUCTURAL DESCRIPTION AS MOLECULAR NETS

LADDER NETWORK

Crystallization of **A** from EtOAc gave solvated crystal **A**•(EtOAc)$_2$ **2** in space group $P\overline{1}$ with half molecule of **A** in the crystallographic unit due to the imposed inversion symmetry. Host molecules make a 1D ladder network through phenol O–H···O hydrogen bonds (O1–H1···O2 1.78 Å, 165°, Table 2) and EtOAc molecules are connected on the sides (O2–H2A···O4 1.75 Å, 173°). Adjacent layers of host and guest molecules are offset in such a way that the ladder rung region is sandwiched between guest molecules of the next layers. In case of **A**•(DMSO)$_2$ **3** solvate (monoclinic space group $P2_1/c$, half molecule of **A**), solvent molecule acts as a connector to convergently directed OH groups of the host via O–H···O hydrogen bonds (O2–H2A···O3, 1.74 Å, 171°; O1–H1A···O3, 1.69 Å, 172°). The difference in O–H···O bonds between the two solvated structures (Figure 11a and 11b) is attributed to the stronger hydrogen bond acceptor basicity of DMSO compared to EtOAc (pK_{HB} scale: S=O 2.58, C=O 1.00).[28] The pK_{HB} scale ranks acceptor groups according to their basicity strength. Higher the pK_{HB} value, stronger is the acceptor. DMSO acts as a dual acceptor of hydrogen bonds from two host molecules and becomes part of the ladder network whereas EtOAc is a single hydrogen bond acceptor to the host ladder. The i-PrOH solvate **A**•(i-PrOH)$_4$ **4** (pK_{HB} Osp^3 0.82) is similar to the EtOAc structure. However, a difference between EtOAc and i-PrOH solvent molecules is that the former behaved as a terminal acceptor whereas the latter is a connector of host ladder nets via helical O–H···O trimer (Figure 11c). There is a half molecule of **A** and two i-PrOH molecules in asymmetric unit of **A**•(i-PrOH)$_4$ **4**, of which one disordered guest molecule is removed using SQUEEZE program (Experimental Section). Small solvent molecules reside in the ladder rung regions to give a close-packed crystal structure (Figure 11).

(a) (b) (c)

(d) (e) (f)

(g)   (h)
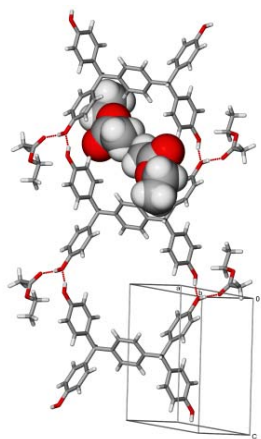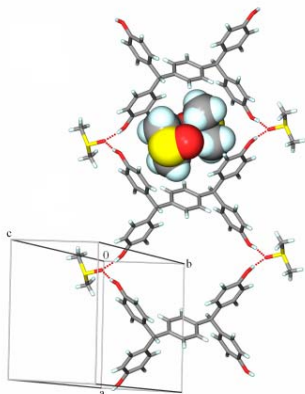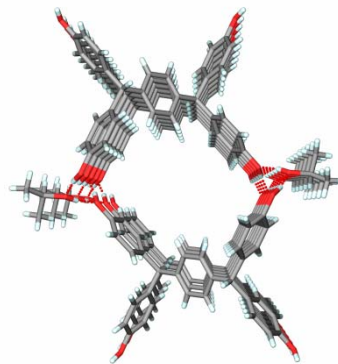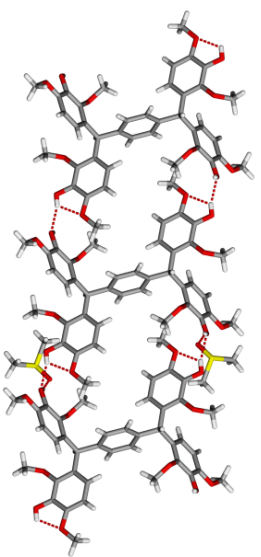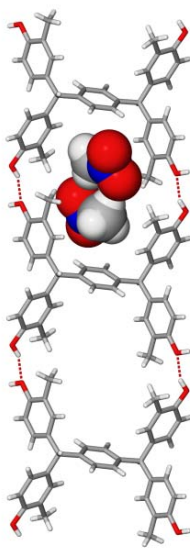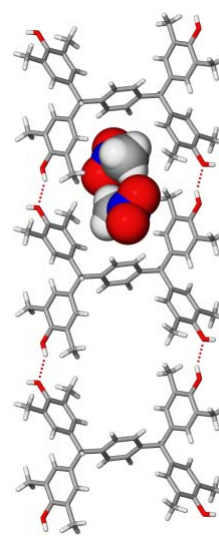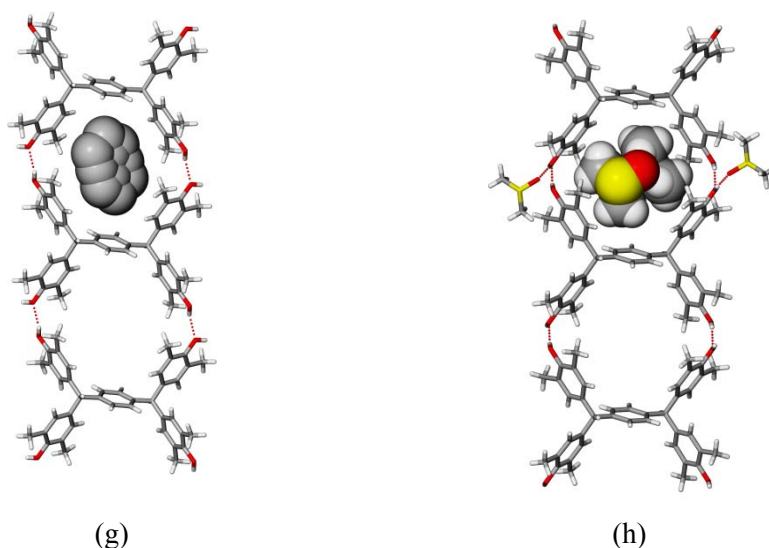
Figure 11 Host Ladder network of **A-D** formed by hydrogen bond between host and the solvent molecule in (a) **A**•(EtOAc)$_2$ **2** along [001] axis. (b) **A**•(DMSO)$_2$ **3** along [100]. (c) **A**•(i-PrOH)$_4$ **4** forming helical O–H···O trimer of host and guest molecules along [010]. (d) **B**•(DMSO)$_2$ **9** where methoxy groups are self-included. (e) **C**•(CH$_3$NO$_2$)$_2$ **12**. (f) **D**•(CH$_3$NO$_2$)$_2$. (g) **D**•(Toluene) **14**. (h) **D**•(DMSO)$_2$ **15**.

A half molecule of **A-D** is present in solvates, cocrystals and guest-free forms that crystallized in space groups with an inversion center, the only exception being **A**•(4,4'-BipyNO)$_2$ **8** cocrystal in space group *Pca*2$_1$. Octamethoxy derivative **B** gives a crystalline solvate **B**•(Dioxane)$_2$ **10** in space group $P\bar{1}$ whose 1D ladder network is structurally similar to **A**•(EtOAc)$_2$ **2**. Adjacent ladders are connected via dioxane (O5–H5···O7 2.06 Å, 138°) to give a 2D sheet structure. A second guest molecule (O8 dioxane) fills the space in the channel framework (Figure 12a). There are two crystallographically distinct solvent molecules, both residing on inversion centers: O7 and O8 dioxane molecules are disordered over two positions, with disorder being modeled in both cases. Compound **C** on crystallization from nitromethane afforded a host ladder network structure **12** (Figure 12b) similar to **D**•(CH$_3$NO$_2$)$_2$ solvate, which extends into a 2D sheet through O–H···O hydrogen bonds. A guest-free form of **D 13** was crystallized from dichloromethane but this crystal structure (Figure 12c) is difficult to classify as a net.

A guest-free form of **A 1** was obtained upon crystallization from CH_3NO_2 in space group $P\bar{1}$ with two half molecules in the asymmetric unit ($Z' = 2$), a situation that arises in crystal structures when the molecule has a packing problem.[21c,29] 1D ladder networks sustained by O–H···O hydrogen bonds (O1–H1A···O3, 1.76 Å, 168°; O2–H2A···O1, 1.82 Å, 167°; O3–H3A···O4, 1.72 Å, 165°) run along [010], and two such networks are inclined at an angle of 73.6° and interpenetrated such that the *p*-phenyl connectors of the second ladder weaved through the rectangular rungs of the first ladder (Figure 12d).

(a)

(b)

(c)

(d)
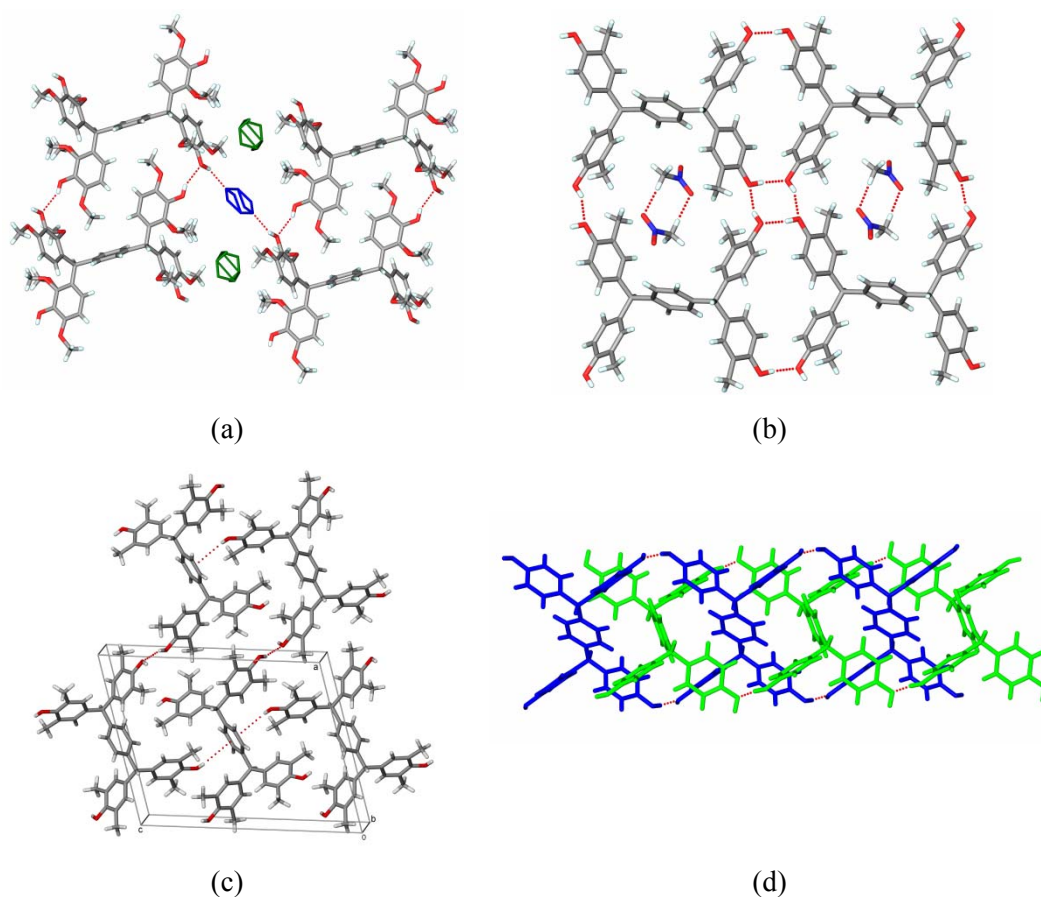
Figure 12 (a) The host ladder network of **B** is connected by dioxane (O7, blue) and filled with a second dioxane molecule in the channels (O8, green) of **B**•(Dioxane)$_2$ **10** solvate. (b) **C**•(CH$_3$NO$_2$)$_2$ **12** shows cooperative O–H···O hydrogen bond tetramer that assembles and connects 1D ladder networks. (c) Close packing of molecules in the crystal structure

of guest-free **D 13**. (d) Double interpenetration of inclined ladders in guest-free form of **A 1**.

Compound **A** and phenazine (Phez) afforded cocrystal **A**•(Phez)$_{1.5}$ **5** with one full and one half molecule of phenazine and two half molecules of **A** in the crystal lattice $P\bar{1}$. One of the host molecules (blue in Figure 13a and 13b) together with a half Phez (green) forms a 2D sheet sustained by O–H⋯O and O–H⋯N hydrogen bonds (O4–H4⋯O3 1.92 Å, 156°; O3–H3A⋯N1 1.99 Å, 165°). The second ladder (red) weaved through the rectangular rung regions of the first ladder, which is part of the 2D sheet, at an inclination of 73° to give a 1D/2D interpenetrated network. The second Phez (light blue) was dangling to the (red) second ladder (O1–H1A⋯O2 1.81 Å, 179°; O2–H2A⋯N1 1.78 Å, 166°) but do not act as a connector.

The crystal structure of **A** with 4,4'-bipyridine,[19] **A**•(4,4'-Bipy)$_2$ make a perfect 1D ladder network (Figure 13c). This structure is compared with 4,4'-bipyridine-*N,N'*-dioxide (4,4'-BipyNO) cocrystal **8** of **A**. Whereas geometrically the co-former is a linear extension in going from pyridine to pyridine-*N*-oxide, the corresponding cocrystal structures are very different. The latter structure is topologically a (6,3) net expanded the ring size by 4,4'-BipyNO and is filled, in part, by self-inclusion of the H-shaped molecule (Figure 13d).

(a)   (b)

(c)   (d)
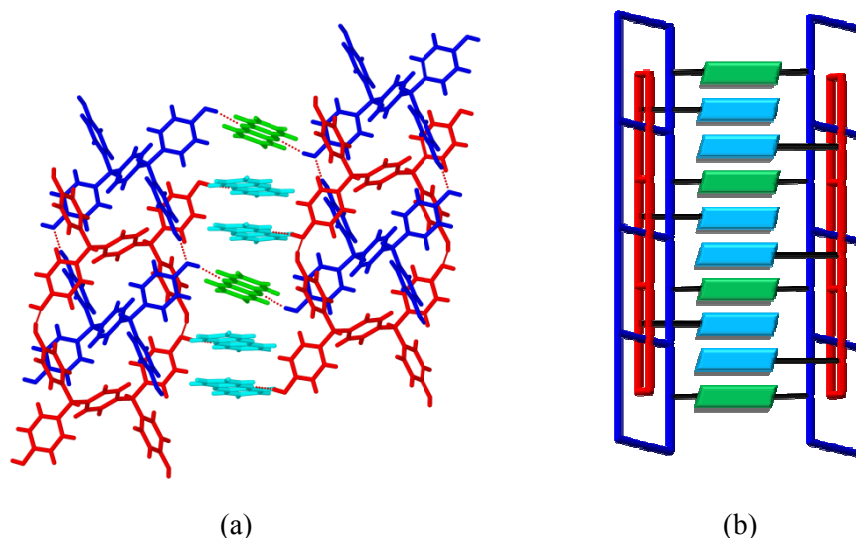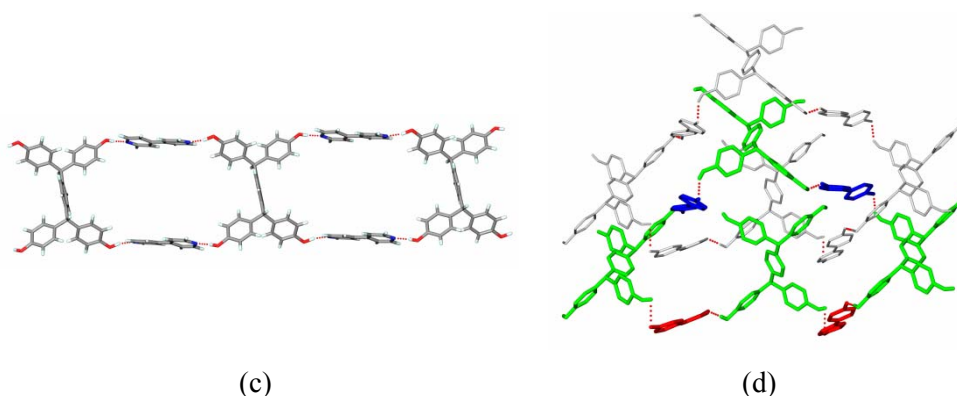
Figure 13 (a) 1D/2D interpenetrated ladder network of **A**•(Phez)$_{1.5}$ cocrystal **5**. (b) Schematic representation of the 1D/2D interpenetrated ladder of **5**. (c) Expanded 1D ladder formed by **A**•(4,4'-Bipy)$_2$ cocrystal. (d) Topological (6,3) net of host molecules self-inclusion in **A**•(4,4'-BipyNO)$_2$ **8** cocrystal.

INTERPENETRATION VS. POLYCATENATION

With DMF solvent, **C** produced a structure having disordered solvent molecules that were removed using the SQUEEZE program (Experimental Section). **C**•(DMF)$_2$ **11** is an example of 2D → 2D interpenetration of (6,3) honeycomb nets. In this structure the host molecule forms a 2D hexagonal net and a second (6,3) net interpenetrated in a parallel fashion (Figure 14) through Hopf links[8,12a] (Figure 2).
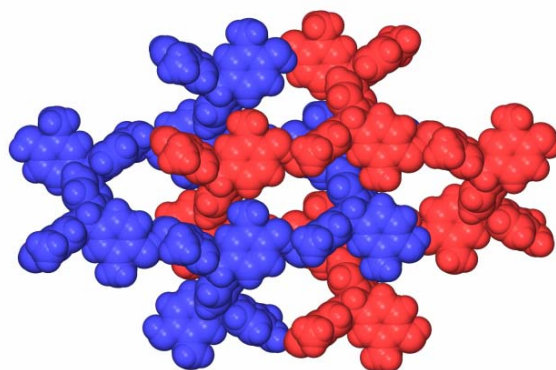
Figure 14 Parallel 2D → 2D 2-fold interpenetration in the crystal structure of **C**•(DMF)$_2$ **11**.

In the cocrystal of **A** with pyrazine-*N*,*N*'-dioxide, **A**•(PyzNO)₂ **7**, the host molecule is hydrogen bonded to the *N*-oxide O acceptor to form a (6,3) network. Due to the tetrahedral angle at the OH donor group and the bent hydrogen bond to PyzNO spacer (O1–H1A···O4 1.72 Å, 161°; O2–H2A···O3 1.78 Å, 170°), the ring size of the (6,3) topological net is actually an expanded 6-membered ring. A single ring of 22.2 × 14.1 × 8.4 Å is occupied by two identical rings to give a 2D → 2D 3-fold interpenetrated network structure (Figure 15) connected by Hopf link.[8,12a]

(a)	(b)
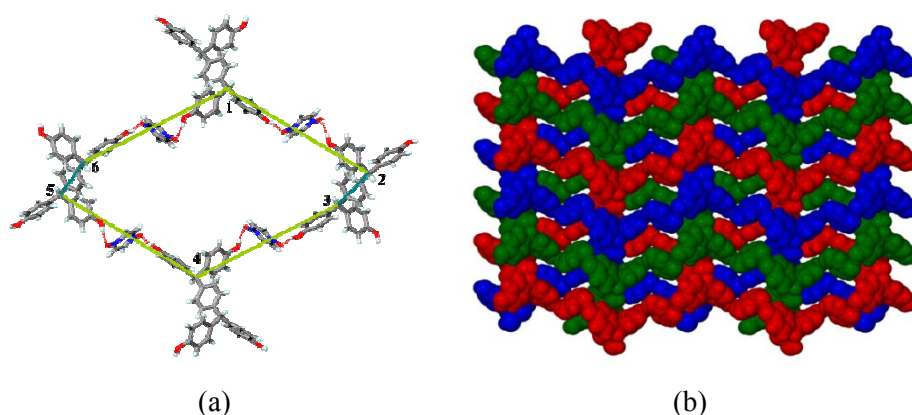
Figure 15 (a) Expanded (6,3) network formed by the host and co-former in **A**•(PyzNO)₂ **7**. (b) 2D → 2D 3-fold interpenetration in **7**.

Crystallization of **A** from CH_3NO_2 with a trace amount of CF_3CH_2OH added (CH_3NO_2 : CF_3CH_2OH ~ 50:1) afforded **A**•(CH_3NO_2)₂ solvate as plate-shaped crystals in space group *Pbca*. Four molecules of **A** are connected via solvent molecules to form an idealized (6,3) net of 18.6 × 13.3 × 10.3 Å cavities. Polycatenation of 2D hexagonal sheets completed the 3D crystal structure (Figure 16). The network in this structure is different from that with PyzNO cocrystal. **A**•(CH_3NO_2)₂ structure is an example of 2D → 3D polycatenation with degree of catenation[12a] (DOC) = 2/2, which means that two layers are catenated within this one hexagonal ring and vice versa. The CH_3NO_2 solvate of **A** is identical to its MeOH and EtOH solvates[19] in terms of stoichiometry, space group, lattice parameters, catenation mode, and the role of solvent as bridge between the host molecules.

(a)   (b)
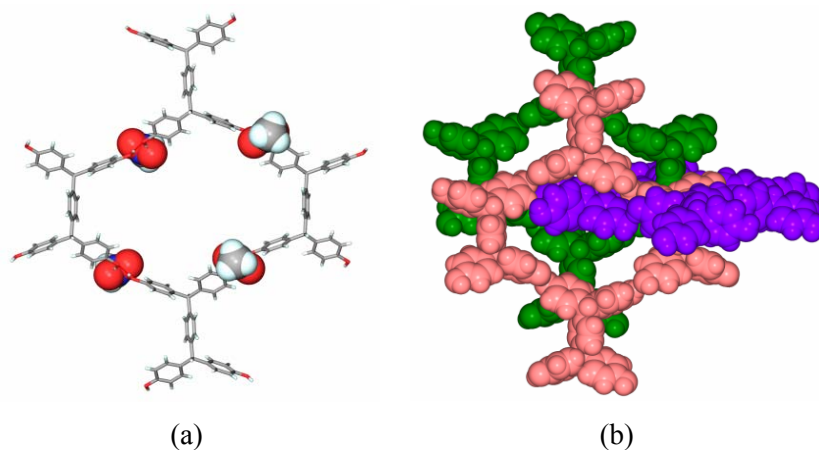
Figure 16 (a) Planar (6,3) honeycomb net formed by four H-shaped molecules with bridged CH_3NO_2 molecules in $A \cdot (CH_3NO_2)_2$ *Pbca* form. (b) 2D → 3D polycatenation with degree of catenation (DOC) = 2/2 to fulfill the 3D structure.

Table 2 Hydrogen bonds in crystal structures of **A-D**.

Compound	Interaction	H···A (Å)	D···A (Å)	D–H···A (º)
A 1	O1–H1A···O3	1.76	2.729(4)	168
	O2–H2A···O1	1.82	2.789(4)	167
	O3–H3A···O4	1.72	2.683(5)	165
	C16–H16···O2	2.45	3.512(5)	167
	C22–H22···O2	2.46	3.389(5)	143
A·(EtOAc)₂ 2	O1–H1···O2	1.78	2.742(1)	165
	O2–H2A···O4	1.75	2.725(1)	173
	C16–H16···O3	2.36	3.426(2)	166
A·(DMSO)₂ 3	O1–H1A···O3	1.69	2.663(3)	172
	O2–H2A···O3	1.74	2.711(3)	171
	C18–H18A···O2	2.32	3.400(6)	173
A·(i-PrOH)₄ 4	O1–H1···O2	1.66	2.629(3)	167
	O2–H2A···O3	1.61	2.588(3)	171
	O3–H3A···O1	1.74	2.715(3)	170
A·(Phez)₁.₅ 5	O1–H1A···O2	1.81	2.791(3)	179
	O2–H2A···N2	1.78	2.739(3)	166
	O3–H3A···N1	1.99	2.950(4)	165
	O4–H4···O3	1.92	2.848(3)	156
	C43–H43···O4	2.33	3.353(7)	157
A·(Quinox)₂ 6	O1–H1A···N1	1.86	2.826(4)	169

	O2–H2A⋯N2	1.84	2.816(4)	173
	C22–H22⋯O2	2.40	3.477(5)	172
A·(PyzNO)$_2$ 7	O1–H1A⋯O4	1.72	2.669(2)	161
	O2–H2A⋯O3	1.78	2.757(3)	170
	C19–H19⋯O2	2.30	3.328(3)	157
	C20–H20⋯O1	2.23	3.283(3)	164
A·(4,4'-BipyNO)$_2$ 8	O1–H1A⋯O5	1.64	2.611(8)	169
	O2–H2A⋯O6	1.64	2.423(11)	133
	O3–H3A⋯O8	1.71	2.682(8)	168
	O4–H4A⋯O7	1.84	2.641(8)	136
	C37–H37⋯O6	2.43	3.513(11)	179
	C52–H52⋯O7	2.41	3.478(11)	168
B·(DMSO)$_2$ 9	O2–H2⋯O5	1.96	2.744(3)	135
	O5–H3⋯O7	1.72	2.653(4)	156
	C6–H6⋯O4	2.36	3.387(4)	157
	C21–H21C⋯O3	2.43	3.355(5)	142
B·(Dioxane)$_2$ 10	O2–H2⋯O5	1.94	2.880(5)	159
	O5–H5⋯O7	2.06	2.867(5)	138
	C19–H19B⋯O1	2.49	3.404(6)	142
	C20–H20B⋯O6	2.49	3.350(6)	135
C·(DMF)$_2$ 11	O1–H1A⋯O2	1.77	2.750(3)	176
	C13–H13⋯O1	2.40	3.365(3)	148
C·(CH$_3$NO$_2$)$_2$ 12	O1–H1A⋯O2	1.75	2.724(3)	171
	O2–H2A⋯O1	1.87	2.789(3)	155
D 13	O1–H1⋯O1	2.33	3.267(3)	158
D·(Toluene) 14	O2–H2⋯O1	2.06	2.935(3)	147
D·(DMSO)$_2$ 15	O1–H1⋯O3	1.80	2.723(5)	155
	O2–H2⋯O1	1.96	2.875(6)	155
	C17–H17A⋯O2	2.40	3.280(7)	137
	C18–H18C⋯O3	2.47	3.233(7)	126
	C22–H22A⋯O3	2.44	3.476(7)	159

CATALAN OR MACMAHON OR $(5,^3_4)$ NETWORK

The use of CH_3NO_2 as the minor component in the solvent mixture (CH_3NO_2: $CF_3CH_2OH \sim 1:6$) gave a solvate polymorph of $A\bullet(CH_3NO_2)_2$ in space group $P2_1/c$ (the other polymorph was solved in *Pbca* space group as mentioned earlier). [25a] The

asymmetric unit contains 0.5 host and 1 guest molecule in both crystal structures. The network in the monoclinic form is best understood by analyzing topologically similar structure of octamethyl derivative **D**•(CHCl$_3$)$_2$ solvate.[25a] Two host molecules are hydrogen bonded by side-on approach via O–H···O tetramer to make pentagons of 5.4 × 5.4 Å voids occupied by the guest species (Fig. 17a). The 2D sheet of pentagonal ($5,^3_4$) nets in (100) plane has four and three connected nodes in 1:2 ratio.[30] This structure and the related **A**•(CH$_3$NO$_2$)$_2$ (Figure 17b) are first examples of organic pentagonal nets. In this pentagonal tiling of ($5,^3_4$) nets (Figure 17c) the sp^3 tetrahedral centers act as 3-connected nodes and the supramolecular 4-connected hydrogen bonded tetramer is auto-generated by joining the 3-connected nodes (Figure 17d). A tetrahedral center can act as a pseudo-trigonal or pseudo-square node[30a] depending on the network topology (Figure 17e). Even though both belong to uniform network topology, hexagonal and ladder nets are under the subclass of platonic net (only one types of n-gons and p-nodes) whereas the **D**•(CHCl$_3$)$_2$ and monoclinic form of **A**•(CH$_3$NO$_2$)$_2$ are uniform network under the subclass of Catalan net (same type of n-gons and two types of nodes, p and q connected).

(a)   (b)

(c)   (d)

(i)   (ii)

(e)
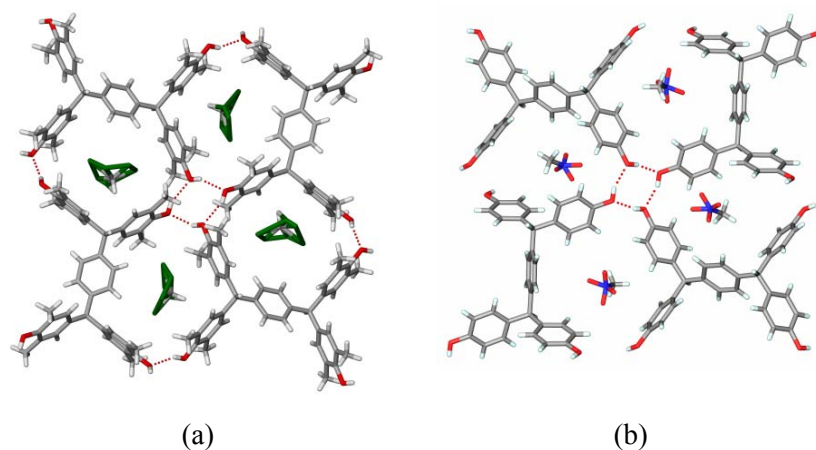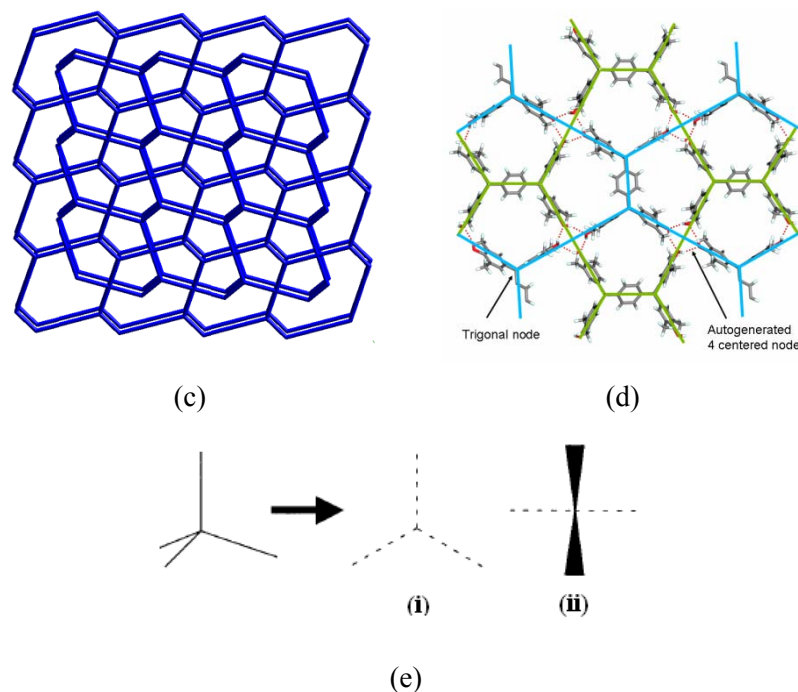
Figure 17 (a) Pentagons of self-assembled **D** are filled with disordered $CHCl_3$ molecules in **D**•$(CHCl_3)_2$ and (b) CH_3NO_2 in the monoclinic form of **A**•$(CH_3NO_2)_2$. (c) Ideal $(5,^3_4)$ or MacMahon or Catalan net. (d) The side-on hydrogen bonding of H-shaped molecules via O–H···O tetramer. Connection of the trigonal carbon centers auto-generates the 4-connected node. (e) Tetrahedral node behaves as 3-connected (i) or 4-connected (ii) node depending on the direction of view along C_3 or C_2 axis.

POLYROTAXANE

Cocrystallization of **A** with quinoxaline afforded single crystals of **A**•$(Quinox)_2$ **6** which solved in monoclinic space group $P2_1/c$ and exhibit a network structure that is of the 1D polyrotaxane or polythreading type.[15] Distinct motifs can be entangled via rotaxane-like mechanical links and this implies the presence of closed loops as well as of connectors that thread through the loops. In contrast to bimolecular rotaxanes in which the loop and thread are made up from different molecules, in **A**•$(Quinox)_2$ **6** the loop and thread belongs to the same binary molecular system (Figure 18). The OH groups at the V-nodes of different H-shaped molecules orient convergently to make a closed loop (ring) with the co-former spacer while the p-substituted benzene ring connects the loops (thread), as

shown in Figure 18b and 18c. This polyrotaxane type of 1D → 1D polythreaded network of alternating rings and rods belongs to the "Euclidean entanglement"[2], i.e. there is no increase in the dimensionality of the network.

(a)

(b)

(c)

(d)
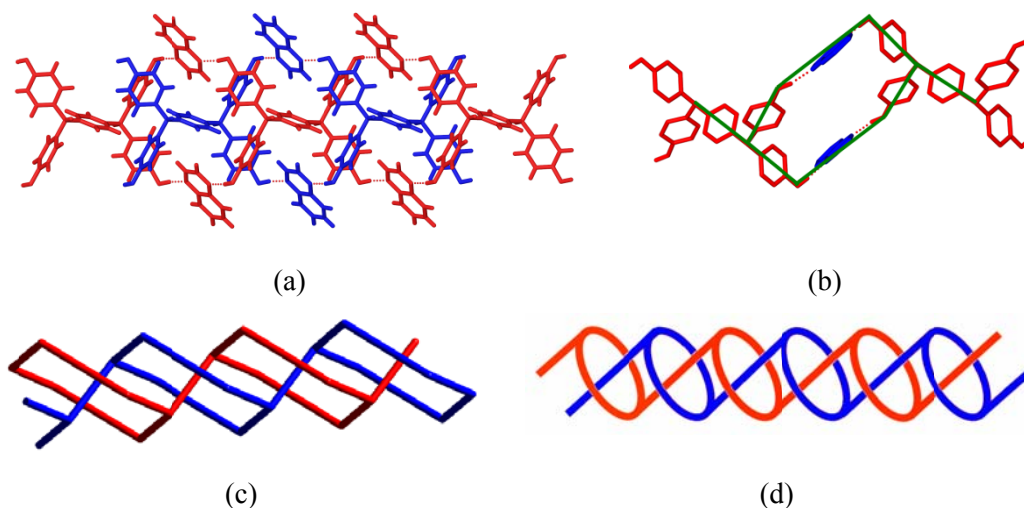
Figure 18 (a) Molecular structure of the polyrotaxane network formed by **A**•(Quinox)$_2$ **6** cocrystal. (b) The V-shaped phenol OHs are inwardly oriented by the aromatic co-former π-stacking to make a ring while the *p*-phenyl connector of **A** is the thread. (c) Skeletal view of the 1D polyrotaxane net. (d) Idealized polyrotaxane.

2.4 NETWORK DIVERSITY AND GUEST INFLUENCE

From the crystal structures of the various host-guest compounds of H-shaped molecule, it can be generalized that solvents having only hydrogen bond acceptor groups such as EtOAc, DMSO, dioxane, CH$_3$CN resulted in a ladder network for **A-D**. The phenol OH groups hydrogen bonded to each other in order to build a 1D ladder and the unused OH of the host molecule is hydrogen bonded to the solvent acceptor, except in DMSO solvate. Because of better acceptor strength of DMSO it behaves as a double hydrogen bond acceptor and is a part of the 1D ladder network. These small solvent molecules reside above and below the rectangular rung regions of host ladders. When bulky methyl or methoxy groups are present (as in **B** and **D**), DMSO solvent could not able to come sufficiently close to the host and accept two hydrogen bonds, perhaps for steric reasons.

Solvents devoid of donor or acceptor groups generally occupied the channel or rung region of host ladder by space filling, e.g., as in D•(Toluene) **14**. The pentagonal Catalan net in **D**•(CHCl$_3$)$_2$ and **D**•(CH$_3$NO$_2$)$_2$ are rare cases[25a] resulted due to the self-assembly of two H-shaped molecules in a side-on manner. Also they are the first example of organic compound apart from few literature reports for metal-organics,[30] metastable form XII and form V of ice.[31] The larger volume of CHCl$_3$ compared to CH$_3$NO$_2$ means that the latter is present as a dimer whereas the former solvent has one molecule in **D** cavity. Small sized solvent molecules, such as MeOH and EtOH, formed 2D hexagonal net of H-shaped phenolic host through hydrogen bonding with the solvent. The close packing of 2D hexagon sheets are achieved through polycatenation or interpenetration.

In case of heteroaromatic cocrystal formers, π-stacking plays an important role. Aromatic stacking is facilitated in larger surface area rings of phenazine and quinoxaline, but not for 4,4'-bipyridine or its *N*-oxide. The ability of extended π-stacking to direct phenol OH groups towards convergent hydrogen bonding with aza heterocycles has been noted in cocrystal systems.[32] π-Stacking of quinoxaline is at longer inter-planar separation than phenazine which resulted in a new kind of polytheading or polyrotaxane network. Usually co-formers with two hydrogen bond acceptor groups, such as 4,4'-bipyridine, acted as spacer to give expanded ladder, e.g., **A**•(4,4'-Bipy)$_2$. However, 4,4'-bipyridine-*N,N'*-dioxide behaved differently to give a distorted 2D net because hydrogen bond donors can approach the stronger N–O acceptor from many directions (in-plane and out-of-plane) whereas donor groups lie mostly in the aromatic plane for pyridyl N acceptor, i.e. co-former functionality directs network variability.

Aoyama's group[20] illustrated organic zeolites constructed from tetraphenol **E**. Similarly the H-shaped molecules also formed large numbers of solvated structures. In host–guest solvates of **A** and D thermo-gravimetric analysis showed the solvent molecules are released at their boiling points or slightly higher temperature (Figure 19). The host is found to be stable up to ~260 °C (Table 3).

(a) DSC of **A** solvates

(b) DSC of **D** solvates

(c) TGA of **A** solvates
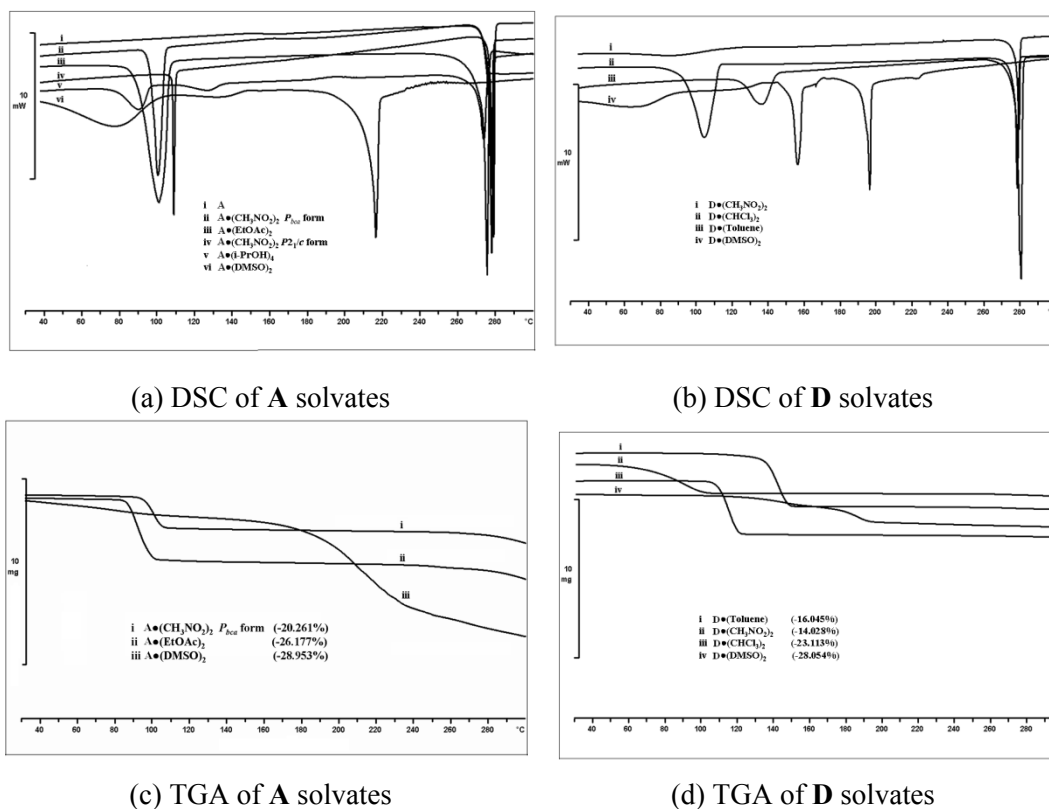
(d) TGA of **D** solvates

Figure 19 DSC and TGA of **A** and **D** solvates.

Table 3 Thermal analysis (TGA and DSC) of inclusion compounds.

Inclusion complex[a]	Observed weight loss from TGA (%)	Calculated weight loss from host-guest ratio in X-ray structure	Guest release T_{on} (°C) (from DSC)	Boiling point of guest (°C)
A•(CH₃NO₂)₂ *Pbca* form	20.3	20.5	96.8	100-103
A•(EtOAc)₂ **2**	26.2	27.1	90.0	77
A•(DMSO)₂ **3**	28.9	24.8	153.7	189
D•(Toluene) **14**	16.1	13.6	125.0	110.6
D•(DMSO)₂ **15**	28.1	21.0	153.1	189
D•(CH₃NO₂)₂	14.0	17.2	60.4	100-103
D•(CHCl₃)₂	23.1	28.9	94.3	61.2

$P2_1/c$ form of A•(CH$_3$NO$_2$)$_2$ and A•(i-PrOH)$_4$ **4** samples could not be generated in sufficient quantity to record TG. They exhibited T$_{on}$ in DSC at 108 °C and 78/ 113 °C, respectively.

2.5 CONCLUSION

Different molecular networks encountered for H-shaped tecton are shown in Figure 20. In metal-organic structures and coordination polymers,[33] network diversity is common but sparse in organic networks before the last one decade. It is clear that conformational flexibility, orientation of OH groups, and solvent hydrogen bonding promoted network diversity of H-shaped tecton. In general, however, prediction of topology and entanglement in organic 2D and 3D network structures is difficult[34] and the most one can say is to rationalize the results after crystal structure determination and analysis.
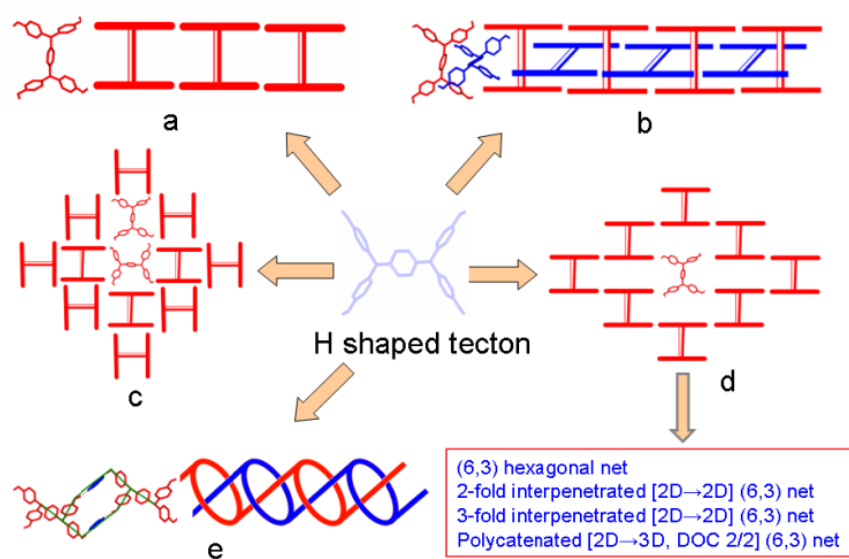
Figure 20 Supramolecular networks in host–guest compounds and cocrystals of H-shaped molecules. (a) 1D ladder, (b) interpenetrated ladders, (c) Catalan or $(5,4^3)$ net, (d) common (6,3) hexagonal or 2D brick wall motif, and (e) polyrotaxane or polythreading.

For different solvates and cocrystals of H-shaped molecule 1D ladder, polyrotaxane, 2D honeycomb and Catalan nets are observed along with various

interpenetration and catenation mode. The most novel and remarkable results are the Catalan $(5,\frac{3}{4})$ net in $\mathbf{D}\bullet(CHCl_3)_2$ and $\mathbf{A}\bullet(CH_3NO_2)_2$, two-component polyrotaxane of $\mathbf{A}\bullet(Quinox)_2$ **6**, 1D/2D interpenetrated ladders in $\mathbf{A}\bullet(Phez)_{1.5}$ **5** cocrystal and 2-fold interpenetration in guest-free form of $\mathbf{A}$ **1**. Network diversity for those multi-component structures is the result of change in guest hydrogen bonding, π-stacking and host molecular conformation. A reason for guest or co-former induced supramolecular diversity is because of the molecular flexibility of H-shaped molecule at three portions – phenol OH group orientation, tetrahedral V-shaped bis(phenol), and *p*-phenyl connector, shown in the overlay diagram of **A** and **D** solvates (Figure 21).

(a)   (b)
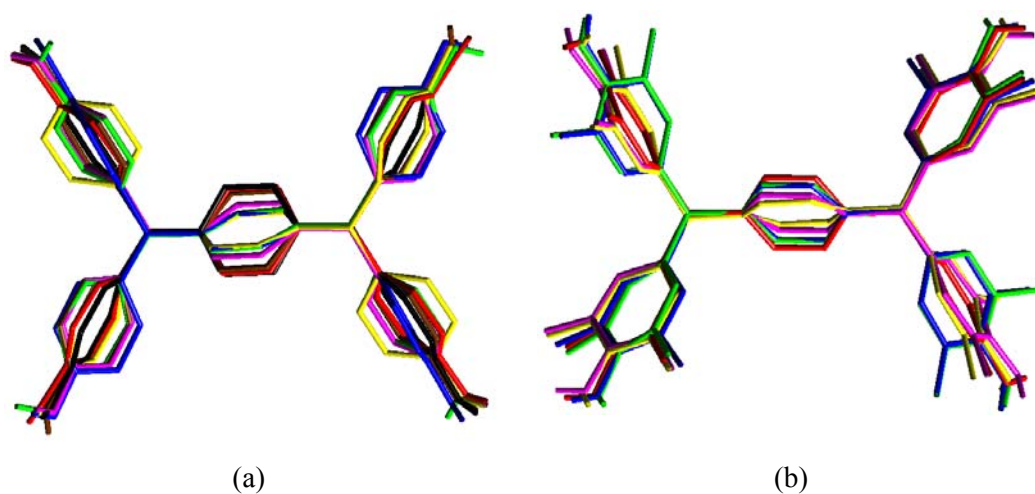
Figure 21 Conformation of H-shaped molecules in crystal structures. (a) guest-free form of **A 1**, molecule A (red) and B (green); CH_3NO_2 solvate, *Pbca* form (blue); CH_3NO_2 solvate, $P2_1/c$ form (magenta); **2** (brown); **3** (yellow); and **4** (black). (b) **D** in guest-free form **13** (green); $CHCl_3$ solvate (red); CH_3NO_2 solvate (blue); **14** (magenta); and **15** (yellow). H atoms of phenol OH only are shown but CH hydrogens are excluded for clarity.

The presence of a second aromatic component gives interplay of hydrogen bonding and π-stacking motifs. The rational construction of novel network architectures from H-shaped molecule should be possible based on a better understanding of network diversity in these structures.

2.6 EXPERIMENTAL SECTION

SYNTHESIS OF HOST MOLECULES

A mixture of terephthaldehyde (500 mg, 3.7 mmol) and phenol (1.8 mL, 14.9 mmol, 4 equiv) in glacial acetic acid (10 mL) was treated dropwise with concentrated HCl (10 mL). The reaction mixture was stirred at room temperature for 24 h, poured onto crushed ice, the precipitate was filtered, and washed with cold water. The dried compound **A** was purified by column chromatography using EtOAc–n-hexane (1:4) to yield 884 mg (50%) of the pure product.

Octamethoxy, tetramethyl and octamethyl derivatives **B**, **C**, **D** were prepared by a similar method using appropriate starting materials.

All compounds were characterized by IR and NMR spectroscopy. NMR spectra were recorded on Bruker Avance spectrometer at 400 MHz and FT-IR spectra were recorded on Jasco 5300 spectrophotometer. NMR chemical shifts on the δ scale (ppm) and J coupling (Hz) are reported. Melting points were recorded on Fisher-Johns apparatus and confirmed by endotherm peak in DSC.

DSC was performed on Mettler Toledo DSC 822e module. Samples were placed in crimped but vented aluminum sample pans. The typical sample size was 3-4 mg, and the temperature range was 30-300 °C at heating rate of 5 °C min^{-1}. Samples were purged by a stream of dry nitrogen flowing at 150 mL min^{-1}. For TGA, the sample size was 7-9 mg, the heating rate was 10 °C min^{-1}, and the N_2 flow was 50 mL min^{-1}.

1,4-di[bis(4′-hydroxyphenyl)methyl]benzene (**A**): IR (KBr, cm^{-1}): 3366, 1599, 1446, 1371, 1224, 760, 636; ^{1}H NMR (δ, DMSO-d$_6$): 5.28 (2H, s, methine CH), 6.64 (8H, d, J=8, Ph CH), 6.85 (8H, d, J=8, Ph CH), 6.97 (4H, s, Ar CH), 9.22 (4H, s, OH). mp 275-278 °C. Yield 50%.

1,4-di[bis(3′-hydroxy, 2′, 4′-dimethoxyphenyl)methyl]benzene (**B**): IR (KBr, cm^{-1}): 3420, 2937, 1616, 1242, 1089, 783, 694; ^{1}H NMR (δ, CDCl$_3$): 3.59 (12H, s, OCH$_3$), 3.84

(12H, s, OCH$_3$), 5.46 (4H, s, OH), 6.06 (2H, s, methine CH), 6.31 (4H, d, J=8, Ph CH), 6.50 (4H, d, J=8, Ph CH), 6.99 (4H, br s, Ar CH). mp 249-251°C. Yield 60%.

1,4-di[bis(4′-hydroxy 3′-methylphenyl)methyl]benzene (**C**): IR (KBr, cm^{-1}): 3468, 2922, 1608, 1454, 1271, 775, 609; ^{1}H NMR (CDCl$_3$, DMSO-d^6): 2.50 (12H, s, CH$_3$), 5.60 (2H, s, methine CH), 7.05 (4H, s, Ar CH), 7.07 (4H, s, Ph CH), 7.18 (4H, s, Ph CH), 7.33 (4H, s, Ph CH), 8.79 (4H, s, OH). mp 254-257 °C. Yield 55%.

1,4-di[bis(4′-hydroxy 3′,5′-dimethylphenyl)methyl]benzene (**D**): IR (KBr, cm^{-1}): 3586, 2918, 1670, 1302, 1147, 760, 694; ^{1}H NMR (CDCl$_3$): 2.17 (24H, s, CH$_3$), 4.48 (4H, s, OH), 5.25 (2H, s, methine CH), 6.70 (8H, s, Ph CH), 6.99 (4H, s, Ar CH). mp 261-264 °C. Yield 60%.

X-RAY CRYSTALLOGRAPHY

Reflections were collected on Bruker SMART CCD diffractometer. Mo-Kα (λ = 0.71073 Å) radiation was used to collect X-ray reflections on all crystals (**A-D**). Data reduction was performed using Bruker SAINT software.[35] Structures were solved and refined using SHELXL-97[36] with anisotropic displacement parameters for non-H atoms. Hydrogen atoms on O were experimentally located in all crystal structures. All C–H atoms were fixed geometrically. A check of the final CIF file using PLATON[37] did not show any missed symmetry. Disordered solvent molecules in **A**•(i-PrOH)$_4$ **4** (one out of two) and **C**•(DMF)$_2$ **11** were removed by SQUEEZE in PLATON. Crystal structures of **A**•(Phez)$_{1.5}$ **5** and **A**•(4,4'-BipyNO)$_2$ **8** could be solved satisfactorily only after fixing hydroxyl H atoms in refinement cycles (HFIX 83 command). Friedel pairs were averaged in case of noncentrosymmetric space group *Pca*2$_1$ for **A**•(4,4'-BipyNO)$_2$ **8** (MERG 4 command). Hydrogens were fixed (HFIX command) and toluene disorder was modelled with isotropic refinement for **D**•(Toluene) **14**. Cif files of all crystal structures contain refinement details under _refine_special_details. Crystallographic parameters for **A-D** structures are summarized in Appendix. Hydrogen bond distances listed in Table 2 are neutron-normalized to fix D–H distance to its accurate neutron value in X-ray crystal

structures (O–H 0.983 Å, N–H 1.009 Å, C–H 1.083 Å). T_{min}, T_{max} values were derived from SHELX based on crystal size since absorption correction was minimal in these light atoms containing crystal structures. Packing diagrams were prepared in X-Seed.[38]

2.7 REFERENCES

1. (a) C. Janiak, *Dalton Trans.*, **2003**, 2781. (b) C. V. K. Sharma and R. D. Rogers, *Materials Today*, 1, **1998**, 27. (c) G. B. Gardner, D. Venkataraman, J. S. Moore and S. Lee, *Nature*, 374, **1995**, 792. (d) J. Lu, A. Mondal, B. Moulton and M. J. Zaworotko, *Angew. Chem. Int. Ed.*, 40, **2001**, 2113. (e) O. M. Yaghi, G. Li and H. Li, *Nature*, 378, **1995**, 703. (f) M. Fujita, Y. J. Kwon, S. Washizu, K. Ogura, *J. Am. Chem. Soc.*, 116, **1994**, 1151. (g) C. C. Stoumpos, R. Inglis, G. Karotsis, L. F. Jones, A. Collins, S. Parsons, C. J. Milios, G. S. Papaefstathiou and E. K. Brechin, *Cryst. Growth Des.*, 9, **2009**, 24. (h) S. R. Batten, *Curr. Opin. Solid State Mater. Sci.*, 5, **2001**, 107.

2. (a) A. F. Wells, *Three-Dimensional Nets and Polyhedra,* Wiley, New York, **1977**. (b) M. O'Keeffe and B. G. Hyde, *Philos. Trans. R. Soc. London, Ser. A,* 295, **1980**, 553. (c) L. Öhrström and K. Larsson, *Molecule-Based Materials*, Elsevier, **2005**. (d) R. Robson, *J. Chem. Soc.*, *Dalton Trans.*, **2000**, 3735. (e) B. Moulton and M. J. Zaworotko, *Chem. Rev.*, 101, **2001**, 1629. (f) G. R. Desiraju, *Chem. Commun.*, **1997**, 1475.

3. (a) S. Basavoju, S. Aitipamula and G. R. Desiraju, *CrystEngComm*, 6, **2004**, 120. (b) B. R. Bhogala, P. Vishweshwar and A. Nangia, *Cryst. Growth Des.*, 5, **2005**, 1271. (c) L. S. Reddy, B. R. Bhogala and A. Nangia, *CrystEngComm*, 7, **2005**, 206. (d) B. K. Saha, S. Aitipamula, R. Banerjee, A. Nangia, R. K. R. Jetti, R. Boese, C.-K. Lam and T. C. W. Mak, *Mol. Cryst. Liq. Cryst.*, 440, **2005**, 295. (e) B. R. Bhogala and A. Nangia, *Cryst. Growth Des.*, 6, **2006**, 32. (f) N. J. Babu and A. Nangia, *Cryst. Growth Des.*, 6, **2006**, 1995. (g) A. Nangia, *Cryst. Growth Des.*, 8, **2008**, 1079.

4. (a) M. Simard, D. Su and J. D. Wuest, *J. Am. Chem. Soc.*, 113, **1991**, 4696. (b) X. Wang, M. Simard and J. D. Wuest, *J. Am. Chem. Soc.*, 116, **1994**, 12119. (c) J.-H. Fournier, T. Maris and J. D. Wuest, *J. Org. Chem.*, 69, **2004**, 1762. (d) J.-H. Fournier, T. Maris, J. D. Wuest, W. Guo and E. Galoppini, *J. Am. Chem. Soc.*, 125, **2003**, 1002. (e) M. W. Hosseini, *Acc. Chem. Res.*, 38, **2005**, 313.

5. (a) O. R. Evans, W. B. Lin, *Acc. Chem. Res.*, 35, **2002**, 511. (b) W. B. Lin, L. Ma and O. R. Evans, *Chem. Commun.*, **2000**, 2263.

6. (*a*) C. J. Kepert, T. J. Prior and M. J. Rosseinsky, *J. Am. Chem. Soc.*, 122, **2000**, 5158. (*b*) D. Bradshaw, J. B. Claridge, E. J. Cussen, T. J. Prior and M. J. Rosseinsky, *Acc. Chem. Res.*, 38, **2005**, 273. (c) J. S. Seo, D. Whang, H. Lee, S. I. Jun, J. Oh, Y. J. Jeon and K. Kim, *Nature*, 404**, 2000**, 982.

7. (a) S. L. James, *Chem. Soc. Rev.*, 32, **2003**, 276. (b) N. L. Rosi, M. Eddaoudi, J. Kim, M. O'Keeffe and O. M. Yaghi, *Angew. Chem. Int. Ed.*, 41, **2002**, 284. (c) C. N. R. Rao, S. Natarajan, A. Choudhury, S. Neeraj and A. A. Ayi, *Acc. Chem. Res.*, 34, **2001**, 80. (d) P. Ryan, L. J. Broadbelt and R. Q. Snurr, *Chem. Commun.*, **2008**, 4132. (e) D. Braga, L. Brammer and N. R. Champness, *CrystEngComm*, 7, **2005**, 1.

8. (a) J. P. Sauvage, *Acc. Chem. Res.*, 31, **1998**, 611. (b) S. S.-Y. Chui, R. Chen and C.-M. Che, *Angew. Chem. Int. Ed.*, 45, **2006**, 1621. (c) S. T. Caldwell, G. Cooke, B. Fitzpatrick, D.-L. Long, G. Rabania and V. M. Rotello, *Chem. Commun.*, **2008**, 5912. (d) J.-Q. Liu, Y.-Y. Wang, L.-F. Ma, G.-L. Wen, Q.-Z. Shi, S. R. Batten and D. M. Proserpio, *CrystEngComm*, 10, **2008**, 1123.

9. (a) E. Cannillo, F. Mazzi and G. Rossi, *Acta Cryst.*, 21, **1966**, 200. (b) D. E. Palin and H. M. Powell, *J. Chem. Soc.*, **1947**, 208. (c) H. M. Powell, *J. Chem. Soc.*, **1950**, 300.

10. (a) L. Carlucci, G. Ciani, D. M. Proserpio and A. Sironi, *J. Am. Chem. Soc.*, 117, **1995**, 4562. (b) S. R. Batten, *CrystEngComm*, 18, **2001**, 1. (c) L. Carlucci, G. Ciani, D. M. Proserpio and S. Rizzato, *CrystEngComm*, 4, **2002**, 413. (d) B. R. Bhogala, P. K. Thallapally and A. Nangia, *Cryst. Growth Des.*, 4, **2004**, 215. (e)

T. R. Shattock, P. Vishweshwar, Z. Wang and M. J. Zaworotko, *Cryst. Growth Des.*, 5, **2005**, 2046. (f) B. R. Bhogala and A. Nangia, *Cryst. Growth Des.*, 3, **2003**, 547. (g) M. R. Montney, R. M. Supkowski and R. L. LaDuca, *CrystEngComm*, 10, **2008**, 111.

11. (a) S. R. Batten and R. Robson, *Angew. Chem. Int. Ed.*, 37, **1998**, 1460. (b) S. R. Batten, B. F. Hoskins, B. Moubaraki, K. S. Murray and R. Robson, *Chem. Commun.*, **2000**, 1095. (c) J.-Q. Liu, Y.-Y. Wang, P. Liu, Z. Dong, Q.-Z. Shia and S. R. Batten, *CrystEngComm*, 11, **2009**, 1207. (d) H. Guo, D. Qiu, X. Guo, S. R. Batten and H. Zhang, *CrystEngComm*, 11, **2009**, 2611. (e) S. R. Batten, *J. Solid State Chem.*, 178, **2005**, 2475.

12. (a) L. Carlucci, G. Ciani and D. M. Proserpio, *Coord. Chem. Rev.*, 246, **2003**, 247. (b) L. Carlucci, G. Ciani and D. M. Proserpio, *CrystEngComm*, 5, **2003**, 269. (c) L. Carlucci, G. Ciani and D. M. Proserpio, *Chem. Commun.*, **2004**, 380. (d) L. Carlucci, G. Ciani, S. Maggini and D. M. Proserpio, *Cryst. Growth Des.*, 8, **2008**, 162. (e) I. A. Baburin, V. A. Blatov, L. Carlucci, G. Ciani and D. M. Proserpio, *Cryst. Growth Des.*, 8, **2008**, 519.

13. A. W. Sleight and R. J. Bouchard, *Inorg. Chem.*, 12, **1973**, 2314.

14. Interpenetration e.g. (a) K. Liang, H. Zheng, Y. Song, M. F. Lappert, Y. Li, X. Xin, Z. Huang, J. Chen and S. Lu, *Angew. Chem. Int. Ed.*, 43, **2004**, 5776. (b) I. A. Baburin, V. A. Blatova, L. Carlucci, G. Ciani and D. M. Proserpio, *J. Solid State Chem.*, 178, **2005**, 2452. (c) B. R. Bhogala, S. Basavoju and A. Nangia, *Cryst. Growth Des.*, 5, **2005**, 1683.
Polycatenation e.g. (d) D. Whang and K. Kim, *J. Am. Chem. Soc.*, 119, **1997**, 451. (e) L. Carlucci, G. Ciani and D. M. Proserpio, *Dalton Trans.*, **1999**, 1799. (f) X.-Q. Yao, D.-P. Cao, J.-S. Hu, Y.-Z. Li, Z.-J. Guo and H.-G. Zheng, *Cryst. Growth Des.*, 11, **2011**, 231.

15. (a) D. Whang, J. Heo, C.-A. Kim and K. Kim, *Chem. Commun.*, **1997**, 2361. (b) C. J. Kuehl, F. M. Tabellion, A. M. Arif and P. J. Stang, *Organomet.*, 20, **2001**, 1956. (c) C. S. A. Fraser, M. C. Jennings and R. J. Puddephatt, *Chem. Commun.*,

2001, 1310. (d) L. Carlucci, G. Ciani and D. M. Proserpio, *Cryst. Growth Des.*, 5, **2005**, 37. (e) K. K. Arora and V. R. Pedireddi, *Cryst. Growth Des.*, 5, **2005**, 1309. (f) A. A. Salaudeen, C. A. Kilner and M. A. Halcrow, *Chem. Commun.*, **2008**, 5200. (g) X.-Y. Cao, Q.-P. Lin, Y.Y. Qin, J. Zhang, Z.-J. Li, J.-K. Cheng and Y.-G. Yao, *Cryst. Growth Des.*, 9, **2009**, 20. (h) B. F. Hoskins, R. Robson, D. A. Slizys, *J. Am. Chem. Soc.*, 119, **1997**, 2952. (i) M. E. Kosal, J.-H. Chou, K. S. Suslick, *J. Porph. Phthal.*, 6, **2002**, 377.

16. (a) X.-L. Wang, C. Qin, E.-B. Wang, Y.-G. Li, Z.-M. Su, L. Xu and L. Carlucci, *Angew. Chem. Int. Ed.*, 44, **2005**, 5824. (b) M. A. Withersby, A. J. Blake, N. R. Champness, P. A. Cooke, P. Hubberstey and M. Schröder, *J. Am. Chem. Soc.*, 122, **2000**, 4044. (c) C. O. Dietrich-Buchecker and J.-P. Sauvage, *Angew. Chem. Int. Ed.*, 28, **1989**, 189. (d) M.-L. Tong, X.-M. Chen and S. R. Batten, *J. Am. Chem. Soc.*, 125, **2003**, 16170. (e) X.-L. Wang, C. Qin, E.-B. Wang, Z.-M. Su, L. Xu and S. R. Batten, *Chem. Commun.*, **2005**, 4789.

17. (a) K. S. Chichak, S. J. Cantrill, A. R. Pease, S.-H. Chiu, G. W. V. Cave, J. L. Atwood, J. F. Stoddart, *Science*, 304, **2004**, 1308. (b) S. J. Cantrill, K. S. Chichak, A. J. Peters and J. F. Stoddart, *Acc. Chem. Res.*, 38, **2004**, 2. (c) R. Liantonio, P. Metrangolo, F. Meyer, T. Pilati, W. Navarrini and G. Resnati, *Chem. Commun.*, **2006**, 1819. (d) M. L. Tong, X.-M. Chen, B.-H. Ye and L.-N. Ji, *Angew. Chem. Int. Ed.*, 38, **1999**, 2237.

18. Y. Ling, L. Zhang, J. Li and A. X. Hu, *Cryst. Growth Des.*, 9, **2009**, 2043.

19. S. Aitipamula and A. Nangia, *Supramol. Chem.*, 17, **2005**, 17.

20. (a) K. Endo, T. Sawaki, M. Koyanagi, K. Kobayashi, H. Masuda and Y. Aoyama, *J. Am. Chem. Soc.*, 117, **1995**, 8341. (b) T. Tanaka, T. Tasaki and Y. Aoyama, *J. Am. Chem. Soc.*, 124, **2002**, 12453. (c) K. Endo, T. Koike, T. Sawaki, O. Hayashida, H. Masuda and Y. Aoyama, *J. Am. Chem. Soc.*, 119, **1997**, 4117. (d) Y. Aoyama, K. Endo, T. Anzai, Y. Yamaguchi, T. Sawaki, K. Kobayashi, N. Kanehisa, H. Hashimoto, Y. Kai and H. Masuda, *J. Am. Chem. Soc.*, 118, **1996**, 5562. (e) K. Tanaka, K. Endo, Y. Aoyama, *Chem. Lett.*, **1999**, 887. (f) Y.

Aoyama, K. Endo, K. Kobayashi and H. Masuda, *Supramol. Chem.*, 4, **1995**, 229.

21. (a) N. Malek, T. Maris, M.-È. Perron and J. D. Wuest, *Angew. Chem. Int. Ed.*, 44, **2005**, 4021. (b) R. Bishop, *Acc. Chem. Res.*, 42, **2009**, 67. (c) S. Aitipamula and A. Nangia, *Chem.-Eur. J.*, 11, **2005**, 6727. (d) V. S. S. Kumar, A. Nangia, M. T. Kirchner and R. Boese, *New J. Chem.*, 27, **2003**, 224.

22. G. R. Swiegers and T. J. Malefetse, *Chem. Rev.*, 100, **2000**, 3483.

23. (a) P. Grosshans, A. Jouaiti, N. Kardouh, M. W. Hosseini and N. Kyritsakas, *New J. Chem.*, 27, **2003**, 1806. (b) F. G. Klärner and B. Kahlert, *Acc. Chem. Res.*, 36, **2003**, 919. (c) M. Harmata, *Acc. Chem. Res.*, 37, **2004**, 862. (d) A. Sygula, F. R. Fronczek, R. Sygula, P. W. Rabideau and M. M. Olmstead, *J. Am. Chem. Soc.*, 129, **2007**, 3842.

24. (a) J.-S. Yang and J.-L. Yanb, *Chem. Commun.*, **2008**, 1501. (b) M. A. Alvarez, I. Amor, M. E. García and M. A. Ruiz, *Inorg. Chem.*, 47, **2008**, 7963.

25. (a) R. Thakuria, B. Sarma and A. Nangia, *Cryst. Growth Des.*, 8, **2008**, 1471. (b) R. Thakuria, B. Sarma and A. Nangia, *New J. Chem.*, 34, **2010**, 623.

26. (a) V. T. Nguyen, P. D. Ahn, R. Bishop, M. L. Scudder and D. C. Craig, *Eur. J. Org. Chem.*, 2001, **2001**, 4489. (b) X.-Q. Lu, M. Pan, J.-R. He, Y.-P. Cai, B.-S. Kanga and C.-Y. Su, *CrystEngComm*, 8, **2006**, 827. (c) V. S. S. Kumar, F. C. Pigge and N. P. Rath, *New J. Chem.*, 27, **2003**, 1554. (d) A. D. Bond, *Chem.-Eur. J.*, 10, **2004**, 1885.

27. (a) B. K. Saha, R. K. R. Jetti, L. S. Reddy, S. Aitipamula and A. Nangia, *Cryst. Growth. Des.*, 5, **2005**, 887. (b) B. R. Bhogala and A. Nangia, *New J. Chem.*, 32, **2008**, 800.

28. C. Laurence and M. Berthelot, *Persp. Drug Dis. Des.*, 18, **2000**, 39.

29. (a) B. Sarma, S. Roy and A. Nangia, *Chem. Commun.*, **2006**, 4918. (b) S. Aitipamula, G. R. Desiraju, M. Jaskólski, A. Nangia and R. Thaimattam, *CrystEngComm*, 5, **2003**, 447. (c) H.-J. Lehmler, L. W. Robertson, S. Parkin and

C. P. Brock, *Acta Cryst.*, B58, **2002**, 140. (d) C. P. Brock, *Acta Cryst.*, B58, **2002**, 1025.

30. (a) B. Moulton, J. Lu and M. J. Zaworotko, *J. Am. Chem. Soc.*, 123, **2001**, 9224. (b) S. W. Keller and S. Lopez, *J. Am. Chem. Soc.*, 121, **1999**, 6306. (c) X.-Q. Liang, X.-H. Zhou, C. Chen, H.-P. Xiao, Y.-Z. Li, J.-L. Zuo and X.-Z. You, *Cryst. Growth Des.*, 9, **2009**, 1041.

31. M. O'Keeffe, *Nature*, 392, **1998**, 879.

32. (a) B. Sarma, L. S. Reddy and A. Nangia, *Cryst. Growth Des.*, 8, **2008**, 4546. (b) L. R. MacGillivray, J. L. Reid and J. A. Ripmeester, *J. Am. Chem. Soc.*, 122, **2000**, 7817. (c) T. Friščić, L. R. MacGillivray, *Chem. Commun.*, **2005**, 5748. (d) G. S. Papaefstathiou, Z. Zhong, L. Geng and L. R. MacGillivray, *J. Am. Chem. Soc.*, 126, **2004**, 9158. (e) L. R. MacGillivray, G. S. Papaefstathiou, T. Frišičič, T. D. Hamilton, D.-K. Bučar, Q. Chu, D. B. Varshney and I. G. Georgiev, *Acc. Chem. Res.*, 41, **2008**, 280.

33. (a) A. J. Blake, N. R. Champness, P. Hubberstey, W.-S. Li, M. A. Withersby and M. Schröder, *Coord. Chem. Rev.*, 183, **1999**, 117. (b) L. Carlucci, G. Ciani, D. M. Proserpio and S. Rizzato, *J. Solid State Chem.*, 152, **2000**, 211. (c) D. K. Kumar, D. A. Jose, A. Das and P. Dastidar, *Inorg. Chem.*, 44, **2005**, 6933. (d) M. R. Montney, S. M. Krishnan, N. M. Patel, R. M. Supkowski and R. L. LaDuca, *Cryst. Growth Des.*, 7, **2007**, 1145. (e) Z. Su, J. Xu, J. Fan, D.-J. Liu, Q. Chu, M.-S. Chen, S.-S. Chen, G.-X. Liu, X.-F. Wang and W.-Y. Sun, *Cryst. Growth Des.*, 9, **2009**, 2801.

34. Y.-B. Men, J. Sun, Z.-T. Huang and Q.-Y. Zheng, *Angew. Chem. Int. Ed.*, 48, **2009**, 2873.

35. *SADABS, Program for Empirical Absorption Correction of Area Detector Data*, G. M. Sheldrick, University of Göttingen, Germany, **1997**.

36. *SHELXS-97 and SHELXL-97, Programs for the Solution and Refinement of Crystal Structures*, G. M. Sheldrick, University of Göttingen, Germany, **1997**.

37. (a) *PLATON*, *A Multipurpose Crystallographic Tool*, Spek, A. L. Utrecht University, Utrecht, Netherland, **2002**. (b) A. L. Spek, *J. Appl. Cryst.*, 36, **2003**, 7.

38. *X-Seed, Graphical Interface to SHELX-97 and POVRay*, L. J. Barbour, University of Missouri-Columbia, Columbia, MO, **1999**.

CHAPTER THREE

COCRYSTALS OF PYROGALLOL AND CATECHOL WITH N-
HETEROCYCLE BASES

3.1 INTRODUCTION

Hydrogen bond and supramolecular synthons are the first step towards crystal enginnering.[1] If the molecules are considered as the bricks for making a supramolecule then hydrogen bond and supramolecular synthons are the cementing materials. Therefore before going into the details of supramolecular assembly it is necessary to be familiarized with *hydrogen bond* and *supramolecular synthon*. Pauling defined hydrogen bond as "*under certain conditions an atom of hydrogen is attracted by rather strong forces to two atoms, instead of only one, so that it may be considered to be acting as a bond between them*".[2] Typically for strong interactions like N–H···O, O–H···O, O–H···X⁻, F–H···F⁻ there is no problem because they are very strong, linear, energetically favorable and spectroscopically identifiable. But this definition did not fit for the weaker interactions like C–H···O, C–H···N, O–H···π, N–H···π and C–H···π interactions which are difficult for analysis crystallographically, spectroscopically or computationally. From then several definitions have been proposed. Prominent among them were by Pimentel and McClellan,[3a] later by Jeffrey and Saenger[3b,c] and then in 1993 by Steiner[3d] and Saenger.[3e] Recently in 2005 the IUPAC core group have stated that "*a typical hydrogen bond may be depicted as X–H···Y–Z, where the three dots denote the bond. X–H represents the hydrogen-bond donor. The acceptor may be an atom or an anion Y, or a fragment or a molecule Y–Z, where Y is bonded to Z. In specific cases X and Y can be the same with both X–H and Y–H bonds being equal. In any event, the acceptor is an electron-rich region such as, but not limited to, a lone pair in Y or a π-bonded pair in Y–Z*".[4] When hydrogen bond forms between the molecular functionalities the supramolecular synthon comes into play. Desiraju defined supramolecular synthon as "*structural units within supermolecules which can be formed and/ or assembled by known or conceivable*

synthetic operations involving intermolecular interactions".[5] The situation is very simple for a homomeric crystal or heteromeric cocrystal with only one or two functionalities, but it becomes complicated when more number of functional groups are present and a synthon competition exists. In such cases Etter's[6] hydrogen bond rules (1990) apply where (1) *all acidic hydrogens available in a molecule will be used in hydrogen bonding in the crystal structure of that compound.* (2) *All good proton acceptors will be used in hydrogen bonding when there are available hydrogen-bond donors.* (3) *The best hydrogen-bond donor and the best hydrogen acceptor will preferentially form hydrogen bonds to one another.* Some common hydrogen bond synthons present in the crystal structures and also encountered in the cocrystals prepared are shown in the Scheme 1.
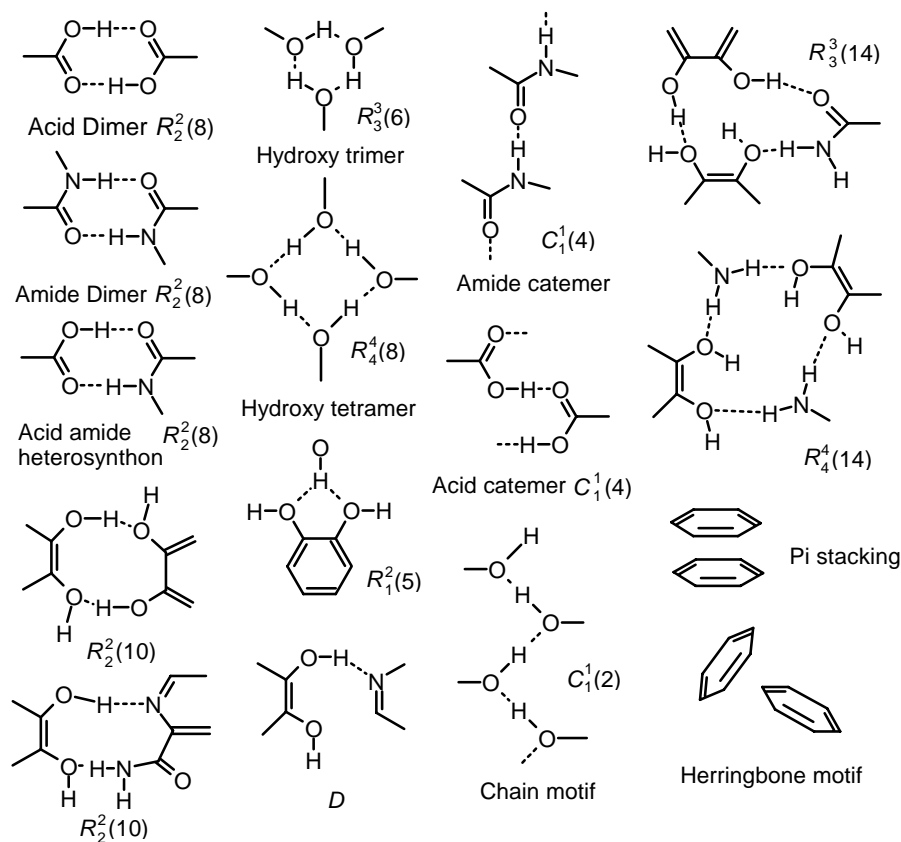
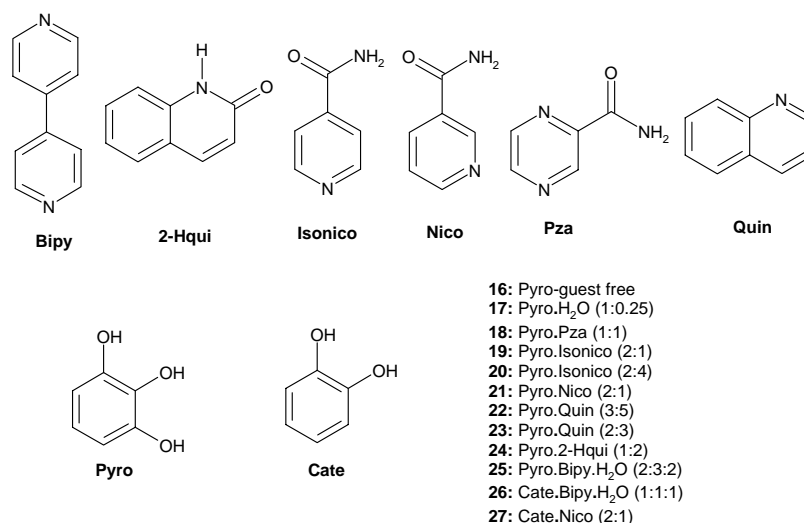**Scheme 1** Some examples of supramolecular synthons.

Cocrystal, also known as a multicomponent crystal under the subset of solid-state chemistry is a familiar word and has 166 year old history. In 1844, Friedrich Wöhler prepared the Quinhydrone[7] from a 1:1 molar combination of quinone and hydroquinone and this can be regarded as the starting point of the cocrystal field. Later after the discovery of X-rays by Röntgen in 1895, in the early 20th century the X-ray crystallography flourished and a large number of cocrystals were determined along with single component crystals. Though they have a long history, cocrystals represent only 0.5% of the crystal structures archived in the Cambridge Structural Database (CSD) as of 2009.[8] Regarding the nomenclature of cocrystals, they are also referred to as co-crystal,[9a] molecular complex,[9b] multicomponent molecular crystal,[9c] molecular compound,[9d] heteromolecular crystal, neutral molecular complex, etc. Again a universal or agreeable definition of cocrystal in the literature is unavailable till date. Various parameters have been applied by Stahly, Nangia, Childs, Jones, Zaworotko etc. to define the cocrystal.[10] According to Aakeröy cocrystal can be defined as "*compounds constructed from discrete neutral molecular species, made from reactants that are solids at ambient conditions and structurally homogeneous crystalline material and contains two or more neutral building blocks that are present in definite stoichiometric amounts*".[10f] There is a scope for confusion in case of certain multi-component crystals like the picric acid with benzene, naphthalene and anthracene. Though stable at room temperature, benzene is a solvent and it is debatable whether it can be categorized as solvate or cocrystal.[11] Therefore in a broader sense all these hydrates, clathrates, solvates and cocrystals can be considered as multi-component systems. Again salts and cocrystals are also closely related to each other and generally the acid ionization constant, pK_a is a common parameter to differentiate between them. The ΔpK_a rule states that when the pK_a difference between the two components is sufficiently large ($\Delta pK_a > 3$) salt formation is very likely,[12] otherwise it is referred to as cocrystal. But there are enormous examples where partial proton transfer occurs. Aakeröy, Childs, Price and coworkers in their recent reports mentioned about the intermediacy of salt and cocrystal structures.[13] Nangia *et. al.* also discussed recently about synthon competition in molecular salts.[12b]

Cocrystals consists of components that interact through non-covalent interactions such as hydrogen bonding, π stacking, van der Waals forces etc. They exhibit physical and chemical properties that can differ from the individual components like the melting point, solubility, chemical stability, and mechanical stability etc.[14] They are widely used in many industries like pharmaceutical, textile, paper, chemical processing, photographic, propellant, and electronics. From the last decade the concept of cocrystallization is widely used in the pharmaceutical industry and a field of *Pharmaceutical cocrystals* has developed. Zaworotko define pharmaceutical cocrystal as "*a multi-component system formed between a molecular or ionic API and a co-crystal former that is a solid under ambient conditions*".[10e] According to a recent analysis by SSCI, the solid state chemistry business of Aptuit have screened about 64 compounds out of which 60 % formed cocrystals other than hydrates or solvates.[10a] Zaworotko and coworkers studied supramolecular heterosynthon as a starting point for cocrystal design.[10e,15] Nangia *et. al.* have studied temperature effects, reactivity of hydrogen-bonding groups in aromatic carboxylic acid and carboxamide cocrystals, also on the amide-N-oxide heterosynthon of model APIs.[16] Jones group explored the methods of preparing cocrystals by liquid-assisted and neat grinding. Based on the grinding technique they explained the mechanism of cocrystal formation and also improvement in chemical and mechanical stability.[17] Rodríguez's group studied the thermodynamics of cocrystal formation and their stability-solubility relationship.[18] Childs group and some of the research and development wings of Merck, Purdue, Pfizer etc have improved the solubility and dissolution of various APIs through their cocrystals.[10c,19]

3.2 RESULTS AND DISCUSSION

It is reported in the literature that aromatic alcohols such as phenols, naphthols etc. readily form cocrystals with aromatic amines, N-heterocyclic aromatics, ureas and acetamide. Cocrystals of antipyrine, an analgesic, with various alcohols like 2-methylphenol, 3-methylphenol, 2-methoxyphenol, resorcinol, pyrogallol etc were reported at the turn of the last century.[20] Apart from that few cocrystals of pyrogallol and

catechol with 4,4' trimethylene-dipyridine, triazine, pyrimidine, HMTA etc were reported by various groups.[21] Pyrogallol or benzene-1,2,3-triol is a white crystalline powder and a powerful reducing agent. It was prepared by Scheele in 1786 by heating gallic acid. It is a common laboratory reagent used to calculate amount of oxygen in air, in making dry nitrogen line, in absorption of moisture, in the early days as dying material and in photography as developing agent. In the recent past, there is a renewed interest on the pharmaceutical utility of pyrogallol as it is a good superoxide generator which induces cell apoptosis. As a result, it has been explored as a potential candidate for anti-lung cancer drug particularly for the non-small cell lung cancer (NSCLC) and Cystic Fibrosis (CF) chronic lung inflammatory disease.[22] In the Cambridge Structural Database (CSD) the crystal structure of pyrogallol is not reported till date, however Becker *et. al.* have determined the cell parameters of the guest-free form and a 0.25-hydrate.[23] Cocrystals of pyrogallol (Pyro) and catechol (Cate) with N-heterocycle bases (Scheme 2) were prepared along with the guest-free form and 0.25-hydrate of pyrogallol and their structural, spectroscopic, solubility and dissolution behavior were studied. All the crystals **16–27** were prepared by solution crystallization method using ethyl acetate-toluene mixture solvent, except cocrystal **25** (from acetonitrile solvent).

16: Pyro-guest free
17: Pyro.H_2O (1:0.25)
18: Pyro.Pza (1:1)
19: Pyro.Isonico (2:1)
20: Pyro.Isonico (2:4)
21: Pyro.Nico (2:1)
22: Pyro.Quin (3:5)
23: Pyro.Quin (2:3)
24: Pyro.2-Hqui (1:2)
25: Pyro.Bipy.H_2O (2:3:2)
26: Cate.Bipy.H_2O (1:1:1)
27: Cate.Nico (2:1)

Scheme 2 Molecular structure of molecules used in the study and the list of cocrystals obtained.

Z' (Z prime) is a common symbol to designate the number of molecules in the asymmetric unit for a single component system. Z' may be defined in relation to the number of molecules in the unit cell: $Z = Z' \times$ number of lattice points $\times$ number of symmetry operations.[24] Eijck and Kroon[25] introduced the symbol Z'' to denote the number of crystallographically non equivalent molecules for multicomponent systems like cocrystals, salts, hydrates and solvates. There is renewed interest on why molecules crystallize with $Z' > 1$ from a structural viewpoint, because the factors leading to its occurrence are still not properly understood. Steed, Padmaja, Gavezzotti and many more research groups[24b,26] studied on the occurrence of more than one molecule in the asymmetric unit. It was mentioned in the literature about awkwardly shaped molecules like monoalcohols, phenols, primary amine etc.[27] which often cannot crystallize out in simple packing modes, give rise to multiple molecules in the asymmetric unit. Apart from that molecular pseudosymmetry,[26h,i] chirality,[26j] strong hydrogen bond,[26k] polymorphs[26l] and modulated structures[26m] are some of the reasons for the occurance of high Z'. As pyrogallol is a noncentrosymmetric molecule with three hydroxyl groups on adjacent side hence most of the cocrystals with N-heterocycle bases having nonstoichiometric donor and acceptor groups resulted in high Z'' structure. But it is difficult to comment about the exact reason for the occurrence of high Z'' in some of the cocrystals of pyrogallol.

Vibrational spectroscopy is a very useful tool to characterize the formation of cocrystal/ salt with respect to the co-formers. Hydrogen bonding between the functional groups alters bond strength thus affecting the stretching and bending vibrations involving them.[28] The common proton donor groups in organic molecules are carboxyl, hydroxyl, amine or amide groups. Common proton acceptor groups are oxygen, nitrogen, the halogens, and even C=C linkage also acts as proton acceptor. When a hydrogen bond forms between $X–H{\cdots}Y–Z$, the strength of $X–H$ bond decreases, the $X–H$ stretching band move to lower frequencies (longer wavelength) usually with increased intensity and band widening. The stretching frequency of the acceptor group also reduces but to a lower extent. The $H–X$ bending vibration shifts to a shorter wavelength but the shift is less pronounced than that of the stretching frequency. The pyrogallol/ catechol cocrystals with

N-heterocycle base were characterized by IR, NIR and Raman spectroscopy. The strong hydrogen bond between the various functional groups present in the cocrystals results in the characteristic changes in stretching and bending vibrations. Apart from X-ray crystallography and vibrational spectroscopy, X-ray photoelectron spectroscopy (XPES) is also a very good technique to differentiate salt/ cocrystal.[29] The FT-IR, NIR and Raman spectra of some of the cocrystals are shown in the Figure 1, 2, 3 and 4 respectively.

(a)

(b)

Figure 1 FT-IR spectra of Pyrogallol 0.25-hydrate **17** and their cocrystals **18**, **19**, **21**, **24** and **25**. Spectral region (a) from 3700–2800 cm^{-1} and (b) from 1800–500 cm^{-1}.

(a)

(b)

Figure 2 FT-IR spectra of Catechol and their cocrystals **26** and **27**. Spectral region (a) from 3600–2200 cm^{-1} and (b) from 2000–500 cm^{-1}.
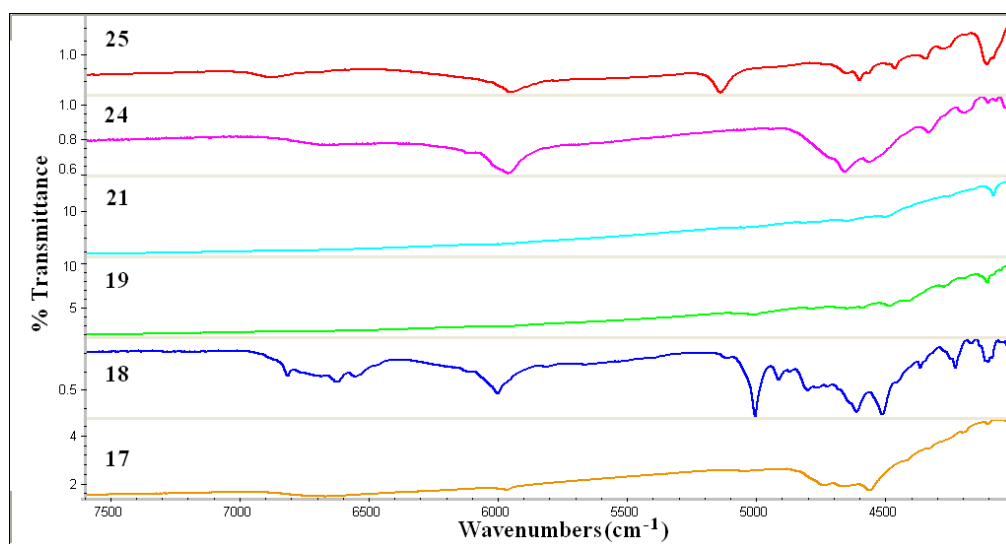
(a)
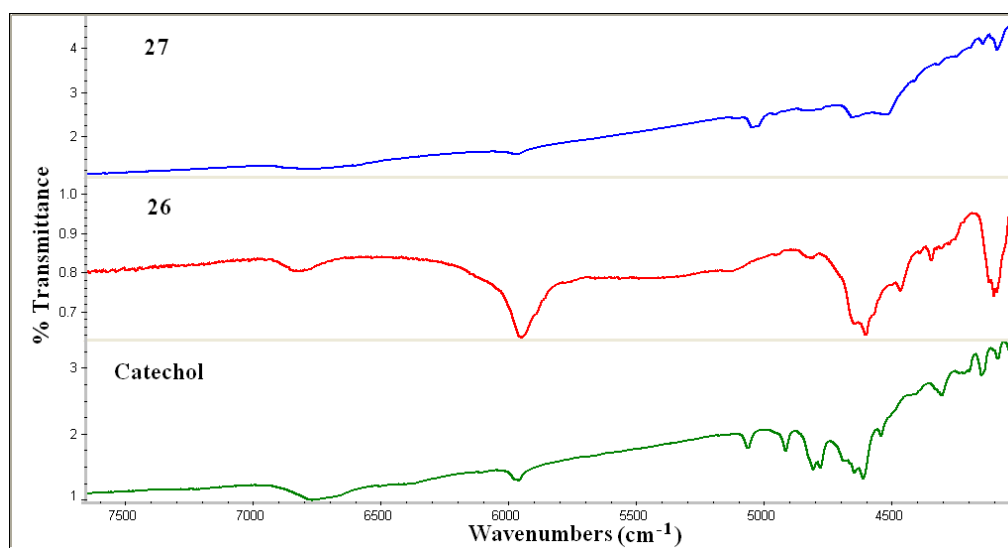
(b)

Figure 3 (a) FT-NIR spectra of Pyrogallol 0.25-hydrate **17** and their cocrystals **18**, **19**, **21**, **24** and **25**. (b) FT-NIR spectra of Catechol and their cocrystals **26** and **27**. Spectral region from 7500–4000 cm^{-1}.
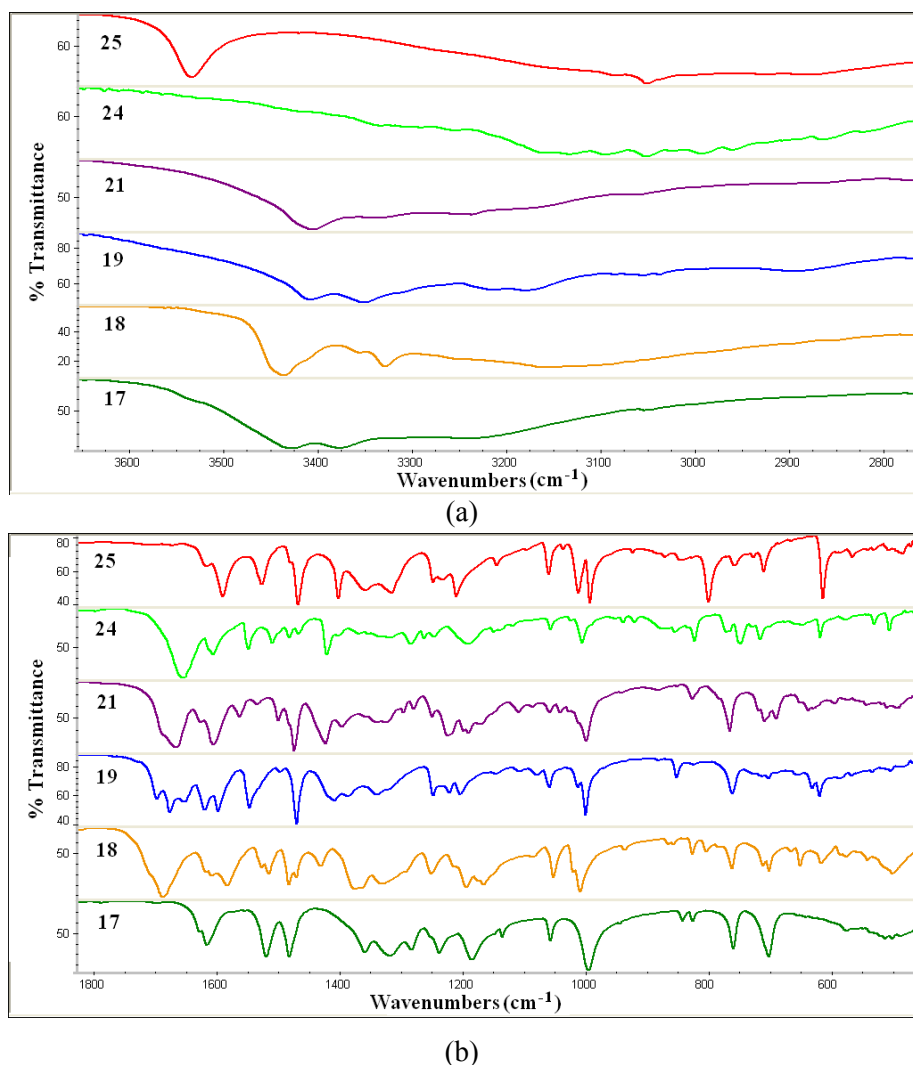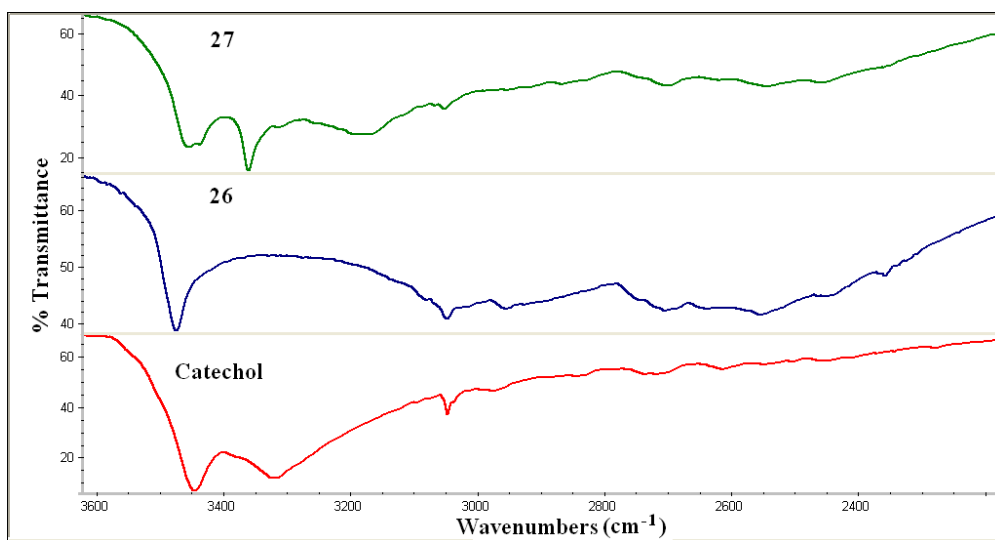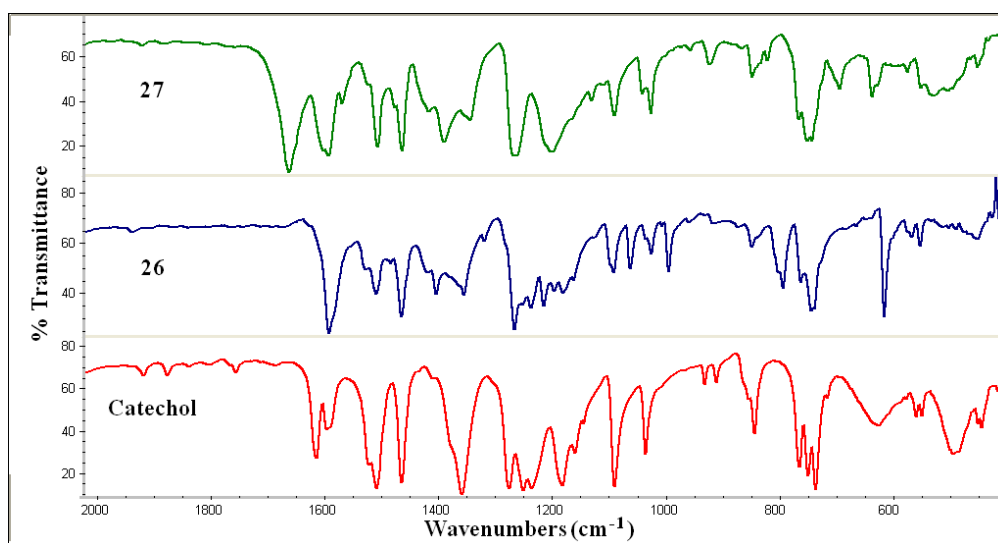
(a)

(b)

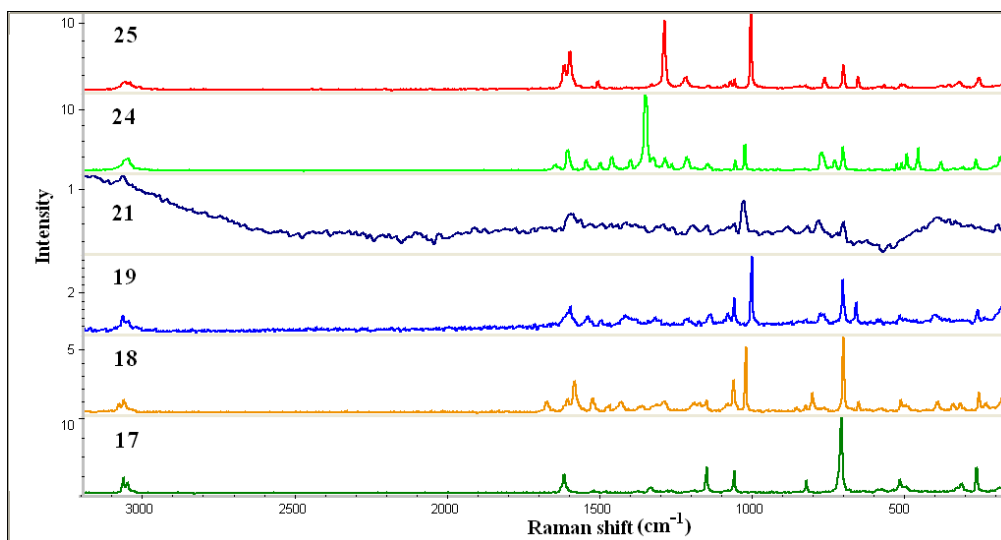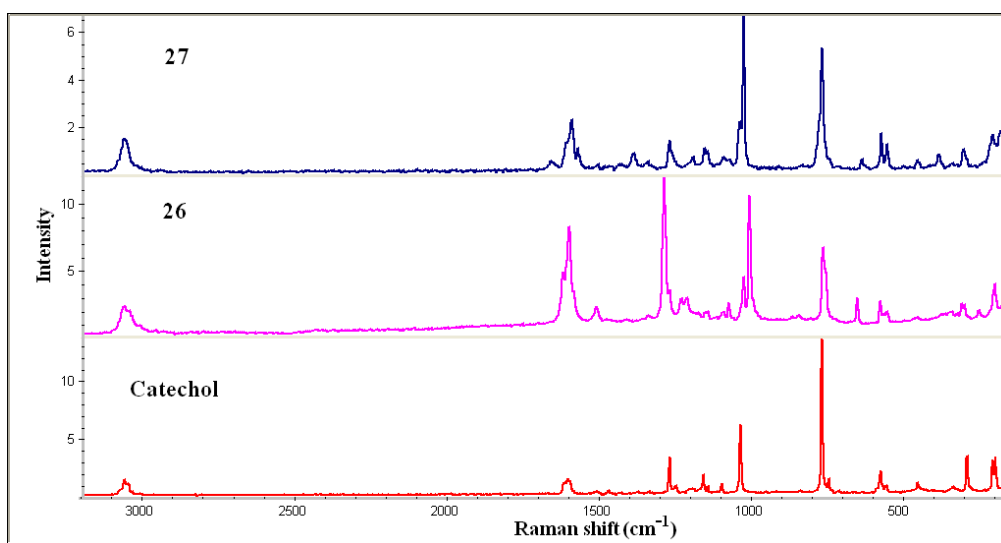**Figure 4** (a) FT-Raman spectra of Pyrogallol 0.25-hydrate **17** and their cocrystals **18**, **19**, **21**, **24** and **25**. (b) FT-Raman spectra of Catechol and their cocrystals **26** and **27**. Spectral region from 3200–400 cm^{-1}.

The hydrogen bond metrics for the crystal structures **16**–**27** are given in Table 1.

Table 1 Hydrogen bond distance in crystal structures.

Compound	Interaction	H···A (Å)	D···A (Å)	D–H···A (º)	Symmetry Code
16	O1–H1···O2	1.96	2.830(2)	145.8	1/2–x,1/2+y,3/2–z
	O2–H2···O3	1.86	2.733(2)	146.5	–x,2–y,1–z
	O1–H1···O2	2.21	2.729(2)	111.5	---[b]
	O2–H2···O3	2.31	2.724(2)	104.0	---[b]
	O3–H3···O1	1.74	2.686(2)	160.2	–1/2+x,3/2–y, –1/2+z
17	O1–H1A···O5	1.83	2.749(3)	155.0	1–y, –1/2+x–1/2+z
	O2–H2A···O4	1.85	2.807(3)	164.2	y,3/2–x,3/2–z
	O1–H1A···O2	2.22	2.715(3)	109.4	---[b]
	O3–H3A···O6	1.76	2.723(3)	166.6	3/2–x,3/2–y, –1+z
	O4–H4A···O3	1.81	2.760(4)	162.5	3/2–y,x,1/2–z
	O5–H5A···*O7	1.91	2.818(5)	152.0	1/2+y,1–x,1/2+z
	O5–H5A···*O7	1.94	2.586(5)	120.7	3/2–y,x,1/2–z
	O6–H6A···O1	1.88	2.767(3)	149.0	1/2+y,1–x,3/2+z
	O6–H6A···O5	2.38	2.746(4)	101.0	---[b]
	O7–H7A···O2	1.95	2.835(6)	148.5	1–x,1–y, –z
18	O1–H1···N1	2.25	2.988(5)	131.1	1–x,2–y,1–z
	O2–H2···O4	1.74	2.697(5)	162.3	–1+x,1+y,z
	O1–H1···O2	2.15	2.710(5)	114.6	---[b]
	O3–H3···N2	1.85	2.819(5)	170.1	1–x,2–y,2–z
	N3–H3A···O2	2.17	3.018(6)	141.1	1–x,2–y,1–z
	N3–H3A···N1	2.33	2.728(6)	102.1	---[b]
	N3–H3B···O1	2.10	3.093(6)	167.8	1–x,1–y,1–z
19	O1–H1···O4	1.76	2.722(2)	164.9	1–x,1–y,1–z
	N1–H1A···O2	1.89	2.896(2)	175.4	---[a]
	N1–H1B···O1	2.06	3.040(2)	162.5	1–x,2–y,1–z
	O2–H2···O6	1.92	2.766(2)	142.7	x,1+y,z
	O2–H2···O3	2.16	2.678(2)	111.0	---[b]
	O3–H3···N2	1.67	2.654(2)	173.4	–1+x,y,1+z
	O4–H4A···O7	1.78	2.732(2)	162.2	---[a]
	O5–H5A···O3	2.02	2.851(2)	140.5	–x,1–y,1–z
	O5–H5A···O6	2.23	2.730(2)	110.0	---[b]
	O6–H6A···O7	1.84	2.818(2)	175.6	–x,1–y,1–z
	C14–H14···O2	2.26	3.241(2)	149.3	1–x,2–y,1–z
20	O1–H1A···N3	1.74	2.699(4)	165.2	x,1+y,z
	O2–H2A···O9	1.89	2.763(4)	145.9	1–x,1/2+y,1–z

	D–H···A	H···A	D···A	D–H···A	symmetry
	O2–H2A···O3	2.22	2.721(4)	110.34	---[b]
	N2–H2B···O9	2.04	3.042(5)	169.2	1–x,1/2+y,1–z
	N2–H2C···O1	1.90	2.895(5)	168.7	x, –1+y,z
	O3–H3A···N7	1.79	2.729(4)	158.6	1–x, –1/2+y,1–z
	O4–H4A···N1	1.74	2.703(5)	165.0	x,1+y, –1+z
	N4–H4B···O4	2.07	2.921(5)	140.4	x,y,1+z
	N4–H4B···O5	2.38	3.251(5)	143.7	x,y,1+z
	N4–H4C···O10	2.15	3.107(5)	157.5	1–x,1/2+y,2–z
	O5–H5A···O10	1.77	2.717(4)	161.4	1–x, –1/2+y,1–z
	O5–H5A···O6	2.23	2.702(4)	103.38	---[b]
	O6–H6A···N5	1.74	2.708(4)	165.4	1–x, –1/2+y,1–z
	N6–H6B···O7	1.94	2.892(4)	156.8	–1+x, –1+y,z
	N6–H6C···O9	1.86	2.846(4)	163.9	–x, –1/2+y,1–z
	N8–H8A···O8	1.86	2.865(5)	171.6	x, –1+y,z
	N8–H8B···O10	1.89	2.862(4)	160.2	1–x, –1/2+y,2–z
	C23–H23···O5	2.28	3.356(4)	172.4	x,y,1+z
	C35–H35···O8	2.44	3.488(5)	162.8	x, –1+y,z
21	O1–H1···O4	1.85	2.787(2)	158.8	1–x, –y,1–z
	N1–H1A···O1	2.40	3.029(2)	119.4	–1+x,1/2–y,1/2+z
	N1–H1A···O2	1.92	2.912(2)	166.0	–1+x,1/2–y,1/2+z
	N1–H1B···O6	2.07	3.066(2)	167.6	–x,1–y,1–z
	O2–H2···O5	1.95	2.781(2)	140.1	1+x,y,z
	O2–H2···O3	2.21	2.696(2)	108.8	---[b]
	O3–H3···N2	1.66	2.632(2)	167.5	1–x,1–y,1–z
	O4–H4···O7	1.68	2.663(2)	176.1	x,1/2–y, –1/2+z
	O5–H5···O7	1.77	2.745(2)	169.5	x,1/2–y, –1/2+z
	O6–H6···O3	1.94	2.763(2)	139.3	–1+x,1/2–y, –1/2+z
	O6–H6···O5	2.23	2.728(2)	110.0	---[b]
	C5–H5A···O4	2.41	3.478(2)	169.2	---[a]
	C14–H14···O6	2.42	3.431(2)	155.5	–x,1–y,1–z
22	O1–H1A···N5	1.69	2.670(6)	171.1	–x,1–y,1–z
	O2–H2A···O6	1.80	2.769(5)	167.8	1–x,1–y,1–z
	O3–H3A···N1	1.65	2.604(6)	161.7	1–x, –y,1–z
	O4–H4A···O5	2.25	2.732(6)	109.1	---[b]
	O4–H4A···O1	2.01	2.905(6)	151.0	–x,1–y,1–z
	O5–H5A···O6	2.28	2.752(5)	108.1	---[b]
	O5–H5A···O3	1.82	2.750(5)	156.6	1–x,1–y,1–z
	O6–H6A···N2	1.68	2.658(6)	171.5	1–x,1–y,1–z
	O7–H7A···O8	2.28	2.770(7)	109.8	---[b]
	O7–H7A···N4	1.89	2.741(7)	143.2	1–x,1–y, –z

	O8–H8A⋯O9	2.25	2.714(6)	107.8	---[b]
	O8–H8A⋯O9	1.96	2.849(6)	148.5	–x,1–y, –z
	O9–H9A⋯N3	1.67	2.633(6)	165.7	–1+x,y,z
	C23–H23⋯O2	2.49	3.312(8)	131.7	---[a]
	C50–H50⋯O2	2.40	3.427(10)	156.9	1–x,1–y,1–z
23	O1–H1A⋯N2	1.76	2.729(2)	167.6	1+x,y,z
	O2–H2A⋯O3	2.07	2.681(2)	118.7	---[b]
	O3–H3A⋯N3	1.72	2.706(2)	178.3	1–x,1–y,1–z
	O4–H4A⋯N1	1.65	2.630(2)	172.0	2–x,1–y, –z
	O5–H5A⋯O4	1.76	2.686(2)	155.7	1–x,2–y, –z
	O5–H5A⋯O4	2.38	2.755(2)	101.9	---[b]
	O6–H6A⋯O5	1.97	2.822(2)	143.4	–x,2–y, –z
	O6–H6A⋯O5	2.26	2.758(2)	109.9	---[b]
	C38–H38⋯O2	2.43	3.377(2)	145.5	x, –1+y,z
24	O1–H1⋯O4	1.69	2.646(2)	164.3	–x,1–y,1–z
	N1–H1A⋯O5	1.81	2.812(2)	170.4	–1+x, –1+y,z
	O2–H2⋯O5	1.74	2.661(2)	155.4	–1+x,y,z
	N2–H2A⋯O4	1.85	2.857(2)	178.9	1–x,1+y,z
	O3–H3⋯O4	1.93	2.869(2)	158.0	1–x,1–y,1–z
	O3–H3⋯O2	2.25	2.727(2)	108.62	---[b]
	C9–H9⋯O2	2.35	3.429(2)	173.6	---[a]
	C13–H13⋯O2	2.33	3.410(2)	173.0	x, –1+y,z
25	O1–H1A⋯N1	1.77	2.736(3)	167.1	1+x,y,z
	O2–H2A⋯O8	1.61	2.572(3)	165.6	---[a]
	O3–H3A⋯N2	1.82	2.727(3)	152.8	–1+x, –1+y,z
	O4–H4A⋯N3	1.82	2.717(3)	150.3	1+x,1+y,z
	O5–H5A⋯O7	1.59	2.551(4)	164.9	---[a]
	O6–H6A⋯N4	1.80	2.763(3)	166.4	–1+x,y,z
	O7–H7A⋯O2	2.14	2.871(4)	129.7	1+x,1+y,z
	O7–H7A⋯O3	2.09	3.010(3)	154.6	1+x,1+y,z
	O7–H7B⋯N6	1.78	2.765(4)	176.8	–1+x,y,z
	O8–H8A⋯O4	2.08	3.010(3)	158.1	–1+x, –1+y,z
	O8–H8A⋯O5	2.19	2.895(3)	127.0	–1+x, –1+y,z
	O8–H8B⋯N5	1.79	2.776(3)	175.1	---[a]
26	O1–H1⋯N1	1.71	2.667(2)	163.3	1–x,1–y,2–z
	O2–H2⋯O3	1.68	2.654(2)	170.2	x,3/2–y,1/2+z
	O3–H3A⋯O1	1.87	2.814(2)	158.9	x,y, –1+z
	O3–H3B⋯N2	1.85	2.821(2)	167.1	---[a]

C5–H5···O2	2.47	3.455(2)	151.4	1+x,y,z
C10–H10···O2	2.37	3.454(2)	178.1	---[a]
C13–H13···O2	2.34	3.376(2)	159.1	---[a]

[a] molecules in the same asymmetric unit
[b] intra molecular H bond

3.3 STRUCTURAL ANALYSIS

PYROGALLOL GUEST-FREE 16

On crystallization of pyrogallol from a mixture of ethyl acetate and toluene plate shaped crystals of guest-free form **16** was obtained in $P2_1/n$ space group. It has all the three hydroxyl groups on the same side, (conformer A) and forms a O–H···O helical trimer synthon along the [010] axis (Figure 5a) and the pyrogallol molecules are stacked through π interaction. In 3D the helical trimer motif of pyrogallol molecules formed an infinite tape parallel to (–101) plane (Figure 5b) and connected to the neighbouring tape through close packing.
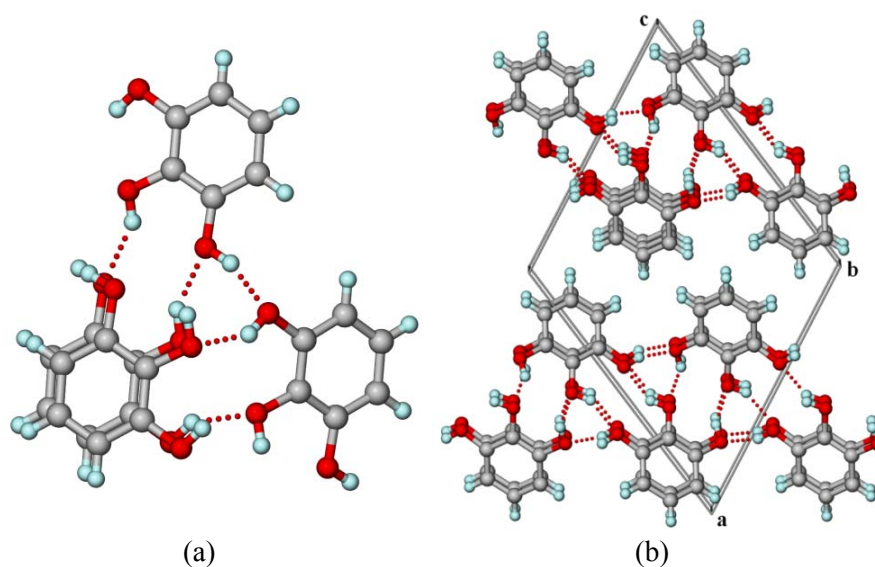

(a)   (b)

Figure 5 (a) O–H···O helical trimer synthon along the [010] axis. (b) 3D packing showing the infinite tape parallel to (–101) plane in **16**.

PYROGALLOL 0.25-HYDRATE 17

On attempted co-crystallization of pyrogallol with pyrazinamide in 1:1 ratio and isonicotinamide in 2:1 ratio respectively in ethyl acetate-toluene mixture solvent two different morphology crystals, needle shaped pyrogallol 0.25-hydrate **17** in tetragonal space group $P4_2/n$ and block shaped crystals of corresponding cocrystals were obtained. The water molecule is present in the crystallographic inversion center with a site occupancy factor of 0.5 along with two pyrogallol molecules (conformer A) in the asymmetric unit. Hence the resulted crystal structure is a 0.25-hydrate. In the crystal structure four pyrogallol molecules forms a helical tetrameric synthon through O–H⋯O hydrogen bond and a water channel resides in the centre of the tetramer along [001] axis (Figure 6).
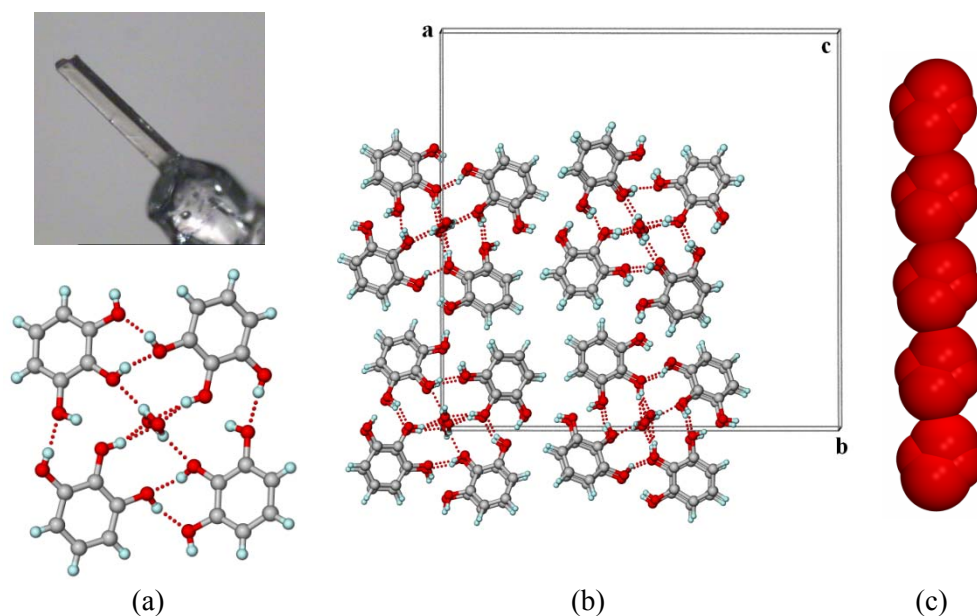

(a)   (b)   (c)

Figure 6 (a) Hydrogen bonded O–H⋯O tetrameric synthon with the shape of a crystal (inset). (b) 3D packing arrangement for pyrogallol 0.25-hydrate **17**. (c) Water channel in **17** along [001] axis.

Presence of the channel water is confirmed by thermal methods like DSC, TGA and hot stage microscopy. In the DSC thermogram an endotherm at 78.8 °C is attributed

to the release of water molecule and the stoichiometry of the released water was further confirmed by TGA analysis which showed a weight loss of 3.18%, matching the theoretical value of 3.12% for 0.25-hydrate (Figure 7). The endotherm at 134.2 °C corresponds to the melting point of pyrogallol. The events are also observed in hot stage microscopic images (Figure 8).
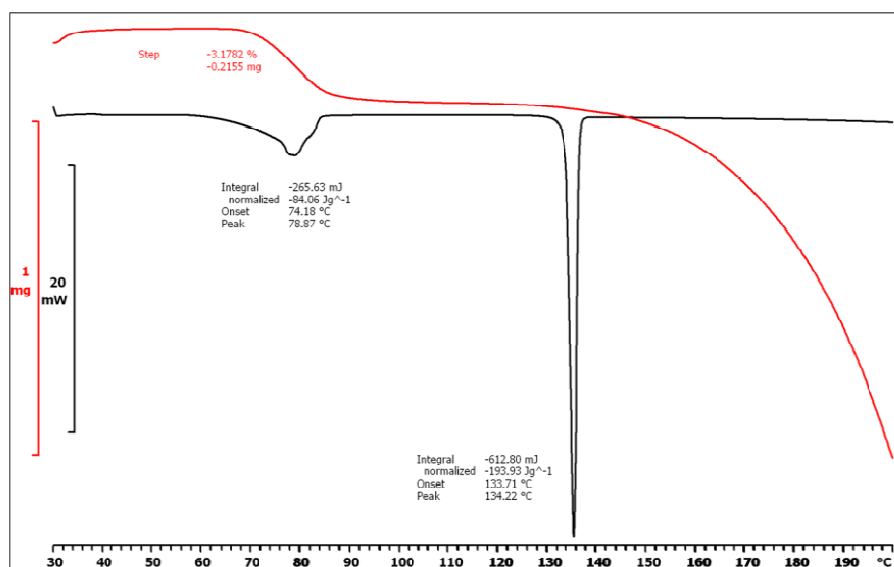

Figure 7 DSC (black) and TGA (red) of pyrogallol 0.25-hydrate crystal **17**.
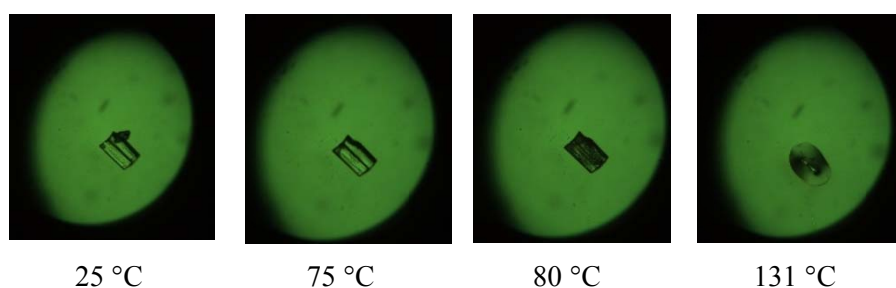

| 25 °C | 75 °C | 80 °C | 131 °C |

Figure 8 HSM snapshots of pyrogallol 0.25-hydrate **17**. The crystal is stable at 25 °C, on heating started getting opaque at 75 °C, 80 °C and melted around 131 °C corresponding to the melting point of pyrogallol guest-free form.

On attempted cocrystallization of pyrogallol with pyrazinamide in 1:1 ratio along with the needle shaped crystals of pyrogallol 0.25-hydrate **17**, blocked shaped cocrystal **18** of pyrogallol and pyrazinamide was obtained. It solved in triclinic space group $P\bar{1}$ containing one molecule each of pyrogallol (conformer A) and pyrazinamide in the asymmetric unit. Pyrogallol is connected to pyrazinamide through O–H⋯O, N–H⋯O and O–H⋯N hydrogen bonding with the graph set notations[30] $R_2^2(10)$, $R_4^4(12)$ and $R_4^4(22)$ to give a tape like structure, where the second layer is connected through $\pi\cdots\pi$ interaction. Pyrogallol and pyrazinamide forms a tetrameric synthon in a non-planar situation as shown in Figure 9.

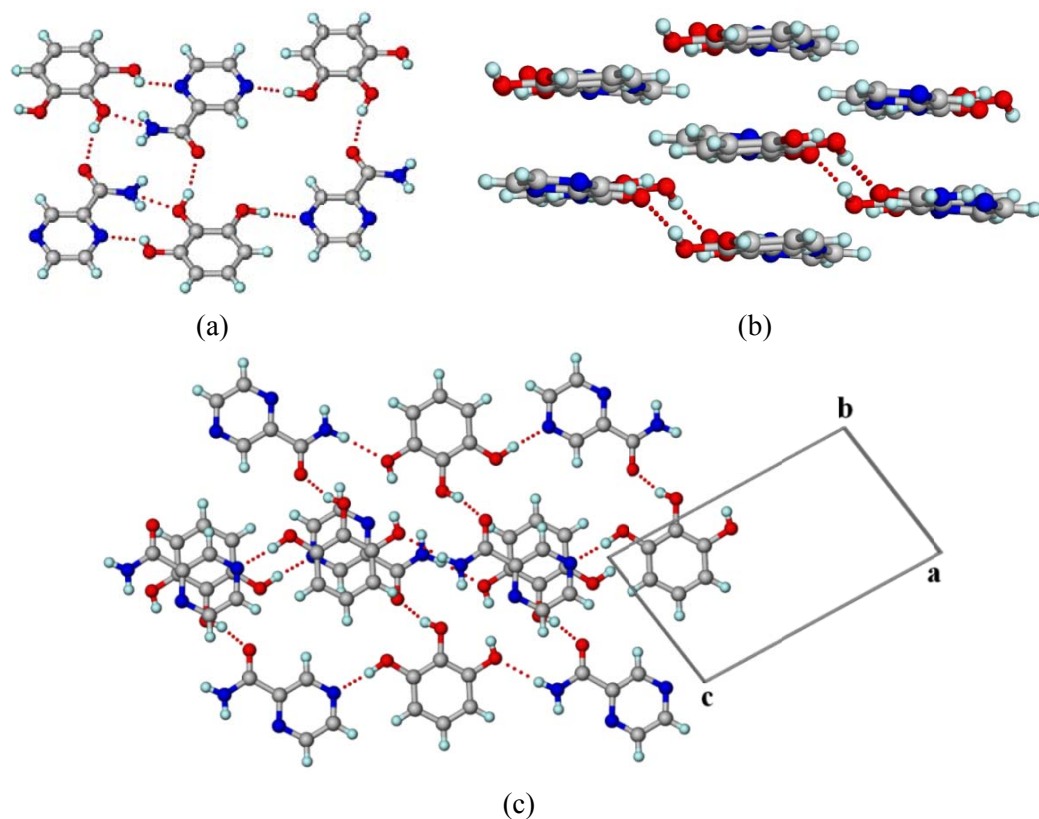(a)   (b)

(c)

Figure 9 (a) $R_2^2(10)$, $R_4^4(12)$ and $R_4^4(22)$ synthon present in cocrystal **18**. (b) Non-planar tetrameric synthon formed by pyrogallol and pyrazinamide and the stacking of layers. (c) 3D packing arrangements of the layers in offset manner in cocrystal **18**.

COCRYSTAL 19: PYRO•ISONICO (2:1)

This cocrystal **19** which crystallized in $P\bar{1}$ space group from ethyl acetate-toluene mixture solvent contained pyrogallol (conformer C) and isonicotinamide in 2:1 ratio. It was obtained as a block shaped crystal in addition to needle shaped crystals of pyrogallol 0.25-hydrate **17**. Because of the strong acceptor groups like pyridine N and amide O and strong donor group O–H in the components, the cocrystal uses all the donor and acceptor groups to form O–H···O, O–H···N and N–H···O hydrogen bonds to give a complicated 3D structure (Figure 10).

(a)

(b)

(c)

(d)
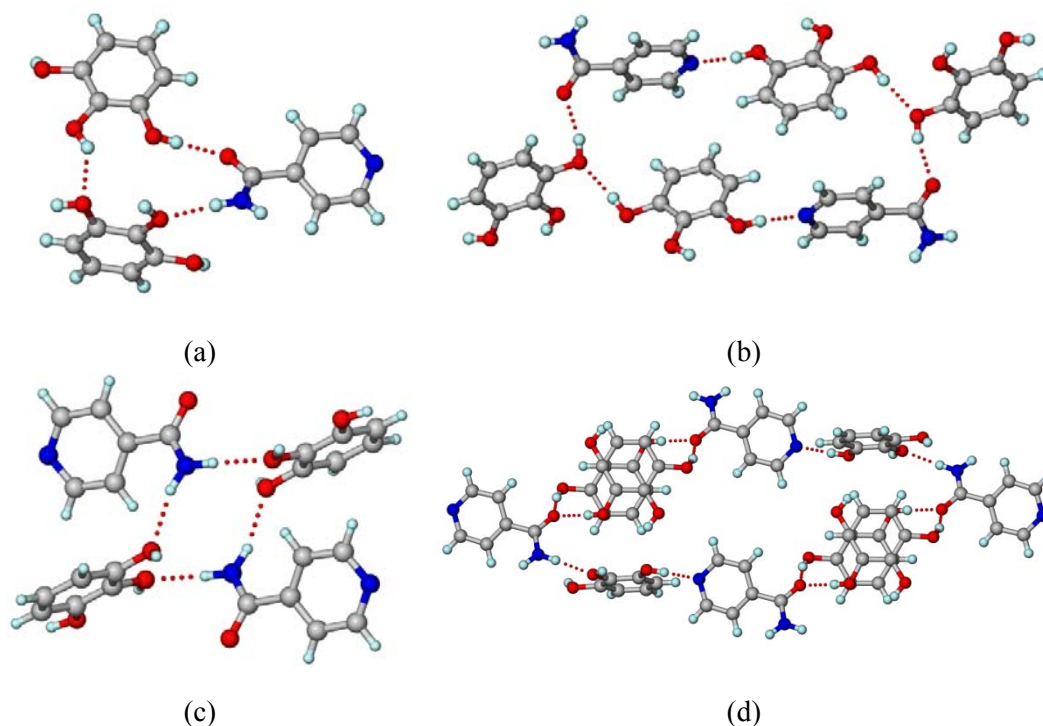
Figure 10 Different hydrogen bonded synthons present in the cocrystal **19**.

COCRYSTAL 20: PYRO•ISONICO (2:4)

On cocrystallizing pyrogallol and isonicotinamide in the reverse ratio i.e. 1:2 from ethyl acetate-toluene mixture a 2:4 cocorystal of pyrogallol and isonicotinamide **20** was obtained. The cocrystal **20** is solved in Sohncke (chiral) space group $P2_1$. Structurally the

two cocrystals **19** and **20** are completely different from each other. While the former is a centrosymmetric structure with a complicated 3D packing without any dimer or catemer synthon between the isonicotinamide molecules, the latter is a chiral structure having two unidirectional catemer networks between two symmetry independent isonicotinamide molecules along the [010] axis. Supramolecular chirality due to hydrogen bonding[31] is the result of occurrence of chiral $P2_1$ space group for cocrystal **20** from two achiral coformers. Isonicotinamide and pyrogallol molecules are connected to each catemer unit through O–H···O and N–H···O hydrogen bond between the amide group of isonicotinamide and hydroxyl group of pyrogallol. These two independent units are further connected by O–H···N hydrogen bond through the hydroxyl group of pyrogallol and the pyridine N of isonicotinamide (Figure 11).

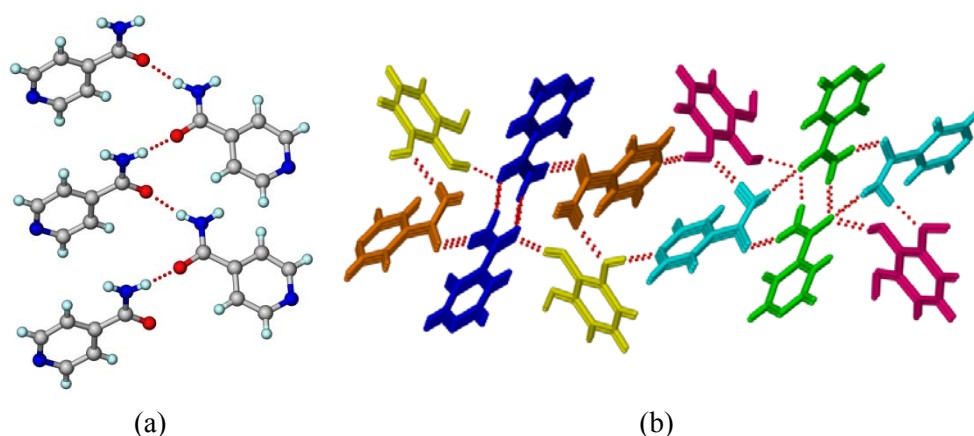(a)   (b)

Figure 11 (a) The catemer synthon formed by the isonicotinamide molecule along [010] axis. (b) 3D molecular packing with the symmetry independent molecules coated with different colors in cocrystal **20**.

COCRYSTAL 21: PYRO•NICO (2:1)

On cocrystallizing pyrogallol and nicotinamide in 2:1 ratio from ethyl acetate-toluene mixture, cocrystal **21** was obtained with two molecules of pyrogallol (conformers C and D) and one molecule of nicotinamide in the asymmetric unit solved in $P2_1/c$ space group. The commonly observed amide dimer or the catemer synthon is absent. Two pyrogallol molecules are hydrogen bonded to the nicotinamide molecule through strong O–H···O,

O–H···N and N–H···O hydrogen bonds (Figure 12). In the 3D structure, one of the pyrogallol (conformer C) and nicotinamide molecules form a layer and a symmetry independent pyrogallol molecule which is offset (conformer D) connects the next layer through O–H···O hydrogen bond. There is π···π stacking between the layers and are separated by a distance of 3.26 Å. A plausible reason for the occurrence of high energy conformer D of pyrogallol is to satisfy all H bonding sites present.
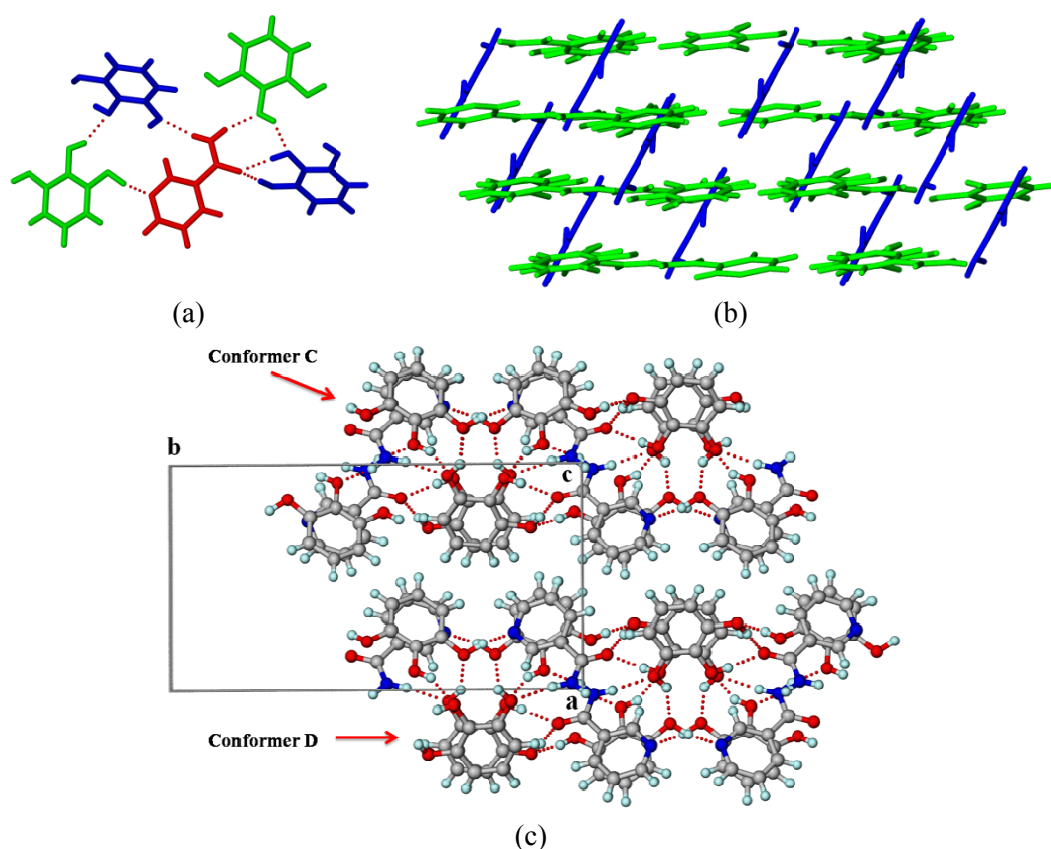

(a)   (b)

(c)

Figure 12 (a) Hydrogen bonded synthon in the cocrystal **21** (different colors are shown for the symmetry independent molecules) (b) Layers formed by pyrogallol and nicotinamide molecules with a second pyrogallol molecule (blue) connecting the layers through O–H···O hydrogen bond. (c) 3D molecular packing of cocrystal **21** along [001] axis.

Cocrystallization of pyrogallol with quinoline was done by adding a solution of quinoline (1 mL of quinoline diluted in 50mL of ethyl acetate-toluene) to 50 mg of pyrogallol and kept for slow evaporation. It resulted in two different stoichiometric cocrystals **22** and **23** from different batches.

The cocrystal **22** is solved in $P\bar{1}$ space group containing three molecules of pyrogallol and five molecules of quinoline in the asymmetric unit. The crystal structure contained two domains. Domain 1 contains two molecules of pyrogallol (conformer A and C) and three molecules of quinoline and domain 2 with one pyrogallol (conformer A) and two quinoline moelcules. In domain 1 pyrogallol molecules are connected to each other through a zigzag tape of O–H···O hydrogen bond and the flanking hydroxyl groups of pyrogallol are connected to the three symmetry independent quinoline molecules through O–H···N hydrogen bond (Figure 13a, b). In domain 2 the pyrogallol molecule forms a centrosymmetric O–H···O dimer synthon and the terminal hydroxyl groups are connected to two symmetry independent quinoline molecules through O–H···N hydrogen bonds. Domain 1 and 2 forms a layer along [100] axis with both the domains stacked together through weak π···π interactions as shown in Figure 13d.

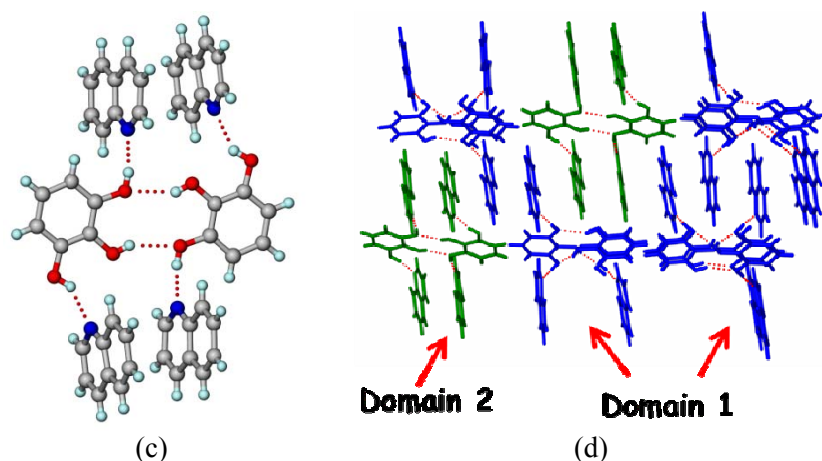(a)   (b)
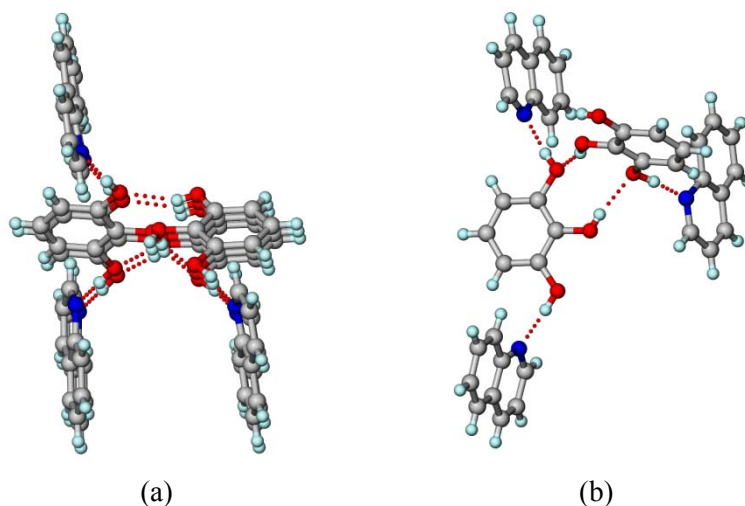
Figure 13 (a) Infinite O–H⋯O zigzag tape of pyrogallol connecting three symmetry independent quinoline molecules through O–H⋯N hydrogen bond (domain 1). (b) Single unit of domain 1 to show the hydrogen bond. (c) Domain 2 with the pyrogallol O–H⋯O dimer synthon connecting the quinoline molecules. (d) 3D molecular packing showing domain 1 and domain 2 with different colors.

COCRYSTAL 23: PYRO•QUIN (2:3)

Along with the cocrystal **22**, pyrogallol and quinoline formed cocrystal **23**, solved in $P\bar{1}$ space group. The asymmetric unit of the cocrystal **23** contains two molecules of pyrogallol and three molecules of quinoline. Like the cocrystal **22**, cocrystal **23** also has the same type of structural domains and conformers of pyrogallol (A and C). The domain 1 has one molecule of pyrogallol (conformer A) and quinoline. The pyrogallol molecule forms an infinite O–H⋯O hydrogen bond chain along [100] axis and one of the terminal hydroxyl group is hydrogen bonded to quinoline molecule through O–H⋯N interaction. In domain 2, one pyrogallol (conformer C) and two quinoline molecules are present. The two symmetry independent quinoline molecules are connected to the terminal hydroxyl groups of the pyrogallol molecule through O–H⋯N hydrogen bond. Domain 1 and 2 are stacked together through π⋯π interaction and fulfill the 3D packing (Figure 14).

(a)   (b)

Domain 1   Domain 2

(c)
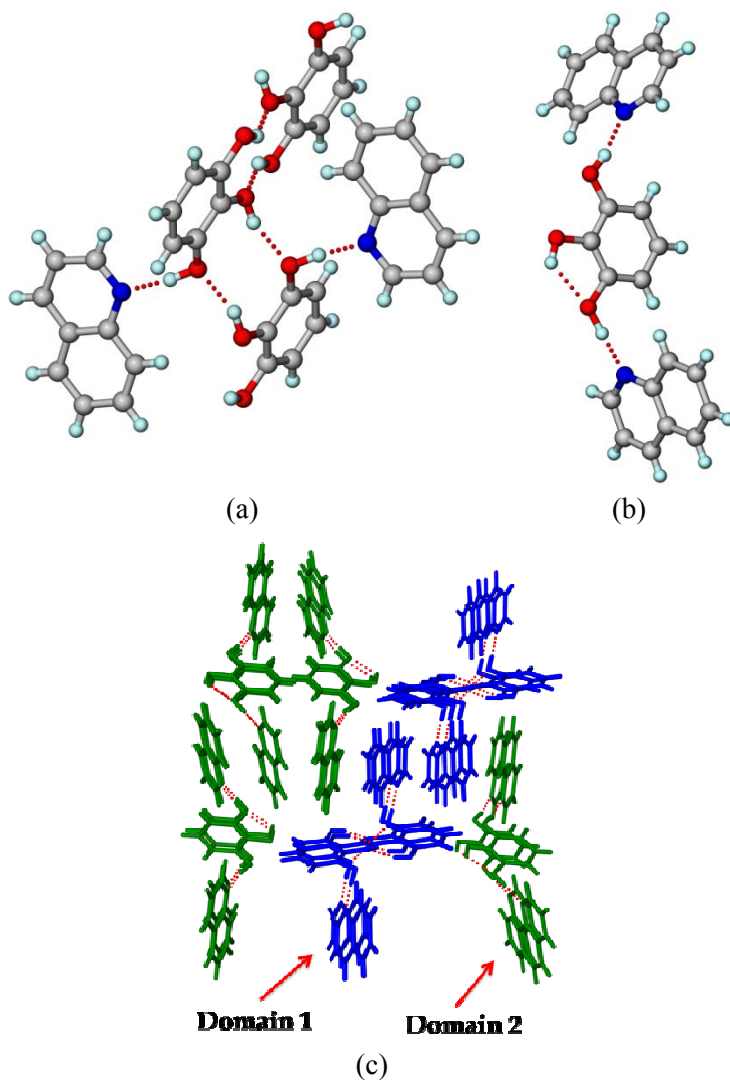
Figure 14 (a) Domain 1 containing infinite O–H···O hydrogen bonded chain along [100] axis. (b) Domain 2 with discrete O–H···N synthon between pyrogallol and quinoline. (c) 3D molecular packing showing the two domains with different colors.

COCRYSTAL 24: PYRO•2HQUI (1:2)

Pyrogallol and 2-Hydroxyquinoline on crystallizing in 1:2 ratio from ethyl acetate-toluene mixture resulted in cocrystal **24** of the same stoichiometry which solved in $P\bar{1}$ space group. 2-Hydroxyquinoline, in its amide tautomeric form results in a

noncentrosymmetric amide dimer synthon with a graph set notation $R_2^2(8)$. The pyrogallol molecules (conformer A) are connected to the 2-hydroxyquinoline dimer motif through O–H···O hydrogen bond forming a tape along [100] axis. The 2-hydroxyquinoline dimer motifs are stacked through $\pi\cdots\pi$ interactions (Figure 15). These 1D tapes are arranged parallel to each other through short contacts.

(a)

(b)   (c)
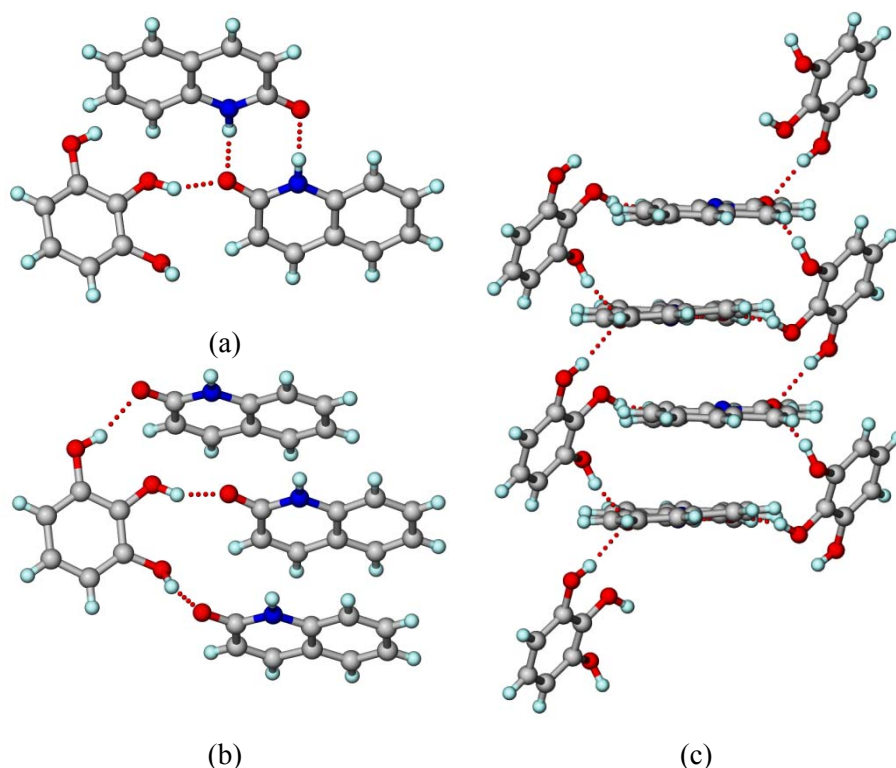
Figure 15 (a) 2-Hydroxyquinoline amide dimer connected to the pyrogallol molecule through O–H···O hydrogen bond. (b) O–H···O hydrogen bond between pyrogallol and 2-Hydroxyquinoline of three different layers. (c) Infinite tape of pyrogallol connecting the π stacked 2-Hydroxyquinoline layers along [100] axis.

COCRYSTAL 25: PYRO•BIPY•H₂O (2:3:2)

Cocrystallization of pyrogallol with bipyridine in 2:3 ratio from acetonitrile resulted in block shaped cocrystals of **25** solved in $P\bar{1}$ space group containing two pyrogallol, three bipyridine along with two water molecules in the asymmetric unit. Structurally the cocrystal **25** consists of an O–H···O tetrameric synthon with graph set notation $R_4^4(8)$

formed by two water molecules and two symmetry independent pyrogallol units (Figure 16a). These pyrogallol-water tetramers are connected to each other by the three symmetry independent bipyridine molecules through O–H⋯N hydrogen bond which forms a layer parallel to the (–12–2) plane. Within the layer, bipyridine molecules are orthogonal to the pyrogallol molecules and the next layer consists of alternate stacks of pyrogallol and bipyridine units through weak C–H⋯π interactions (Figure 16).
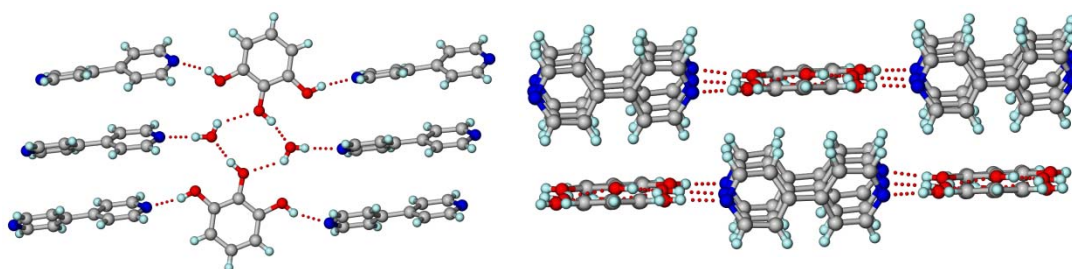
Figure 16 (a) O–H⋯O tetrameric synthon between pyrogallol and water which is connected to the bipyridine through O–H⋯N hydrogen bond. (b) Two pyrogallol-bipyridine layers connected through weak C–H⋯π interaction.

COCRYSTAL 26: CATE•BIPY•H₂O (1:1:1)

Similarly like the cocrystal **25** of pyrogallol, on crystallizing catechol (having one hydroxyl group less than pyrogallol) with bipyridine from ethyl acetate-toluene mixture solvent, afforded cocrystal **26** having one catechol, one bipyridine and a water of crystallization in the asymmetric unit. The cocrystal **26** solved in $P2_1/c$ space group and is different from **25** due to the lack of one hydroxyl group and consequently the tetrameric synthon. Catechol along with the water molecule forms an infinite O–H⋯O chain along [001] axis and the bipyridine molecule acts as a spacer which connect the hydrogen bonded chains (Figure 17).

<div align="center">(a)   (b)</div>
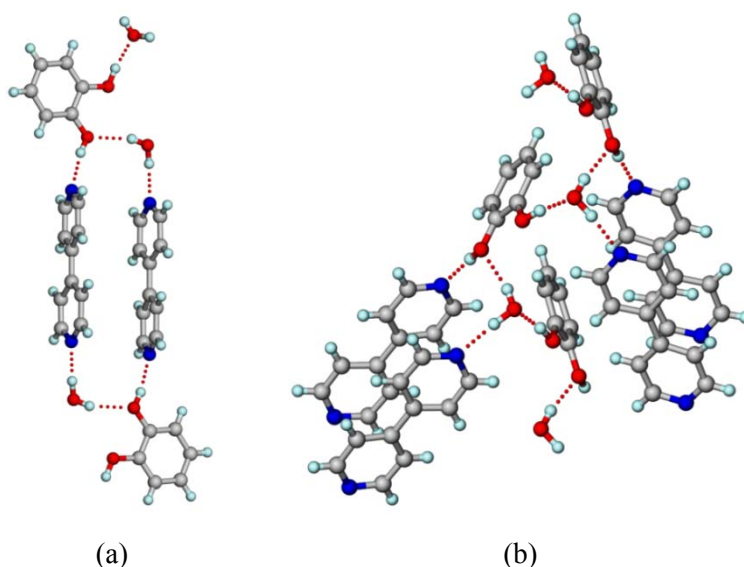
Figure 17 (a) O–H···O and O–H···N hydrogen bonding that connects the bipyridine to water and catechol molecules in cocrystal **26**. (b) Infinite O–H···O hydrogen bonded chain of catechol and water along [001] axis.

COCRYSTAL 27: CATE•NICO (2:1)

Cocrystallizing catechol and nicotinamide in 2:1 ratio from ethyl acetate-toluene mixture resulted in cocrystal **27** which solved in *Pca*2$_1$ space group with two catechol and one nicotinamide molecules in the asymmetric unit. In the crystal structure **27** nicotinamide molecule is disordered over two positions with the site occupancy factor 0.63 and 0.37 (Figure 18). The two symmetry independent catechol molecules form an O–H···O hydrogen bonded zigzag chain along [001] axis and the flanking hydroxyl groups are connected to the disordered nicotinamide molecule through O–H···N hydrogen bond (Figure 19).
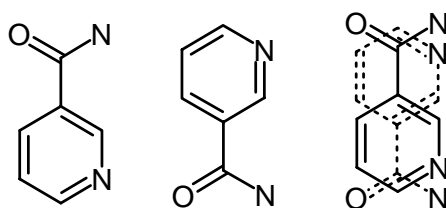
Figure 18 Positional disorder of two nicotinamide molecules.

(a) (b)
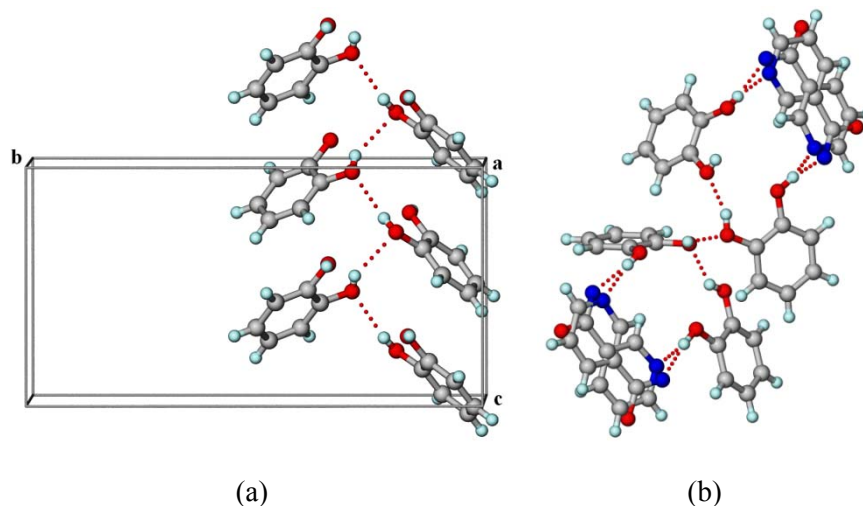
Figure 19 (a) Infinite O–H···O hydrogen bonded chain along [001] axis. (b) Catechol molecules of the chain that connect the disordered nicotinamide molecules through O–H···N hydrogen bond in cocrystal **27**.

3.4 CONFORMATIONAL ANALYSIS

Dihydroxy and trihydroxy benzene molecules generally show positional isomerism. Among them pyrogallol, 1,2,4 trihydroxybenzene and catechol have intramolecular hydrogen bond (Scheme 3). M. Gerhards *et al.*[32] have calculated conformational energy possible for the different conformers of pyrogallol of which it was found that conformer A is the most stable one having 1664 cm^{-1} (4.76 kcal mol^{-1}) less energy than the metastable conformer C. Conformer D and E have higher energy due to inter-atomic repulsion term, similar to the case of catechol conformers B and C.
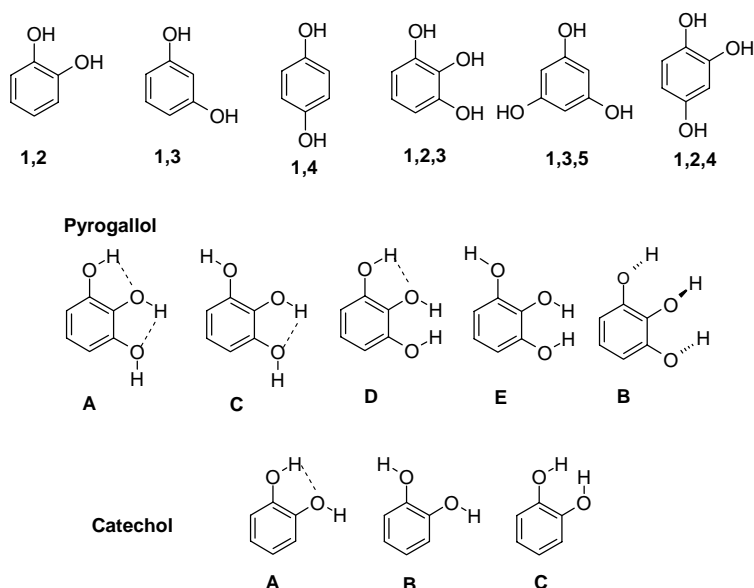
Scheme 3 Positional isomers of dihydroxy and trihydroxy benzene and various conformers of pyrogallol and catechol molecules.

The hydroxyl group conformations of pyrogallol and catechol obtained in the crystal structures **16–27** are listed in Table 2. The stable conformer A is found for most of the cocrystals of pyrogallol along with its guest-free form and 0.25-hydrate followed by the conformer C, and conformer D for structure **21** (Table 2). The occurrence of high energy conformers for structures **21** and **26** is to satisfy all possible hydrogen bond donor/acceptor sites available.

Table 2 Conformers present in the crystal structures **16–27**.

Structure	OH group Conformer	Structure	OH group Conformer
16	Conformer A[a]	**22**	Conformer A and C[a]
17	Conformer A[a]	**23**	Conformer A and C[a]
18	Conformer A[a]	**24**	Conformer A[a]
19	Conformer C[a]	**25**	Conformer C[a]
20	Conformer C[a]	**26**	Conformer B[b]
21	Conformer C and D[a]	**27**	Conformer A[b]

[a] pyrogallol, [b] catechol.

3.5 LIQUID ASSISTED GRINDING AND XRPD ANALYSIS

Cocrystals of pyrogallol and catechol with N-heterocycle bases obtained from solution crystallization were prepared in bulk quantity using liquid assisted grinding method. For the liquid assisted grinding both the components were taken in stoichiometric amount in a mortar pestle and a few drops of ethyl acetate solvent was used and ground thoroughly for 15-20 min and XRPD of the materials were recorded. The powder patterns of the materials match the calculated XRD patterns (Figure 20).
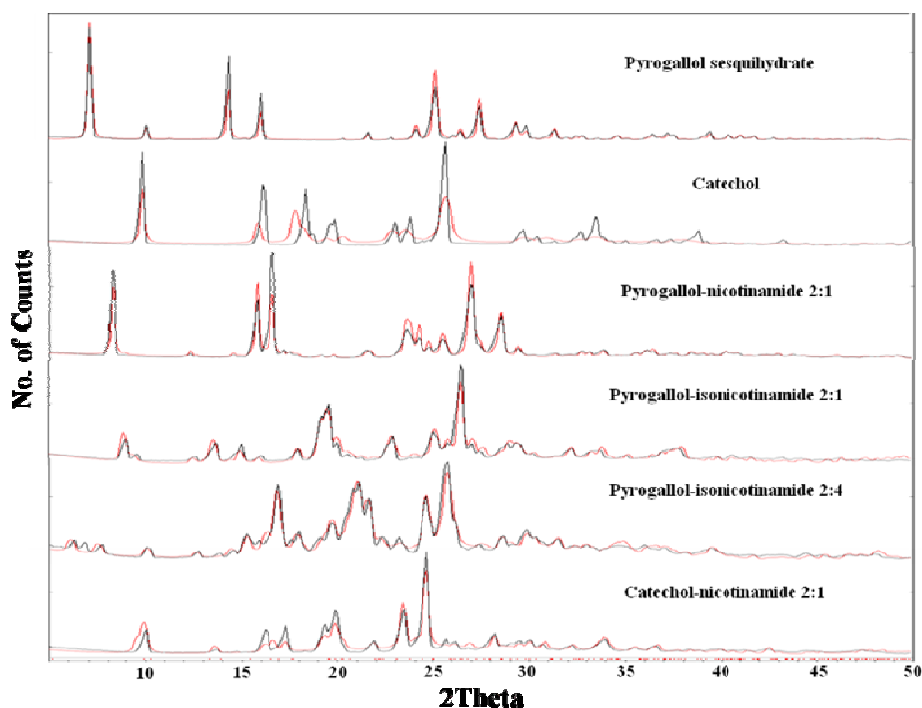
Figure 20 Overlay of the calculated X-ray crystal structure (red) and experimental XRPD pattern (black) of the bulk material of **17**, Catechol, **19**, **20**, **21** and **27**.

3.6 SOLUBILITY AND DISSOLUTION

As reported in the literature, pyrogallol is responsible for cell apoptosis and is also an active compound responsible for the anti-inflammatory effect[22f] of Emblica officinalis, a medicinal plant, due to which it may be a potential candidate as an anti-lung cancer

drug.[22e] Therefore it is important to study the solubility and dissolution behavior of pyrogallol and their cocrystals in order to have a better knowledge about the bioavailability of the molecule. Solubility and dissolution of pyrogallol and catechol and their cocrystals with nicotinamide and isonicotinamide were studied. Pyrogallol is highly soluble in water with a solubility value of 611.99 mg/mL but the solubility of the isonicotinamide cocrystals **19**, **20** (187.36, 156.13 mg/mL respectively) and nicotinamide **21** (187.22 mg/mL) are less than that of the parent molecule. Similar observation is obtained in case of catechol (337.72 mg/mL) and its nicotinamide **27** (162.08 mg/mL) cocrystal. In addition the dissolution profile (Figure 21) shows that pyrogallol and catechol have higher IDR values than their respective cocrystals. The 2:1 and 2:4 isonicotinamide cocrystals of pyrogallol have almost same dissolution rate.

(a)   (b)
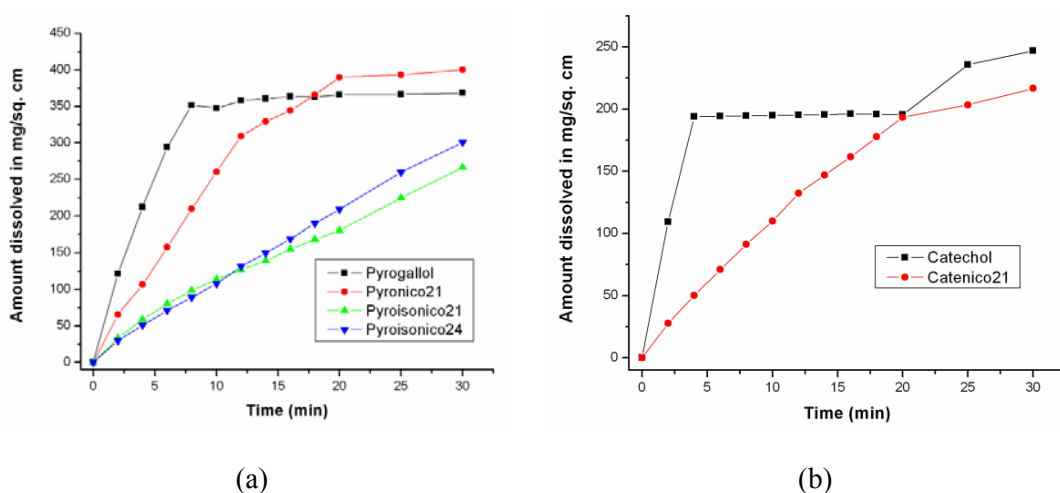
Figure 21 Dissolution patterns of pryogallol, catechol, and their cocrystals **19**, **20**, **21** and **27** in distilled water recorded upto 30 min.

3.7 CONCLUSION

Cocrystals of pyrogallol and catechol with various N-heterocycle bases were prepared. It is observed that in most of the cocrystals there are more than two molecules in the asymmetric unit. The awkward shape of the pyrogallol/ catechol molecules and the strong hydrogen bonding requirements of the OH group can dominate the crystal packing. Thus

the frustration between the conflicting needs to achieve close packing and maximal hydrogen bonding of the lone OH groups resulted in high Z'' structures of the cocrystals. The cocrystal **20**, that solved in chiral noncentrosymmetric space group $P2_1$ is the reason for 6 molecules in the asymmetric unit (Z'') compared to 3 molecules for the centrosymmetric case. But it is difficult to conclude in one line for the occurrence of high Z' in crystal structures. In the course of time with more number of high Z' structures deposited in the CSD can help in understanding the structural reasons for high Z'.

Over the last two decades based on the hydrogen bonding and supramolecular synthon approach, cocrystals were prepared. Therefore to have a better understanding of the non-covalent interactions, cocrystallization is a good approach from the crystal engineering point of view. The field of cocrystal chemistry is maturing from the supramolecular perspective towards the structure-property relationship of materials. Similar to the salt form of drugs, the utility of cocrystals for modifying the physical and chemical properties of drugs has increased its importance in pharmaceutical industry. So far there is no drug cocrystal formulation in the market but a large number of patent applications are filed for pharmaceutical cocrystals and are undergoing bioavailability and animal studies. It is only a matter of time before this imagination becomes a reality.

3.8 EXPERIMENTAL SECTION

X-RAY CRYSTALLOGRAPHY

X-ray reflections for all compounds were collected at 100 K (except **25** at 298K) on Bruker SMART APEX CCD equipped with a graphite monochromator and Mo-Kα fine-focus sealed tube (λ = 0.71073 Å). Data integration was done using SAINT.[33] Intensities for absorption were corrected using SADABS.[34] Structure solution and refinement were carried out using Bruker SHELXTL.[35] The hydrogen atoms were refined isotropically and the heavy atoms were refined anisotropically. N–H and O–H hydrogens were located from difference electron density maps and C–H hydrogens were fixed using HFIX command in SHELXTL. In case of cocrystal **27** the nicotinamide molecule is disordered over two positions. It was modeled using FVAR command with s.o.f. of 0.63 and 0.37

respectively refining the disordered non-hydrogen atoms isotropically. Crystallographic data were summarized in Appendix. Packing diagrams were prepared in X-Seed.[36]

X-RAY POWDER DIFFRACTION

X-ray powder diffraction of all samples were recorded on Bruker D8 Advance diffractometer using Cu-Kα X-radiation (λ = 1.54056 Å) at 40 kV and 30 mA. Diffraction patterns were collected over a 2θ range of 5-50° at a scan rate of 1° min^{-1}. Powder Cell 2.4 was used for Rietveld refinement.[37]

VIBRATIONAL SPECTROSCOPY

Nicolet 6700 FT-IR spectrometer with an NXR FT-Raman module was used to record IR, NIR and Raman spectra. IR and NIR spectra were recorded on samples dispersed in KBr pellets. Raman spectra were recorded on solid samples contained in standard NMR diameter tubes or on compressed samples contained in a gold-coated sample holder.

THERMAL ANALYSIS

DSC was performed on Mettler Toledo DSC 822e module. Samples were placed in crimped but vented aluminum sample pans. The typical sample size was 3-4 mg, and the temperature range was 30-200 °C at heating rate of 5 °C min^{-1}. Samples were purged by a stream of dry nitrogen flowing at 150 mL min^{-1}. For TGA, the sample size was 7-9 mg, the heating rate was 10 °C min^{-1}, and the N_2 flow was 50 mL min^{-1}. HSM was performed on a Wagner & Munz PolythermA Hot Stage and Heiztisch microscope. A Moticam 1000 (1.3 MP) camera supported by software Motic Image Plus 2.0ML was used to record images.

INTRINSIC DISSOLUTION TESTING OF DISC

IDR measurements were carried on a USP-certified Electrolab TDT-08 L Dissolution Tester. Equilibrium solubility was determined in water using the shakeflask method. Excess amount of the powdered materials were added to 5 mL of water, and the resulting

suspension was stirred at room temperature for 24 hr. The suspension was then filtered through 2.5 μm Whatman filter paper. The concentration of the solution thus obtained was determined on a Thermo Scientific Evolution 300 UV-vis spectrometer based on the absorbance maxima with appropriate dilution using a predetermined calibration curve.

For IDR experiments, 200 mg of the pure pyrogallol, catechol and the cocrystals **19**, **20**, **21** and **27** were taken in the intrinsic attachment and compressed to a 0.5 cm^2 pellet using a hydraulic press at a pressure of 2.5 ton inch^{-2} for 5 min. There is no polymorphic transformation or dissociation of the sample upon compression. The intrinsic attachment was placed in a jar of 900 mL of water at 37 °C and rotated at 50 rpm. 7 mL aliquots were collected at specific time intervals and concentrations of the aliquots were determined with proper dilution from the predetermined calibration curves of the respective materials using their individual molar extinction coefficients (Pyrogallol 0.67, Catechol 2.48, cocrystal **19** 4.30, **20** 11.78, **21** 4.45 and **27** 5.97 /mmol/cm) by UV-Vis spectrophotometry. The IDR values were 34.75, 19.48, 11.39, 10.78, 26.07 and 10.99 mg/cm^2/min (at 10 min interval) respectively.

Calculation: Beer Lambert's Law: $A = \varepsilon c l$

where A is the absorbance, ε is coefficient of absorbance, c is the concentration and l is path length of the sample.

3.9 REFERENCES

1. (a) G. M. Schmidt, *J. Pure Appl. Chem.*, 27, **1971**, 647. (b) G. R. Desiraju, *Crystal Engineering. The Design of Organic Solids*, Elsevier: Amsterdam, **1989**. (c) D. Braga, F. Grepioni and G. R. Desiraju, *Chem. Rev.*, 98, **1998**, 1375. (d) B. Moulton and M. J. Zaworotko, *Chem. Rev.*, 101, **2001**, 1629.

2. L. Pauling, *The Nature of the Chemical Bond*, Cornell University Press, Ithaca, **1939**.

3. (a) G. C. Pimentel and A. L. McClellan, *The Hydrogen Bond*, W. H. Freeman, San Francisco, **1960**. (b) G. A. Jeffrey and W. Saenger, *Hydrogen Bonding in Biological Structures*, Springer, Berlin, **1991**. (c) G. A. Jeffrey, *An Introduction*

to Hydrogen Bonding, Oxford University Press, Oxford, **1997**. (d) T. Steiner, *Angew. Chem. Int. Ed.*, 41, **2002**, 48. (e) T. Steiner and W. Saenger, *J. Am. Chem. Soc.*, 115, **1993**, 4540.

4. (a) G. R. Desiraju, *Angew. Chem. Int. Ed.*, 50, **2011**, 52. (b) G. R. Desiraju, *Acc. Chem. Res.*, 35, **2002**, 565.

5. (a) G. R. Desiraju, *Perspectives in Supramolecular Chemistry: The Crystal as a Supramolecular Entity*, Ed., Vol. 2, Wiley: Chichester, **1996**. (b) G. R. Desiraju, *Angew. Chem. Int. Ed.*, 34, **1995**, 2311.

6. (a) M. C. Etter, *J. Am. Chem. Soc.*, 104, **1982**, 1095. (b) M. C. Etter, *Acc. Chem. Res.*, 23, **1990**, 120. (c) M. C. Etter, *J. Phys. Chem.*, 95, **1991**, 4601.

7. F. Wöhler, *Annalen Chem. Pharm.*, 51, **1844**, 145.

8. S. L. Childs and M. J. Zaworotko, *Cryst. Growth Des.*, 9, **2009**, 4208.

9. (a) J. D. Dunitz, *CrystEngComm*, 4, **2003**, 506. (b) G. R. Desiraju, *CrystEngComm*, 5, **2003**, 466. (c) A. D. Bond, *CrystEngComm*, 9, **2007**, 833. (d) A. R. Ling and J. L. Baker, *J. Chem. Soc.*, 63, **1893**, 1314.

10. (a) G. P. Stahly, *Cryst. Growth Des.*, 7, **2007**, 1007. (b) B. R. Bhogala and A. Nangia, *New J. Chem.*, 32, **2008**, 800. (c) S. L. Childs and K. I. Hardcastle, *Cryst. Growth Des.*, 7, **2007**, 1291. (d) W. Jones, W. D. Motherwell and A. V. Trask, *MRS Bull.*, 341, **2006**, 875. (e) P. Vishweshwar, J. A. McMahon, J. A. Bis and M. J. Zaworotko, *J. Pharm. Sci.*, 95, **2006**, 499. (f) C. B. Aakeröy and D. J. Salmon, *CrystEngComm*, 7, **2005**, 439. (g) C. B. Aakeröy, J. Desper, M. Fasulo, I. Hussain, B. Levin and N. Schultheiss, *CrystEngComm*, 10, **2008**, 1816.

11. (a) H. Takayanagi, Y. Toubai, M. Goto, S. Yamaguchi and H. Ogura, *Chem. Pharm. Bull.*, 39, **1991**, 2491. (b) A. Banerjee and C. J. Brown, *Acta Cryst.*, C41, **1985**, 82. (c) F. H. Herbstein and M. Kaftory, *Acta Cryst.*, B32, **1976**, 387.

12. (a) S. L. Johnson and K. A. Rumon, *J. Phys. Chem.*, 69, **1965**, 74. (b) B. Sarma, N. K. Nath, B. R. Bhogala and A. Nangia, *Cryst. Growth Des.*, 9, **2009**, 1546. (c) B. R. Bhogala, S. Basavoju and A. Nangia, *CrystEngComm*, 7, **2005**, 551.

13. (a) C. B. Aakeröy, M. E. Fasulo and J. Desper, *Mol. Pharm.*, 4, **2007**, 317. (b) S. L. Childs, G. P. Stahly and A. Park, *Mol. Pharm.*, 4, **2007**, 323. (c) S. Mohamed, D. A. Tocher, M. Vickers, P. G. Karamertzanis and S. L. Price, *Cryst. Growth Des.*, 9, **2009**, 2881.

14. (a) N. Schultheiss and A. Newman, *Cryst. Growth Des.,* 9, **2009**, 2950. (b) J. H. ter Horst, M. A. Deij and P. W. Cains, *Cryst. Growth Des.,* 9, **2009**, 1531. (c) G. P. Stahly, *Cryst. Growth Des.,* 9, **2009**, 4212. (d) N. Blagden, D. J. Berry, A. Parkin, H. Javed, A. Ibrahim, P. T. Gavan, L. L. De Matosa and C. C. Seaton, *New J. Chem.*, 32, **2008**, 1659. (e) C. C. Sun and H. Hou, *Cryst. Growth Des.,* 8, **2008**, 1575. (f) C. B. Aakeröy, J. Desper, M. Fasulo, I. Hussain, B. Levina and N. Schultheiss, *CrystEngComm*, 10, **2008**, 1816.

15. J. A. Bis, P. Vishweshwar, D. Weyna and M. J. Zaworotko, *Mol. Pharm.*, 4, **2007**, 401.

16. (a) L. S. Reddy, P. M. Bhatt, R. Banerjee, A. Nangia and G. J. Kruger, *Chem.-Asian J.*, 2, 2007, 505. (b) N. J. Babu, L. S. Reddy and A. Nangia, *Mol. Pharm.*, 4, **2007**, 417.

17. (a) T. Friščić and W. Jones, *Cryst. Growth Des.,* 9, **2009**, 1621. (b) S. Karki, T. Friščić, L. Fábián, P. R. Laity, G. M. Day and W. Jones, *Adv. Mater.*, 21, **2009**, 3905. (c) D. Cinčić, T. Friščić and William Jones, *J. Am. Chem. Soc.*, 130, **2008**, 7524. (d) S. Karki, T. Friščić, W. Jones and W. D. S. Motherwell, *Mol. Pharm.*, 4, **2007**, 347. (e) T. Friščić and W. Jones, *Faraday Discuss.*, 136, **2007**, 167. (f) T. Friščić, A. V. Trask, W. Jones and W. D. S. Motherwell, *Angew. Chem. Int. Ed.*, 45**, 2006**, 7546. (g) A. V. Trask, W. D. S. Motherwell and W. Jones, *Int. J. Pharm.*, 320, **2006**, 114.

18. (a) A. Jayasankar, D. J. Good and N. Rodríguez-Hornedo, *Mol. Pharm.*, 4, **2007**, 360. (b) K. Seefeldt, J. Miller, F. Alvarez-Núñez and N. Rodríguez-Hornedo, *J. Pharm. Sci.*, 96, **2007**, 1147. (c) N. Rodríguez-Hornedo, S. J. Nehm, K. F. Seefeldt, Y. Pagán-Torres and C. J. Falkiewicz, *Mol. Pharm.*, 3, **2006**, 362. (d) S.

J. Nehm, B. Rodríguez-Spong and N. Rodríguez-Hornedo, *Cryst. Growth. Des.*, 6, **2006**, 592.

19. (a) S. L. Childs, L. J. Chyall, J. T. Dunlap, V. N. Smolenskaya, B. C. Stahly and G. P. Stahly, *J. Am. Chem. Soc.*, 126, **2004**, 13335. (b) A. M. Chen, M. E. Ellison, A. Peresypkin, R. M. Wenslow, N. Variankaval, C. G. Savarin, T. K. Natishan, D. J. Mathre, P. G. Dormer, D. H. Euler, R. G. Ball, Z. Ye, Y. Wang and I. Santos, *Chem. Commun.*, **2007**, 419. (c) Z. J. Li, Y. Abramov, J. Bordner, J. Leonard, A. Medek and A. V. Trask, *J. Am. Chem. Soc.*, 128, **2006**, 8199. (d) N. Variankaval, R. Wenslow, J. Murry, R. Hartman, R. Helmy, E. Kwong, S.-D. Clas, C. Dalton and I. Santos, *Cryst. Growth. Des.*, 6, **2006**, 690.

20. (a) H. Helbing, *Modern Materia Medica*, 4th Ed., Lehn & Fink: New York, **1895**, p 18, 122. (b) E. Springer, *Pharm. Ztg.*, 46, **1901**, 430.

21. (a) L. Dobrzańska, *Acta Cryst.*, E61, **2005**, o3416. (b) L. Dobrzańska, *Acta Cryst.*, E61, **2005**, o2981. (c) M. Tremayne and C. Glidewell, *Chem. Commun.*, **2000**, 2425. (d) C. J. Brown, *Acta Cryst.*, 21, **1966**, 170. (e) M. R. Caira, A. Horne, L. R. Nassimbeni and F. Toda, *Perkin Trans.*, 2, **1997**, 1717. (f) P. Daka and K. A. Wheeler, *Acta Cryst.*, E62, **2006**, o5477.

22. (a) Y. H. Han, S. Z. Kim, S. H. Kim and W. H. Park, *Int. J. Mol. Med.*, 21, **2008**, 721. (b) Y. Takemura, D.-H. Wang, R. Sauriasari, M. Horita, K. Tsutsui, K. Sano, N. Masuoka, T. Takigawa, J. Takaki and K. Ogino, *Bull Environ Contam Toxicol.*, 84, **2010**, 347. (c) Y. H. Han and W. H. Park, *Arch Toxicol.*, 84, **2010**, 631. (d) Y. H. Han, S. Z. Kim, S. H. Kim and W. H. Park, *Chem.-Bio. Inter.*, 177, **2009**, 107. (e) C.-J. Yang, C.-S. Wang, J.-Y. Hung, H.-W. Huang, Y.-C. Chia, P.-H. Wang, C.-F. Weng and M.-S. Huang, *Lung Cancer*, 66, **2009**, 162. (f) E. Nicolis, I. Lampronti, M. C. Dechecchi, M. Borgatti, A. Tamanini, N. Bianchi, V. Bezzerri, I. Mancini, M. G. Giri, P. Rizzotti, R. Gambari and G. Cabrini, *Int. Immunopharm.*, 8, **2008**, 1672.

23. P. Becker, H. Brusset and H. Gillier-Pandraud, *C. R. Acad. Sci., Ser.C (Chim)*, 274, **1972**, 1043.

24. (a) C. P. Brock, *J. Res. Natl. Inst. Stand. Technol.*, 101, **1996**, 321. (b) J. W. Steed, *CrystEngComm*, 5, **2003**, 169. (c) G. R. Desiraju, *CrystEngComm*, 9, **2007**, 91. (d) W. Clegg and G. S. Nichol, *Acta Cryst.*, E60, **2004**, 1433.

25. (a) B. P. van Eijck, J. Kroon, *Acta Cryst.*, B56, **2000**, 535. (b) P. van der Sluis and J. Kroon, *J. Cryst. Growth*, 97, **1989**, 645.

26. (a) K. M. Anderson, K. Afarinkia, H Yu, A. E. Goeta and J. W. Steed, *Cryst. Growth Des.*, 6, **2006**, 2109. (b) K. M. Anderson, A. E. Goeta, K. S. B. Hancock and J. W. Steed, *Chem. Commun.*, **2006**, 2138. (c) N. Padmaja, S. Ramakumar and M. A. Viswamitra, *Acta Cryst.*, A46, **1990**, 725. (d) A. Gavezzotti and G. Filippini, *J. Am. Chem. Soc.*, 117, **1995**, 12299. (e) A. Gavezzotti and G. Filippini, *J. Phys. Chem.*, 98, **1994**, 4831. (f) S. Aitipamula and A. Nangia, *Chem.-Eur. J.*, 11, **2005**, 6727. (g) V. S. S. Kumar, A. Addlagatta, A. Nangia, W. T. Robinson, C. K. Broder, R. Mondal, I. R. Evans, J. A. K. Howard and F. H. Allen, *Angew. Chem. Int. Ed.*, 41, **2002**, 3848. (h) J. D. Wallis and J. D. Dunitz, *Acta Cryst.*, C44, **1988**, 1037. (i) G. R. Desiraju, J. C. Calabrese and R. L. Harlow, *Acta Cryst.*, B47, **1991**, 77. (j) S. E. Gibson, H. Ibrahim and J. W. Steed, *J. Am. Chem. Soc.*, 124, **2002**, 5109. (k) N. J. Babu and A. Nangia, *Cryst. Growth Des.*, 6, **2006**, 1995. (l) B. Sarma, S. Roy and A. Nangia, *Chem. Commun.*, **2006**, 4918. (m) S. K. Chandran and A. Nangia, *CrystEngComm*, 8, **2006**, 581.

27. (a) C. P. Brock and J. D. Dunitz, *Chem. Mater.*, 6, **1994**, 118. (b) H. J. Lehmler, L. W. Robertson, S. Parkin and C. P. Brock, *Acta Cryst.*, B58, **2002**, 140.

28. (a) R. M. Silverstein, F. X. Webster and D. J. Kiemle, *Spectroscopic Identification of Organic Compounds*, John Wiley & Sons, **2005**. (b) B. T. G. Lutz, J. Jacob and J. H. van der Maas, *Vib. Spectros.*, 12, **1996**, 197. (c) H. G. Brittain, *Cryst. Growth Des.*, 9, **2009**, 2492.

29. J. S. Stevens, S. J. Byard and S. L. M. Schroeder, *J. Pharm. Sci.*, 99, **2010**, 4453.

30. (a) M. C. Etter, J. C. Macdonald and J. Bernstein, *Acta Cryst.*, B46, **1990**, 256. (b) J. Bernstein, R. E. Davis, L. Shimoni and N.-L. Chang, *Angew. Chem., Int. Ed.,* 34, **1995**, 1555.

31. (a) H. Koshima, *J. Mol. Struct.*, 552, **2000**, 111. (b) T. Matsuura and H. Koshima, *J. Photochem. Photobio. C: Photochem. Rev.*, 6, **2005**, 7. (c) E. Pidcock, *Chem. Commun.*, **2005**, 3457.

32. H. Gier, W. Roth, S. Schumm and M. Gerhards, *J. Mol. Struct.*, 610, **2002**, 1.

33. *SAINT-Plus*, version 6.45, Bruker AXS Inc., Madison, WI, **2003**.

34. G. M. Sheldrick, *SADABS, Program for Empirical Absorption Correction of Area Detector Data*, University of Göttingen, Germany, **1997**.

35. *SHELXS-97 and SHELXL-97, Programs for the Solution and Refinement of Crystal Structures*, G. M. Sheldrick, University of Göttingen, Germany, **1997**.

36. *X-Seed, Graphical Interface to SHELX-97 and POVRay*, L. J. Barbour, University of Missouri-Columbia, Columbia, MO, **1999**.

37. Powder Cell 2.4, Program for structure visualization, powder pattern calculation and profile fitting, www.ccp14.ac.uk.

CHAPTER FOUR

OLANZAPINIUM SALTS/SOLVATES

4.1 INTRODUCTION

From the ancient time during the isolation and purification of 'vegetable alkalis', the nitrogen-containing bases later known as alkaloids are extracted from plants in the form of salts. In contrast to the free bases, the salts are found to be water-soluble and more stable. Such properties qualified the salts of these biologically active compounds as the preferred forms for use as therapeutic agents. For example Morphine hydrochloride, atropine sulfate, pilocarpine nitrate, codeine phosphate, etc. are few of them. Salt formation is an acid-base reaction involving either a proton transfer or neutralization reaction and is therefore controlled by factors influencing such reactions. Substance that exhibits acid or base characteristics participates in salt formation. The salt formation and stability depend on the acidity/ basicity of the species involved in the reaction.

The dissociation of a monoprotic acid HA to its conjugate base A^- can be described by the following equilibrium:

$$[HA] \xrightleftharpoons{K_a} [H^+] + [A^-]$$
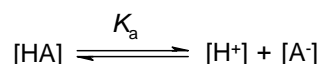
The equilibrium constant K_a of this reaction is the ionization constant and defined as

$$K_a = \frac{[H^+].[A^-]}{[HA]}$$

Because ionization constants are small and inconvenient numbers, they are expressed as their negative logarithms:

$$pK_a = -\log K_a$$

The acid ionization constant pK_a is a key parameter to predict the molecular ionization state, despite the fact that pK_a values are only valid under the solution equilibrium conditions at which they are determined. When the ΔpK_a is sufficiently large, salt formation is very likely, and there have been many propositions for the minimum ΔpK_a required to be confident of salt formation. By contrast, in the range $0 < \Delta pK_a < 3$ experimental evidence shows that

crystallization may result in a salt, cocrystal, or mixed ionization solid form with partial proton transfer, with the location of the acidic proton dependent on the specific crystal packing environment.[1]

Salt preparation in is not only essential for isolation and purification of substances but also pharmaceutically important because of better solubility and stability compared to the acidic/ basic drug.[2] Determination of solubility and alteration if required is an essential step in pharmaceutical development. The bioavailability of an orally administered drug depends primarily on solubility in the gastrointestinal tract and permeability across the cell membrane. This solubility and permeability forms the basis for biopharmaceutical classification system (BCS) devised by Amidon et al.,[3] According to the Biopharmaceutics Classification System all the drugs can be classified into four categories (Figure 1).
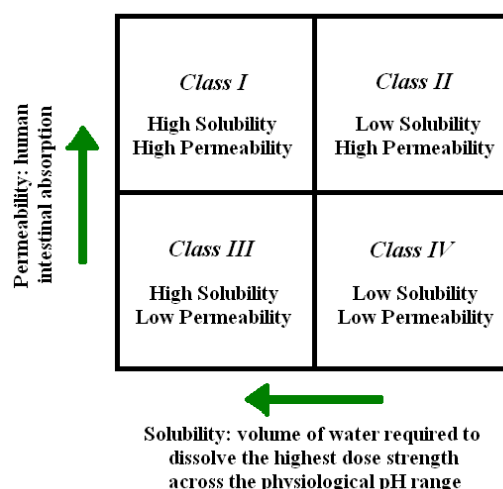
Figure 1 The Biopharmaceutics Classification System. This diagram is culled from *AAPS Journal*, American Association of Pharmaceutical Scientists publication (reference 3d).

Class I – High **Permeability**, High **Solubility**

These compounds are well absorbed and their absorption rate is usually higher than excretion.

Class II – High **Permeability**, Low **Solubility**

The bioavailability of these products is limited by their solvation rate.

Class III – Low **Permeability**, High **Solubility**

> The absorption is limited by the permeation rate but the drug is solvated very fast.

Class IV – Low **Permeability**, Low **Solubility**

> These compounds have a poor bioavailability. Usually they are not well absorbed over the intestinal mucosa and a high variability is expected.

Absorption number (A_n), dissolution number (D_n), and dose number (D_o) are the three main dimensionless parameters in the Biopharmaceutics Classification System. The BCS is one of the most significant tools created to facilitate oral drug product development in recent years and has been adopted by the US Food and Drug Administration (US-FDA), the European Medicines Agency (EMEA), and the World Health Organization (WHO) for setting bioavailability/ bioequivalence (BA/ BE) standards for immediate-release (IR) oral drug products. According the BCS there is a basic need for the improvement of Class II and Class IV drug for better effect on human health.

Even though solubility enhancement is a primary area of focus during drug development phase, several situations are there, like for sustained release products, taste masking, and enhancement of chemical stability where decrease in solubility is required. Solubility and dissolution are related to each other. The concentration of the solute in the solvent, at which the rate of molecules leaving the bulk solute surface becomes equal to the rate of redeposition, is the thermodynamic solubility. The rate at which this equilibrium is achieved is defined as the dissolution rate. Therefore solubility is an equilibrium process while dissolution is a kinetic phenomenon. According to Noyes–Whitney, dissolution rate of a solute in a solvent is directly proportional to its solubility described by the equation[4]

$$\text{Dissolution rate} \; = \; \frac{dQ}{dt} \; = \; \frac{DA}{h} \, (C_s - C_b)$$

where:

dQ/ dt is the rate of mass transfer

D is the diffusion coefficient (cm^2/ sec)

A is the surface area of the drug (cm^2)

h is the diffusion layer thickness (cm)

C_s is the saturation solubility of the drug

C_b is bulk solution concentration.

Biological activity of a drug molecule is influenced by two factors: its chemical structure and effect at a specific site; and its ability to reach and then be removed from the site of action. Thus, a knowledge of the physicochemical properties of a compound that influence its absorption, distribution, metabolism, and excretion (ADME) is essential for a complete understanding of the onset and duration of action, the relative toxicity, and the possible routes of administration. The salt form is known to influence a number of physicochemical properties of the parent drug including dissolution rate, solubility, stability, and hygroscopicity.[5] These properties, in turn, affect the bioavailability and formulation characteristics of the drug. Consequently, the pharmaceutical industry has systematically engaged in extensive preformulation studies of the physicochemical properties of each new drug entity to determine the most suitable form for drug formulation.

4.2 RESULTS AND DISCUSSION

2-methyl-4-(4-methyl-1-piperazinyl)-10*H*-thieno[2,3-*b*][1,5]benzodiazepine (Figure 2) commonly known as Olanzapine is a psychotropic agent that belongs to the thienobenzodiazepine class.[6] The drug is available in the market under the brand name of ZYPREXA manufactured by Eli Lilly and Company that obtained approval by FDA in the year 1996 and is one of the top 20 prescription drugs based on a recent survey.[7] According to the Biopharmaceutics Classification System (BCS), Olanzapine belongs to class II category, i.e., a drug of low solubility and high permeability. It is a yellow crystalline solid, which is practically insoluble in water (43 mg/L), sparingly soluble in acetonitrile, ethyl acetate and freely soluble in chloroform. The drug is stable at ambient temperature and humidity and its melting point is 190–195 °C. Each tablet contains 2.5-20 mg of the active ingredient (8-64 μmol), i.e. a D_o value of 2 at the highest dose, thus making OLN a low solubility drug. This suggested the possibility of developing more soluble solid forms of this lipophilic drug (cLogP = 3.39). Olanzapine molecule has a central seven-membered diazepine ring which is fused with benzene, a thiophene and an N-methyl-piperazine substituent ring. The boat

conformation of the central 1,5-diazepine ring defines the overall butterfly shape of the molecule, but the N-methyl-piperazine ring can have conformational variation. Two butterfly like molecules form centrosymmetric dimers stabilized by C–H···π interactions between their cavities. In patent literature total six forms of the drugs are claimed[8] and characterized by XRPD, but so far only the form-II crystal structure is reported[9] in the Cambridge Structure Database (CSD).[10] Olanzapine is a dibasic molecule with pK_a 7.37 and 4.69 corresponding to the N3 of piperazine and N1 of diazepine ring, respectively. Therefore according to the ΔpK_a rule[11] it should form salts with acids of $pK_a < 5$ (Table 1).
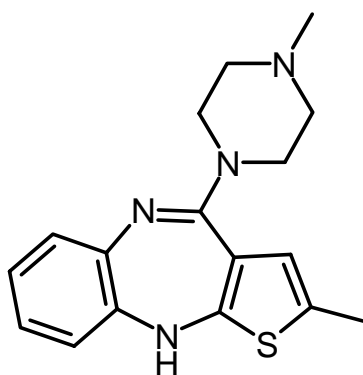
Figure 2 Molecular structure of Olanzapine

Table 1 pK_a values of Olanzapine[12] and acids[13] used in this study.

Molecule	pK_a value	Product complex	ΔpK_a value
Olanzapine	7.37, 4.69	Olanzapine and maleic acid 1:1	5.45
Maleic acid	1.92, 6.27	Olanzapine and maleic acid 1:2	5.45, 2.77
Malonic acid	2.83, 5.69	Olanzapine malonic acid 1:1	4.54
Fumaric acid	3.03, 4.44	Olanzapine and fumaric acid	4.34
PABA	4.65	Olanzapine and PABA	2.72
Salicylic acid	2.97	Olanzapine and Salicylic acid	4.4

A few salts of Olanzapine were reported in patent literature.[14] Two salts Olanzapinium nicotinate and benzoate were reported by Ravikumar et al.[15] The free base Olanzapine also has the tendency to form solvates and cocrystals.[16] Dihydrate polymorphs, higher hydrate, methanol hydrate, ethanol hydrate, buthanol hydrate, THF hydrate, dichloromethane, etc. solvates were reported in the literature by several groups like Koziol, Ravikumar, Larsen, Byrn, etc.[9b,17] All the reported salts and solvates contains the Olanzapine dimer motif. Few salts of Olanzapine base with acids like malonic acid, maleic acid, fumaric acid, salicylic acid, p-amino benzoic acid were prepared in order to improve the solubility and dissolution behavior of this Class II drug, and also to study structure-solubility relationship. Along with the salts of Olanzapine some solvates with ethanol, acetone, acetonitrile, etc. were obtained. Basing on the mechanochemistry method two amorphous forms of Olanzapinium maleate salts were prepared by us.[18] The preparation and characterization of these amorphous salt forms was discussed in Chapter 5. On an attempted cocrystallization of Olanzapine with nicotinamide in 1:1 ratio, form IV crystal structure of Olanzapine was obtained.

4.3 STRUCTURAL ANALYSIS

OLANZAPINE FORM IV 28

On cocrystallization of Olanzapine with nicotinamide in 1:1 ratio block shaped pale yellow crystals of Olanzapine form IV **28** in space group $P2_1/c$ were obatined. The asymmetric unit contains one molecule of Olanzapine, having a single hydrogen bond donor, N4–H, and two acceptors, the imine N1 and piperazine N3, which are exposed in the crystal building blocks to near neighbor dimers. In the crystal structure of form II, N–H⋯N hydrogen bond interaction between the N4–H and imine N1 links the crystal building blocks into two-dimensional layers. These sheets stack on one another to give the 3D structure. The piperazine N3 does not participate in hydrogen bonding in this crystal form. The crystal structure of the form IV is almost similar to the reported form II (in some literature named as form I). In this form IV the N–H⋯N hydrogen bond is slightly longer than the form II structure. But both the form II and form IV structures have the same centrosymmetric dimer,

which is stabilized by weak C–H⋯π interaction between the N-methylpiperazine fragment and the phenyl/ thiophene system. Theoretical calculation reported in the literature stated that total C–H⋯π binding energy was about 8 kcal mol^{-1}.[17a] In the two structures the packing of the dimer motif is completely different, form II consists of parallel dimer whereas form IV has herringbone type arrangement of the neighboring dimers (Figure 3).
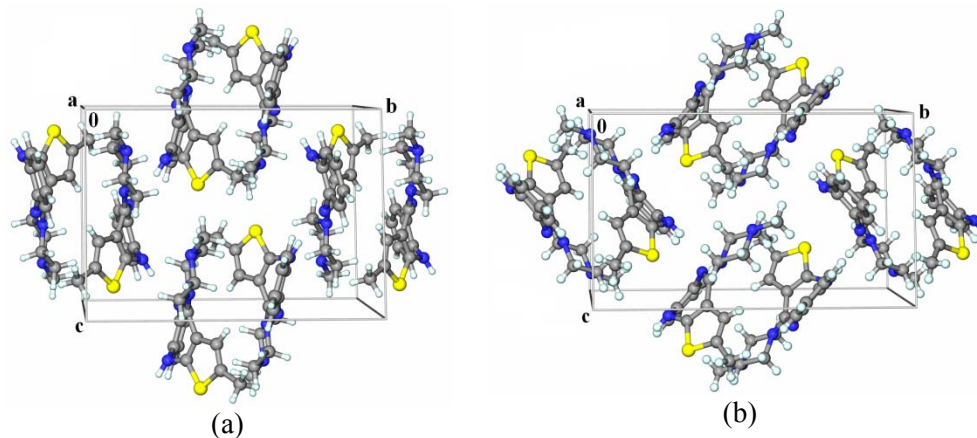

Figure 3 (a) Parallel stacking of the Olanzapine dimer in form II crystal structure. (b) Herringbone type of arrangement of the dimer in Olanzapine form IV **28** structure.

OLANZAPINIUM HYDROGENMALONATE (1:1) SALT 29

Olanzapinium hydrogenmalonate salt was prepared by crystallization of Olanzapine and malonic acid in 1:1 ratio from ethyl acetate-acetone mixture solvent. In crystal structure **29**, one proton of malonic acid is transferred to N3 of the piperazine ring (N$^+$–H⋯O$^-$) of Olanzapine molecule. The malonic acid molecule is connected to two Olanzapine molecule through bifurcated N–H⋯O$^-$/ N$^+$–H⋯O$^-$ hydrogen bond to give a cyclic synthon with graph set notation[19] $R_4^2(22)$. Two such units are connected to each other through C–H⋯π interactions between two Olanzapine molecules to give the dimer synthon (Figure 4). The second carboxylic hydrogen of the malonic acid molecule forms intramolecular hydrogen bonding with the carboxylate O atom with a graph set notation of $S(6)$.
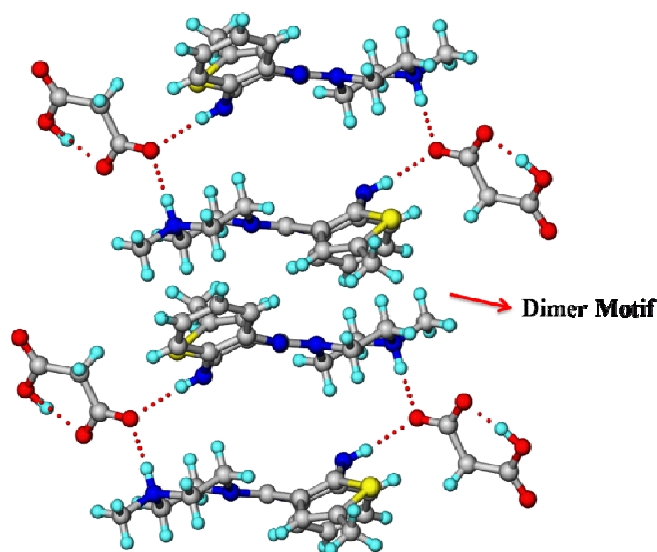
Figure 4 Bifurcated N–H⋯O⁻/ N⁺–H⋯O⁻ hydrogen bond between two Olanzapinium and one malonate ion. Two such cyclic synthons were connected by the Olanzapine dimer synthon.

Mechanical grinding of Olanzapine with maleic acid in two different ratios 1:1 and 1:2 resulted in salts of Olanzapinium monomaleate and dimaleate respectively. Liquid assisted grinding gave the crystalline salt whereas neat grinding resulted in the corresponding amorphous salts.[18] The analysis of these two salts was discussed in Chapter 5.

OLANZAPINIUM DIMALEATE MONOFUMARIC ACID (1:2:1) SALT COCRYSTAL 30

As Olanzapine is a dibasic molecule and forms dimaleate salt, with the idea of preparing a ternary cocrystal/ salt,[20] Olanzapine was crystallized with maleic and fumaric acid in 1:0.5:1 ratio from ethyl acetate-acetone-nitromethane mixture solvent. The resulting material is a salt cocrystal **30** of Olanzapinium dimaleate monofumaric acid (1:2:1). In the crystal structure **30**, two protons were transferred from two symmetry independent maleic acid molecule to imine N1 position of the diazepine ring and piperazine N3 of Olanzapine molecule. One of the maleate ion is bifurcated to the imine N1 (N⁺–H⋯O⁻) and N4 (N–H⋯O⁻) of the diazepine ring (Figure 5) to give a cyclic synthon with graph set notation

$R_4^2(14)$. The second maleate ion is connected to N3 of the piperazine ring (N⁺–H···O⁻) with a discrete *D* hydrogen bond motif. The two symmetry independent half fumaric acid molecules act as connectors which link two Olanzapinium maleate motifs through O–H···O hydrogen bond. In one of the fumaric acid molecule the carboxylic proton is shared by both fumaric and maleate ion (hydrogen bonded to N3 of piperazine ring), is a case of partial proton transfer. Therefore this structure can be considered as a salt cocrystal. The common Olanzapine dimer motif is absent in this crystal structure **30**. This is a first case of maleic acid and fumaric acid coformers in a ternary cocrystal.
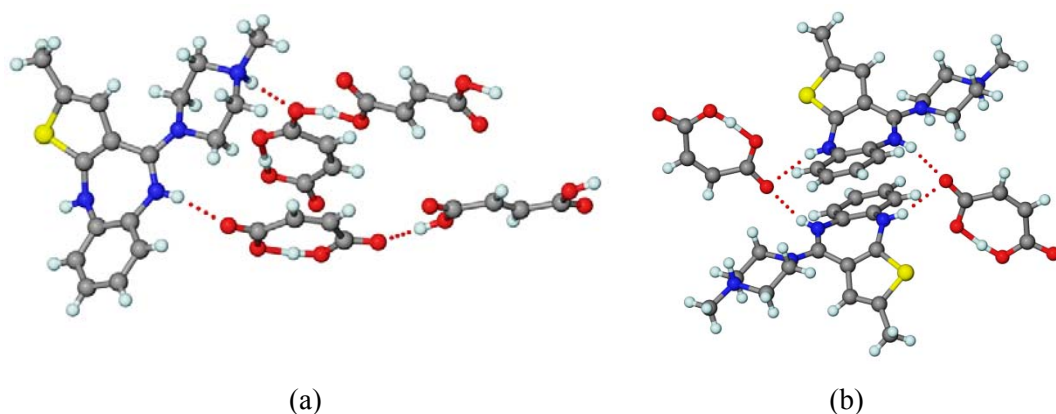

(a)   (b)

Figure 5 (a) Two symmetry independent maleate ions connected to Olanzapinium dication through N⁺–H···O⁻ hydrogen bond further bonded to two fumaric acid molecules via O–H···O hydrogen bonding. (b) Bifurcated maleate ion connects two Olanzapinium dications.

OLANZAPINIUM p-AMINOBENZOATE HEMIHYDRATE (1:1:0.5) SALT HYDRATE 31

On crystallizing Olanzapine and p-aminobenzoic acid (PABA) in 1:1 ratio from acetonitrile solvent, a hemihydrate salt of Olanzapine-PABA in 1:1:0.5 ratio was obtained. The occupancy of the water molecule is fixed at 0.5 because the isotropic displacement for the water O atom is large (0.1032(13) Å²) compared to the other heavy atom (O2 of 0.0209(4) Å²) and also the R-factor drops down when the occupancy of the water is fixed at 0.5. In crystal structure **31**, a proton is transferred from the carboxyl group of PABA to the piperazine N3 of Olanzapine molecule. Both the carboxylate and carbonyl O are bifurcated; carboxylate O to N3 of piperazine ring (N⁺–H···O⁻) and water (O–H···O⁻) molecule and the

carbonyl O to N4 of the diazepine ring (N–H···O) and amino group (N–H···O) of a second PABA molecule (Figure 6). In this salt hydrate **31**, the common Olanzapine dimer synthon is present similar to most of the salts and solvates reported in the literature and discussed here.
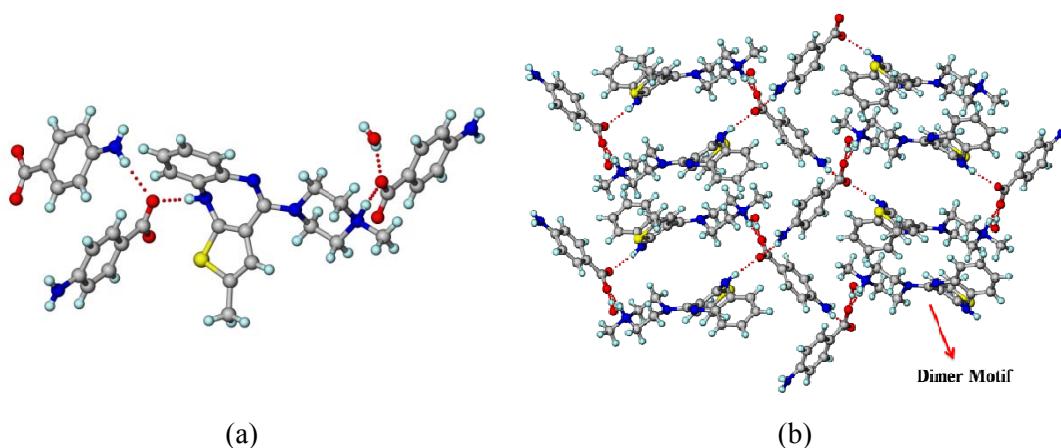

| (a) | (b) |

Figure 6 (a) N–H···O⁻/ N⁺–H···O⁻ and O–H···O⁻ hydrogen bond connecting the PABA and water molecule to Olanzapinium ion. (b) 3D packing of the salt hydrate **31** showing the common Olanzapine dimer motif.

OLANZAPINIUM SALICYLATE BENZENE (1:1:1.5) SALT SOLVATE 32

Olanzapine salicylate benzene (1:1:1.5) salt solvate **32** was obtained on crystallizing 1:1 mixture of Olanzapine and salicylic acid from benzene solvent. Apart from benzene, all common laboratory solvents like methanol, ethanol, acetone and ethyl acetate, etc. resulted in pasty material. The asymmetric unit of the crystal structure **32** consists of one Olanzapinium, one salicylate ion, one full and an inversion related half molecule of benzene. A proton is transferred from the carboxyl group of salicylic acid to the piperazine N3 (N⁺–H···O⁻) of Olanzapine molecule and the carbonyl O is hydrogen bonded to N4 of diazepine ring forming a cyclic synthon with graph set notation $R_4^4(26)$ (Figure 7a). The adjacent cyclic motif is close packed via C–H···π interaction of the Olanzapine dimer. In 3D packing, the Olanzapine dimer forms a layer with flanking salicylate ion on both ends. The cavities formed by the Olanzapine dimer and the salicylate molecules are occupied by the two symmetry independent benzene molecules (Figure 7b).
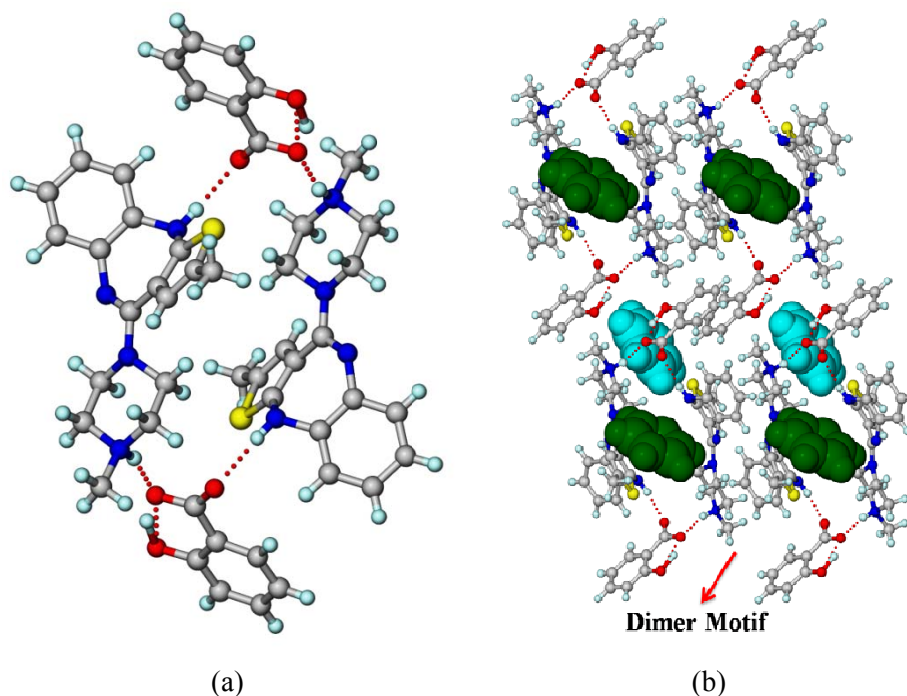
<div align="center">(a)   (b)</div>

Figure 7 (a) Cyclic $R_4^4(26)$ synthon formed by two Olanzapinium and salicylate molecules with the help of N–H⋯O/ N$^+$–H⋯O$^-$ hydrogen bond. (b) 3D packing of the salt solvate **32** with the Olanzapine dimer synthon and two symmetry independent benzene solvent molecules (green and light blue) occupying the void space.

OLANZAPINE SOLVATES

OLANZAPINE ACETONE MONOHYDRATE (1:0.5:1) 33

Crystallizing Olanzapine in acetone solvent yielded block shaped crystals of acetone monohydrate solvate **33** in *C*2/*c* space group. The water molecule is hydrogen bonded to two different Olanzapine molecules, one to N3 of piperazine and the other to N4 of diazepine ring through O–H⋯N and N–H⋯O hydrogen bonds respectively. The packing is driven by the spatial complementarity of the opposite enantiomers of two Olanzapine molecule forming a dimer through C–H⋯π interaction. The Olanzapine dimer aligned orthogonally to each other forming a layer parallel to the (100) plane and the water molecule occupies the sites between the Olanzapine dimers. The acetone molecules are sit between two Olanzapine

dimer layers along with the water molecules (Figure 8). The Olanzapine dimer motif of the next layer is orthogonal to each other, shown in Figure 8c.

(a)

(b)   (c)
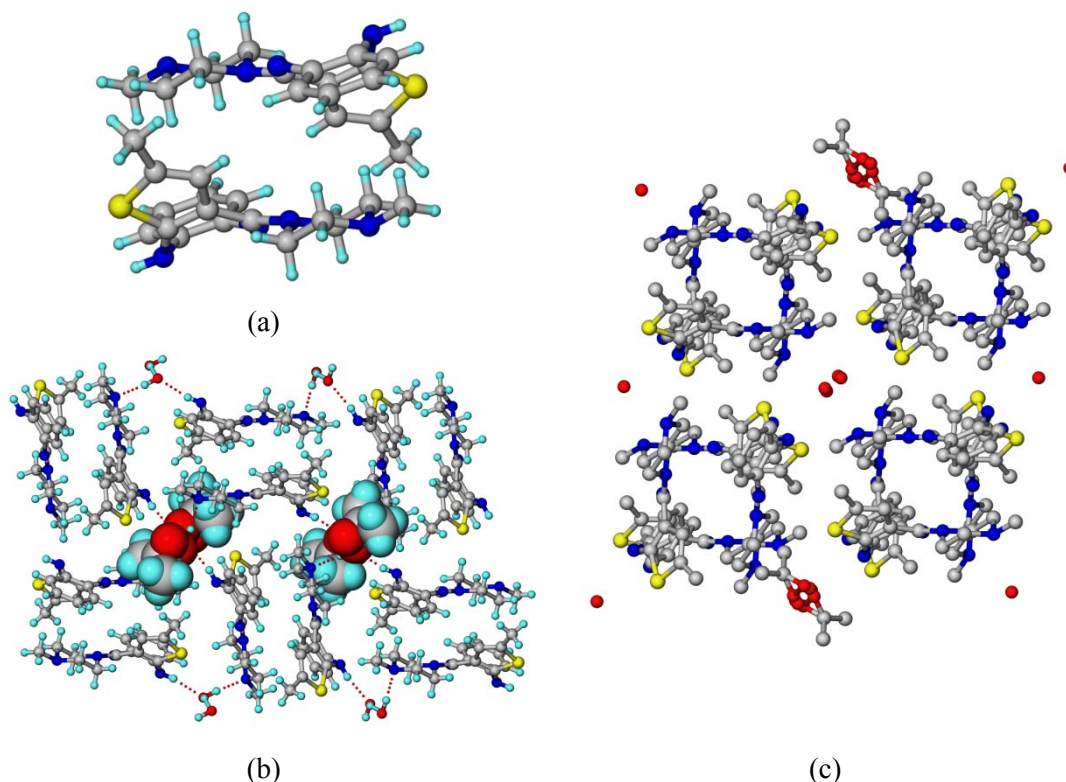
Figure 8 (a) Olanzapine dimer synton. (b) water and acetone solvent associated via hydrogen bond with the Olanzapine molecule. (c) Two Olanzapine dimers stacked orthogonally with the water and acetone molecules occupying the void space (hydrogen atoms are removed for clarity).

Olanzapine acetonitrile monohydrate **34**, ethanol monohydrate (1:0.5:1) **35** and Olanzapine nitromethane monohydrate **36** solvates were prepared similarly by crystallizing with acetonitrile, ethanol and nitromethane respectively. All the solvates solved in *C*2/*c* space group having similar cell values and are isostructural with the acetone monohydrate solvate **33**. The packing diagrams of the solvates are shown in Figure 9. The Olanzapine ethanol monohydrate solvate **35** is different from the crystal structure reported earlier by Koziol et al.,[17a] with stoichiometry 2:1:2. As mentioned by Byrn et al.,[9b] it is isostructural to the higher hydrate reported by them. The reported ethanol hydrate has Olanzapine dimer

parallel to each other, whereas structure **35** has orthogonal arrangement of the dimer motif with ethanol and water molecules occupying the cavity (Figure 9c and 9d).

(a)   (b)

(c)   (d)
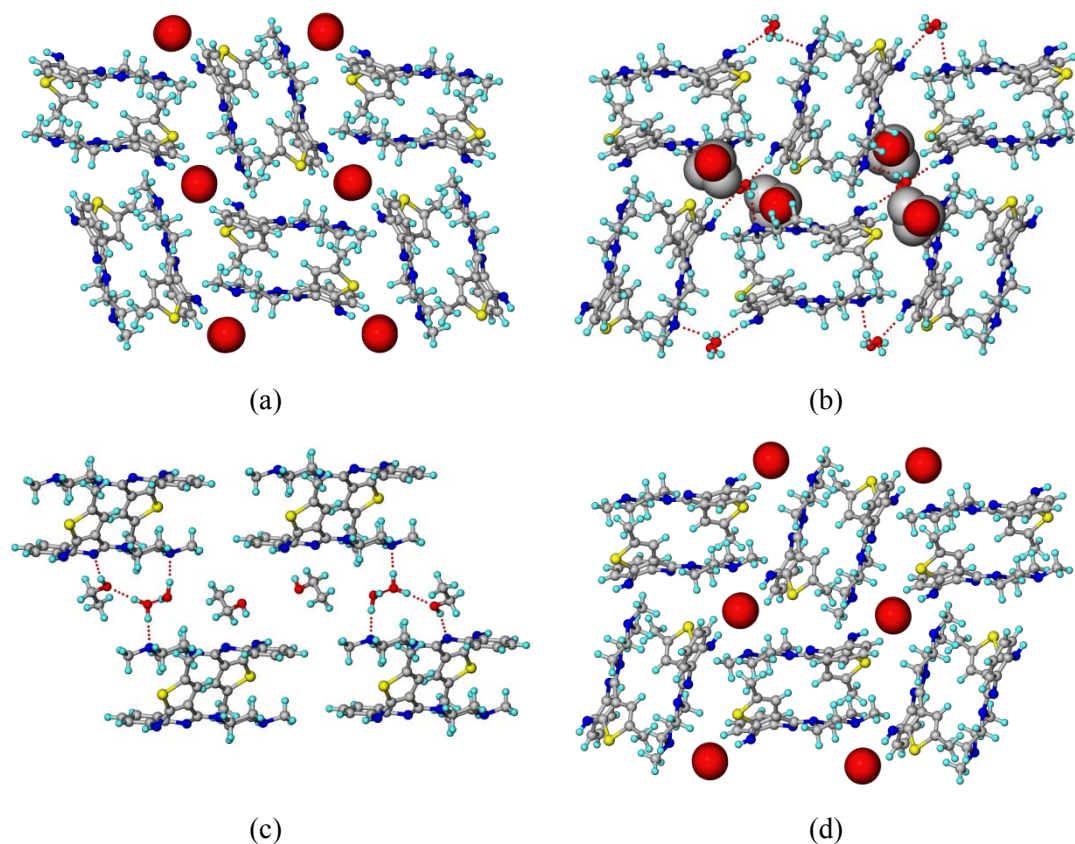
Figure 9 3D packing of the (a) Olanzapine acetonitrile hydrate **34**, (b) ethanol hydrate polymorph **35**, (c) ethanol hydrate (reported) and (d) nitromethane hydrate **36** with the Olanzapine dimer motif.

4.4 Solvent Assisted Grinding and XRPD Analysis

Mechanochemistry[21,20c] has been successfully applied to the synthesis of systems based on covalent, coordination and supramolecular bonds. The earliest example of mechanochemical cocrystallization dates from 1893 with the formation of the quinhydrone cocrystal from equimolar amounts of *p*-benzoquinone and hydroquinone.[22] The effects of solubility and solvent competition can be avoided in grinding methodology compared to solution

crystallization. Neat grindging and liquid assisted grinding[23] are the two methods used for cocrystallization via mechanochemistry. Neat grinding consists of mixing the coformers together and grinding them either manually using a mortar and pestle, or mechanically, using a ball mill or a vibratory mill. The second technique known as liquid assisted grinding (or kneading) requires a small (catalytic) amount of an additional liquid along with the coformers. Both these grinding techniques have been established as highly efficient methods for preparing cocrystals, salts, and polymorphic forms of pharmaceutical compounds and the same are used for the preparation of Olanzapinium salts. Apart from solution crystallization, macroscopic amounts of the salts are prepared through acetonitrile-assisted grinding. The materials were grounded thoroughly for about 15–20 minute and the XRPD was recorded. The XRPD of the materials matches with the calculated powder pattern of the corresponding salts (Figure 10). In case of Olanzapinium salicylate the experimental XRPD pattern does not match with the calculated one as the corresponding structure **32** is a benzene solvate.
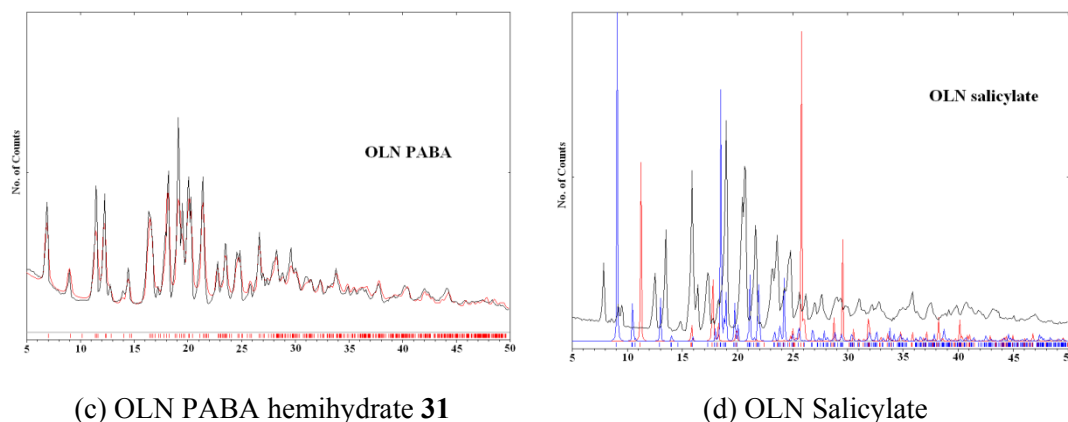

(a) OLN Form IV **28**   (b) OLN Malonate **29**

(c) OLN PABA hemihydrate **31**   (d) OLN Salicylate
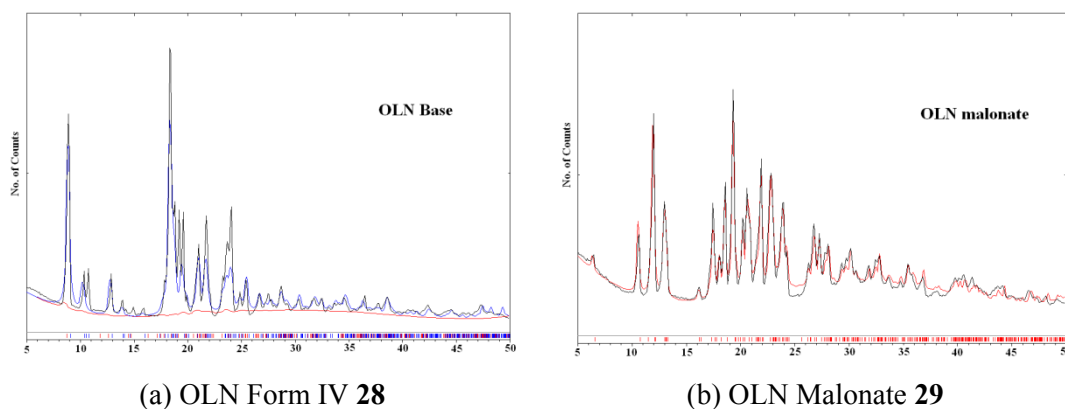
Figure 10 Overlay of the calculated X-ray crystal structure (red and blue) and experimental XRPD pattern (black) of the bulk material. (a) OLN form IV matches with the calculated pattern of **28**. (b) OLN malonate **29**. (c) OLN PABA hemihydrate **31**. (d) OLN salicylate with calculated **28** (blue) and salicylic acid (red) patterns respectively.

4.5 SPECTROSCOPIC AND THERMAL ANALYSIS

Olanzapine base and the carboxylic acid salts were further confirmed with FT-IR, NIR and Raman spectroscopy. For FT-IR spectroscopy peak shift of 10–15 cm^{-1} due to the formation of hydrogen bond indicates the formation of salt/ cocrystal. A neutral carboxylic acid group (–COOH) normally displays a strong C=O stretching band around 1700 cm^{-1} and a weaker C–O stretch around 1200 cm^{-1}, while for a carboxylate anion (–COO⁻) due to resonance, the observed peak is only a single C–O stretch in the fingerprint region of 1000–1400 cm^{-1}.[24] For a dicarboxylic acid with one proton transfer the peak around 1700 cm^{-1} indicates the presence of an unionized carboxylic group whereas for monoacid like **31**, Olanzapinium salicylate and nicotinate, the absence of this peak is a clear indication of salt formation. FT-IR, NIR and Raman spectra of the corresponding Olanzapinium salts respectively are shown in Figures 11, 12 and 13.
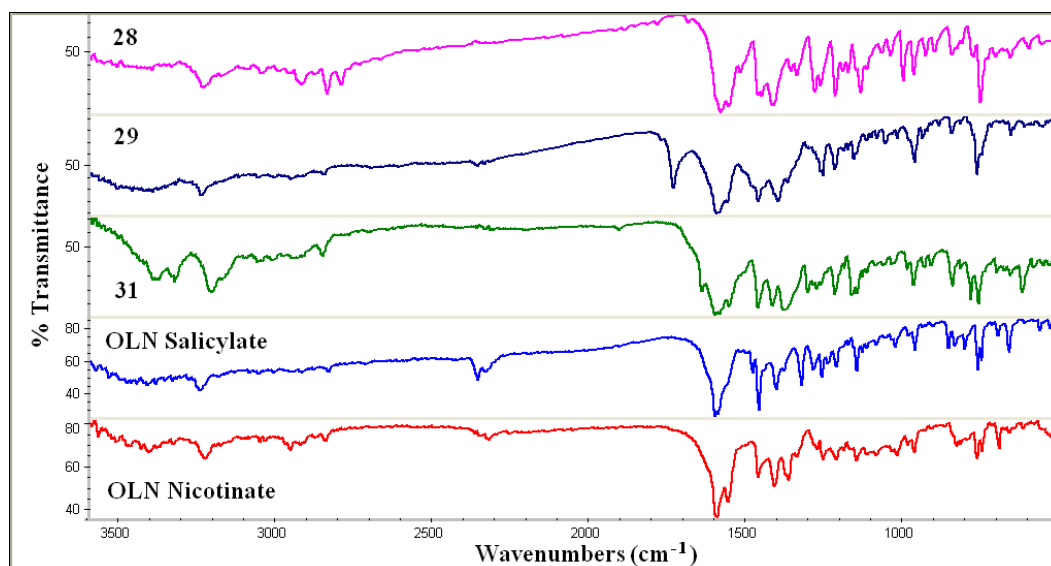
Figure 11 FT-IR spectra of Olanzapine **28** and Olanzapinium salts **29**, **31**, salicylate and nicotinate. Spectral region from 3500–500 cm^{-1}.
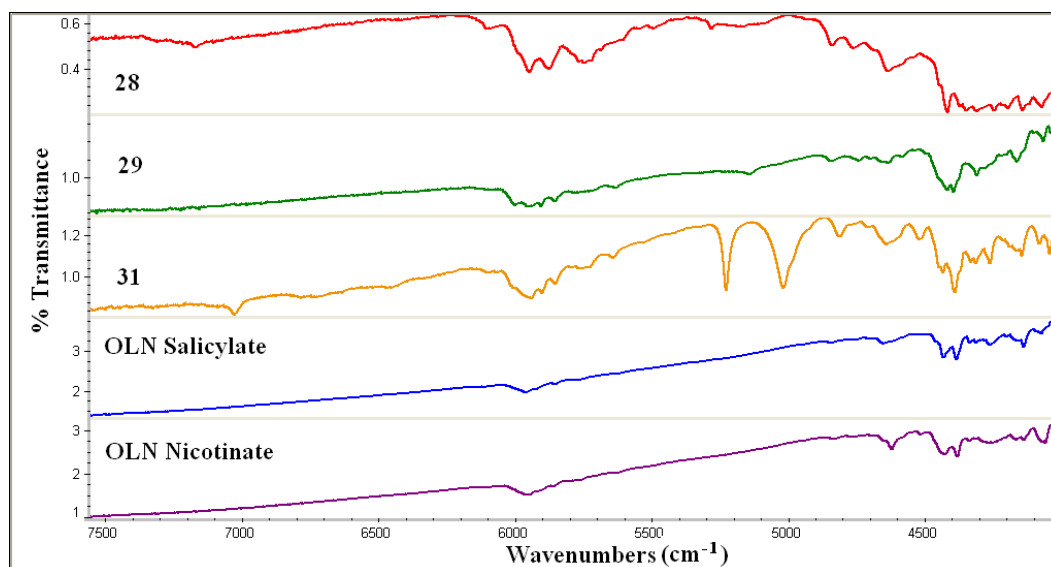
Figure 12 FT-NIR spectra of Olanzapine **28** and Olanzapinium salts **29**, **31**, salicylate and nicotinate. Spectral region from 7500–4000 cm^{-1}.
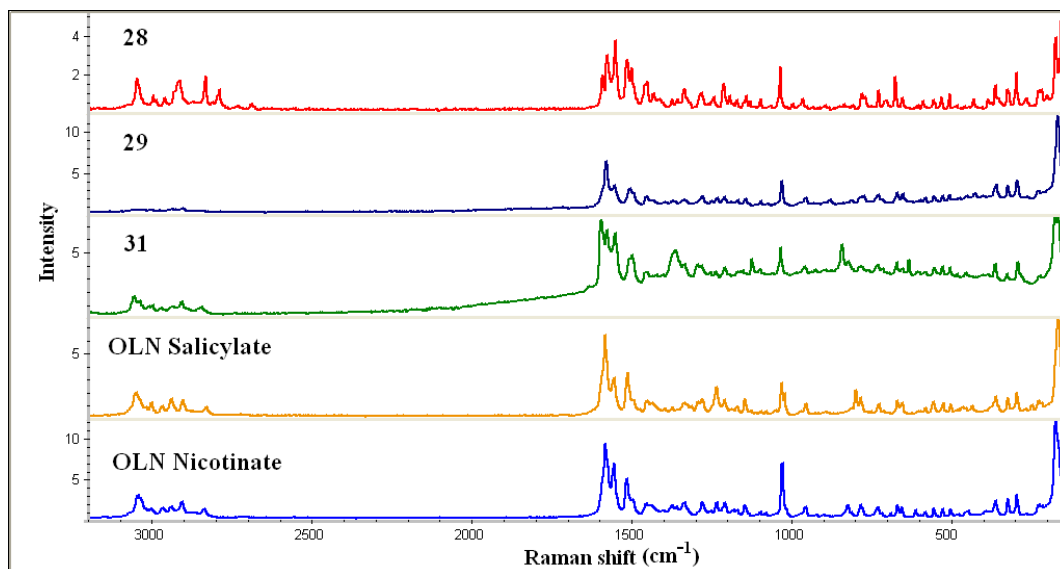
Figure 13 FT-Raman spectra of Olanzapine **28** and Olanzapinium salts **29**, **31**, salicylate and nicotinate. Spectral region from 3200–450 cm^{-1}.

The hydrogen bond distances and symmetry codes are listed in Table 2.

Table 2

Interaction	H···A/ Å	D···A/ Å	∠D–H···A/ °	Symmetry code
Olanzape form IV **28a**				
N4–H4··· N1	2.32	3.176(2)	165.7	x,1/2–y,1/2+z
Olanzapinium Hmalonate **29**				
N3$^+$–H3···O1$^-$	1.83	2.697(2)	167.4	---[a]
O3–H3A···O2	1.62	2.521(3)	155.7	---[b]
N4–H4···O1$^-$	2.09	2.898(2)	168.8	2–x,1–y,2–z
C15–H15B···N4	2.56	3.484(3)	158.6	2–x,1–y,2–z
C16–H16A···O4	2.53	3.483(4)	165.7	2–x,1–y,1–z
C18–H18B···N1	2.30	2.684(2)	102.3	---[b]
Olanzapinium dimaleate monofumaric acid **30**				
N1$^+$–H1···O4$^-$	2.08	2.819(6)	162.1	---[a]

N3$^+$–H3···O8$^-$	1.93	2.789(6)	140.9	---[a]
N4–H4···O3	2.36	3.108(6)	145.6	1−x,1−y,−z
N4–H4···O4$^-$	2.39	3.212(6)	159.4	1−x,1−y,−z
O6–H6···O7	1.46	2.472(7)	177.3	---[b]
O8$^-$–H9···O9	1.36	2.652(6)	167.1	---[a]
O8$^-$–H9···O10	2.58	3.518(6)	126.7	---[a]
O11–H11A···O1	1.69	2.573(7)	162.7	x,1+y,z
C8–H8···O2	2.44	3.294(6)	153.3	−1+x,1+y,z
C10–H10C···O4$^-$	2.58	3.379(7)	141.0	x,1+y,z
C16–H16B···O12	2.30	2.979(7)	126.7	---[a]
C19–H19B···O10	2.52	3.358(6)	145.3	−x,1−y,1−z
C19–H19C···O10	2.58	3.521(7)	167.6	---[a]
C31–H31···O11	2.41	2.738(9)	100.5	1−x,1−y,1−z

Olanzapinium p-aminobenzoate hemihydrate **31**

N3$^+$–H3A···O1$^-$	1.53	2.589(2)	171.6	1−x,1−y,−z
N3$^+$–H3A···O2	2.57	3.294(2)	125.2	1−x,1−y,−z
O3–H3B···O1$^-$	2.10	2.825(4)	154.7	1−x,1−y,−z
N4–H4A···O2	2.00	2.884(2)	176.3	−1+x,y,z
N5–H5A···N1	2.27	3.101(2)	167.3	---[a]
N5–H5B···O2	2.16	3.017(2)	166.2	1−x,−1/2+y,1/2−z
C10–H10C···O3	2.48	3.307(4)	141.7	−1+x,y,z
C12–H12···N4	2.59	3.447(2)	150.5	−x,−1/2+y,1/2−z
C17–H17A···O3	2.55	3.269(4)	129.7	---[a]
C18–H18A···N1	2.37	2.722(2)	100.1	---[b]

Olanzapinium salicylate benzene **32**

N3$^+$–H3···O1$^-$	1.84	2.685(5)	159.3	1−x,−y,−z
N4–H4···O2	2.02	2.861(4)	165.6	---[a]
C18–H18A···N1	2.29	2.663(4)	100.8	---[b]
C29–H29···O2	2.40	3.247(6)	148.6	---[a]
C32–H32···O1$^-$	2.50	3.273(6)	138.4	x,1+y,z

Olanzapine acetone water **33**

O2–H2A···O2	1.97	2.901(5)	158.6	1/2−x,3/2−y,1−z
N4–H4···O2	2.08	2.918(3)	168.6	---[a]

Olanzapine ethanol water **35**

O2–H2B···O1	2.30	2.996(6)	131.3	x,1−y,1/2+z
N4–H4···O2	1.97	2.893(4)	165.6	---[a]

[a] molecules/ ions in the same asymmetric unit
[b] intra molecular H bond

Differential scanning calorimetry (DSC) is an important technique to determine phase behavior of polymorphs and to characterize materials.[25] The DSC thermograms of the Olanzapine form II and IV show that form IV converted to form II indicated by the small endotherm (Figure 14a). The phase transition of form IV→II at 122 °C means that form IV and form II are enantiotropically related and Olanzapine form II melts at around 192 °C. Similar events were seen under a hot stage microscope (HSM) (Figure 15). The Olanzapinium salts **29**, **31** and salicylate were further confirmed by their DSC thermograms which show higher melting temperature than the individual components. The DSC thermogram of Olanzapinium dimaleate monofumaric acid salt cocrystal **30** could not be recorded as the XRPD of the material obtained from manual grinding of the stoichiometric components did not match with the calculated pattern of the crystal structure **30**. The DSC thermograms of Olanzapinium salts are shown in Figure 14.

(a)   (b)

(c)

(d)
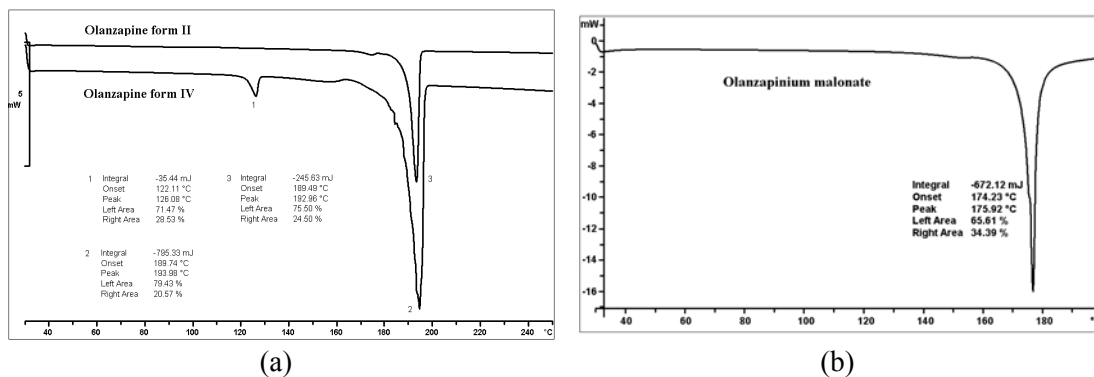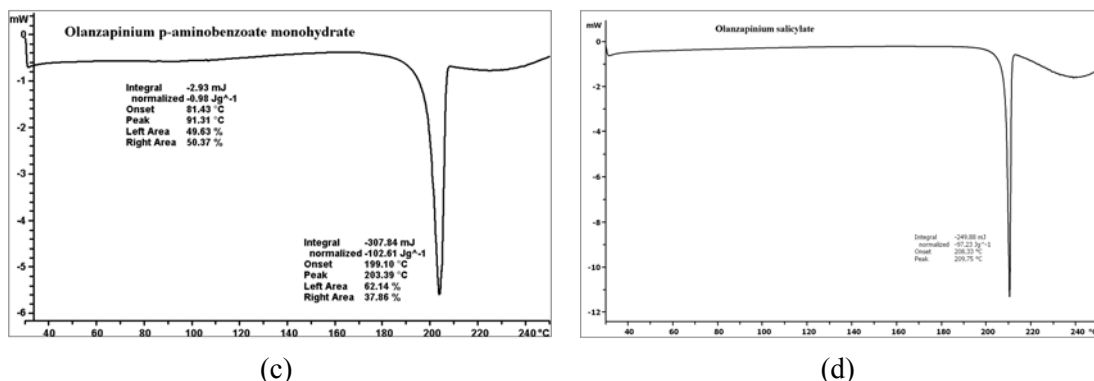
Figure 14 DSC of Olanzapine form IV **28** crystals along with **29**, **31** and Olanzapinium salicylate powder material.

25 °C

120 °C

122 °C

125 °C

179 °C
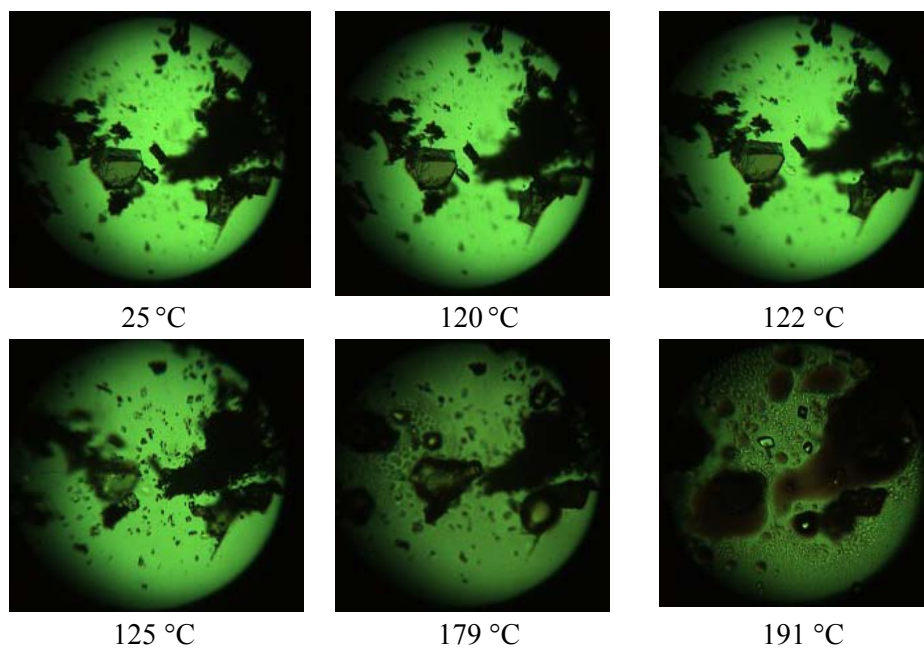
191 °C

Figure 15 HSM snapshots of Form IV material **28** at different temperatures. Material sublimes at 125 °C correspond to form II, with melting at 191 °C.

The lattice energy calculation (Cerius^2) of the two forms of Olanzapine shows that Olanzapine form II is stable than the form IV by 1.507 kcal mol^{-1}. This is further supported by the crystal density and packing fraction given in Table 3.

Table 3 Lattice energy, crystal density and packing fraction of the two polymorphs

Polymorph	Lattice Energy (Dreiding) (kcal mol^{-1})	Crystal Density (g cm^{-3})	Packing Fraction (%)
Form II (298 K)	–41.298	1.296	67.7
Form IV **28a** (298 K)	–39.791	1.279	66.4

4.6 SOLUBILITY AND DISSOLUTION

The key stage in the development of a new drug begins from optimization of lead compound properties through early stage clinical trials. During this phase, one of the important physicochemical parameters optimized is solubility of the API, and consequently, the dissolution rate. Therefore a proper understanding of these intrinsic properties can impact on formulation design and speed of progression through development. Thus, measuring and understanding solubility and dissolution rate of a new API in early development provides a good indication of the associated risks.[26] Based on its solubility (43 mg/L in water) Olanzapine comes under Class II category of the Biopharmaceutical Classification System (BCS).

Improvement of dissolution rate of weakly acidic or weakly basic drugs that are poorly soluble is one of the primary reasons for preparation of pharmaceutical salts. Therefore various salts of Olanzapine with malonic acid, maleic acid, fumaric acid, p-aminobenzoic acid, salicylic acid and nicotinic acid etc. were prepared in order to improve and control the solubility and therefore the dissolution rate of the drug. The dissolution profile of Olanzapine salts is shown in Figure 16.
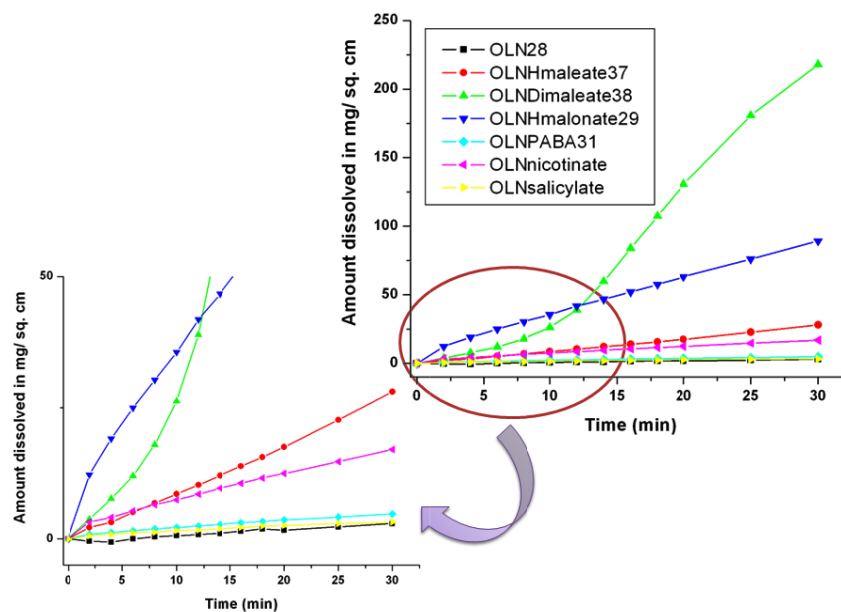
(a) Plot of amount dissolved per unit area vs. time
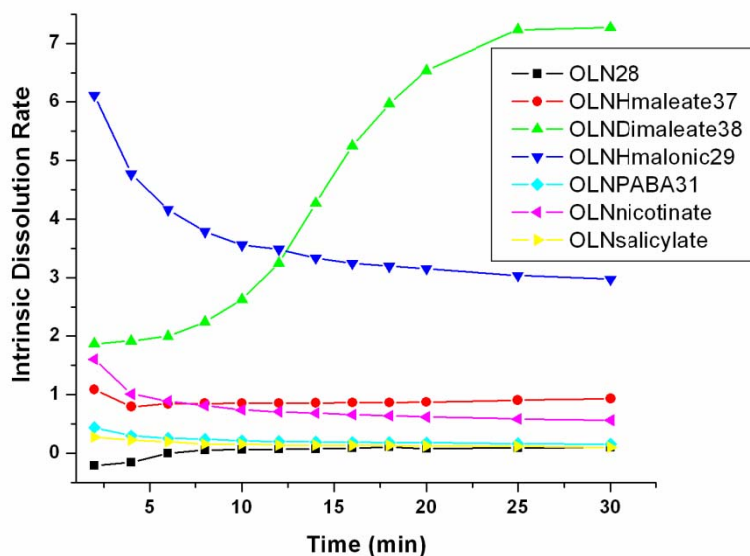
(b) Plot corresponding to IDR vs. time

Figure 16 (a) Dissolution profiles of crystalline OLN **28**, OLN monomaleate **37**, OLN dimaleate **38**, OLN malonate **29**, OLN PABA hemihydrate **31**, OLN nicotinate, OLN salicylate in distilled water. (b) IDR vs. time curve of the corresponding salts.

From the solubility and dissolution profiles it is seen that Olanzapinium dimaleate **38** (7.23 mg/cm^2/min) salt is having the highest intrinsic dissolution rate (IDR) followed by malonate salt **29** (3.04 mg/cm^2/min) and then Olanzapinium monomaleate **37** (0.91 mg/cm^2/min) and nicotinate (0.59 mg/cm^2/min). The IDR of PABA hemihydrate **31** (0.17 mg/cm^2/min) and salicylate (0.12 mg/cm^2/min) are equal to the pure base **28** (0.09 mg/cm^2/min) after an interval of 25 min (Figure 16b). Berge et al.,[2a] stated that in general, salt combinations with monocarboxylic acids are insoluble in water compared to dicarboxylic acids if one carboxylic group is free, and this phenomenon is also observed in the series of Olanzapinium salts studied. In some cases, salt used to precipitate out which decreases the solubility and dissolution rate. Therefore it is important to characterize the material by XRPD after the dissolution experiment in order to establish the stability of the salt. The XRPD of Olanzapinium salts after the dissolution experiment (Figure 17) reveal that they are stable under the experimental conditions.[27]
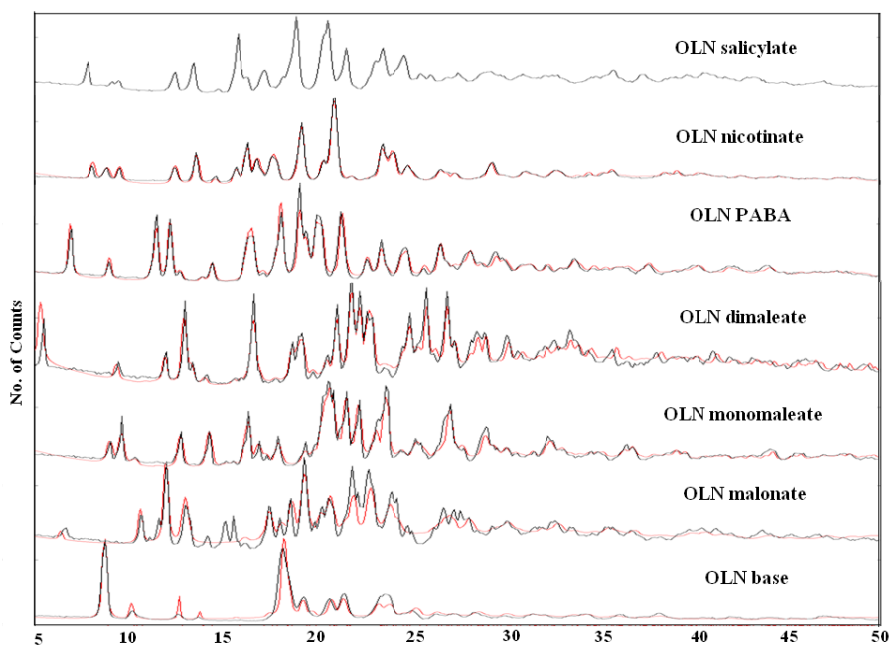

Figure 17 XRPD patterns of the samples of Olanzapine base **28** and the crystalline salts **29**, **37**, **38**, **31**, nicotinate and salicylate after the dissolution experiment and overlay of the

calculated lines from the crystal structure confirm that the salts were stable during the dissolution experiment.

4.7 CONCLUSION

Polymorphism, salt forms and solvates of Olanzapine was studied. So far in the CSD only form II structure is deposited but during cocrystallization of Olanzapine with nicotinamide, form IV crystal structure was solved and the phenomenon is not unusual as several reports are there in the literature.[28] Structurally both the form II and IV are similar with centrosymmetric dimer as the major synthon. Binary salts of Olanzapinium malonate, ternary Olanzapinium dimaleate monofumaric acid salt cocrystal, Olanzapinium p-aminobenzoate hemihydrate, Olanzapinium salicylate benzene salt solvates were discussed from their structural analysis. The butterfly like thienobenzodiazepine ring is conformationally rigid, but the N-methyl-piperazine part of the molecule has conformational variation as seen from the overlay diagram (Figure 18) of crystal structures. But this conformational variation hardly affects the crystal packing, as the dimer motif is observed in all salts and solvate structures (except salt **30** and **38**).
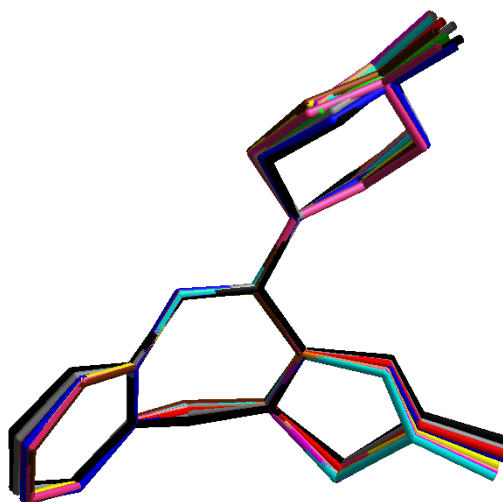

Figure 18 Molecular overlay for the Olanzapine conformers in the crystal structures. Olanzapine form II (red); form IV **28** (blue); **29** (brown); **30** (dark grey); **31** (green); **32**

(yellow); **33** (sky blue); **34** (magenta); **35** (orange); **36** (light brown); **37** (pink) and **38** (black). H atoms of the molecules are excluded for clarity.

The Olanzapinium salts were further characterized by XRPD, vibrational spectroscopy (FT-IR, FT-NIR, FT-Raman) and thermal methods (DSC and HSM). The proton transfer in all the Olanzapine crystal structures is consistent with the rule of 3. The solubility and dissolution study of the corresponding Olanzapinium salts reveal significant improvement for maleate and malonate salts (diacids) compared to the salicylate or p-aminobenzoate salts (monoacids). However, IDR is almost equal to the basic drug for the latter two cases. The salt formation to improve the physico-chemical properties is well appreciated in the pharmaceutical literature. The physico-chemical study of Olanzapinium salts is not studied till date.

4.8 EXPERIMENTAL SECTION

X-RAY CRYSTALLOGRAPHY

X-ray reflections for all compounds were collected at 298 K (crystal structure **28**, **31** and **32** at 100K) on Bruker SMART APEX CCD equipped with a graphite monochromator and Mo-Kα fine-focus sealed tube (λ = 0.71073 Å). Data integration was done using SAINT.[29] Intensities for absorption were corrected using SADABS.[30] Structure solution and refinement were carried out using Bruker SHELXTL.[31] The hydrogen atoms were refined isotropically and the heavy atoms were refined anisotropically. N–H and O–H hydrogens were located from difference electron density maps and C–H hydrogens were fixed using HFIX command in SHELXTL. Disordered solvent molecules acetonitrile and nitromethane in Olanzapine acetonitrile hydrate **34** and Olanzapine nitromethane hydrate **36** respectively were removed by SQUEEZE in PLATON. Crystallographic data are summarized in Appendix. Packing diagrams were prepared in X-Seed.[32]

X-RAY POWDER DIFFRACTION

X-ray powder diffraction of all samples were recorded on Bruker D8 Advance diffractometer using Cu-Kα X-radiation (λ = 1.54056 Å) at 40 kV and 30 mA. Diffraction patterns were collected over a 2θ range of 5-50° at a scan rate of 1° min^{-1}. Powder Cell 2.4 was used for Rietveld refinement.[33]

VIBRATIONAL SPECTROSCOPY

Nicolet 6700 FT-IR spectrometer with an NXR FT-Raman module was used to record IR, NIR and Raman spectra. IR and NIR spectra were recorded on samples dispersed in KBr pellets. Raman spectra were recorded on solid samples contained in standard NMR diameter tubes or on compressed samples contained in a gold-coated sample holder.

THERMAL ANALYSIS

DSC was performed on Mettler Toledo DSC 822e module. Samples were placed in crimped but vented aluminum sample pans. The typical sample size was 3-4 mg, and the temperature range was 30-300 °C at heating rate of 5 °C min^{-1}. Samples were purged by a stream of dry nitrogen flowing at 150 mL min^{-1}. HSM was performed on a Wagner & Munz PolythermA Hot Stage and Heiztisch microscope. A Moticam 1000 (1.3 MP) camera supported by software Motic Image Plus 2.0ML was used to record images.

INTRINSIC DISSOLUTION TESTING OF DISC

IDR measurements were carried on a USP-certified Electrolab TDT-08 L Dissolution Tester. Equilibrium solubility was determined in water using the shakeflask method. 200 mg of the powdered materials of the Olanzapinium salts (**29**, **31**, **37**, **38**, salicylate and nicotinate) and pure base were added to 5 mL of water, and the resulting suspension was stirred at room temperature for 48 hr. The suspension was then filtered through 2.5 μm Whatman filter paper. The concentration of the solution thus obtained was determined on a Thermo Scientific Evolution 300 UV-Vis spectrometer based on the absorbance maxima with appropriate dilution using a predetermined calibration curve.

For IDR experiments, 200 mg of the Olanzapinium salts and pure base were taken in the intrinsic attachment and compressed to a 0.5 cm^2 pellet using a hydraulic press at a pressure of 2.5 ton inch^{-2} for 5 min. There is no polymorphic transformation or dissociation of the salts upon compression. The intrinsic attachment was placed in a jar of 900 mL of water at 37 °C and rotated at 50 rpm. 7 mL aliquots were collected at specific time intervals and concentrations of the aliquots were determined with proper dilution from the predetermined calibration curves of the respective salts using their individual molar extinction coefficients (Olanzapine base **28** 18.92, Olanzapinium hydrogenmalonate **29** 20.29, Olanzapinium monomaleate 24.09, Olanzapinium dimaleate 23.07, Olanzapinium PABA hemihydrate **31** 31.56, Olanzapinium salicylate 18.97 and Olanzapinium nicotinate 22.20 /mmol/cm) by UV-Vis spectrophotometry. The IDR values were 0.09, 3.04, 0.91, 7.23, 0.17, 0.12 and 0.59 mg/cm^2/min (at 25 min interval) for Olanzapine base and their salts respectively.

Calculation: Beer Lambert's Law: $\qquad$ $\mathbf{A = \varepsilon c}\mathit{l}$

where A is the absorbance, ε is coefficient of absorbance, c is the concentration and l is path length of the sample.

4.9 REFERENCES

1. (a) P. H. Stahl and C. G. Wermuth(Eds.), *Handbook of Pharmaceutical Salts: Properties, Selection, and Use*; Wiley-VCH, **2002**. (b) M. B. Smith, J. March, *March's advanced organic chemistry: reactions, mechanisms, and structure*, 5th Ed., J. Wiley: New York, **2001**. (c) B. R. Bhogala, S. Basavoju and A. Nangia, *CrystEngComm*, 7, **2005**, 551.

2. (a) S. M. Berge, L. D. Bighley and D. C. Monkhouse, *J. Pharm. Sci.*, 66, **1977**, 1. (b) L. D. Bighley, S. M. Berge and D. C. Monkhouse, *Salt forms of drugs and absorption*, in: J. Swarbrick, J. Boylan (Eds.), *Encyclopaedia of Pharmaceutical Technology*, vol. 13, Dekker, New York, **1996**, p 453–499. (c) A. T. M. Serajuddin, *Adv. Drug Deliv. Rev.*, 59, **2007**, 603. (d) P. L. Gould, *Int. J. Pharm.*, 33, **1986**, 201. (e) W. H. Streng, S. K. Hsi, P. E. Helms and H. G. Tan, *J. Pharm. Sci.*, 73, **1984**,

1679. (f) A. V. Trask, D. A. Haynes, W. D. S. Motherwell and W. Jones, *Chem. Commun.*, **2006**, 51. (g) D. A. Haynes, W. Jones and W. D. S. Motherwell, *CrystEngComm*, 7, **2005**, 538. (h) S. L. Morissette, Ö. Almarsson, M. L. Peterson, J. F. Remenar, M. J. Read, A. V. Lemmo, S. Ellis, M. J. Cima and C. R. Gardner, *Adv. Drug Deliv. Rev.*, 56, **2004**, 275. (i) E. C. Ware and D. R. Lu, *Pharm. Res.*, 21, **2004**, 177.

3. (a) G. L. Amidon, H. Lennernäs, V. P. Shah and J. R. Crison, *Pharm. Res.*, 12, **1995**, 413. (b) R. Löbenberga and G. L. Amidon, *Eur. J. Pharm. Biopharm.*, 50, **2000**, 3. (c) N. A. Kasim, M. Whitehouse, C. Ramachandran, M. Bermejo, H. Lennernäs, A. S. Hussain, H. E. Junginger, S. A. Stavchansky, K. K. Midha, V. P. Shah and G. L. Amidon, *Mol. Pharm.*, 1, **2004**, 85. (d) A. Dahan, J. M. Miller and G. L. Amidon, *The AAPS Journal*, 11, **2009**, 740.

4. (a) A. A. Noyes and W. R. Whitney, *J. Am. Chem. Soc.*, 19, **1897**, 930. (b) W. E. Hamlin, J. I. Northam and J. G. Wagner, *J. Pharm. Sci.*, 54 , **1965**, 1651.

5. (a) L.-F. Huang and W.-Q. (Tony) Tong, *Adv. Drug Deliv. Rev.*, 56, **2004**, 321. (b) J. F. Remenar, J. M. MacPhee, B. K. Larson, V. A. Tyagi, J. H. Ho, D. A. McIlroy, M. B. Hickey, P. B. Shaw and Ö. Almarsson, *Org. Proc. Res. Dev.*, 7, **2003**, 990. (c) R. J. Bastin, M. J. Bowker and B. J. Slater, *Org. Proc. Res. Dev.*, 4, **2000**, 427. (d) B. D. Anderson and R. A. Conradi, *J. Pharm. Sci.*, 74, **1985**, 815. (e) E. A. Zannou, Q. Ji, Y. M. Joshi and A. T. M. Serajuddin, *Int. J. Pharm.*, 337, **2007**, 210.

6. (a) L. B. Marangell and J. M. Martinez, *Concise Guide to Psychopharmacology*, 2nd Ed., American Psychiatric Publishing, Inc., **2006**. (b) C. R. Craig and R. E. Stitzel (Eds.), *Modern Pharmacology with Clinical Applications*, Little Brown & Company, 5th Ed., Boston, **1997**, p 385–405. (c) J. K. Chakrabarti, L. Horsman, T. M. Hotten, I. A. Pullar, D. E. Tupper and F. C. Wright, *J. Med. Chem.*, 23, **1980**, 878. (d) B. J. Kinon, A. L. Hill, H. Liu and S. Kollack-Walker, *Int. J. Neuropsychopharm.*, 6, **2003**, 97.

7. (a) C. W. Lindsley, *ACS Chem. Neurosci.*, 1, **2010**, 407. (b) G. Miller, *Science*, 329, **2010**, 502.

8. (a) C. A. Bunnell, B. A. Hendriksen and S. D. Larsen, US 5,736,541, **1998**. (b) Y. K. Hamied, R. N. Kankan and D. R. Rao, US 6,348,458 B1, **2002**. (c) V. Sundaram, S. Pandurang, V. Dayaram and S. K. R. Bommareddy, WO 2006/102176 A2, **2006**. (d) B. R. Reguri and R. Chakka, US 2005/0153954 A1, **2005**.

9. (a) I. Wawrzycka-Gorczyca, A. E. Koziol, M. Glice and J. Cybulski, *Acta Cryst.*, E 60, **2004**, o66. (b) S. M. Reutzel-Edens, J. K. Bush, P. A. Magee, G. A. Stephenson and S. R. Byrn, *Cryst. Growth Des.*, 3, **2003**, 897.

10. Cambridge Structural Database, ver. 5.31, ConQuest 1.12, November **2009** release, Aug **2010** update; www.ccdc.cam.ac.uk.

11. (a) S. L. Johnson and K. A. Rumon, *J. Phys. Chem.*, 69, **1965**, 74. (b) B. Sarma, N. K. Nath, B. R. Bhogala and A. Nangia, *Cryst. Growth Des.*, 9, **2009**, 1546. (c) S. L. Childs, G. P. Stahly and A. Park, *Mol. Pharm.*, 4, **2007**, 323.

12. S. Ulrich, *Therapeutic Drug Monitoring*, 27, **2005**, 463.

13. (a) D. R. Lide, *CRC Handbook of Chemistry & Physics*, 86th Ed.; Taylor & Francis., p 8: 42–51. (b) www.wikipedia.org.

14. (a) R. Keltjens, US 2005/0272721 A1, **2005**. (b) I. Simonic, R. Lenarsic, B. Kotar-Jordan, R. Zupet and J. Gnidovec, WO 2006/010620 A2, **2006**. (c) T. Kozluk, WO 2007/032695 A1, **2007**. (d) J. K. Bush, US 2008/0096871 A1, **2008**. (e) T. Mesar, A. Copar, H. Sturm and J. Ludescher, US 2008/0161557 A1, **2008**.

15. (a) K. Ravikumar, G. Y. S. K. Swamy, B. Sridhar and S. Roopa, *Acta Cryst.*, E61, **2005**, o2720. (b) B. Sridhar and K. Ravikumar, *J. Struct. Chem.*, 48, **2007**, 198.

16. (a) Ö. Almarsson, M. B. Hickey, M. Peterson, M. J. Zaworotko, B. Moulton and N. Rodríguez-Hornedo, US 2007/0059356 A1, **2007**. (b) M. B. Hickey and J. Remenar, US 2006/0223794 A1, **2006**.

17. (a) I. Wawrzycka-Gorczyca, P. Borowski, J. Osypiuk-Tomasik, L. Mazur, A. E. Koziol, *J. Mol. Struct.*, 830, **2007**, 188. (b) B. Capuano, I. T. Crosby, G. D. Fallon, E. J. Lloyd, E. Yuriev and S. J. Egan, *Acta Cryst.*, E59, **2003**, o1367. (c) K. Ravikumar, G. Y. S. K. Swamy, B. Sridhar and S. Roopa, *Acta Cryst.*, E61, **2005**, o2720. (d) I. Wawrzycka-Gorczyca, A. E. Koziol, M. Glice and J. Cybulski, *Acta*

Cryst., E60, **2004**, o66. (e) S. D. Larsen, US 5,637,584, **1997**. (f) C. A. Bunnell, T. M. Hotten, S. D. Larsen and D. E. Tupper, US 5,703,232, **1997**. (g) B. Kotar-Zordan, R. Lenarsic, M. Grcman, M. Smrkolj, A. Meden, I. Simonic, R. Zupet, J. Gnidovec and P. Benkic, WO 2005/085256 A1, **2005**. (h) D. Barjoan and B. Bellmunt, WO 2006/013435 A1, **2006**. (i) D. Barjoan and H. Espinal, WO 2007/077134 A1, **2007**.

18. R. Thakuria and A. Nangia, *CrystEngComm*, DOI: 10.1039/c0ce00787k.

19. (a) M. C. Etter, J. C. Macdonald and J. Bernstein, *Acta Cryst.*, B46, **1990**, 256. (b) J. Bernstein, R. E. Davis, L. Shimoni and N.-L. Chang, *Angew. Chem., Int. Ed.,* 34, **1995**, 1555.

20. (a) B. R. Bhogala, S. Basavoju and A. Nangia, *Cryst. Growth Des.*, 5, **2005**, 1683. (b) T. Friščić, A. V. Trask, W. Jones and W. D. S. Motherwell, *Angew. Chem., Int. Ed.*, 45, **2006**, 7546. (c) T. Friščić and W. Jones, *Cryst. Growth Des.*, 9, **2009**, 1621. (d) M. Pop, P. Sieger and P. W. Cains, *J. Pharm. Sci.*, 98, **2009**, 1820.

21. (a) J. J. Gilman, *Science*, 274, **1996**, 65. (b) V. V. Boldyrev, *J. Mat. Sci.*, 39, **2004**, 5117. (c) K. L. Nguyen, T. Friščić, G. M. Day, L. F. Gladden and W. Jones, *Nat. Mater.*, 6, **2007**, 206. (d) N. Shan, F. Toda and W. Jones, *Chem. Commun.*, **2002**, 2372. (e) A. V. Trask, D. A. Haynes, W. D. S. Motherwell and W. Jones, *Chem. Commun.*, **2006**, 51.

22. F. Wöhler, *Annalen Chem. Pharm.*, 51, **1844**, 145.

23. (a) T. Friščić, L. Fábián, J. C. Burley, W. Jones and W. D. S. Motherwell, *Chem. Commun.*, **2006**, 5009. (b) S. Karki, T. Friščić, W. Jones and W. D. S. Motherwell, *Mol. Pharm.*, 4, **2007**, 347. (c) S. Karki, T. Friščić and W. Jones, *CrystEngComm*, 11, **2009**, 470. (d) A. V. Trask, N. Shan, W. D. S. Motherwell, W. Jones, S. Feng, R. B. H. Tan and K. J. Carpenter, *Chem. Commun.*, **2005**, 880.

24. (a) R. M. Silverstein, F. X. Webster and D. J. Kiemle, *Spectroscopic Identification of Organic Compounds;* John Wiley & Sons, **2005**. (b) H. G. Brittain, *Polymorphism in Pharmaceutical Solids*, 2nd Ed.; **2009**. (c) C. B. Aakeröy, D. J. Salmon, M. M. Smith and J. Desper, *Cryst. Growth Des*., 6, **2006**, 1033.

25. (a) T. L. Threlfall, *Org. Pro. Res. Dev.*, 13, **2009,** 1224. (b) J. C. Silva, T. S. Plivelic, M. L. Herrera, N. Ruscheinsky, T. G. Kieckbusch, V. Luccas, and I. L. Torriani, *Cryst. Growth Des.*, 9, **2009**, 5155.

26. (a) M. Mirmehrabi, S. Rohani, K. S. K. Murthy and B. Radatus, *Int. J. Pharm.*, 282, **2004**, 73. (b) J. Bauer, S. Spanton, R. Henry, J. Quick, W. Dziki, W. Porter, J. Morris, *Pharm. Res.*, 18, **2001**, 859. (c) M. L. Cheney, N. Shan, E. R. Healey, M. Hanna, L. Wojtas, M. J. Zaworotko, V. Sava, S. Song and J. R. Sanchez-Ramos, *Cryst. Growth Des.*, 10, **2010**, 394. (d) H. Parshad, K. Frydenvangb, T. Liljefors, H. O. Sorensen and C. Larsen, *Int. J. Pharm.*, 269, **2004**, 157. (e) R. T. Forbes, P. York and J. R. Davidson, *Int. J. Pharm.*, 126, **1995**, 199. (f) K. M. O'Connor and O. I. Corrigan, Int. J. Pharm., 226, **2001**, 163. (g) T. Tao, Y. Zhao, J. Wu and B. Zhou, *Int. J. Pharm.*, 367, **2009**, 109.

27. (a) K. Greco and R. Bogner, *Mol. Pharm.*, 7, **2010**, 1406. (b) M. Hawley and W. Morozowich, *Mol. Pharm.*, 7, **2010**, 1441.

28. (a) M. Rafilovich and J. Bernstein, *J. Am. Chem. Soc.*, 128, **2006**, 12185. (b) M. Wenger and J. Bernstein, *Mol. Pharm.*, 4, **2007**, 355. (c) M. Lang, J. W. Kampf and A. J. Matzger, *J. Pharm. Sci.*, 91, **2002**, 1186. (d) C. P. Price, A. L. Grzesiak and A. J. Matzger, *J. Am. Chem. Soc.*, 127, **2005**, 5512. (e) J. Li, S. A. Bourne and M. R. Caira, *Chem. Commun.*, 47, **2011**, 1530. (f) N. K. Nath and A. Nangia, *CrystEngComm*, 13, **2011**, 47.

29. *SAINT-Plus*, version 6.45, Bruker AXS Inc., Madison, WI, **2003**.

30. G. M. Sheldrick, *SADABS*, *Program for Empirical Absorption Correction of Area Detector Data*, University of Göttingen, Germany, **1997**.

31. *SHELXS-97 and SHELXL-97, Programs for the Solution and Refinement of Crystal Structures*, G. M. Sheldrick, University of Göttingen, Germany, **1997**.

32. *X-Seed, Graphical Interface to SHELX-97 and POVRay*, L. J. Barbour, University of Missouri-Columbia, Columbia, MO, **1999**.

33. Powder Cell 2.4, Program for structure visualization, powder pattern calculation and profile fitting, www.ccp14.ac.uk.

CHAPTER FIVE

OLANZAPINIUM MALEATE SALTS

5.1 INTRODUCTION

The bioavailability of an active pharmaceutical ingredient (API) plays a vital role in pharmaceutical industry and hence there is an urgent need to improve the bioavailability by increasing the solubility and dissolution rate.[1] Therefore to improve the solubility and dissolution modification is carried out by affecting bulk property such as particle size or on a molecular level for ionizable molecules by salt preparation.[2] For nonionizable molecules improvement may be gained through metastable polymorph, amorphization or cocrystallization.[3] In the last few decades there has been a high level of interest and study on the use of amorphous solids of API as an attractive means of improving the oral bioavailability of poorly soluble drugs.[4] Compared to crystalline solids, glass or amorphous solids have only short range order like the liquids, possess high thermodynamic properties (Figure 1) including free energy, enthalpy, entropy and volume. It imparts high solubility and dissolution compared to the crystalline form and can be further improved if the amorphous material is dispersed in a hydrophilic polymer matrix.[4d,5] These excess quantities are termed as "configurational" quantities. There are four most common ways to prepare amorphous material of pharmaceutical solids.[6] These are (1) condensation from the vapor state, (2) supercooling of the melt, (3) mechanical activation of crystalline mass, for example during milling and cryo-milling and (4) rapid precipitation from solution, for example during freeze-drying or spray drying.
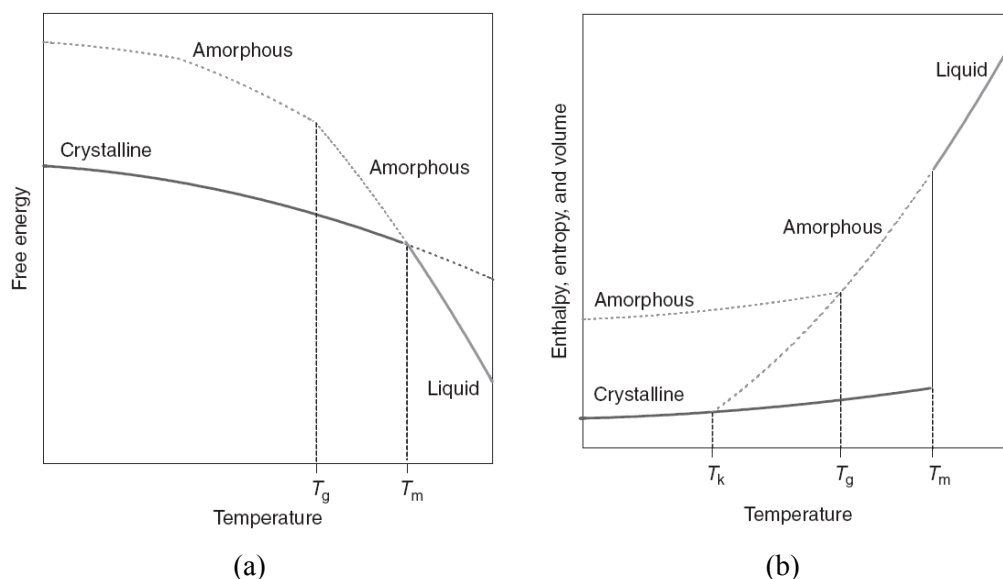
Figure 1 Phase diagrams of amorphous and crystalline solids (a) Free energy. (b) Enthalpy, entropy, and volume. The diagram is adapted from the book *Developing Solid Oral Dosage Forms: Pharmaceutical Theory and Practice*, published by Elsevier (reference 1a).

Grinding or milling is a usual process in the course of drug formulation, which may change the physical state of the end product. William Jones et al. discussed thoroughly about this technique in literature.[7] Amorphous and crystalline salts of Olanzapinium maleate were prepared using the grinding (or milling) technique. Despite many advantages of amorphous materials still a number of challenges need to be addressed in order to take a practical benefit. For example, a major problem of the amorphous APIs is that they are inherently metastable, which can lead to phase transformation during storage as well as during dissolution.[8] Hence there is an urge for the study of amorphous materials and their stability in improving the bioavailability of APIs. The stability of an amorphous material is related to its glass transition temperature (T_g). During cooling of a liquid the molecules "get stuck" when their relaxation times exceed the time scale associated with cooling. The temperature at which this process occurs is roughly the glass transition temperature (T_g) of the material. Below the glass transition temperature amorphous material is stable and above which it converts to the

crystalline phase. Therefore glass transition temperature is an important parameter to establish the stability of an amorphous material. It is mentioned about the importance of the onset of glass transition temperature with respect to the temperature attained during milling. Generally milling at low temperature leads to an increase in the amorphization tendency whereas milling above T_g can produce a crystal-to-crystal transformation between polymorphic forms. The two grinding techniques, namely neat grinding and liquid assisted grinding affect the amorphization of a material extensively. Water (T_g of – 137 °C) and other common solvents are potential plasticizers that lower the T_g and enhance the rate of crystallization of amorphous materials.[9] Generally for stabilization of an amorphous material it is dispersed in a polymer matrix used as a stabilizer. By varying the composition of the stabilizer to the API stability can be improved (enhancement in the T_g) based on the Gordon Taylor equation.[10]

For an amorphous material one more parameter is the Kauzmann temperature (T_K) which is defined as "*the temperature at which the extrapolated entropy of the supercooled liquid becomes equal to the crystalline phase*".[11]

GORDON TAYLOR EQUATION

Several empirical or semi-empirical equations were proposed in order to determine the T_g of a mixture to the T_g's of its components, such as Fox, Couchman and Gordon-Taylor.[10] All these equations are approximation since the nature of interaction between pharmaceutical components varies depending on the molecular size and ionic state. The Gordon-Taylor equation is widely used to calculate the theoretical glass transition temperature of a mixture. The equation is written as

$$\boldsymbol{T_{g12} = (w_1 T_{g1} + K w_2 T_{g2})/ (w_1 + K w_2)} \qquad \text{where } \boldsymbol{K = \rho_1 \Delta\alpha_1/ \rho_2 \Delta\alpha_2}$$

here T_{gi} indicating the glass transition temperature of component i, w_i indicating the weight fraction of component i in the mixture, ρ_i indicating the true density of the component i and $\Delta\alpha_i$ the change in thermal expansivity for component i.

As values for $\Delta\alpha_i$ are not readily available for many materials, K is often approximated using the Simha-Boyer rule presented as

$$K \cong \rho_1 T_{g1} / \rho_2 T_{g2}$$

Now correlating the theoretical and experimental T_g value the miscibility of the system can be assessed.

5.2 RESULTS AND DISCUSSION

As discussed in the Chapter 4, Olanzapine (OLN) is a blockbuster psychotropic agent that belongs to Class II category (low solubility and high permeability) according to the Biopharmaceutical Classification System (BCS).[12] The drug has a solubility of 43 mg/L in water, it is sparingly soluble in acetonitrile and ethyl acetate, and freely soluble in chloroform. The D_o value of Olanzapine is 2 at its highest dose which suggests the need of modification to make more soluble solid form of this lipophilic drug (cLogP = 3.39). Olanzapine is a dibasic molecule with pK_a 7.37 and 4.69 corresponding to the N3 of piperazine and N1 of diazapine ring, respectively. Therefore according to the ΔpK_a rule typical acids of pK_a < 5 should form salts (Table 1).[13] The salts of Olanzapine with malonic acid, fumaric acid, salicylic acid, p-aminobenzoic acid and the solvates are discussed in the Chapter 4.

Table 1 Calculated pK_a values in gas phase for Olanzapine[14a] and maleic acid[14b].

Molecule	pK_a	Molecular component	ΔpK_a
Olanzapine	7.37, 4.69	Olanzapine and maleic acid 1:1	5.45
Maleic acid	1.92, 6.27	Olanzapine and maleic acid 1:2	5.45, 2.77

Preparation and characterization of the amorphous and crystalline salts of Olanzapine with maleic acid (MA) are discussed along with the enhancement in solubility and dissolution of the crystalline salts.

5.3 STRUCTURAL ANALYSIS

Crystallization of Olanzapine with maleic acid in 2:1 ratio (typically on 0.1 mmol Olanzapine scale) using liquid-assisted grinding by adding a few drops of ethyl acetate and kept for slow evaporation in a mixture of ethyl acetate-acetone solvent. It afforded single crystals of Olanzapinium monomaleate (1:1) salt **37** in which one proton is transferred from the diacid to N3 of Olanzapine piperazine ring. $OLNH^+$ and MA^- ions are arranged in a zigzag chain having a graph set notation[15] ($C_3^2(15)[S(7)]$) and sustained by $N^+–H{\cdots}O^-$ hydrogen bond (1.73 Å, 156.0º) from the protonated OLN to monomaleate (Figure 2). In the crystal structure **37** the common Olanzapine dimer motif is present (Figure 2a) and assembled by parallel stacking of the infinite zigzag chains along [010] axis.
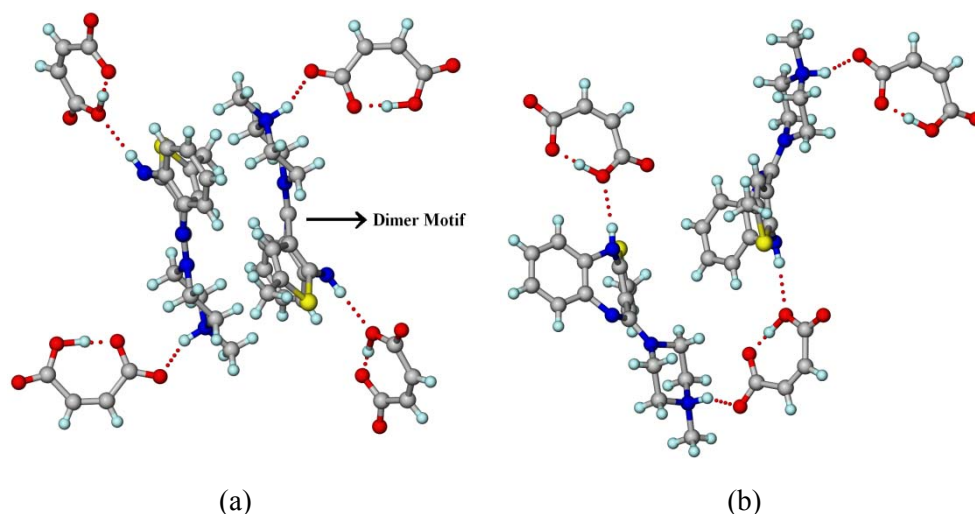

(a)   (b)

Figure 2 (a) Hydrogen bond synthon with dimer motif in 1:1 salt **37**. (b) Zigzag chain of $OLNH^+$ and MA^- in **37**.

When a 1:1:0.5 mixture of Olanzapine, aspirin and maleic acid were ground and crystallized from ethyl acetate-nitromethane mixture solvent, in an attempt to prepare a two drug ternary cocrystal,[16] the product surprisingly was Olanzapinium dimaleate **38** as confirmed by X-ray diffraction. In crystal structure **38** both N3 of the piperazine and N1 of diazepine ring are protonated and bonded via $N^+–H{\cdots}O^-$ hydrogen bonds (1.69 Å,

170.3°; 1.97 Å, 160.4°; Table 2) to different monomaleate anions (Figure 3). One maleate ion is bonded to piperazinyl $OLNH^+$ via *D* motif whereas the second maleate is bifurcated with one benzodiazepine $OLNH^+$ and another $OLNH$ donor to give a ring motif with the graph set notation $R_4^2(14)$. Surprisingly the Olanzapine dimer motif is absent in this salt **38** structure. The structures of both salts could be unambiguously established only by crystal X-ray diffraction. Good quality single crystals were obtained only using the above stoichiometry and crystallization conditions and a 1:1 or 1:2 stoichiometry of the drug and coformer resulted in pasty material.

Accidental appearance of new polymorph, solvate, etc. on attempted cocrystallization with additives/ coformers is not uncommon.[17] Bernstein reported cases where on attempted cocrystallization yielded four polymorphs of benzidine with benzophenone and diphenyl sulfoxide,[17a] dimorphic sesquihydrate of oxalic acid with asparagine/ glutamine;[17b] Matzger group reported where carbamazepine form IV was obtained in presence of hydroxypropylcellulose,[17c] and several API polymorphs using polymer as additives.[17d] Recently Caira[17e] and Nangia[17f] also reported serendipitous finding of new polymorphs of nicotinamide/ isonicotinamide and tolbutamide respectively.

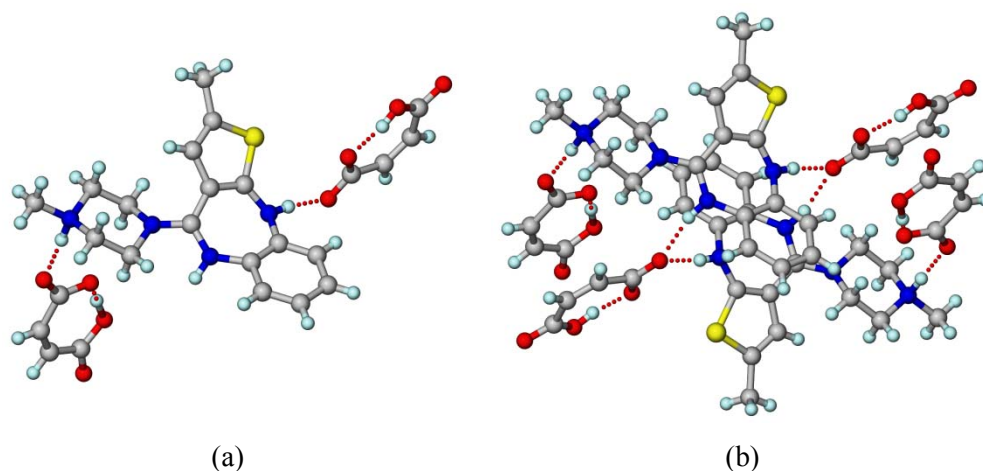(a)   (b)

Figure 3 (a) Discrete H bond connecting two MA^- ions by $OLN2H^+$. (b) $OLN2H^+$ is flanked by MA^- ions in the 1:2 salt. The protonated benzodiazepine is hydrogen-bonded to maleate ions on both sides.

Table 2 Hydrogen bonds in crystal structures of **37** and **38** salts.

Interaction	H···A/ Å	D···A/ Å	∠D–H···A/ °	Symmetry code
Olanzapinium monomaleate 1:1 salt **37**				
N3$^+$–H3···O4$^-$	1.73	2.648(2)	156.0	---
N4–H4···O1	2.18	3.018(3)	163.1	½–x, –½+y, 3/2–z
C16 –H16A···N4	2.63	3.537(3)	156.1	½+x, ½–y, ½+z
C18–H18B···N1	2.28	2.680(3)	103.8	[a]
Olanzapinium dimaleate 1:2 salt **38**				
N1$^+$–H1···O1$^-$	1.97	2.825(5)	160.4	1–x, –y, 1–z
N3$^+$–H3···O5$^-$	1.69	2.656(5)	170.3	x, –1+y, z
N4–H4···O1	2.04	2.885(5)	167.6	x, y, –1+z
O3–H3A···O2	1.62	2.436(6)	160.8	[a]
C10–H10A···O7	2.55	3.397(6)	148.0	1+x, y, z
C15–H15A···O6	2.45	3.348(6)	153.0	x, –1+y, z
C19–H19A···O5$^-$	2.41	3.359(6)	171.3	2–x, 1–y, 1–z
C19–H19B···O8	2.42	3.290(7)	150.3	1–x, 1–y, 1–z

[a] Intramolecular hydrogen bond.

5.4 NEAT AND LIQUID-ASSISTED GRINDING

Olanzapinium maleate salts **37** and **38** were prepared in larger quantity for spectral and physical measurements using both solid-state and liquid-assisted grinding method. The two components were taken in stoichiometric amount and ground thoroughly in a mortar-pestle for about 15 min and then XRPD were recorded. Neat grinding resulted in amorphous material characterized by the appearance of a hump in XRPD pattern (Figure 4) and the glass transition temperature (T_g) from DSC. CHN analysis of the two amorphous salts was consistent with their calculated microanalysis (see Experimental Section).

In case of liquid-assisted grinding the two components were taken in stoichiometric amount, a few drops (6-8) of CH$_3$CN solvent were added, the material was ground in mortar-pestle for about 15–20 min resulted in crystalline materials. XRPD of

the salts were recorded which matched with the calculated powder pattern of **37** and **38** crystal structures (Figure 4).
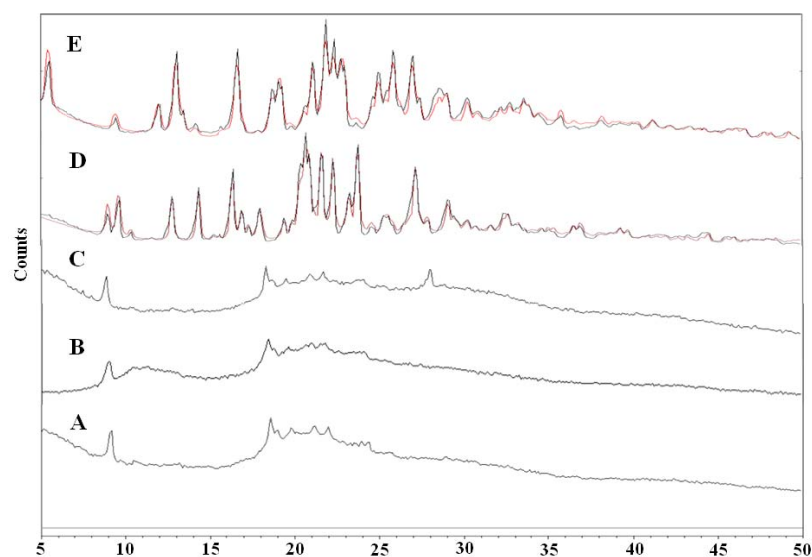

Figure 4 XRPD of (A) OLN maleate. 1:1 amorphous salt, (B) 1:1 amorphous salt mixed with 50% PVP K–90, (C) 1:2 amorphous salt, (D) 1:1 crystalline salt (black experimental, red calculated), and (E) 1:2 crystalline salt (black experimental, red calculated).

The formation of amorphous materials in the absence of solvent suggested a two step mechanism of crystallization with the amorphous phase as an intermediate.[18] Amorphous forms of organic solids are difficult to detect due to their low T_g. Amorphous salts of Olanzapine obtained during dry milling at room temperature have T_g of ~60 °C (Figure 5), higher than the temperature attained during grinding. Water and other organic solvents are potential plasticizers which lower the T_g, hence liquid-assisted grinding gave the crystalline phase. Dry grinding of the crystalline salts in the absence of solvent did not convert them to the amorphous state (Experimental Section).
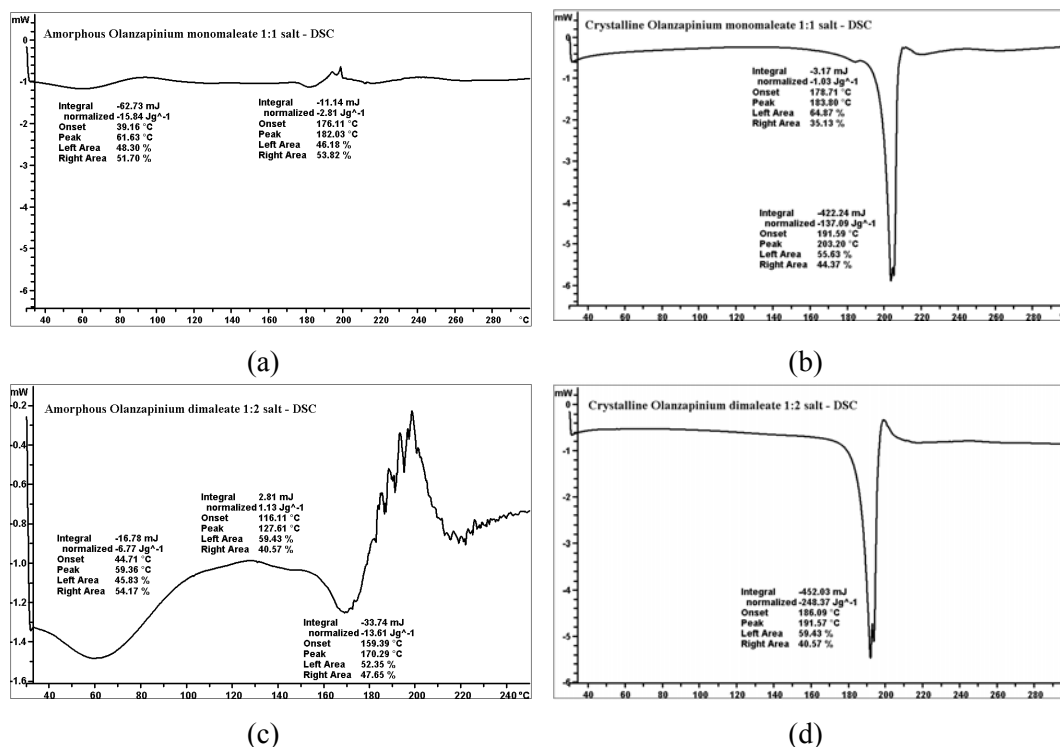
Figure 5 DSC thermograms of Olanzapinium monomaleate **37** and dimaleate **38** amorphous (a), (c) and crystalline (b), (d) forms respectively.

5.5 SPECTRAL ANALYSIS OF MALEATE SALTS

The pure base Olanzapine and both the amorphous and crystalline maleate salts **37** and **38** were well characterized by IR, NIR, Raman and ss-NMR spectroscopy. Generally in case of salt or cocrystal the formation of hydrogen bond leads to changes in bond strength of both the acceptor and donor groups. The frequency of the donor X–H stretching vibration is more sensitive to the formation of hydrogen bond, therefore the common changes in the FT-IR spectra include (i) red shift in absorbance band (due to lengthening of the X–H bond by hydrogen bond formation), (ii) band broadening, and (iii) band intensification.[19] The band broadening and intensification increases strongly upon formation of a hydrogen bond therefore it is more prominent in crystalline phase than solution or amorphous phase where the molecules are disordered. Therefore vibrational spectroscopy is a well known

technique to differentiate and quantify amorphous and crystalline compounds.[20] Amorphous materials are characterized by broad unresolved peaks with low intensity.

(i)

(ii)

Figure 6 FT-IR spectra of (a) OLN base, (b) OLN monomaleate **37** amorphous, (c) **37** crystalline, (d) OLN dimaleate **38** amorphous, (e) **38** crystalline, (f) Maleic acid. (i) spectral range from 4000–2000 cm^{-1} (ii) spectral range from 2000–400 cm^{-1}.

The red shift of the N–H stretching vibration from 3441 cm^{-1} (Olanzapine base) to 3433 cm^{-1} (Olanzapinium monomaleate) to 3432 cm^{-1} (Olanzapinium dimaleate) and increase in band intensity confirmed the formation of the salts (Figure 6).
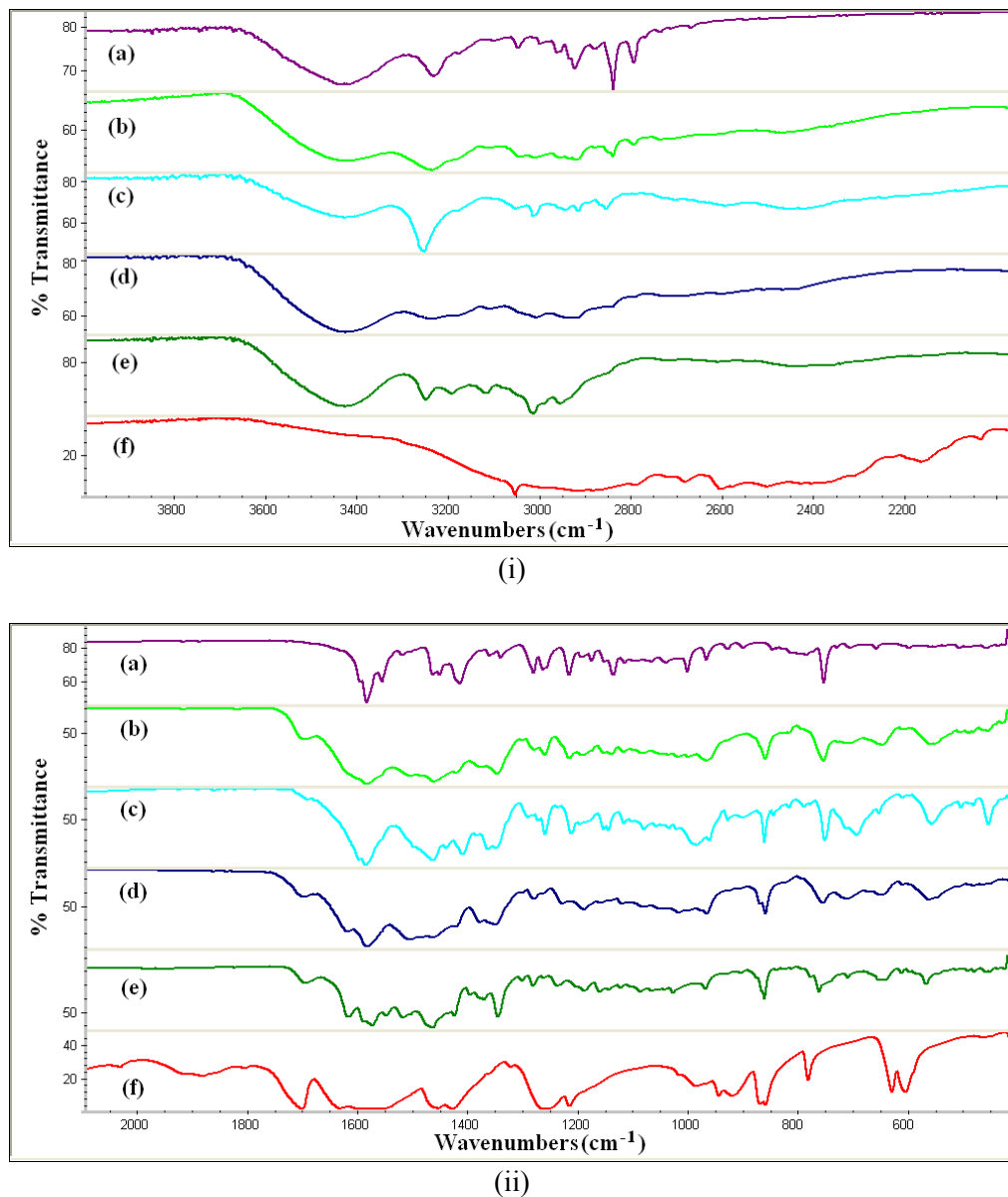

Figure 7 FT-NIR spectra of (a) OLN base, (b) OLN monomaleate **37** amorphous, (c) **37** crystalline, (d) OLN dimaleate **38** amorphous, (e) **38** crystalline, (f) Maleic acid.

(i)

(ii)

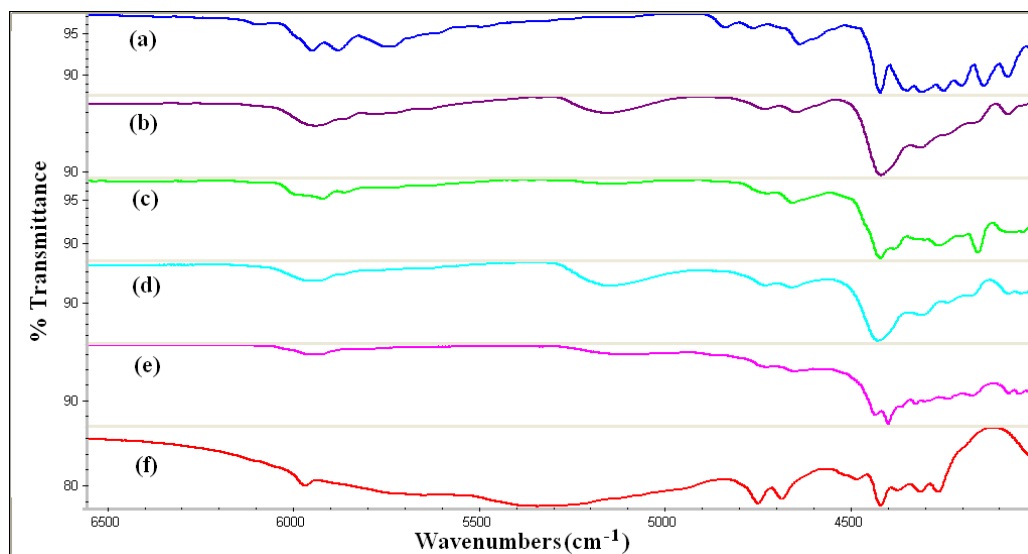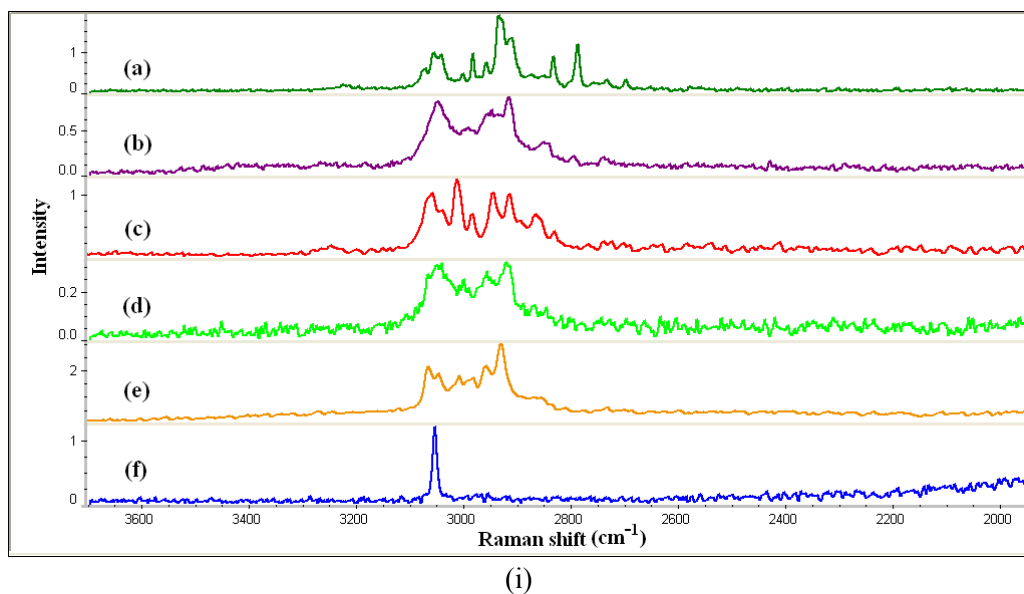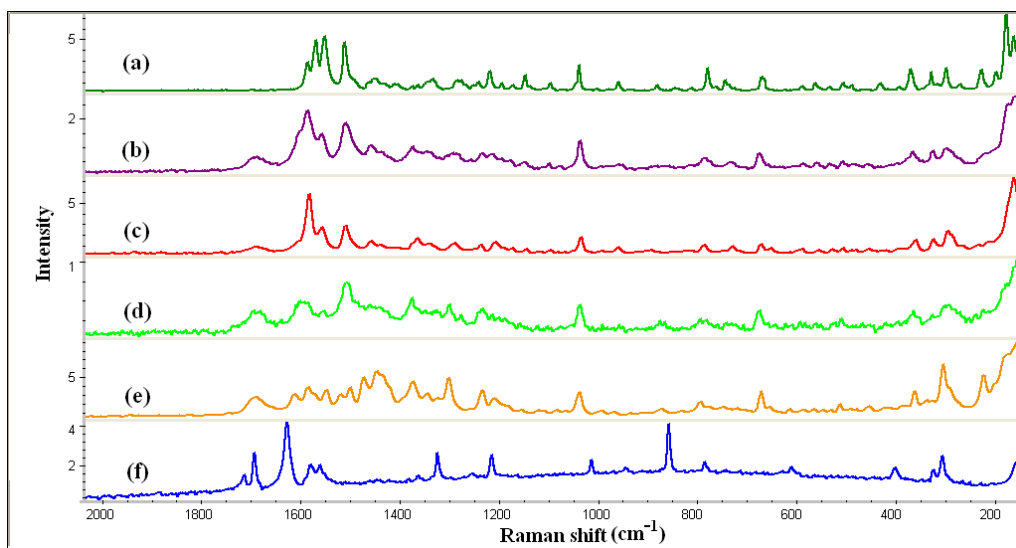**Figure 8** FT-Raman spectra of (a) OLN base, (b) OLN monomaleate **37** amorphous, (c) **37** crystalline, (d) OLN dimaleate **38** amorphous, (e) **38** crystalline, (f) Maleic acid. (i) spectral range from 3700–2000 cm^{-1} (ii) spectral range from 2000–200 cm^{-1}.
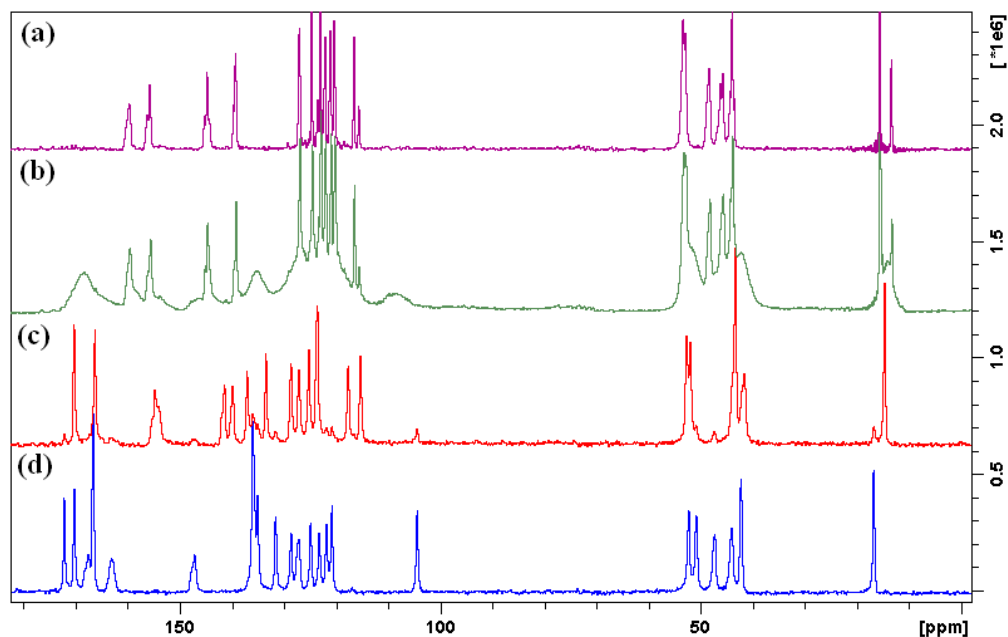
Figure 9 ss-NMR of (a) OLN base, (b) OLN monomaleate **37** amorphous, (c) **37** crystalline, (d) OLN dimaleate **38** crystalline.

NIR, Raman and ss-NMR also confirmed the formation of the corresponding salts (Figure 7, 8 and 9).

5.6 STABILITY OF THE AMORPHOUS PHASE

The stability of amorphous forms were studied in slurry experiments and by dynamic vapor sorption/ desorption (DVS).[21] Olanzapinium dimaleate is quite unstable as it converted to the crystalline 1:2 salt **38** in aqueous slurry within 1 hr. The 1:1 monomaleate amorphous salt do not show water uptake in DVS up to 50% humidity, but after that stage it showed 7% water uptake in the sorption cycle. The water content is 4% after one desorption cycle (Figure 10). At this point the amorphous material is converted to the crystalline 1:1 salt **37** as confirmed by XRPD of the product material after sorption/ desorption cycle for 12 hr (Figure 10c).
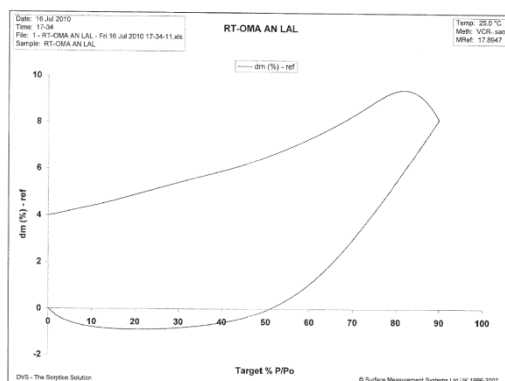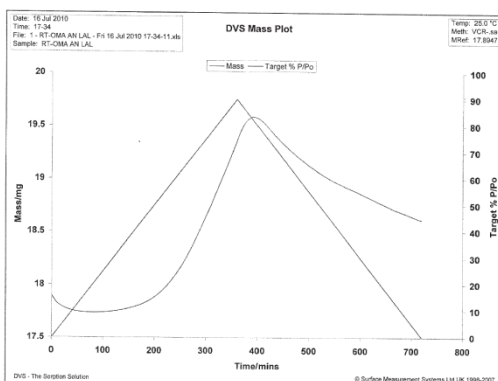
(a)   (b)
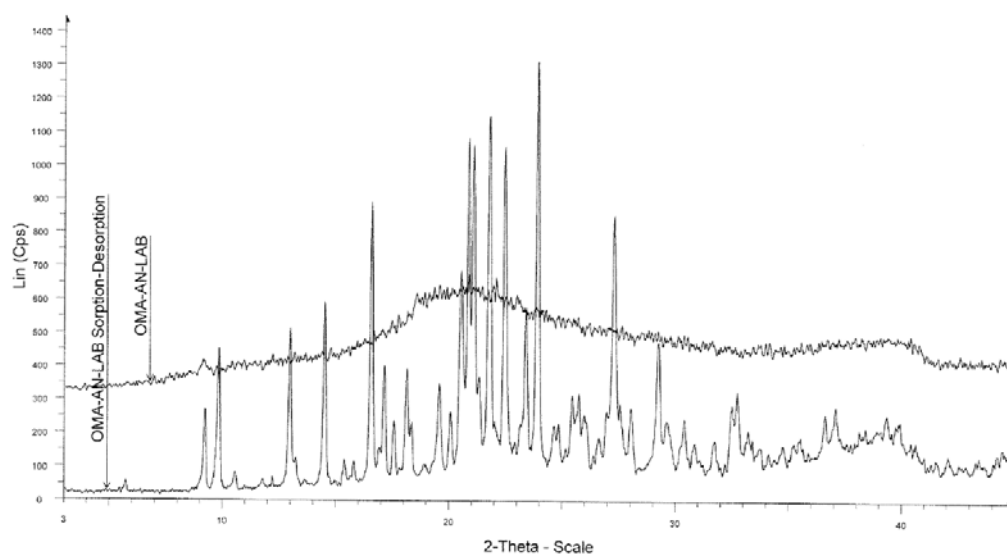
(c)

Figure 10 Dynamic vapour sorption of amorphous OLN monomaleate. (a) isotherm plot shows 7% water sorption and desorption gives sample with 4% water content, (b) Mass plot as a function of time (12 hr), (c) XRPD of the sample before DVS (OLN monomaleate amorphous) and after one sorption-desorption cycle of 12 hr up to 90% RH gave the crystalline 1:1 salt **37**.

Polymers, like PVP which have a high T_g (167.5 °C) are used as stabilizers for amorphous materials. The amorphous drug is dispersed in a solid solvent of hydrophilic polymer to result in a single homogeneous amorphous phase of higher T_g according to the Gordon-Taylor equation.[10c,22] A qualitative energy profile showing the amorphous drug, crystalline drug and single phase amorphous solid dispersion (SD) is represented in Figure 11.
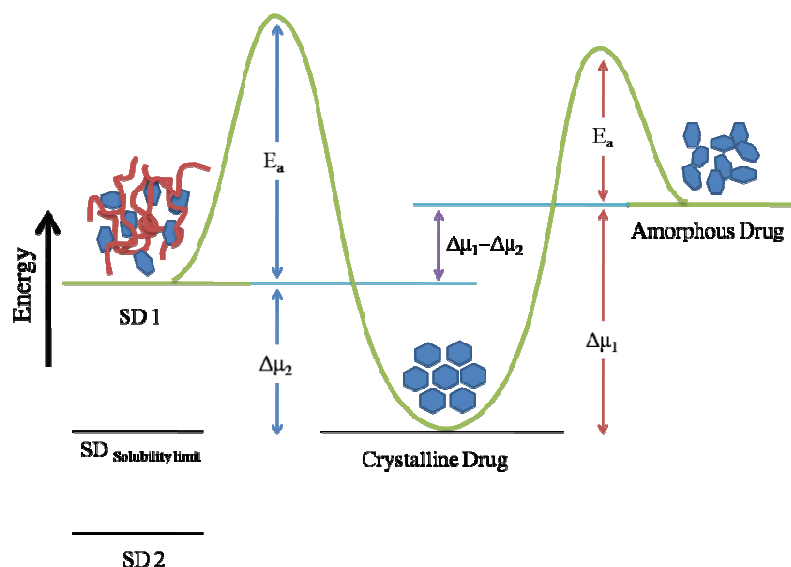
Figure 11 Schematic energy profile diagram showing amorphous drug, crystalline drug and two amorphous solid dispersions (SD 1 and SD 2), (μ represents the chemical potential of the drug and E_a represents the activation energy barrier for crystallization). The figure is taken from *AAPS Newsmagazine*, Sept 2009, American Association of Pharmaceutical Scientists publication.

On addition of 50% by weight PVP K-90 the T_g of amorphous Olanzapinium monomaleate increases from 60 °C to 74 °C (Figure 12). The amorphous nature of the solid dispersion is intact after the addition of polymer as confirmed by XRPD (Figure 4).
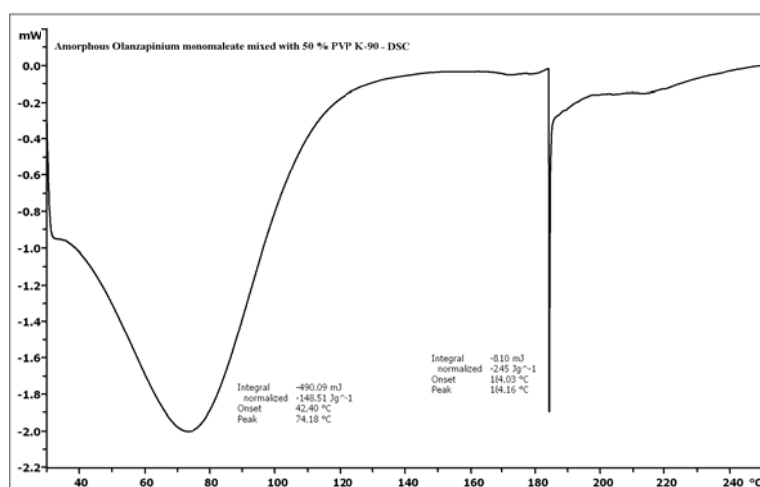
Figure 12 DSC thermogram of amorphous Olanzapinium monomaleate mixed with 50% PVP K-90 polymer.

The amorphous nature of Olanzapinium monomaleate salt was further confirmed by transmission electron microscopy (TEM) and electron diffraction (ED) pattern (Figure 13). The samples were prepared by making a dispersed solution of amorphous and crystalline monomaleate salt in n-hexane drop casted on the carbon coated TEM grid of 200 mesh size. The diffuse rings in ED indicate the amorphous phase whereas the series of discrete concentric rings mean a polycrystalline phase.[23] The morphology of the crystalline and amorphous mono and dimaleate salts of Olanzapine are revealed in the SEM images (Figure 14).

(a)

(b)
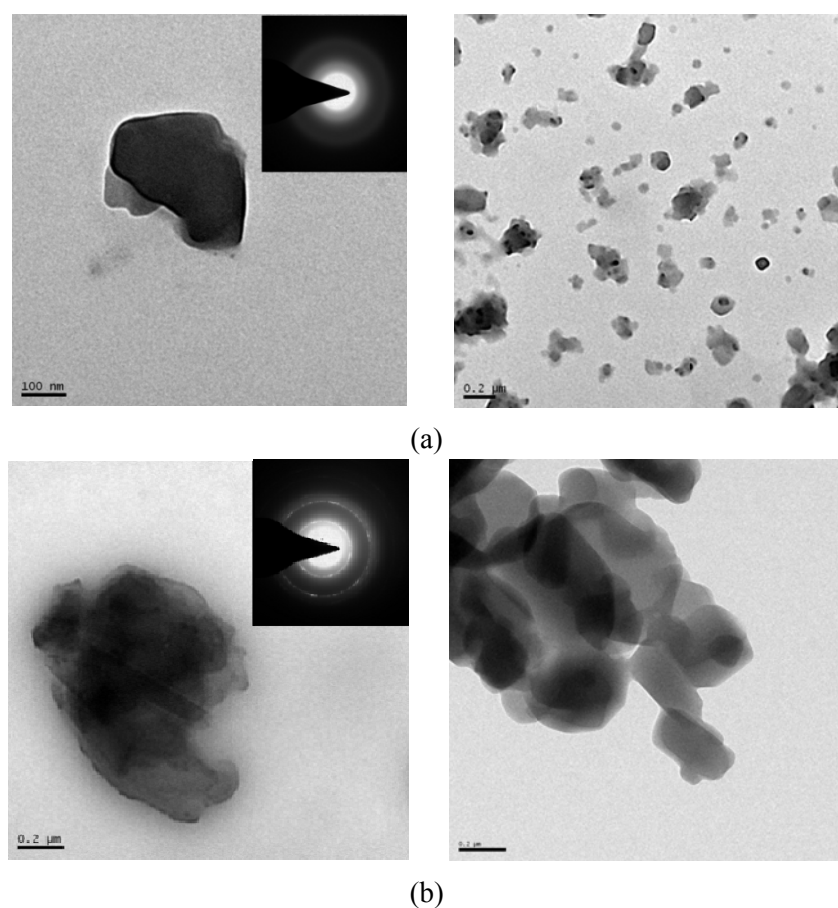
Figure 13 TEM micrographs of Olanzapinium monomaleate **37** amorphous (a) and crystalline (b) materials. The ED pattern is shown in inset. The left and right images are at different magnification.
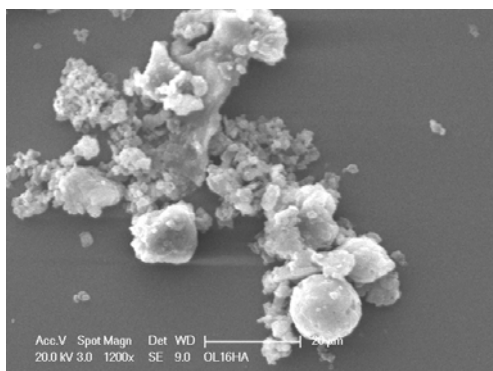
(a) Amorphous salt of **37**
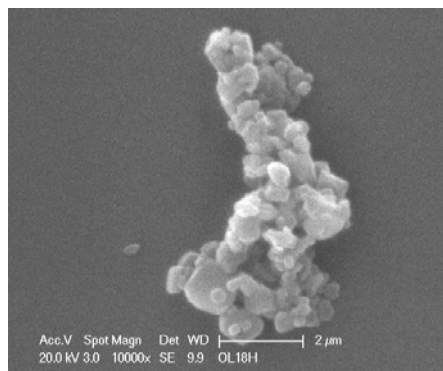
(b) Crystalline salt of **37**
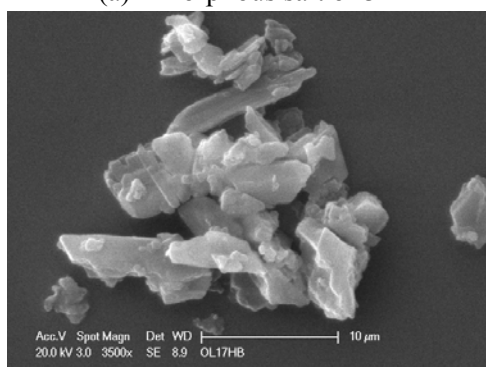
(c) Amorphous salt of **38**
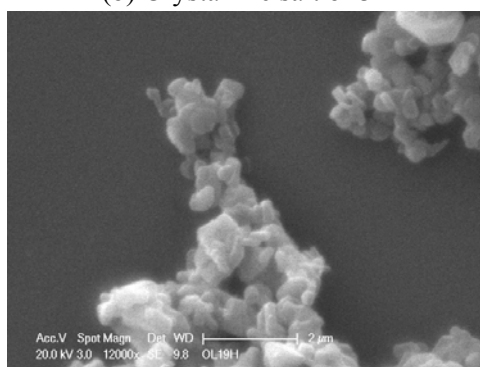
(d) Crystalline salt of **38**

Figure 14 SEM images of the Olanzapinium monomaleate **37** and dimaleate **38** amorphous (a), (c) and crystalline (b), (d) salts respectively.

5.7 SOLUBILITY AND DISSOLUTION

Since the amorphous materials are found to convert to their crystalline phases, the equilibrium solubility of only the crystalline salts was measured. The solubility of the two salts **37** and **38** were measured using the shake flask method.[24] The concentration of the solutions were determined on a UV-Vis spectrometer using the Beer Lambert's equation. The UV-Vis spectra of Olanzapine base is shown in Figure 15.

(a)   (b)
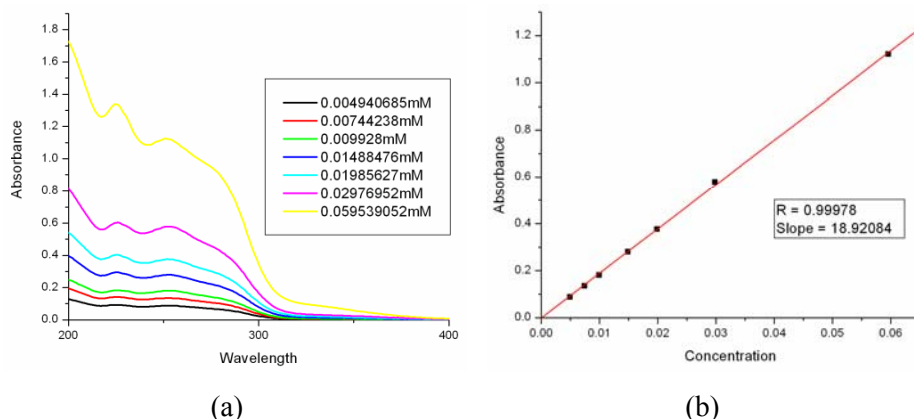
Figure 15 (a) Absorbance vs. wavelength and (b) absorbance vs. concentration curve for the standard solution of Olanzapine free base in distilled water.

The solubility (measured after 48 hr) of crytstalline Olanzapinium monomaleate **37** is 9.68 mg/mL and that of Olanzapinium dimaleate **38** is 23.61 mg/mL, several hundred fold higher (225 and 550 times respectively) than that of the free base (0.043 mg/mL). The higher solubility of the 1:2 salt **38** compared to 1:1 salt **37** is reflected in their intrinsic dissolution rates (Figure 16). The intrinsic dissolution rate (IDR) of the crystalline mono and dimaleate salts were measured on compressed pellet/ disk in 900 mL of water at 37 °C at 50 rpm. The IDR values are 0.76 and 5.75 mg/cm^2/min (at 10 min interval) for mono and dimaleate salts respectively.

(a)   (b)
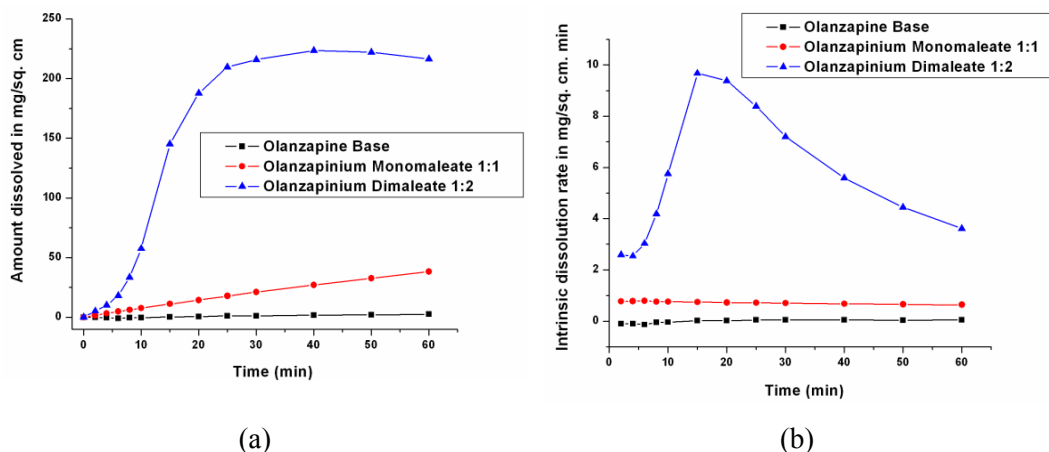
Figure 16 Dissolution profiles of crystalline **37** and **38** salts in distilled water. The more soluble dimaleate **38** shows faster dissolution than monomaleate salt **37**. (a) The amount of drug dissolved plateaus after 20 min (blue curve) because most of the drug was consumed for the faster dissolving salt. (b) The dissolution rate falls for dimaleate **38** (blue) after 15 min because the sample was almost completely dissolved by that time.

When the more soluble salt has higher IDR, it indicates that the solid form is stable to the experimental conditions.[8a,25] This was verified by recording the XRPD of the sample after dissolution experiment, which matches with the starting crystalline phase (Figure 17).
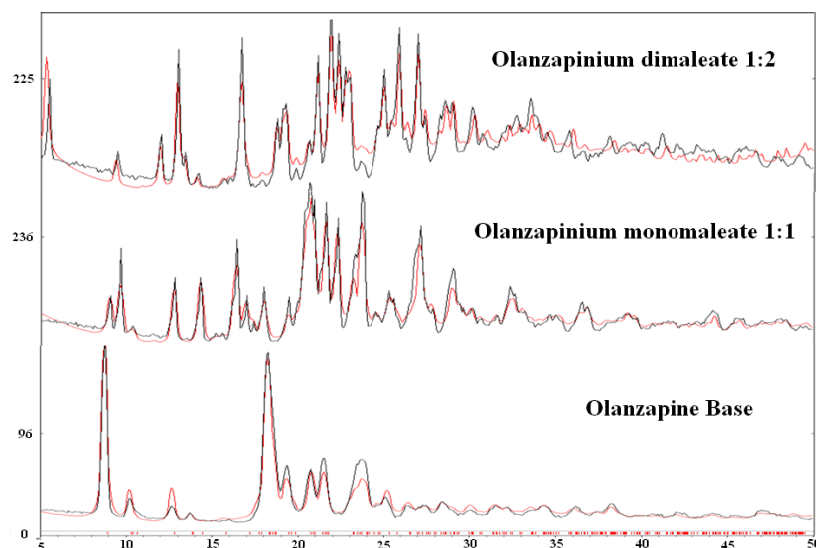
Figure 17 XRPD patterns of the samples of Olanzapine base and the crystalline salts **37** and **38** after the dissolution experiment and overlay of the calculated lines from the crystal structure confirm that the salts are stable during the dissolution experiment.

5.8 STRUCTURE SOLUBILITY RELATIONSHIP

The higher solubility and dissolution rate of Olanzapinium dimaleate **38** compared to monomaleate **37** is understood from the hydrogen bonding in the crystal structure. Even though maleic acid is not in the GRAS list, but some of the maleate salts of well known APIs like enalapril maleate, amlodipine maleate are approved drugs in the market and a

large number of maleate salts of API are reported in the literature.[12c,13c,26] Maleic acid has a very high solubility in water (solubility 780 mg/mL) and if two maleate ions are present for one drug cation **38**, then the solubility would obviously be higher compared to the 1:1 monomaleate salt **37**. In general, a higher charge on the counter ion results in higher hydration energy hence greater solubility of the salt. Conversely, the more stable crystalline lattice use to have lower solubility. Olanzapinium monomaleate **37** has higher melting point compared to dimaleate salt **38** (203 °C, 192 °C DSC plots in Figure 5) and moreover crystal lattice energy of Olanzapinium dimaleate **38** is higher (i.e. less stable) than that of monomaleate salt **37** (Cerius^2: Dreiding –475.81, –559.78 kcal/mol; Compass –486.07, –658.49 kcal/mol). Both melting point and lattice energy values are consistent with the higher solubility of the 1:2 salt. Analysis of the hydrogen bonding in the crystal structures suggest interesting rationale for the higher solubility and dissolution rate of Olanzapinium dimaleate **38**.

(1) The salt structure has an infinite chain motif for the 1:1 stoichiometry **37** whereas it is a finite motif of maleate anions flanking the drug dication in the 1:2 salt **38**. The breaking of hydrogen bonds in the 1:1 salt structure requires many more bonds to be cleaved for drug solvation and dissolution to occur. On the other hand, cleaving apart the maleate anion on either side of the drug use to release the ionized drug from the 1:2 salt.

(2) The environment of maleate anion in 1:1 salt is such that two out of the four available O acceptors are bonded to N$^+$–H donors in monomaleate, whereas only one out of four is H bonded in dimaleate.

A survey of the Cambridge Structural Database[27] for maleate anion of $S(7)$ motif surrounded by O–H donors give all total 48 hits. It shows that for maleate anion of $S(7)$ motif one O acceptor is the most common environment, and can have 2 or up to 3 O–H donors bonded to different O atoms (Figure 18).
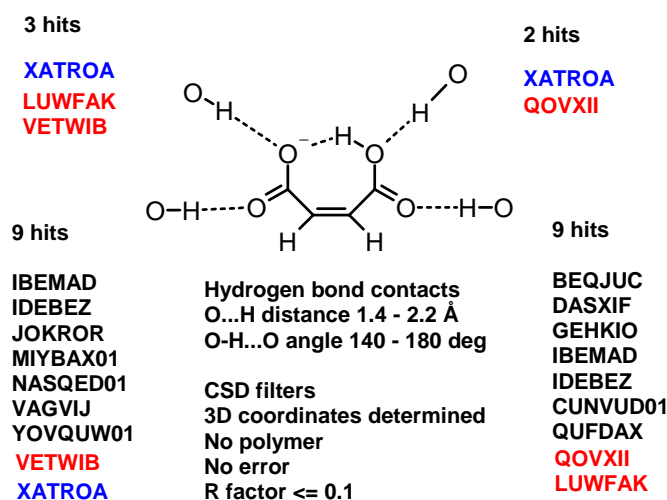
Figure 18 O–H donor environment for the 48 maleate ions in the CSD. The Refcode for O–H$_{donor}$···O$_{maleate}$ hydrogen bond from one donor (black, 14 hits), two donors (red, 3 hits), and three donors (blue, 1 hit) are shown.

OH donors were analyzed to get a statistical distribution of the maleate surroundings. The carbonyl O is the preferred acceptor site for H bonding and carboxylate O is next best. Since the carboxylate O is free in the dimaleate anion (but H bonded in monomaleate), it is possible for water molecules to H bond with the maleate anion more easily in the dimaleate salt. Therefore the 1:2 salt can be hydrated more easily and could be an important reason for its high solubility and dissolution rate. This kind of detailed crystal structure-to-dissolution rate comparison is possible only when accurate 3D structures are known.[28]

Finally Olanzapinium maleate salts **37** and **38** can be distinguished by their color (Figure 19). Extended conjugation of the protonated benzodiazepine ring with the maleate counterion on both sides give bright orange color to the 1:2 salt, whereas the 1:1 salt is light orange and the free base is yellow in color.

Figure 19 (a) Olanzapine free base, (b) Olanzapinium monomaleate **37** and (c) Olanzapinium dimaleate **38**.

5.9 CONCLUSION

Apart from the structural landscape of Olanzapine polymorphs, solvates, hydrates and one nicotinate salt in the literature[29] there is a dearth of physico-chemical and pharmaco-kinetic study of this Class II drug in order to improve the properties. Therefore the solubility and dissolution study of the highly soluble Olanzapinium monomaleate (1:1) **37** and dimaleate (1:2) **38** salts place this drug in the ideal BCS Class I category. The formation of an amorphous phase upon solid state grinding suggested a two-step mechanism for the crystalline salt formation. The higher solubility and dissolution rate of dimaleate is explained by the crystal structure analysis and hydrogen bonding sites on the maleate anion. The crystalline and amorphous salts are further characterized by spectroscopy, XRD, SEM, TEM, ED to confirm the bulk phase and the amorphous nature. The property enhancement of API using salt and cocrystal modification is widely appreciated in pharmaceutical science.

5.10 EXPERIMENTAL SECTION

BULK PREPARATION

Amorphous Olanzapinium maleate salts 37 and 38: To prepare both the 1:1 and 1:2 salts of Olanzapine, 30 mg (0.1 mmol) of Olanzapine was mixed with stoichiometric amount of maleic acid in a mortar-pestle and was manually ground for 10-15 min without addition of any solvent (neat grinding).

Crystalline Olanzapinium maleate salts 37 and 38: 1:1 and 1:2 salt of Olanzapine were prepared in bulk by mixing 30 mg (0.1 mmol) of Olanzapine with stoichiometric amount of maleic acid in a mortar-pestle, 10-15 drops of acetonitrile was added and was manually ground for 15-20 min (liquid-assisted grinding).

CHN ANALYSIS OF THE AMORPHOUS SALTS:

Compound	Amorphous salt of **37** (mw 428.50 gm)		Amorphous salt of **38** (mw 544.57 gm)	
Atom	Calculated %	Experimental %	Calculated %	Experimental %
C	58.81	58.69	55.08	55.16
H	5.60	5.56	5.14	5.51
N	13.07	13.28	10.28	10.22

X-RAY CRYSTALLOGRAPHY

X-ray reflections for all compounds were collected at 298 K on Bruker SMART APEX CCD equipped with a graphite monochromator and Mo-Kα fine-focus sealed tube (λ = 0.71073 Å). Data integration was done using SAINT.[30] Intensities for absorption were corrected using SADABS.[31] Structure solution and refinement were carried out using Bruker SHELXTL.[32] The hydrogen atoms were refined isotropically and the heavy atoms were refined anisotropically. N–H and O–H hydrogens were located from difference electron density maps and C–H hydrogens were fixed using HFIX command in SHELXTL. Crystallographic data are summarized in Appendix. Packing diagrams were prepared in X-Seed.[33]

X-RAY POWDER DIFFRACTION

X-ray powder diffraction of all samples were recorded on Bruker D8 Advance diffractometer using Cu-Kα X-radiation (λ = 1.54056 Å) at 40 kV and 30 mA. Diffraction patterns were collected over a 2θ range of 5-50° at a scan rate of 1° min^{-1}. Powder Cell 2.4 was used for Rietveld refinement.[34]

VIBRATIONAL SPECTROSCOPY

Nicolet 6700 FT-IR spectrometer with an NXR FT-Raman module was used to record IR, NIR and Raman spectra. IR and NIR spectra were recorded on samples dispersed in KBr pellets. Raman spectra were recorded on solid samples contained in standard NMR diameter tubes or on compressed samples contained in a gold-coated sample holder.

THERMAL ANALYSIS

DSC was performed on Mettler Toledo DSC 822e module. Samples were placed in crimped but vented aluminum sample pans. The typical sample size was 3-4 mg, and the temperature range was 30-300 °C at heating rate of 5 °C min^{-1}. Samples were purged by a stream of dry nitrogen flowing at 150 mL min^{-1}.

INTRINSIC DISSOLUTION TESTING OF DISC

IDR measurements were carried on a USP-certified Electrolab TDT-08 L Dissolution Tester. Equilibrium solubility was determined in water using the shakeflask method. 200 mg of the powdered Olanzapinium maleate salts (**37** and **38**) and pure base were added to 5 mL of water, and the resulting suspension was stirred at room temperature for 48 hr. The suspension was then filtered through 2.5 μm Whatman filter paper. The concentration of the solution thus obtained was determined on a Thermo Scientific Evolution 300 UV-Vis spectrometer based on the absorbance maxima with appropriate dilution using a predetermined calibration curve.

For IDR experiments, 200 mg of the pure base and maleate salts were taken in the intrinsic attachment and compressed to a 0.5 cm^2 pellet using a hydraulic press at a pressure of 2.5 ton inch^{-2} for 5 min. There is no polymorphic transformation or dissociation of the salts upon compression. The intrinsic attachment was placed in a jar of 900 mL of water at 37 °C and rotated at 50 rpm. 7 mL aliquots were collected at specific time intervals and concentrations of the aliquots were determined with proper dilution from the predetermined calibration curves of the respective salts using their individual molar extinction coefficients (Olanzapine base 18.92, Olanzapinium monomaleate 24.09

and Olanzapinium dimaleate 23.07 /mmol/cm) by UV-Vis spectrophotometry. The IDR values are –0.04, 0.76 and 5.75 mg/cm^2/min (at 10 min interval) for Olanzapine base, mono and dimaleate salts respectively.

Calculation: Beer Lambert's Law: $A = \varepsilon c l$

where A is the absorbance, ε is coefficient of absorbance, c is the concentration and l is path length of the sample.

Olanzapine base in distilled water: For the saturated solution A = 0.130 (20 times dilution) at $\lambda = 253$ nm, $l = 1$ cm, $\varepsilon = 18.92084$ /mmol/cm.

Hence concentration of the saturated solution is **0.04293 mg/mL** or **42.93 mg/L.**

The solubility of Olanzapinium maleate salts were calculated in the same way.

5.11 REFERENCES

1. (a) Y. Qiu, Y. Chen, G. G. Z. Zhang, L. Liu and W. Porter, *Developing Solid Oral Dosage Forms: Pharmaceutical Theory and Practice*; 1st Ed., Academic Press Publications, **2009**. (b) C. Leuner and J. Dressman, *Eur. J. Pharm. Biopharm.*, 50, **2000**, 47. (c) C. A. Lipinski, F. Lombardo, B. W. Dominy and P. J. Feeney, *Adv. Drug Deliv. Rev.*, 23, **1997**, 3.

2. (a) P. H. Stahl and C. G. Wermuth(Eds.), *Handbook of Pharmaceutical Salts: Properties, Selection, and Use*; Wiley-VCH, **2002**. (b) S. M. Berge, L. D. Bighley and D. C. Monkhouse, *J. Pharm. Sci.*, 66, **1977**, 1. (c) A. T. M. Serajuddin, *Adv. Drug Deliv. Rev.*, 59, **2007**, 603.

3. (a) L. Yu, *Adv. Drug Deliv. Rev.*, 48, **2001**, 27. (b) J. F. Willart and M. Descamps, *Mol. Pharm.*, 5, **2008**, 905. (c) J. Bauer, S. Spanton, R. Henry, J. Quick, W. Dziki, W. Porter and J. Morris, *Pharm. Res.*, 18, **2001**, 859. (d) Ö. Almarsson and M. J. Zaworotko, *Chem. Commun.*, **2004**, 1889. (e) N. Schultheiss and A. Newman, *Cryst. Growth Des.*, 9, **2009**, 2950.

4. (a) M. Savolainen, K. Kogermann, A. Heinz, J. Aaltonen, L. Peltonen, C. Strachan and J. Yliruusi, *Eur. J. Pharm. Biopharm.*, 71, **2009**, 71. (b) K. A. Graeser, C. J. Strachan, J. E. Patterson, K. C. Gordon and T. Rades, *Cryst.*

Growth Des., 8, **2008**, 128. (c) S. B. Murdande, M. J. Pikal, R. M. Shanker and R. H. Bogner, *J. Pharm. Sci.*, 99, **2010**, 1254. (d) J. C. DiNunzio, D. A. Miller, W. Yang, J. W. McGinity and R. O. Williams III, *Mol. Pharm.*, 5, **2008**, 968. (e) B. C. Hancock and M. Parks, *Pharm. Res.*, 17, **2000**, 397. (f) C. S. Towler, T. Li, H. Wikström, D. M. Remick, M. V. Sanchez-Felix and L. S. Taylor, *Mol. Pharm.*, 5, **2008**, 946.

5. (a) F. Qian, J. Huang and M. A. Hussain, *J. Pharm. Sci.*, 99, **2010**, 2941. (b) D. S. Hsieh, B. A. Sarsfield, M. Davidovich, L. M. Dimemmo, S.-Y. Chang and S. Kiang, *J. Pharm. Sci.*, 99, **2010**, 4096. (c) J. P. Lakshman, Y. Cao, J. Kowalski and A. T. M. Serajuddin, *Mol. Pharm.*, 5, **2008**, 994. (d) R. Nair, N. Nyamweya, S. Gönen, L. J. Martínez-Miranda and S. W. Hoag, *Int. J. Pharm.*, 225, **2001**, 83. (e) S. L. Shamblin, E. Y. Huang and G. Zografi, *J. Therm. Anal.*, 47, **1996**, 1567.

6. (a) H. G. Brittain, *Polymorphism in Pharmaceutical Solids*, 2nd Ed., Ed., Inc. New York, **2009**, Chapter 16, p 587–629. (b) B. C. Hancock and G. Zografi, *J. Pharm. Sci.*, 86, **1997**, 1. (c) J. E. Patterson, M. B. James, A. H. Forster, R. W. Lancaster, J. M. Butler and T. Rades, *Int. J. Pharm.*, 336, **2007**, 22.

7. (a) N. Shan, F. Toda and W. Jones, *Chem. Commun.*, **2002**, 2372. (b) A. V. Trask, D. A. Haynes, W. D. S. Motherwell and W. Jones, *Chem. Commun.*, **2006**, 51. (c) S. Karki, T. Friščić and W. Jones, *CrystEngComm*, 11, **2009**, 470. (d) S. Karki, T. Friščić, L. Fábián, P. R. Laity, G. M. Day and W. Jones, *Adv. Mater.*, 21, **2009**, 3905. (e) T. Friščić and W. Jones, *Cryst. Growth Des.*, 9, **2009**, 1621.

8. (a) D. Zhou, G. G. Z. Zhang, D. Law, D. J. W. Grant and E. A. Schmitt, *Mol. Pharm.*, 5, **2008**, 927. (b) K. Greco and R. Bogner, *Mol. Pharm.*, 7, **2010**, 1406. (c) D. E. Alonzo, G. G. Z. Zhang, D. Zhou, Y. Gao and L. S. Taylor, *Pharm. Res.*, 27, **2010**, 608.

9. (a) E. Y. Shalaev and G. Zografi, *J. Pharm. Sci.*, 85, **1996**, 1137. (b) E. Schmitt, C. W. Davis and T. S. Long, *J. Pharm. Sci.*, 85, **1996**, 1215. (c) M. Descamps, J. F. Willart, E. Dudognon and V. Caron, *J. Pharm. Sci.*, 96, **2007**, 1398. (d) S. Strydom, W. Liebenberg, L. Yu and M. de Villiers, *Int. J. Pharm.*, 379, **2009**, 72.

10. (a) T. G. Fox, *Bull. Am. Phys. Soc. Ser.*, II, 1, **1956**, 123. (b) P. R. Couchman, *Polymer Eng. Sci.*, 24, **1984**, 135. (c) M. Gordon and J. S. Taylor, *J. Appl. Chem.*, 2, **1952**, 493.

11. (a) W. Kauzmann, *Chem. Rev.*, 43, **1948**, 219. (b) S. F. Swallen, K. L. Kearns, M. K. Mapes, Y. S. Kim, R. J. McMahon, M. D. Ediger, T. Wu, L. Yu and S. Satija, *Science*, 315, **2007**, 353. (c) H. Tanaka, *Physical Rev.*, E68, **2003**, 011505–1.

12. (a) G. L. Amidon, H. Lennernäs, V. P. Shah and J. R. Crison, *Pharm. Res.*, 12, **1995**, 413. (b) A. Dahan, J. M. Miller and G. L. Amidon, *The AAPS Journal*, 11, **2009**, 740. (c) N. A. Kasim, M. Whitehouse, C. Ramachandran, M. Bermejo, H. Lennernäs, A. S. Hussain, H. E. Junginger, S. A. Stavchansky, K. K. Midha, V. P. Shah and G. L. Amidon, *Mol. Pharm.*, 1, **2004**, 85.

13. (a) B. Sarma, N. K. Nath, B. R. Bhogala and A. Nangia, *Cryst. Growth Des.*, 9, **2009**, 1546. (b) S. L. Johnson and K. A. Rumon, *J. Phys. Chem.*, 69, **1965**, 74. (c) S. L. Childs, G. P. Stahly and A. Park, *Mol. Pharm.*, 4, **2007**, 323. (d) E. A. Sudbeck, W. B. Gleason and M. C. Etter, *J. Chem. Cryst.*, 25, **1995**, 555.

14. (a) S. Ulrich, *Therapeutic Drug Monitoring*, 27, **2005**, 463. (b) D. R. Lide, *CRC Handbook of Chemistry & Physics*, 86th Ed., Taylor & Francis. pp 8: 42–51.

15. (a) M. C. Etter, J. C. Macdonald and J. Bernstein, *Acta Cryst.*, B46, **1990**, 256. (b) J. Bernstein, R. E. Davis, L. Shimoni and N.-L. Chang, *Angew. Chem., Int. Ed.*, 34, **1995**, 1555.

16. (a) B. R. Bhogala, S. Basavoju and A. Nangia, *Cryst. Growth Des.*, 5, **2005**, 1683. (b) T. Friščić, A. V. Trask, W. Jones and W. D. S. Motherwell, *Angew. Chem., Int. Ed.*, 45, **2006**, 7546. (c) Z. Ma and B. Moulton, *Mol. Pharm.*, 4, **2007**, 373.

17. (a) M. Rafilovich and J. Bernstein, *J. Am. Chem. Soc.*, 128, **2006**, 12185. (b) M. Wenger and J. Bernstein, *Mol. Pharm.*, 4, **2007**, 355. (c) M. Lang, J. W. Kampf and A. J. Matzger, *J. Pharm. Sci.*, 91, **2002**, 1186. (d) C. P. Price, A. L. Grzesiak and A. J. Matzger, *J. Am. Chem. Soc.*, 127, **2005**, 5512. (e) J. Li, S. A. Bourne

and M. R. Caira, *Chem. Commun.*, 47, **2011**, 1530. (f) N. K. Nath and A. Nangia, *CrystEngComm*, 13, **2011**, 47.

18. (a) A. Jayasankar, A. Somwangthanaroj, Z. J. Shao and N. Rodríguez-Hornedo, *Pharm. Res.*, 23, **2006**, 2381. (b) K. Seefeldt, J. Miller, F. Alvarez-Núñez and N. Rodríguez-Hornedo, *J. Pharm. Sci.*, 96, **2007**, 1147. (c) D. Erdemir, A. Y. Lee and A. S. Myerson, *Acc. Chem. Res.*, 42, **2009**, 621. (d) A. Dey, P. H. H. Bomans, F. A. Müller, J. Will, P. M. Frederik, G. de With and N. A. J. M. Sommerdijk, *Nat. Mat.*, 9, **2010**, 1010.

19. (a) R. M. Silverstein, F. X. Webster and D. J. Kiemle, *Spectroscopic Identification of Organic Compounds;* John Wiley & Sons, **2005**. (b) B. T. G. Lutz, J. Jacob and J. H. van der Maas, *Vib. Spectros.*, 12, **1996**, 197. (c) T. Steiner, *Angew. Chem., Int. Ed.*, 41, **2002**, 48.

20. (a) A. M. Kaushal, A. K. Chakraborti and A. K. Bansal, *Mol. Pharm.*, 5, **2008**, 937. (b) L. S. Taylor and G. Zografi, *Pharm. Res.*, 15, **1998**, 755. (c) T. Okumura and M. Otsuka, *Pharm. Res.*, 22, **2005**, 1350. (d) F. Atassi, C. Mao, A. S. Masadeh and S. R. Byrn, *J. Pharm. Sci.*, 99, **2010**, 3684.

21. (a) K. S. Howard, Z. K. Nagy, B. Saha, A. L. Robertson and G. Steele, *Org. Pro. Res. Dev.*, 13, **2009**, 590. (b) J. Ortiz, U. S. Kestur, L. S. Taylor and L. J. Mauer, *J. Agric. Food Chem.*, 57, **2009**, 4691. (c) D. Murnane, C. Marriott and G. P. Martin, *Cryst. Growth Des.*, 8, **2008**, 2753. (d) J. Lu and S. Rohani, *Org. Pro. Res. Dev.*, 13, **2009**, 1269.

22. (a) B. Albertini, C. Cavallari, N. Passerini, M. L. González-Rodríguez and L. Rodriguez, *Eur. J. Pharm. Biopharm.*, 56, **2003**, 479. (b) M. M. Feldstein, *Polymer*, 42, **2001**, 7719.

23. (a) Y. Huang, D. J. H. Cockayne, C. Marsh, J. M. Titchmarsh and A. K. Petford-Long, *App. Surf. Sci.*, 252, **2005**, 1954. (b) E. Karavas, M. Georgarakis, A. Docoslis and D. Bikiaris, *Int. J. Pharm.*, 340, **2007**, 76. (c) E. Karavas, E. Georgarakis, M. P. Sigalasc, K. Avgoustakis and D. Bikiaris, *Eur. J. Pharm. Biopharm.*, 66, **2007**, 334.

24. (a) P. Schneider, S. S. Hosseiny, M. Szczotka, V. Jordan and K. Schlitter., *Phytochem. Lett.*, 2, **2009**, 85. (b) C. L. Liu, T. C. Chang, S. M. Wu and H. J. Chiang, *J. Chinese Chem. Soc.*, 53, **2006**, 851. (c) A. Avdeef, *Adv. Drug Deliv. Rev.*, 59, **2007**, 568.

25. M. Hawley and W. Morozowich, *Mol. Pharm.*, 7, **2010**, 1441.

26. (a) M. E. Davison and J. I. Wells, US 4879303, **1989**. (b) C. V. N. Prasad, R. N. Saha and P. Parimoo, *Pharm. Pharmacol. Commun.*, 5, **1999**, 383. (c) E. A. Zannou, Q. Ji, Y. M. Joshi and A. T. M. Serajuddin, *Int. J. Pharm.*, 337, **2007**, 210.

27. Cambridge Structural Database, ver. 5.31, ConQuest 1.12, November **2009** release, Aug **2010** update; www.ccdc.cam.ac.uk.

28. (a) A. Portell, R. Barbas, M. Font-Bardia, P. Dalmases, R. Prohens and C. Puigjaner, *CrystEngComm*, 11, **2009**, 791. (b) L. S. Reddy, S. J. Bethune, J. W. Kampf and N. Rodríguez-Hornedo, *Cryst. Growth Des.*, 9, **2009**, 378.

29. (a) S. M. Reutzel-Edens, J. K. Bush, P. A. Magee, G. A. Stephenson and S. R. Byrn, *Cryst. Growth Des.*, 3, **2003**, 897. (b) K. Ravikumar, G. Y. S. K. Swamy, B. Sridhar and S. Roopa, *Acta Cryst.*, E61, **2005**, o2720. (c) B. Capuano, I. T. Crosby, G. D. Fallon, E. J. Lloyd, E. Yuriev and S. J. Egan, *Acta Cryst.*, E59, **2003**, o1367. (d) I. Wawrzycka-Gorczyca, A. E. Koziol, M. Glice and J. Cybulski, *Acta Cryst.*, E60, **2004**, o66. (e) Y. K. Hamied, R. N. Kankan and D. R. Rao, US 6348458 B1, **2002**. (f) Ö. Almarsson, M. B. Hickey, M. Peterson, M. J. Zaworotko, B. Moulton and N. Rodriguez-Hornedo, US 2007/0059356 A1, **2007**. (g) T. Kozluk, WO 2007/032695 A1, **2007**. (h) R. Keltjens, US 2005/0272721 A1, **2005**. (i) M. B. Hickey and J. Remenar, WO 2004/089313 A2, **2004**.

30. *SAINT-Plus*, version 6.45, Bruker AXS Inc., Madison, WI, **2003**.

31. G. M. Sheldrick, *SADABS*, *Program for Empirical Absorption Correction of Area Detector Data*, University of Göttingen, Germany, **1997**.

32. *SHELXS-97 and SHELXL-97, Programs for the Solution and Refinement of Crystal Structures*, G. M. Sheldrick, University of Göttingen, Germany, **1997**.

33. *X-Seed, Graphical Interface to SHELX-97 and POVRay*, L. J. Barbour, University of Missouri-Columbia, Columbia, MO, **1999**.

34. Powder Cell 2.4, Program for structure visualization, powder pattern calculation and profile fitting, www.ccp14.ac.uk.

CHAPTER SIX

MOLECULAR SALTS OF AN ANTI-DEPRESSANT DRUG MIRTAZAPINE

6.1 INTRODUCTION

Salt formation is an acid-base reaction involving either a proton transfer or neutralization. Theoretically any compound having an acidic or basic moiety can form salt, but generally the strength of the salt depends on the pK_a difference between the acid and the base. An empirical rule is that if the ΔpK_a between the conjugate acid of base and the carboxylic acid is > 3, then salt formation will result.[1] Choosing the appropriate salt is a very difficult task, since each salt imparts unique property to the parent compound. Therefore salt formation is one of the ways to alter the physical and chemical characteristics of a drug without modifying its chemical structure.[2] Currently salt formation is one of the primary solid-state approaches to modify the physical properties of an API, and it is estimated that almost half of the drugs on the market are administered as salts.[3] The most widely used salt formers are HCl, acetate, sulfate, mesylate, fumarate, etc. However the main limitation in this approach is that the API must possess a suitable ionizable site (acidic or basic).

Mirtazapine, (±)-1,2,3,4,10,14b-hexahydro-2-methylpyrazino[2,1-a]pyrido[2,3-c]benzazepine with empirical formula $C_{17}H_{19}N_3$ (Figure 1) having a tetracyclic skeleton belongs to the piperazino-azepine group of compounds. It is a drug used in the treatment of depression and anxiety, and as an anxiolytic, hypnotic, antiemetic, appetite stimulant and antihistamine.[4] S-(+)-mirtazapine is under development for the treatment of insomnia. Mirtazapine is commercially marketed as the hemihydrate of an R/S-racemate (at the carbon marked *) with the brand name Remeron and is the most popular anti-depressant among the top 12 SNRI and SSRI drugs according to a very recent survey.[5]

(a) **(b)**
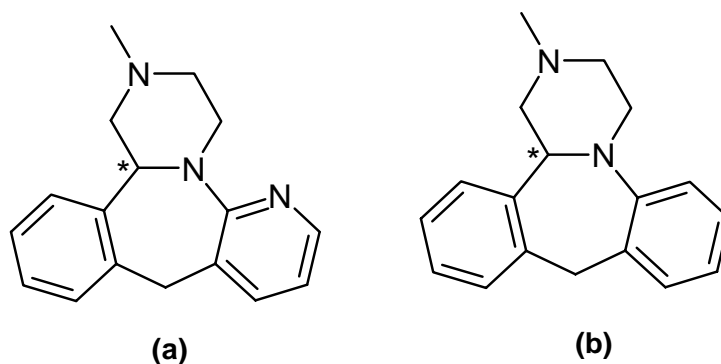
Figure 1 Molecular structure of (a) Mirtazapine and (b) Mianserin.

Mirtazapine is a white to creamy white crystalline powder and a class I drug (solubility in water 1 mg/mL) according to the Biopharmaceutics Classification System[6] with D_o (min) and D_o (max) values of 0.059 and 0.180, respectively, and half-life of 20-40 hours.[7] Where D_o can be defined as "*the ratio of the dose to the amount of drug that will dissolve in 250 mL of test solution at the lowest solubility within the pH range 1 to 8*".[6] i.e.,

$$D_o = (M_o \, / \, V_o) \, / \, C_s$$

where M_o is the highest dose strength (milligrams), C_s is the solubility (milligrams per milliliter), and $V_o = 250$ mL.

Racemic Mirtazapine is supplied for oral administration as scored film-coated tablets containing 15 or 30 mg of mirtazapine base, and unscored film-coated tablets containing 45 mg of the drug. Each tablet also contains corn starch, hydroxypropyl cellulose, magnesium stearate, colloidal silicon dioxide, lactose, and other inactive ingredients.[8]

According to the mode of action, Mirtazapine is believed to act as an antagonist at the alpha 2-adrenergic presynaptic receptor sites. This results in an enhancement of noradrenergic and serotonergic activity. Mirtazapine shows little activity at serotonergic and muscarinic receptor sites. The drug has potent sedative effects due to antagonistic actions at the histamine (H1) receptor but it is not an inhibitor of cytochrome P-450 isoenzymes.[9]

6.2 RESULTS AND DISCUSSION

In Mirtazapine molecule the N-methyl basic site of the piperazine group has a pK_a of 7.1. In the literature only the pK_a of N-methyl piperazinyl site is reported and there is no report for the pK_a of pyridyl N atom. Structurally related 2-N,N-dimethyl pyridine N atom has a pK_a of 7.0.[10a] From the Sparc online pK_a calculator the two pK_a values for N-methyl piperazinyl site and pyridyl N atom of Mirtazapine are found to be 6.62 and 6.13 respectively.[2b,10b] The "rule of 3" implies that it will form salts with acids having p$K_a < 4$. A major stability problem of the drug is that it sublimes at ambient temperature and this poses problems for tablet formulation. Non-subliming salts of S-Mirtazapine, namely maleate, fumarate, and hydrobromide are published in the patent literature along with the crystal structure of Mirtazapine hemihydrate.[11] Molecular salts of rac-Mirtazapine salts with hydrochloric acid, maleic acid, malonic acid, adipic acid, salicylic acid, fumaric acid and hemihydrate of the free base were prepared (Scheme 1) in order to study and understand the hydrogen bonding, molecular packing and hydration state. A Cambridge Structural Database search (CSD version 5.31)[12] was done using piperazino-azepine sub-structure (Scheme 2) that resulted in only 7 hits, among which there were only two CNS drugs, Mianserin and Mirtazapine containing the search moiety. Both these drugs have high solubility (0.2 mg/mL for Mianserin, 1 mg/mL for Mirtazapine) even though they do not contain hydrogen bond donor groups. A guest-free form of Mianserin (CSD Refcode BUCVAW) and its HCl and HBr salts (Refcodes HIJDEJ and MIANSB) were reported.[13] There is only one salt crystal structure of Mirtazapinium saccharinate hydrate (Refcode YANNAD) reported by Desiraju[14] in the published literature. Therefore a structural analysis of Mirtazapine salts is carried out to fill the gap in the available crystallographic data and also to understand the salt crystal structures for their enhanced stabilities.
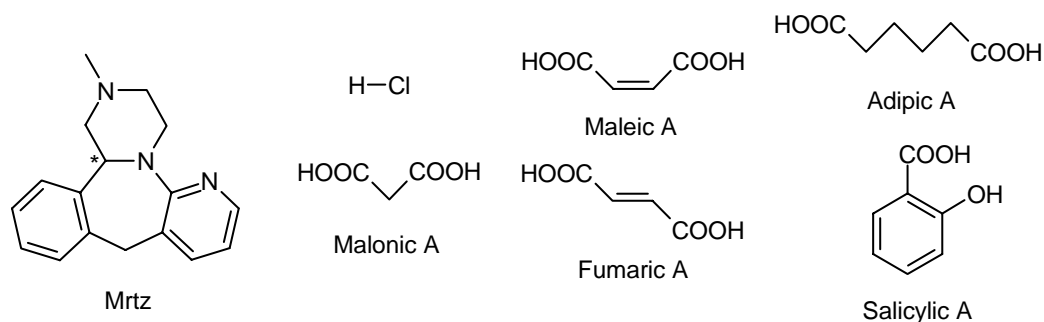
Scheme 1 Mirtazapine and the salt formers used to prepare the Mirtazapinium salts and the corresponding salt composition. Salts 40 and 43 are crystallized as hydrated salt along with the hemihydrate of the pure base.

No	Compounds	No	Compounds
39	Mrtz hemihydrate (1:0.5)	42	Mrtz Hmaleate (1:1)
40	Mrtz diHCl trihydrate (1:2:3)	43	Mrtz Hfumarate monohydrate (1:1:1)
41	Mrtz Hmalonate (1:1)	44	Mrtz hemiadipate (1:0.5)
		45	Mrtz Salicylate (1:1)
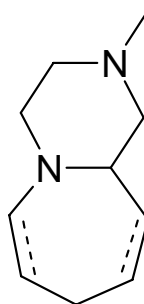
Scheme 2 Piperazino-azepine sub-structure for CSD search gave only four crystal structures of drugs listed in Figure 1.

6.3 STRUCTURAL ANALYSIS

MIRTAZAPINE HEMIHYDRATE (1:0.5) 39

Crystallization of Mirtazapine from EtOH produced block-shaped crystals of Mirtazapine hemihydrate 39 confirmed by X-ray diffraction (space group $P2_1/c$). Water hydrogen

atoms cannot be located in the difference electron density map. There are no strong hydrogen bond donor groups on the Mirtazapine molecule, and the water acts as a bridge to connect the drug molecules. However, the difficulty in locating water hydrogen positions makes the structure not as informative for hydrogen bonding analysis. Water molecule is located in channels down the [010] axis (Figure 2). The isotropic displacement for the water O atom is large (0.133(2) Å^2) for a heavy atom in an otherwise good quality X-ray crystal structure. The difference electron density map gives two sites for O1 separated by 1.75 Å. Since the van der Waals radius of O is 1.52 Å, another O atom at 1.75 Å distance is physically unreasonable. The two O1 sites across the inversion center are assigned occupancy of 0.50 each. Therefore a single unit cell contains 4 Mirtazapine and 2 water molecules to give a hemihydrate stoichiometry. The R-factor is lower when the O1 site occupancy is fixed at 0.5 compared to 1.0. It is difficult to estimate the water content by TGA because Mirtazapine sublimes much below 100 °C in TGA (melting endotherm in DSC at 121 °C). Sublimation around 65 °C is also visualized under a hot stage microscope (HSM) (Figure 12).
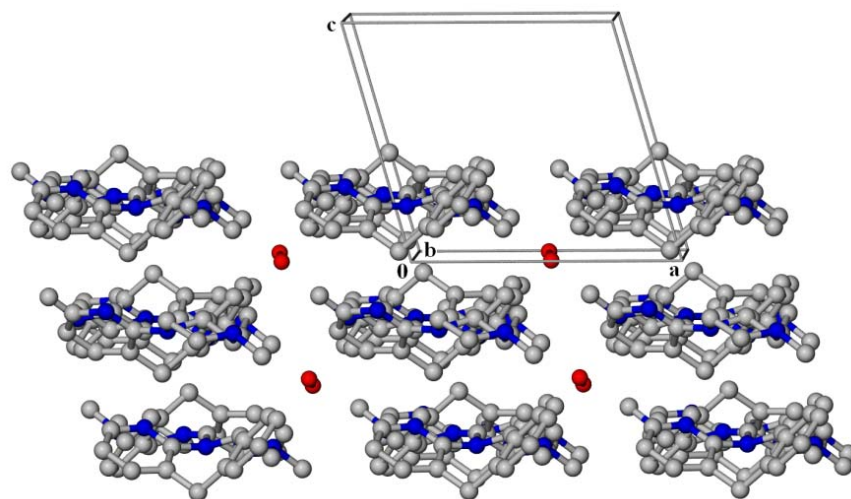
Figure 2 Water molecules reside in channels along [010] in the crystal structure of Mirtazapine hemihydrate **39** (hydrogen atoms are removed for clarity).

MIRTAZAPINIUM DIHYDROCHLORIDE TRIHYDRATE (1:2:3) 40

Mirtazapinium dihydrochloride salt was prepared (see experimental Section for details) to give a trihydrate salt **40** in which protonation occurred at two basic sites, N3 of the piperazine ring and N1 of the pyridine ring. The three water molecules and two chloride ions make a hydrogen-bonded chain along the *a*-axis (Figure 3). Both the N^+–H donors are bonded to Cl^- ions which are in turn hydrated through O–H⋯Cl^- hydrogen bonds.

(a)	(b)
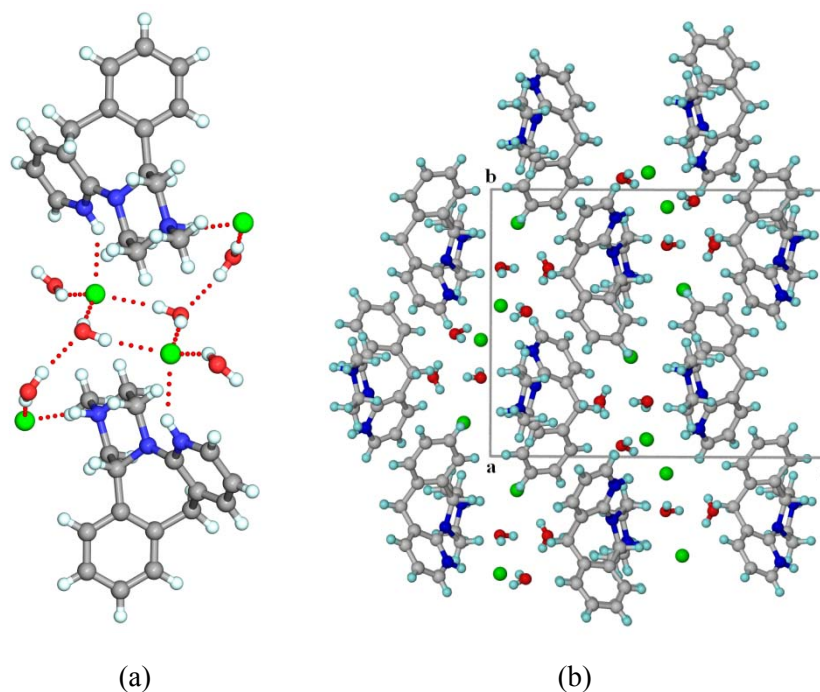
Figure 3 (a) N^+–H⋯Cl^- hydrogen bond connecting Mirtazapinium and chloride ion. (b) Hydrogen bonding motifs of water molecules and chloride ions along [100] in **40**.

MIRTAZAPINIUM HYDROGENMALONATE (1:1) 41

Crystallization of Mirtazapine with malonic acid in methanol give a 1:1 salt **41** (Figure 4) in which one proton of malonic acid is transferred to N3 of the piperazine ring (N^+–H⋯O^-) of Mirtazapine. The Mirtazapinium hydrogenmalonate **41** units are connected by C–H⋯O interactions to the nearby Mirtazapinium molecule.

(a)   (b)
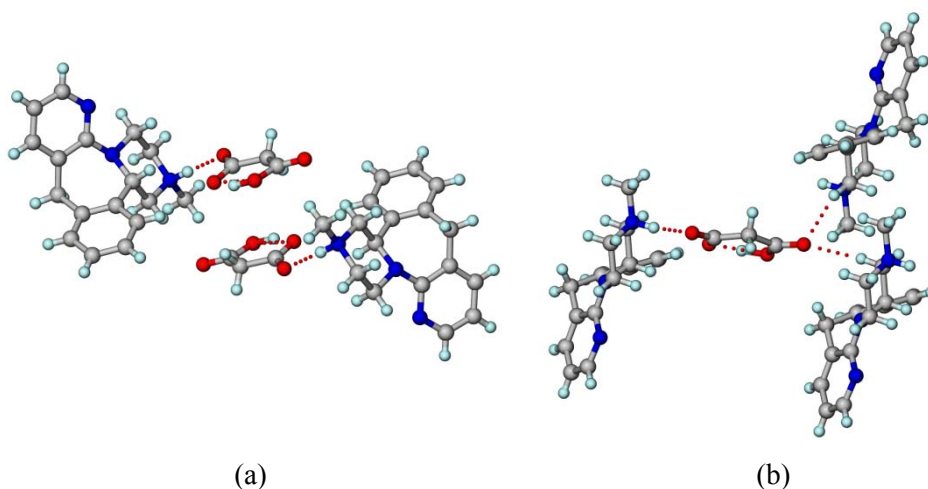
Figure 4 (a) Piperazine–acid N^+–H···O^- hydrogen bond in Mirtazapinium hydrogenmalonate structure **41**. (b) C–H···O hydrogen bond connects one Mirtazapinium hydrogenmalonate **41** to the neighboring Mirtazapinium unit.

MIRTAZAPINIUM HYDROGENMALEATE (1:1) 42

Co-crystallization of Mirtazapine and maleic acid from methanol resulted in a 1:1 salt **42**, similar to the previous cases. Surprisingly, the crystal structure is in chiral noncentrosymmetric space group $P2_12_12_1$ for this racemic salt, a phenomenon that occurs in no more than 10% structures.[15] Mirtazapinium hydrogenmaleate units are arranged along the [100] direction (Figure 5).

(a)   (b)
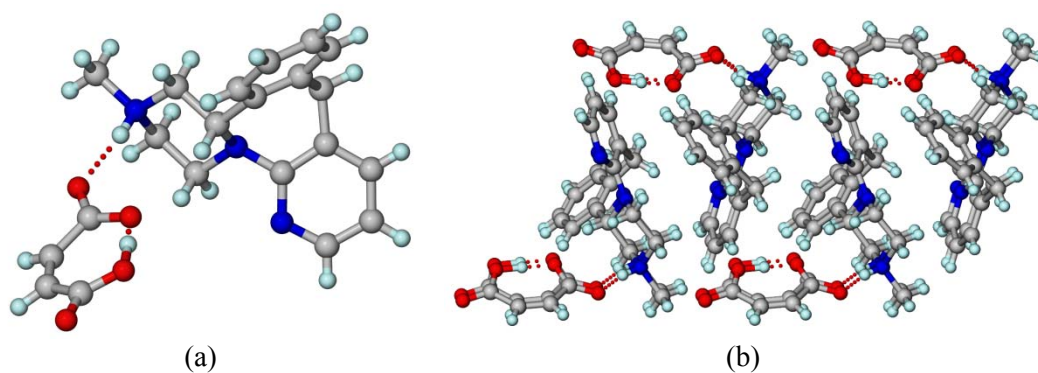
Figure 5 (a) N^+–H···O^- ionic hydrogen bond connecting Mirtazapinium and maleate ions and (b) molecular packing along the [100] axis.

MIRTAZAPINIUM HYDROGENFUMARATE MONOHYDRATE (1:1:1) 43

Co-crystallization of Mirtazapine with fumaric acid in methanol resulted in Mirtazapinium hydrogenfumarate monohydrate **43** crystal. One molecule of Mirtazapine, two half fumaric acid molecules, and a water of crystallization are present in the asymmetric unit of the crystal structure. One of the half fumarate ion resides about an inversion center while the other half about a twofold axis. The latter half is disordered over two positions and was modeled using a site occupancy factor of 0.5 each. An infinite zigzag chain is formed by the hydrogenfumarate anions along the c-axis and Mirtazapinium cations are pendent over the chain (Figure 6). Hydrogenfumarate chains are connected by water molecules, although a detailed hydrogen bonding analysis is not possible because water H atoms could not be located in the X-ray structure. The N^+–H donor of Mirtazapinium is bonded to fumarate O^- as shown below.

(a)   (b)

(c)
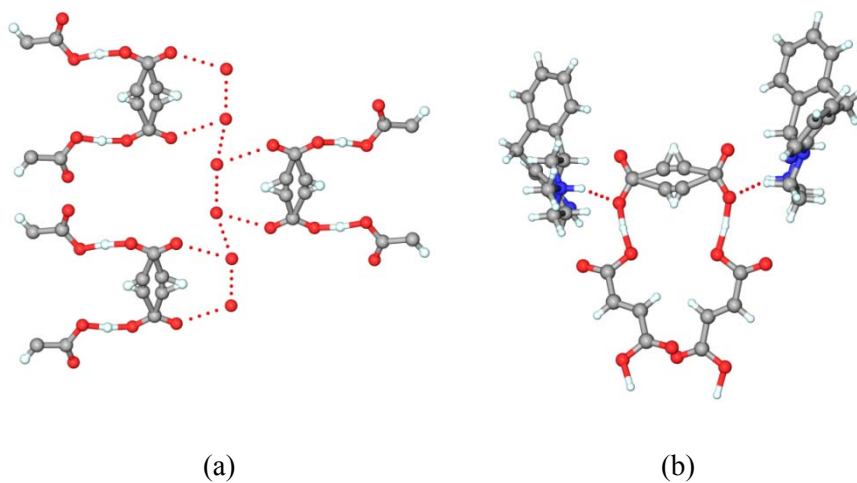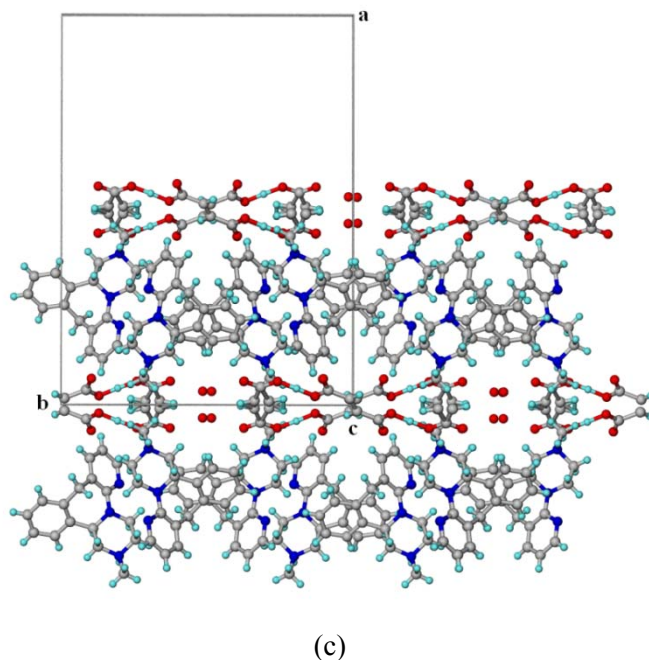
Figure 6 (a) A chain of water molecules along [001] connects fumarate ions. (b) N^+–H$\cdots$O$^-$ hydrogen bond connecting Mirtazapinium to hydrogenfumarate ion. (c) Overall packing showing the hydrogen bond pattern forming layers of Mirtazapinium and hydrogenfumarate ion and water channel connecting the anions.

MIRTAZAPINIUM HEMIADIPATE (1:0.5) 44

In case of Mirtazapinium hemiadipate salt **44** the proton resides partially between the acidic and basic groups. In structure **44** with respect to one Mirtazapinium molecule half molecule of adipate ion is present which resides about an inversion center. Drug molecule layers are connected via adipate through N^+–H$\cdots$O$^-$ hydrogen bonds (Figure 7). In contrast to previous salts wherein only one hydrogen atom of diacid is transferred, here a dianion is bonded to two cationic drug molecules.

| (a) | (b) |
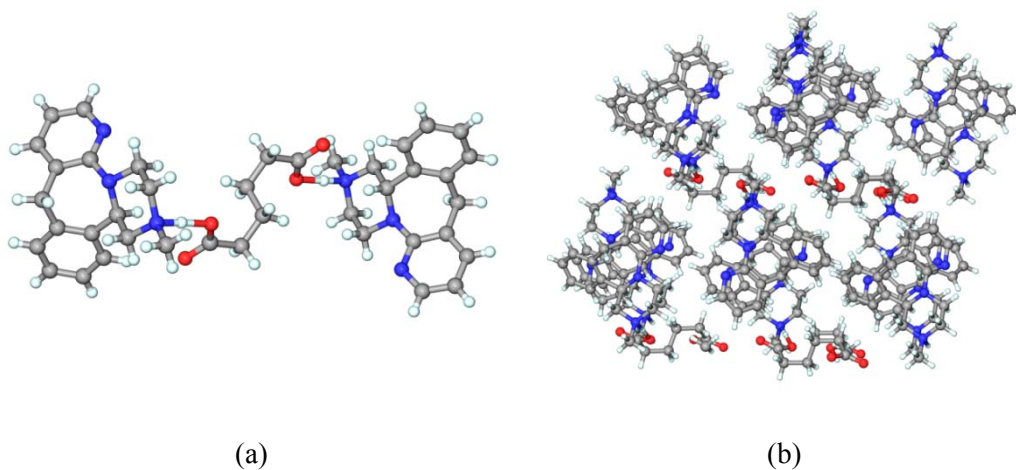
Figure 7 (a) One adipate anion connects two Mirtazapinium cations through N^+–H···O^- hydrogen bond and (b) the overall molecular packing of **44** viewed along [010] axis.

MIRTAZAPINIUM SALICYLATE (1:1) 45

Co-crystallization of Mirtazapine with salicylic acid resulted in 1:1 salt of Mirtzapinium salicylate **45** where the carboxylic proton remains in between the acidic and basic group, as in the adipate salt. The crystal structure of Mirtazapinium salicylate **45** is also a salt structure with the ionic units close packed in the monoclinic $P2_1/c$ space group (Figure 8). As shown in the figure, Mirtazapinium ion forms a layer with the hydrogen bonded salicylate group pointing outwards.

| (a) | (b) |
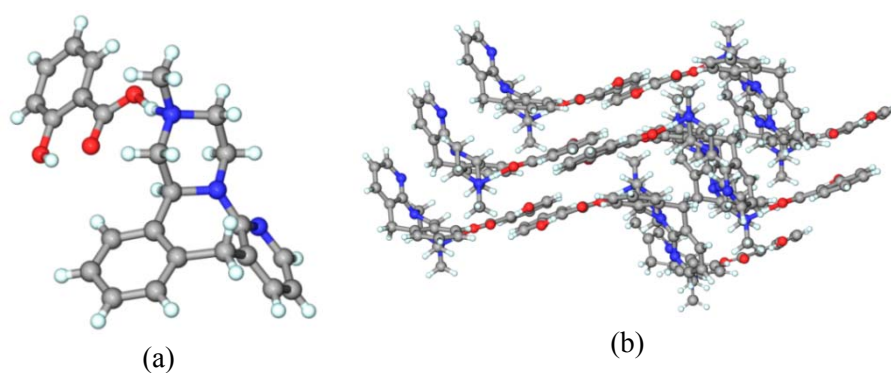
Figure 8 (a) N^+–H···O^- ionic hydrogen bond connecting Mirtazapinium and salicylate ions and (b) the zigzag layer packing in the structure **45**.

The hydrogen bond parameters for all the Mirtazapinium salts and the monohydrate are listed in the Table 1.

Table 1 Hydrogen bonds and short contacts in crystal structures.

Compound	Interaction	H···A (Å)	D···A (Å)	D–H···A (º)	Symmetry Code
Mirtazapine hemihydrate **39**	C1–H1···O1	2.50	3.428(7)	175.2	−1+x, 3/2−y, 1/2+z
Mirtazapinium diHCl trihydrate **40**	N1$^+$–H1A···Cl2$^-$	2.41	3.172(2)	144.1	1−x, 1/2+y, 1/2−z
	O1–H1B···O2	2.24	3.027(5)	171.1	---[a]
	O1–H1C···Cl2$^-$	2.35	3.210(3)	153.5	1−x, −1/2+y, 1/2−z
	O2–H2A···O3	2.01	2.804(4)	170.6	---[a]
	O2–H2B···Cl1$^-$	2.37	3.162(3)	172.7	---[a]
	N3$^+$–H3A···Cl1$^-$	2.07	3.032(2)	169.3	1−x, 1−y, 1−z
	O3–H3B···Cl2$^-$	2.37	3.188(3)	170.9	x, 1/2−y, 1/2+z
	O3–H3C···Cl2$^-$	2.39	3.197(3)	165.6	−x, −1/2+y, 1/2−z
	C3–H3···Cl1$^-$	2.72	3.504(3)	142.9	−x, 1/2+y, 1/2−z
	C13–H13A···Cl1$^-$	2.77	3.692(3)	159.4	1+x, y, z
	C14–H14B···Cl2$^-$	2.75	3.703(3)	167.9	1+x, 3/2−y, 1/2+z
Mirtazapinium hydrogenmalonate **41**	N3$^+$–H3A···O1$^-$	1.72	2.634(3)	169.3	---[a]
	O4–H4A···O2$^-$	1.46	2.468(3)	155.7	---[c]
	C13–H13A···O3	2.47	3.371(3)	154.5	1−x, 1−y, 1−z
	C13–H13B···O3	2.45	3.397(3)	167.4	x, 1+y, z
	C19–H19B···N1	2.47	3.344(3)	149.6	−x, 1−y, 1−z
	[b]C12–H12···O2$^-$	2.68	3.424	135.9	x, y, z
Mirtazapinium hydrogenmaleate **42**	N3$^+$–H3A···O2$^-$	1.84	2.709(3)	158.7	x, 1+y, z
	C13–H13A···O4	2.55	3.371(3)	142.6	1/2+x, 3/2−y, −z
	C17–H17A···O4	2.44	3.279(3)	145.8	1/2+x, 3/2−y, −z
	C17–H17B···O4	2.57	3.377(3)	142.3	---[a]
	C20–H20···O1$^-$	2.58	3.484(3)	165.3	−1/2+x, 1/2−y, −z
	[b]C12–H12···O1$^-$	2.67	3.587	153.7	x, 1+y, z

Mirtazapinium	O2–H2A⋯O3⁻	1.30	2.580(5)	174.2	---[a]
hydrogenfumarate	N3⁺–H3A⋯O3⁻	1.89	2.768(4)	157.5	1/2–x, 1/2–y, 1–z
monohydrate **43**	N3⁺–H3A⋯O4⁻	2.27	3.043(5)	140.6	1/2–x, 1/2–y, 1–z
	C13–H13A⋯O5	2.55	3.420(6)	148.7	---[a]
	C14–H14B⋯O1	2.54	3.458(5)	158.4	1/2–x, 1/2–y, 1–z
	C19–H19⋯O2	2.47	2.794(5)	100.6	–x, –y, 1–z [c]
	C21A–H21A⋯O5	2.55	3.407(9)	153.2	1/2–x, 1/2+y, 1/2–z
	C21B–H21B⋯O2	2.50	3.339(8)	150.6	---[a]
	[b]C12–H12⋯O4⁻	2.84	3.487	125.4	1/2–x, 1/2–y, 1–z
Mirtazapinium	N3⁺–H3A⋯O1⁻	2.60	3.377(4)	122.7	–1+x, y, z
hemiadipate **44**	N3⁺–H3A⋯O2⁻	1.42	2.592(4)	175.3	–1+x, y, z
	C2–H2⋯O1⁻	2.46	3.312(5)	150.0	---[a]
	C8–H8⋯N1	2.53	3.453(4)	163.3	x, 3/2–y, 1/2+z
	C10–H10⋯O1⁻	2.50	3.384(4)	155.1	–1+x, y, z
	C14–H14B⋯O2⁻	2.50	3.402(4)	151.5	1–x, 2–y, –z
	[b]C12–H12⋯O1⁻	2.69	3.383	125.5	–1+x, y, z
Mirtazapinium	O3–H3B⋯O2⁻	1.80	2.563(7)	142.9	---[a]
Salicylate **45**	N3⁺–H3A⋯O1⁻	1.34	2.521	166.3	---[a]
	[b]C12–H12⋯O2⁻	2.79	3.560	133.2	---[a]

[a] molecules/ ions in the same asymmetric unit
[b] ionic C–H⋯O⁻ H bond of the $R_2^2(8)$ synthon shown in Figure 14
[c] intra molecular H bond

6.4 XRPD and Spectroscopic Analysis

Apart from single crystal X-ray diffraction, XRPD and spectroscopic methods are useful tools for characterizing the formation of a salt/ cocrystal. The bulk material of Mirtazapinium salts were prepared by liquid assisted grinding[16] using 4–5 drops of methanol solvent, stoichiometric amount of Mirtazapine and the corresponding salt former for 10-15 min. The XRPD of Mirtazapinium salts are shown in Figure 9 match with the calculated powder pattern (red) which confirms the formation of the salts and the R_p values (refinement parameter) of the Rietveld refinement are satisfactory. In case of

Mirtazapinium dihydrochloride trihydrate **40** the experimental powder pattern do not match with the calculated one which may be because of release of water molecule from the channel during the grinding of the sample, which was confirmed by the thermal analysis.
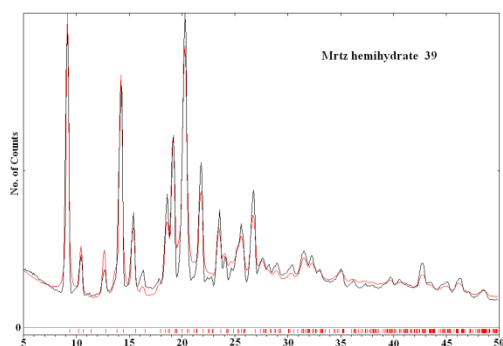
(a) Mirtazapine hemihydrate **39**
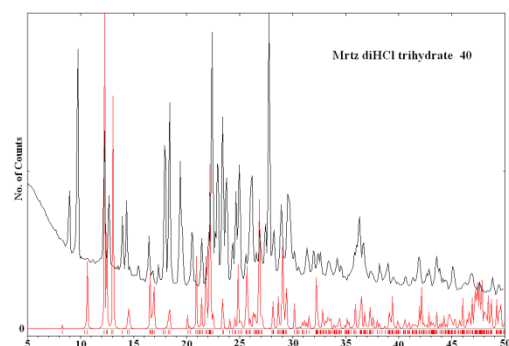
(b) Mirtazapinium diHCl trihydrate **40**
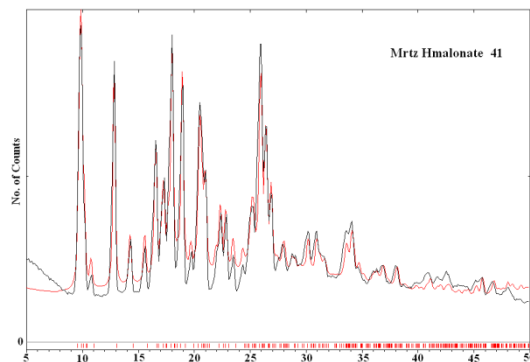
(c) Mirtazapinium Hmalonate **41**
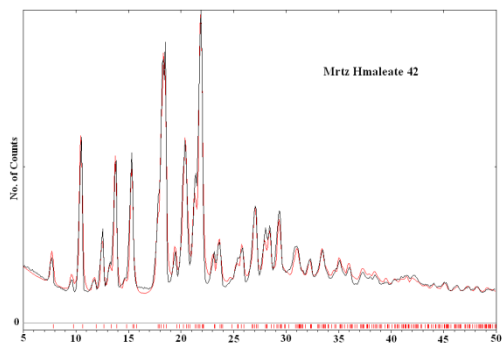
(d) Mirtazapinium Hmaleate **42**
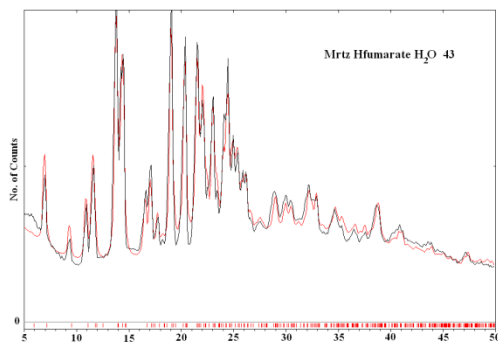
(e) Mirtazapinium Hfumarate H_2O **43**

(f) Mirtazapinium hemiadipate **44**   (g) Mirtazapinium salicylate **45**
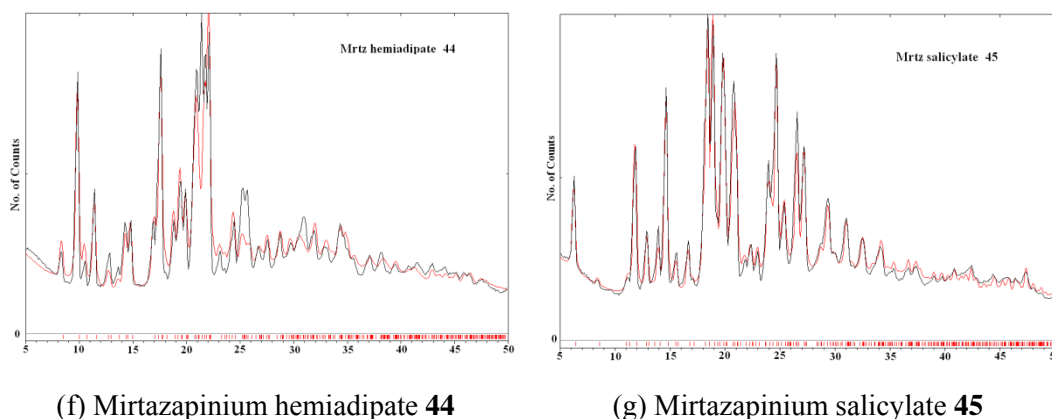
Figure 9 Overlay of the calculated X-ray crystal structure (red) and experimental XRPD pattern (black) of the bulk material.

Infrared spectroscopy is a very useful tool in detecting cocrystal/salt formation. The peak shift of 10–15 cm^{-1} due to the formation of hydrogen bond indicates the formation of salt/ cocrystal. Here in Mirtazapinium salts, carboxylic acids are present as salt formers and the difference in stretching frequency should be observed between a neutral carboxylic acid moiety and a carboxylate anion. A neutral carboxylic acid group (–COOH) normally displays a strong C=O stretching band around 1700 cm^{-1} and a weaker C–O stretch around 1200 cm^{-1}, while for a carboxylate anion (–COO$^-$) due to resonance, the observed peak is only a single C–O stretch in the fingerprint region of 1000–1400 cm^{-1}. But for a dicarboxylic acid with one proton transfer the peak around 1700 cm^{-1} indicates the presence of an unionized carboxylic group whereas for monoacid like **45** the absence of this peak is a clear indication of salt formation. Again, if a neutral intermolecular O–H⋯N hydrogen bond is present then two broad peaks around 2500 and 1900 cm^{-1} will be observed which are resulted for Fermi resonance of OH proton stretching and overtones of bending modes.[17] Moreover the intermolecular hydrogen bond between two components results in red shift of stretching frequency. For Raman spectra also the same characteristic features are observed except that intensities are weaker for the asymmetric vibrations. All the salts showed characteristic IR and Raman spectra in the solid state (Figure 10, 11).
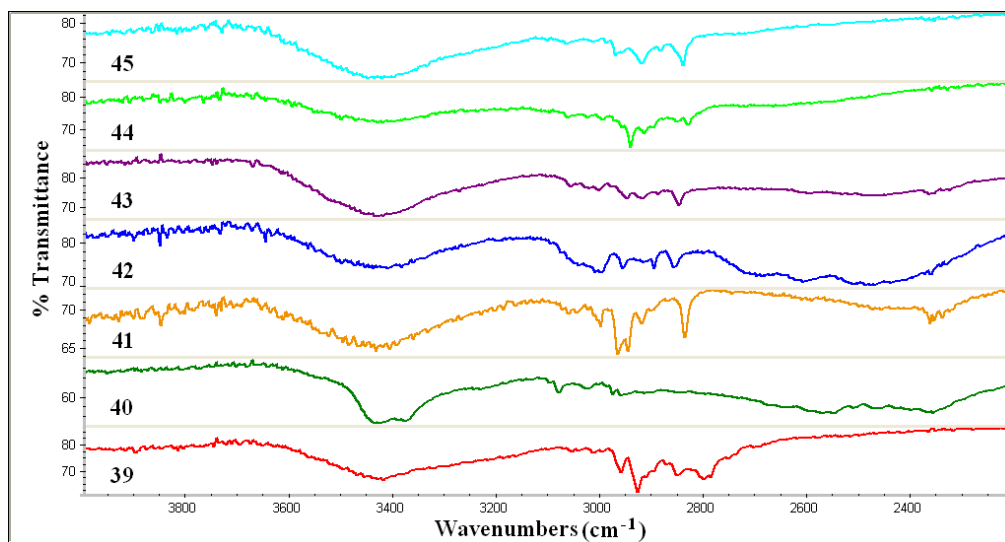
(a)
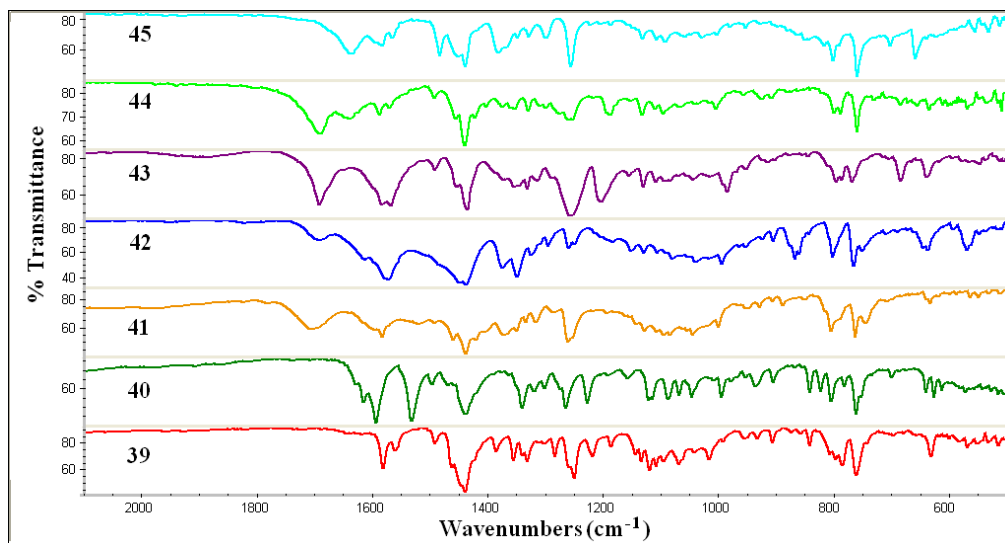
(b)

Figure 10 FT-IR spectra of Mirtazapine salts **39**–**45**. Spectral region (a) from 4000–2200 cm^{-1} and (b) from 2200–500 cm^{-1}.
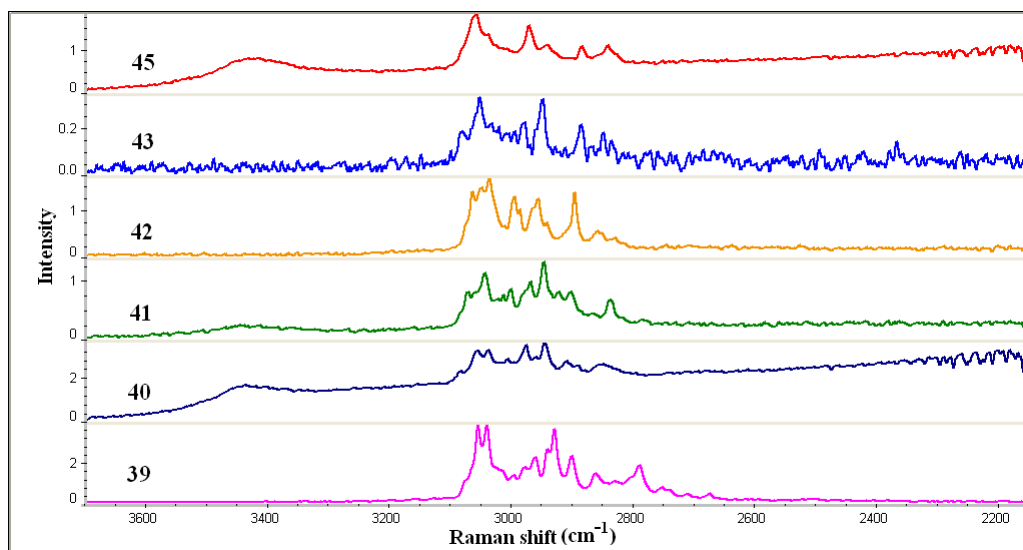
(a)
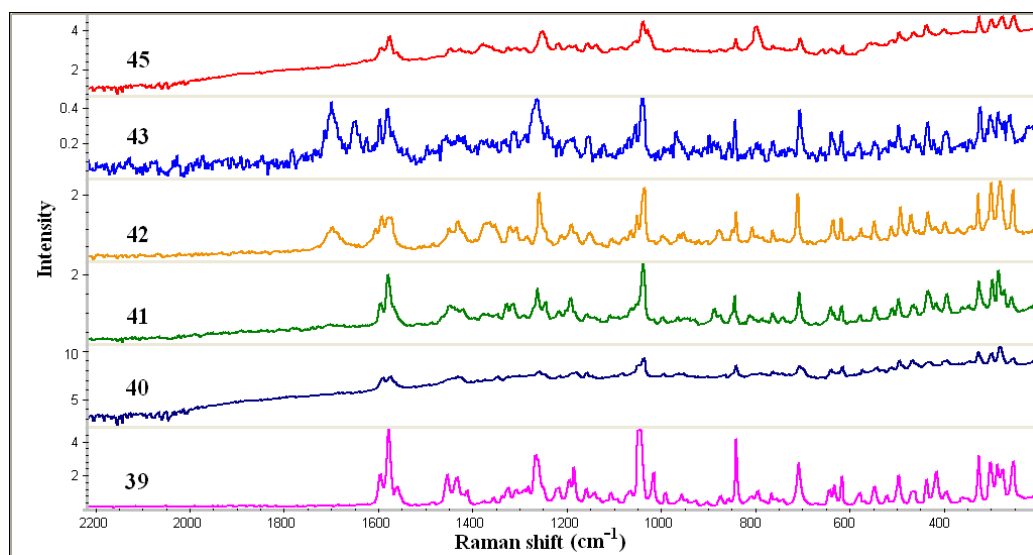
(b)

Figure 11 FT-Raman spectra of Mirtazapine salts **39**–**45**. Spectral region (a) from 3700–2200 cm^{-1} and (b) from 2200–200 cm^{-1}.

Note: Mirtazapinium hemiadipate **44** could not be recorded because the sample was charred by the laser.

6.5 THERMAL ANALYSIS

Differential Scanning Calorimetry (DSC), Thermo Gravimetric Analysis (TGA) and Hot Stage Microscopic (HSM) studies were done in order to study the thermal stability of Mirtazapinium salts prepared. The TGA of Mirtazapine hemihydrate **39** showed a gradual weight loss starting at about 65 °C. The sublimation of Mirtazapine base started at 65 °C as seen under a hot stage microscope (Figure 12) and the sudden drop in TGA curve at 120 °C corresponds to the melting point of Mirtazapine based on the DSC endotherm at T_{peak} = 121 °C.

24 °C   65 °C   90 °C

95 °C

| 95-98 °C | 103 °C | 109 °C |
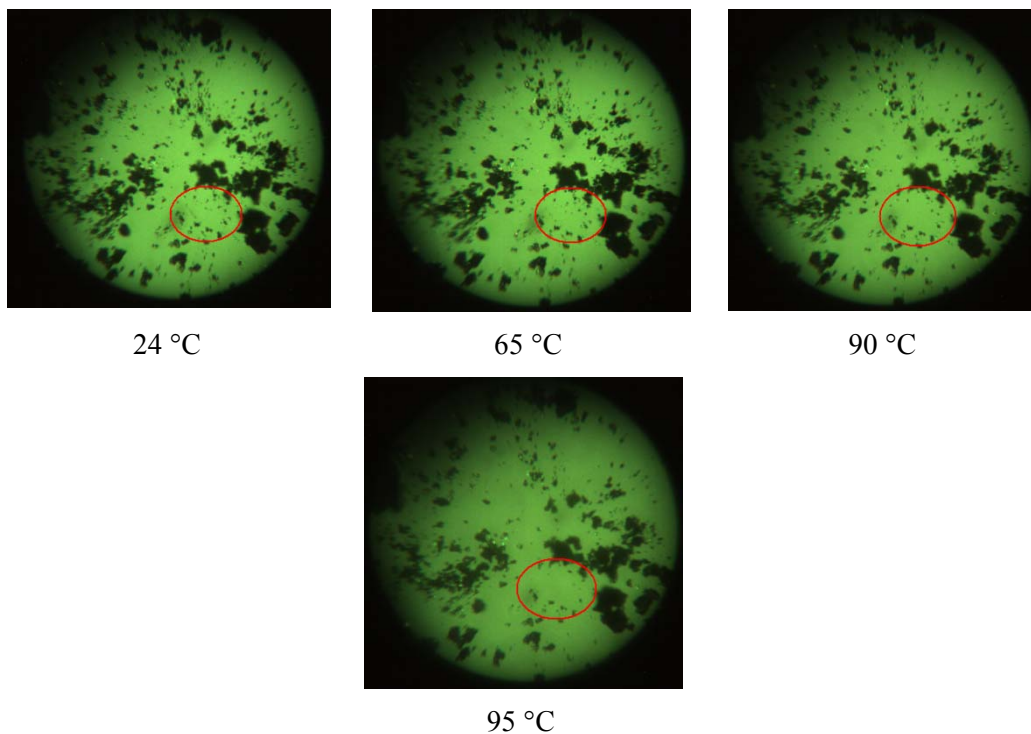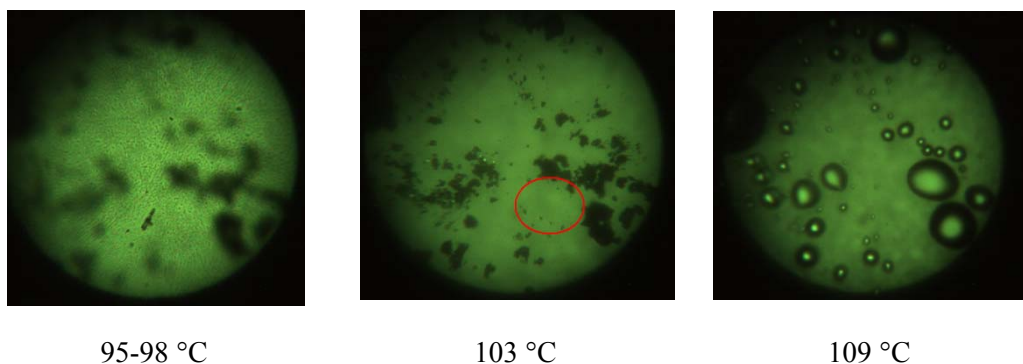
Figure 12 HSM snapshots of Mirtazapine hemihydrate **39**. The solid particles in the red circle started disappearing with heating and made a cloudy deposition on the glass slide at 95 °C and melted by 110 °C. Visual observation suggests that sublimation begins around 65 °C and melting occurred at 110 °C. The glass lid is filled with the sublimed material at 95-98 °C.

In case of Mirtazapinium dihydrochloride trihydrate salt **40** the weight loss of 8.97% corresponds to the loss of two water molecules based on theoretical weight (calc. 9.18%). Mirtazapinium dihydrochloride is a trihydrate according to the crystal structure. Therefore it is possible that part of the water escaped from the channel structure to give a lower water content in TGA. The loss of one water stoichiometry could have happened at the time of powdering the sample for XRPD and a possible reason for not matching the experimental XRD lines with that of calculated pattern for the trihydrate salt **40**. For Mirtazapinium hydrogenfumarate monohydrate salt **43** the observed weight loss of 4.04% corresponds to one stoichiometric water molecule (calc. 4.52%).

Interestingly, in contrast to the immediate sublimation of Mirtazapine hemihydrate **39**, the salt forms of Mirtazapine prepared in our study do not show any evidence of sublimation in TGA and/ or HSM, which justify the need to analyze the crystal structures of salts to understand the improvement in the stability of Mirtazapine. The DSC and TGA thermograms of the Mirtazapinium salts are shown in Figure 13.
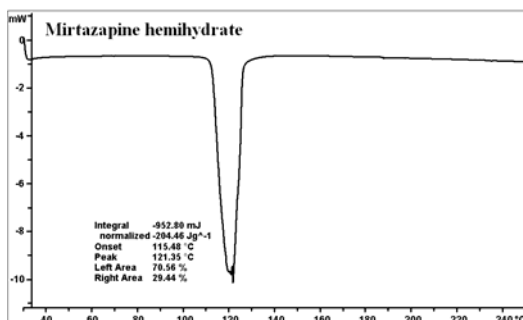
(a) DSC of **39**
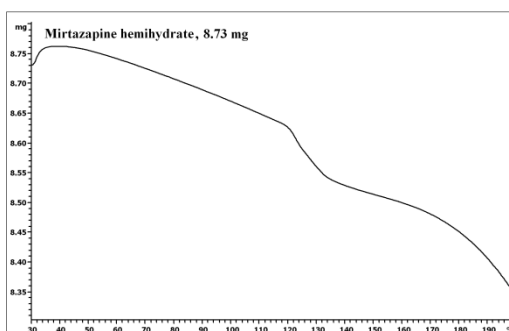
(b) TGA of **39**
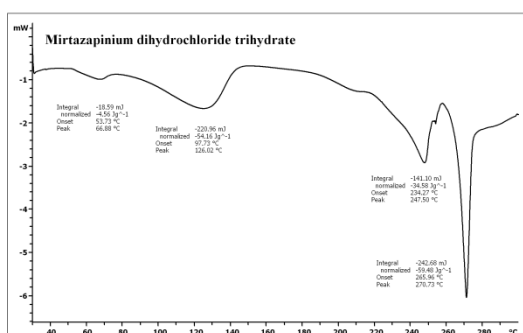
(c) DSC of **40**
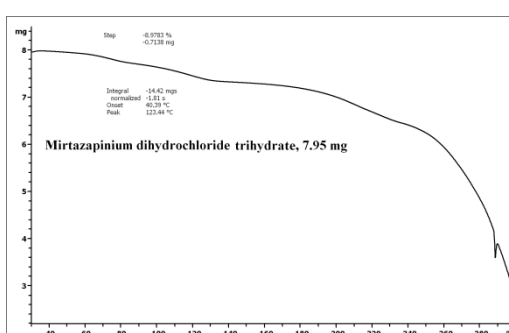
(d) TGA of **40**

(e) DSC of **43**

(f) TGA of **43**
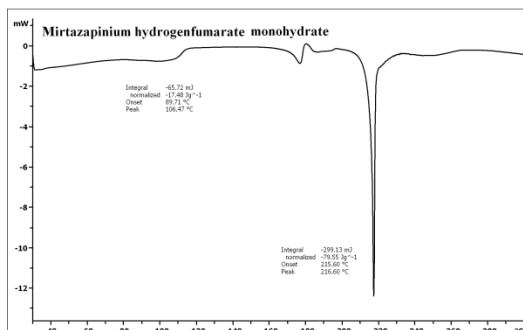
(g) DSC of **41**

(h) DSC of **42**

(i) DSC of **44**

(j) DSC of **45**
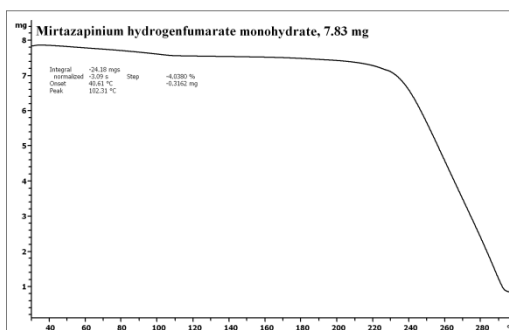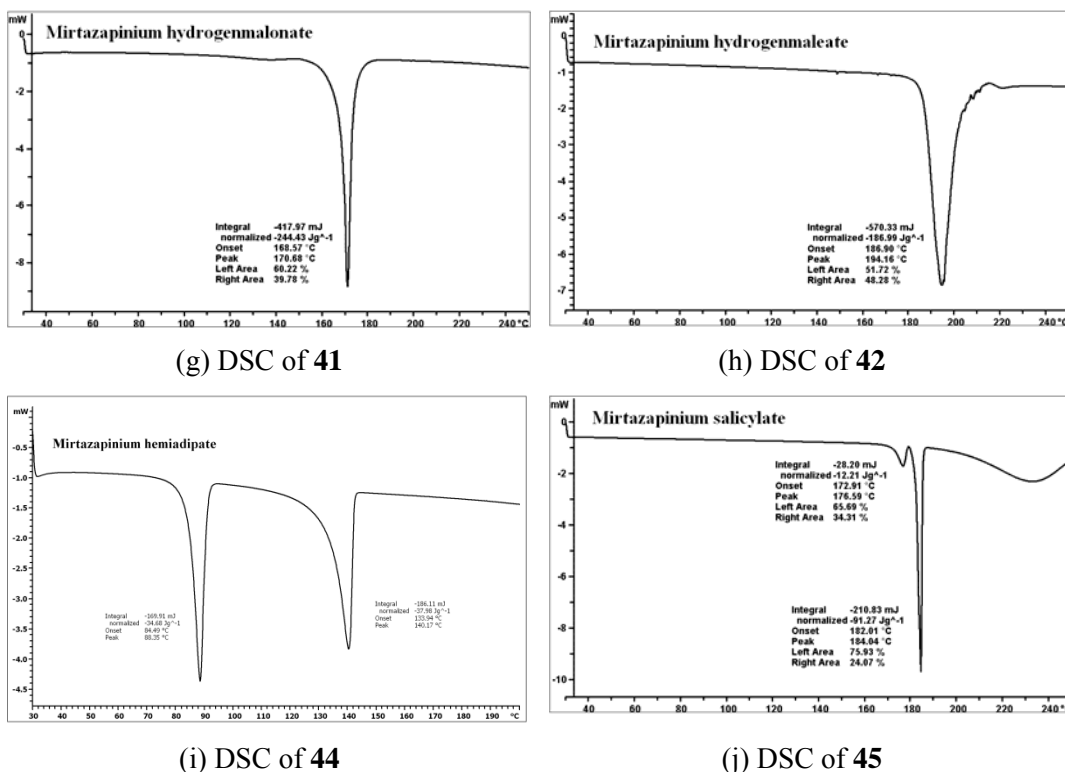
Figure 13 DSC and TGA of Mirtazapinium salts along with hemihydrate **39**.

6.6 HYDROGEN BOND SYNTHON

From the crystal structure point of view it is seen that all acid coformer with $pK_a < 4$ formed salts (Table 2) and all Mirtazapinium carboxylate salts possess an ionic, two-point synthon $R_2^2(8)$ formed by the carboxylate anion with the protonated N-methyl site and the activated H attached to the asymmetric C atom of the piperazine ring of Mirtazapine. The C–H donor is both benzylic and α to tertiary amine being sandwiched between these functional groups, and hence activated as a carbon acid.[18] In the adipate salt two protons are transferred to two molecules of Mirtazapine even though $\Delta pK_a < 3$. The formation of strong N^+–H···O^- and C–H···O^- two-point synthons (Figure 14) compared to the neutral motifs, N···H–O and C–H···O, is the reason for the proton transfer and the salt formation. This special synthon situation is applicable to five carboxylate structures which have the $R_2^2(8)$ motif of C–H···O distance 2.68, 2.67, 2.84,

2.69 and 2.79 Å for structures **41**, **42**, **43**, **44** and **45** respectively (interaction labeled b in Table 1). This two-point synthon $R_2^2(8)$ is not serendipitous contact as the ionic one-point synthon is also possible. There is limited structural data on the piperazino-azepine ring system in the CSD, and more crystal structures are needed to understand the structural significance of this newly identified synthon in Mirtazapine salts.

Ionic, one-point **Ionic, two-point** **Neutral, two-point**
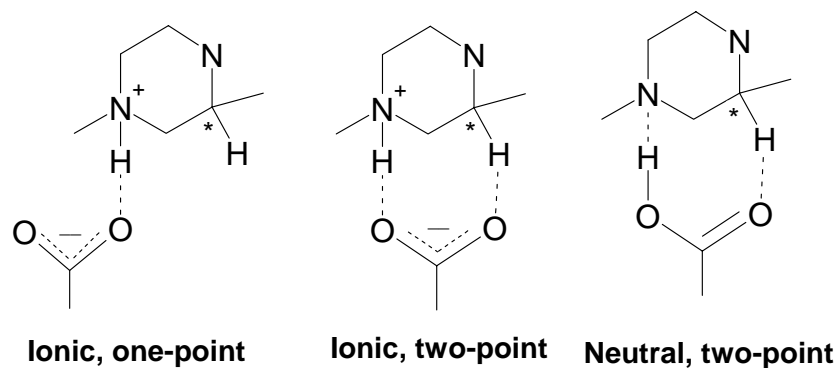
Figure 14 Possible carboxylic acid–piperazine hydrogen bonding motif for Mirtazapine base and carboxylic acid. The stronger ionic two-point synthon is preferred over the neutral motif.

Table 2 pK_a values of Mirtazapine[19] and acids[20] used in this study.

Molecule	pK_a value	Product complex	ΔpK_a value
Mirtazapine	7.1		
HCl	–7	Mirtazapinium HCl	14.1
Fumaric acid	3.03, 4.44	Mirtazapinium hydrogenfumarate	4.07
Malonic acid	2.83, 5.69	Mirtazapinium hydrogenmalonate	4.27
Maleic acid	1.92, 6.27	Mirtazapinium hydrogenmaleate	5.18
Adipic acid	4.43, 5.41	Mirtazapinium hemiadipate	2.67, 1.69
Salicylic acid	2.97	Mirtazapinium salicylate	4.13

6.7 CONCLUSION

Salt formation is the first-choice method to improve the physical stability and solubility of drug substances. A few non-subliming salts of Mirtazapine along with the hemihydrate

of the parent drug were crystallized. The proton transfer in these crystal structures is consistent with the ΔpK_a rule except in the hemiadipate salt for which the difference < 3. All salts are fully characterized by diffraction, spectroscopic and thermal methods. Except the dihydrochloride and fumarate salts, all other Mirtazapine salts are non-hygroscopic in nature. Whereas the free base undergoes sublimation at slightly above ambient temperature, the maleate, salicylate and fumarate salts do not sublime even at elevated temperatures. There is very little crystallographic information on the piperazino-azepine class of drugs to make definitive structure–property conclusions which could be possible in the near future when sufficient data is available.

6.8 EXPERIMENTAL SECTION

PREPARATION OF SALTS

50 mg (0.2 mmol) of Mirtazapine and stoichiometric amount of the carboxylic acid were mixed in a mortar-pestle, 4-5 drops of methanol was added, the material was manually ground for 15 min, and then dissolved in 10 mL methanol and left for slow evaporation at room temperature. The resulting solid was analyzed by X-ray diffraction and vibrational spectroscopy.

Mirtazapinium diHCl trihydrate salt was prepared by gradual addition of a dilute solution of HCl in acetonitrile (prepared by adding 2 drops of concentrated HCL in 10 mL of acetonitrile) to a solution of Mirtazapine (50 mg ie. 0.2 mmol in 10 mL acetonitrile). The addition continued till the hydrochloride salt precipitates out. The solid was filtered, dried and kept for crystallization in methanol for X-ray diffraction quality crystals.

X-RAY CRYSTALLOGRAPHY

X-ray reflections for all compounds were collected at 298 K (Mirtazapinium hemiadipate data collected at 100K) on Bruker SMART APEX CCD equipped with a graphite monochromator and Mo-Kα fine-focus sealed tube (λ = 0.71073 Å). Data integration was done using SAINT.[21] Intensities for absorption were corrected using SADABS.[22]

Structure solution and refinement were carried out using Bruker SHELXTL.[23] The hydrogen atoms were refined isotropically and the heavy atoms were refined anisotropically. N–H and O–H hydrogens were located from difference electron density maps and C–H hydrogens were fixed using HFIX command in SHELXTL. In case of Mirtazapinium fumarate monohydrate, among the two symmetry independent half fumarate molecules, the methylene carbon of the furamate ion that resides over the two-fold axis was disordered over two positions. It was modeled using FVAR command with s.o.f. of 0.5 each. For the Mirtazapine hemihydrate the oxygen atom of the water molecule has s.o.f. of 0.5 and is situated near the inversion center. Crystallographic data are summarized in Appendix. Packing diagrams were prepared in X-Seed.[24]

X-RAY POWDER DIFFRACTION

X-ray powder diffraction of all samples were recorded on Bruker D8 Advance diffractometer using Cu-Kα X-radiation (λ = 1.54056 Å) at 40 kV and 30 mA. Diffraction patterns were collected over a 2θ range of 5-50° at a scan rate of 1° min^{-1}. Powder Cell 2.4 was used for Rietveld refinement.[25]

VIBRATIONAL SPECTROSCOPY

Nicolet 6700 FT-IR spectrometer with an NXR FT-Raman module was used to record IR and Raman spectra. IR spectra were recorded on samples dispersed in KBr pellets. Raman spectra were recorded on solid samples contained in standard NMR diameter tubes or on compressed samples contained in a gold-coated sample holder.

THERMAL ANALYSIS

DSC was performed on Mettler Toledo DSC 822e module. Samples were placed in crimped but vented aluminum sample pans. The typical sample size was 3-4 mg, and the temperature range was 30-300 °C at heating rate of 5 °C min^{-1}. Samples were purged by a stream of dry nitrogen flowing at 150 mL min^{-1}. For TGA, the sample size was 7-9 mg, the heating rate was 10 °C min^{-1}, and the N_2 flow was 50 mL min^{-1}. HSM was performed

on a Wagner & Munz PolythermA Hot Stage and Heiztisch microscope. A Moticam 1000 (1.3 MP) camera supported by software Motic Image Plus 2.0ML was used to record images.

6.9 REFERENCES

1. (a) S. L. Johnson and K. A. Rumon, *J. Phys. Chem.*, 69, **1965**, 74. (b) B. Sarma, N. K. Nath, B. R. Bhogala and A. Nangia, *Cryst. Growth Des.*, 9, **2009**, 1546. (c) B. R. Bhogala, S. Basavoju and A. Nangia, *CrystEngComm*, 7, **2005**, 551. (d) S. L. Childs, G. P. Stahly and A. Park, *Mol. Pharm.*, 4, **2007**, 323.

2. (a) C. L. Cooke and R. J. Davey, *Cryst. Growth Des.*, 8, **2008**, 3483. (b) M. Mirmehrabi, S. Rohani, K. S. K. Murthy and B. Radatus, *Int. J. Pharm.*, 282, **2004**, 73. (c) M. L. Cheney, N. Shan, E. R. Healey, M. Hanna, L. Wojtas, M. J. Zaworotko, V. Sava, S. Song and J. R. Sanchez-Ramos, *Cryst. Growth Des.*, 10, **2010**, 394.

3. (a) P. H. Stahl, C. G. Wermuth (Eds.), *Handbook of Pharmaceutical Salts: Propertiesm Selection, and Use*; Wiley-VCH, **2002**. (b) S. M. Berge, L. D. Bighley and D. C. Monkhouse, *J. Pharm. Sci.*, 66, **1977**, 1. (c) S. L. Morissette, Ö. Almarsson, M. L. Peterson, J. F. Remenar, M. J. Read, A. V. Lemmo, S. Ellis, M. J. Cima and C.R. Gardner, *Adv. Drug Deliv. Rev.*, 56, **2004**, 275.

4. (a) C. R. Craig and R. E. Stitzel, *Modern Pharmacology with Clinical Applications*. 5th Ed.; Boston: Little Brown & Company. pp 385–396. (b) V. J. Nickolson, AU 2001273932 B2. (c) J. S. Andrews, W. Drinkenburg and N. M. Ward, US 2005/0090488 A1. (d) A. Houghton, G. Stephanus and F. Ruigt, US 2007/0270413 A1.

5. A. Cipriani, T. A. Furukawa, G. Salanti, J. R Geddes, J. P. T. Higgins, R. Churchill, N. Watanabe, A. Nakagawa, I. M. Omori, H. McGuire, M. Tansella and C. Barbui, *Lancet*, 373 (9665), **2009**, 746.

6. (a) R. Löbenberg and G. L. Amidon, *Eur. J. Pharm. and Biopharm.*, 50, **2000**, 3. (b) N. A. Kasim, M. Whitehouse, C. Ramachandran, M. Bermejo, H. Lennernäs,

A. S. Hussain, H. E. Junginger, S. A. Stavchansky, K. K. Midha, V. P. Shah and G. L. Amidon, *Mol. Pharm.*, 1, **2004**, 85.

7. C. J. Timmer, J. M. Ad Sitsen and L. P. Delbressine, *Clin. Pharmacokinetics*, 38, **2000**, 461.

8. A. Puncuh-Kolar, U. Turk, M. Kincl, T. Rajer, A. Ferlan, B. Gartnar and L. Cernosa, WO 2006/005578 A2.

9. (a) T. D. Boer, *Intern. Clin. Psychopharmacol*., 10, **1995**, 19. (b) A Orjales, R. Mosquera, A. Toledo, M. C. Pumar, N. García, L. Cortizo, L. Labeaga and A. Innerárity, *J. Med. Chem.*, 46, **2003**, 5512.

10. (a) A. F. Pozharskii, V. V. Kuźmenko, V. A. Azimov and L. N. Yakhontov, *Chem. Hetero. Compd.*, 9, **1973**, 1119. (b) http://sparc.chem.uga.edu/.

11. (a) S. H. Moolenaar, G. J. Kemperman and K. V. D. V. Maarschalk, WO 2005/102352 A1. (b) P. Aluri, J. Babu, S. S. Rao and S. Gogia, US 2007/0298107 A1. (c) E. Iishi and Y. Imamiya, US 6552189 B2.

12. Cambridge Structural Database, ver. 5.31, ConQuest 1.12, November **2009** release, Aug **2010** update; www.ccdc.cam.ac.uk.

13. (a) M. van Meerssche and V. P. Declercq, *Bull. Soc. Chim. Belg.*, 92, **1983**, 307. (b) A. Dalpiaz, V. Ferretti, P. Gilli and V. Bertolasi, *Acta Cryst.*, B52, **1996**, 509. (c) C. van Ru and D. Feil, *Tetrahedron*, 29, **1973**, 1891.

14. P. M. Bhatt, N. V. Ravindra, R. Banerjee and G. R. Desiraju, *Chem. Commun.*, **2005**, 1073.

15. (a) A. Collet, M.-J. Brienne and J. Jacques, *Chem. Rev.*, 80, **1980**, 215. (b) J. Jacques, A. Collet and S. H. Wilen, in *Enantiomers*, *Racemates and Resolution*, Wiley-Interscience, New York, **1981**. (c) D. K. Kondepudi and K. Asakura, *Acc. Chem. Res.*, 34, **2001**, 946. (d) L. Pérez-García and D. B. Amabilino, *Chem. Soc. Rev.*, 31, **2002**, 342; 36, **2007**, 941. (e) E. Pidcock, *Chem. Commun.*, **2005**, 3457. (f) M. A. Sephton, C. R. Emerson, L. N. Zakhrov and P. R. Blakemore, *Chem. Commun.*, 46, **2010**, 2094.

16. (a) N. Shan, F. Toda and W. Jones, *Chem. Commun.*, **2002**, 2372. (b) A. V. Trask, D. A. Haynes, W. D. S. Motherwell and W. Jones, *Chem. Commun.*, **2006**, 51. (c) T. Friščić and W. Jones, *Cryst. Growth Des.*, 9, **2009**, 1621.

17. (a) R. M. Silverstein, F. X. Webster and D. J. Kiemle, *Spectroscopic Identification of Organic Compounds;* John Wiley & Sons, **2005**. (b) H. G. Brittain, *Polymorphism in Pharmaceutical Solids*, 2nd Ed.; **2009**. (c) C. B. Aakeröy, D. J. Salmon, M. M. Smith and J. Desper, *Cryst. Growth Des.*, 6, **2006**, 1033. (d) J. P. Castaneda, G. S. Denisov, S. Y. Kucherov, V. M. Schreiber and A. V. Shurukhina, *J. Mol. Struct.*, 660, **2003**, 25.

18. G. R. Desiraju and T. Steiner, *The Weak Hydrogen Bond In Structural Chemistry and Biology*; Oxford University Press. pp 50–53.

19. (a) T. L. Lemke, D. A. Williams, V. F. Roche and S. W. Zito, *Foye's Principles of Medicinal Chemistry*. 6th Ed.; Lippincott Williams & Wilkins. pp 547–600. (b) S. R. Kuchekar, M. L. Kundlik and B. H. Zaware, *J. Saudi Chem. Soc.*, **2010**, doi:10.1016/j.jscs.2010.07.001.

20. (a) D. R. Lide, *CRC Handbook of Chemistry & Physics*, 86th Ed.; Taylor & Francis. pp 8: 42–51. (b) www.wikipedia.org.

21. *SAINT-Plus*, version 6.45, Bruker AXS Inc., Madison, WI, **2003**.

22. G. M. Sheldrick, *SADABS*, *Program for Empirical Absorption Correction of Area Detector Data*, University of Göttingen, Germany, **1997**.

23. (a) *SMART* (Version 5.625) and *SHELX-TL* (Version 6.12), Bruker AXS Inc., Madison, WI, **2000**. (b) G. M. Sheldrick, *SHELXS-97* and *SHELXL-97*, University of Göttingen, Germany, **1997**.

24. *X-Seed, Graphical Interface to SHELX-97 and POVRay*, L. J. Barbour, University of Missouri-Columbia, Columbia, MO, **1999**.

25. Powder Cell 2.4, Program for structure visualization, powder pattern calculation and profile fitting, www.ccp14.ac.uk.

CHAPTER SEVEN

CONCLUSION AND FUTURE PROSPECTS

Solid-state chemistry is important from the synthesis and structural point of view in order to generate solid materials with new properties.[1] Novel functional materials for guest inclusion, gas absorption, isomers separation, targeted drug delivery, magnetism, conductivity and catalysis, etc. can be designed through the network approach.[2] In the pharmaceutical solids area, apart from polymorphism, salt preparation, amorphization and cocrystallization are practical approaches in pharmaceutical drug design to improve the physico-chemical properties such as solubility, dissolution, bioavailability, stability, hygroscopicity, etc.[3]

Different molecular networks generated from a H-shaped tecton, 1,4-Di[bis(4'-hydroxyphenyl)methyl]benzene **A** and its methoxy and methyl derivatives **B**–**D** were described in Chapter 2. These H-shaped molecules **A**–**D** formed numerous solvates and cocrystals that resulted in diverse network structures like 1D ladder, polyrotaxane, 2D honeycomb net and Catalan nets with various interpenetration and catenation modes from the same starting tecton. The presence of a second aromatic component facilitated interplay between hydrogen bonding and π-stacking motifs. Network diversity for these multi-component structures is the result of change in guest hydrogen bonding, π-stacking and host molecular conformation.

Structural aspects of cocrystals of pyrogallol and catechol with various N-heterocycle bases was the subject matter of Chapter 3. It was observed that in most of the cocrystals there are more than two molecules in the asymmetric unit. Some reasons for higher Z' structure are awkwardly shaped molecules (like monoalcohols, phenols, primary amine, etc.), molecular pseudosymmetry, chirality, strong hydrogen bond, polymorphs and modulated structures etc. In case of pyrogallol and catechol cocrystals, the awkward shape of molecule and strong hydrogen bonds may be the reasons for higher Z''. For cocrystal **20** that solved in chiral noncentrosymmetric space group $P2_1$, a reason for 6 molecules in the asymmetric unit (Z'') in contrast to 3 molecules for

centrosymmetric case is the chiral space group. On the whole it is difficult to summarize in one line the reason for the occurrence of high Z' in crystal structures. In the recent past several articles have been published on the pharmaceutical utility of pyrogallol which is explored as a potential candidate for anti-lung cancer drug particularly for the non-small cell lung cancer (NSCLC) and Cystic Fibrosis (CF) chronic lung inflammatory disease. The structural study of the N-heterocycle bases with pyrogallol/ catechol and their solubility and dissolution comprise a model study that could be useful from the pharmaceutical perspective.

Chapter 4 focused on structural aspects of a polymorph (Form IV), few solvates and molecular salts of a BCS Class II anti-psychotic drug, Olanzapine (Zyprexa). There are six polymorphs reported for Olanzapine, but so far only one form is reported in the CSD. Form IV crystals of Olanzapine was obtained from cocrystallization with nicotinamide. Other derivatives of Olanzapine are acetone monohydrate, acetonitrile monohydrate, ethanol monohydrate, nitromethane monohydrate solvates and binary and ternary (salt cocrystal/ salt solvate) salts. The solubility and dissolution of the Olanzapinium salts were studied and improved to a significant extent compared to the practically insoluble Olanzapine base (43 mg/L). These salts were further characterized by XRPD, molecular spectroscopy (FT-IR, FT-NIR, FT-Raman) and thermal methods (DSC and HSM). The proton transfer in all the Olanzapinium salts was consistent with the ΔpK_a rule of 3.

In Chapter 5, two different stoichiometric salts of Olanzapine with maleic acid in both crystalline and amorphous forms were discussed. Olanzapinium monomaleate (1:1) **37** and dimaleate (1:2) **38** salts were prepared by mechanical grinding. Solid-state grinding resulted in amorphous form and liquid assisted grinding gave the crystalline salts. The two step model of salt formation with amorphous material as an intermediate is discussed. The two maleate salts have higher solubility (225–550 times) and dissolution rate. Enhancement in solubility and dissolution rate of dimaleate was explained by crystal structure analysis and hydrogen bonding sites on the maleate anion. The crystalline and amorphous salts were further characterized by spectroscopy, XRD, SEM, TEM and ED

to confirm the bulk material and the amorphous nature. Salts are well documented as a means to improve the physico-chemical properties of drugs. Olanzapinium salts were shown to exhibit improved solubility and variable stoichiometry.

The preparation and structural aspects of hemihydrate of the free base, some molecular salts of Mirtazapine with HCl, malonic acid, maleic acid, fumaric acid, adipic acid and salicylic acid in order to understand the hydrogen bonding, molecular packing and hydration states were also discussed. (±)-1,2,3,4,10,14b-hexahydro-2-methylpyrazino[2,1-a]pyrido[2,3-c]benzazepine commonly known as Mirtazapine sublimes at ambient temperature and this poses stability problem for tablet formulation. With respect to the free base all Mirtazapinium salts were found to be non-hygroscopic and non-subliming in nature (except the dihydrochloride and fumarate salt) and are stable as confirmed by Thermal analysis (DSC and TGA).

In summary various important aspects of solid state chemistry of materials are discussed in this thesis. Organic network solids were designed, structural aspects along with improvement in solubility, dissolution and stability of some APIs were studied to obtain superior drug products.

REFERENCES

1. (a) J.-M. Lehn, *Supramolecular Chemistry: Concepts and Perspectives*, VCH: Weinheim, **1995**. (b) M. G. Kanatzidis and K. R. Poeppelmeier (Organizers), *Prog. in Solid State Chem.*, 36, **2007**, 1.

2. (a) A. F. Wells, *Three-Dimensional Nets and Polyhedra,* Wiley, New York, **1977**. (b) L. Öhrström and K. Larsson, *Molecule-Based Materials*, Elsevier, **2005**. (c) N. L. Rosi, M. Eddaoudi, J. Kim, M. O'Keeffe and O. M. Yaghi, *Angew. Chem. Int. Ed.*, 41, **2002**, 284. (d) L. Carlucci, G. Ciani and D. M. Proserpio, *Coord. Chem. Rev.*, 246, **2003**, 247.

3. (a) H. G. Brittain, *Polymorphism in Pharmaceutical Solids*, 2nd Ed., Inc. New York, **2009**. (b) P. H. Stahl and C. G. Wermuth (Eds.), *Handbook of Pharmaceutical Salts: Properties, Selection, and Use*; Wiley-VCH, **2002**. (c) L.

Yu, *Adv. Drug Deliv. Rev.*, 48, **2001**, 27. (d) P. Vishweshwar, J. A. McMahon, J. A. Bis and M. J. Zaworotko, *J. Pharm. Sci.*, 95, **2006**, 499. (e) Y. Qiu, Y. Chen, G. G. Z. Zhang, L. Liu and W. R. Porter (Eds.), *Developing Solid Oral Dosage Forms: Pharmaceutical Theory And Practice*, 1st Ed., Elsevier, **2009**.

APPENDIX

Crystallographic data for the crystal structures discussed in this thesis.

Crystal Data	1	2•EtOAc	3•DMSO
Emp. Formula	$C_{32}H_{26}O_4$	$C_{40}H_{42}O_8$	$C_{36}H_{38}O_6S_2$
Formula wt.	474.53	650.74	630.78
Crystal system	Triclinic	Triclinic	Monoclinic
Space group	$P\bar{1}$	$P\bar{1}$	$P2_1/c$
T [K]	100	100	100
a [Å]	10.1926(10)	7.3791(5)	11.0387(11)
b [Å]	11.0478(10)	10.4359(8)	7.4017(7)
c [Å]	13.0960(14)	11.3692(8)	19.4980(19)
α [°]	101.849(2)	93.3570(10)	90
β [°]	102.082(2)	95.2410(10)	96.343(2)
γ [°]	115.675(2)	100.8240(10)	90
Z	2	1	2
Volume [Å^3]	1224.1(2)	853.77(11)	1583.3(3)
D_{calc} [g cm^{-3}]	1.287	1.266	1.323
μ/mm^{-1}	0.084	0.087	0.214
Reflns. collected	12394	7902	15752
Unique reflns.	4633	3323	3127
R_1 [I>2σ(I)], wR_2	0.0786, 0.1032	0.0401, 0.1049	0.0603, 0.1273
GOF	0.991	1.048	1.062

4•isoPrOH	5•Phez	6•Quinox	7•PyzNO
$C_{44}H_{58}O_8$	$C_{50}H_{38}N_3O_4$	$C_{48}H_{38}N_4O_4$	$C_{40}H_{34}N_4O_8$
714.90	744.83	734.82	698.71
Monoclinic	Triclinic	Monoclinic	Monoclinic
$C2/c$	$P\bar{1}$	$P2_1/c$	$P2_1/c$
100	298	298	298
33.506(3)	10.2976(8)	14.472(6)	13.064(2)
5.8797(4)	11.2084(9)	16.115(6)	7.6296(11)
22.036(2)	18.4225(15)	8.057(3)	16.929(3)
90	96.0410(10)	90	90
115.061(2)	103.7210(10)	93.044(7)	99.722(2)
90	102.7000(10)	90	90
4	2	2	2
3932.5(6)	1987.1(3)	1876.3(13)	1663.1(4)
1.207	1.245	1.301	1.395
0.082	0.079	0.084	0.099
19346	20835	11675	16408
3880	7790	3678	3273
0.0759, 0.2116	0.0651, 0.1538	0.0829, 0.1429	0.0599, 0.1334
1.042	1.016	1.118	1.141

8•BipyNO	9•DMSO	10•Dioxane	11•DMF
$C_{52}H_{42}N_4O_8$	$C_{44}H_{54}O_{14}S_2$	$C_{48}H_{58}O_{16}$	$C_{42}H_{48}N_2O_6$
850.90	870.99	890.94	676.82
Orthorhombic	Monoclinic	Triclinic	Monoclinic
$Pca2_1$	$P2_1/c$	$P\bar{1}$	$C2/c$
298	100	298	100
20.631(4)	10.8550(7)	9.039(4)	23.799(2)
7.1465(14)	14.2040(9)	10.605(4)	8.0974(8)
28.309(5)	14.8984(9)	13.461(6)	18.3595(15)
90	90	101.940(7)	90
90	111.1700(10)	98.428(8)	113.226(5)
90	90	112.198(7)	90
4	2	1	4
4173.9(14)	2142.1(2)	1132.4(8)	3251.3(5)
1.354	1.350	1.307	1.383
0.092	0.192	0.098	0.092
40714	21901	11616	11912
4257	4227	4379	3202
0.1264, 0.2843	0.0641, 0.1565	0.0751, 0.1797	0.0670, 0.1694
1.150	1.000	0.990	0.978

12•MeNO$_2$	13	14•Toluene	15•DMSO
$C_{38}H_{40}N_2O_8$	$C_{40}H_{42}O_4$	$C_{47}H_{50}O_4$	$C_{44}H_{54}O_6S_2$
652.72	586.74	678.87	742.99
Triclinic	Monoclinic	Triclinic	Monoclinic
$P\bar{1}$	$P2_1/c$	$P\bar{1}$	$P2_1/n$
298	100	100	298
5.5173(5)	15.0090(17)	8.7313(7)	11.340(2)
12.0094(12)	5.5072(6)	10.2761(9)	8.2249(15)
12.9806(13)	18.887(2)	11.4745(10)	21.892(4)
91.144(2)	90	64.9820(10)	90
96.446(2)	104.850(2)	75.9800(10)	102.049(4)
91.410(2)	90	86.5800(10)	90
1	2	1	2
854.17(14)	1509.0(3)	904.07(13)	1996.9(6)
1.269	1.291	1.247	1.236
0.089	0.082	0.078	0.180
8866	14825	9481	19868
3331	2970	3553	3891
0.0594, 0.1388	0.0604, 0.1338	0.0764, 0.1760	0.1189, 0.1888
1.023	1.042	1.074	1.181

	16	17•H$_2$O	18	19
	C$_6$H$_6$O$_3$	C$_6$H$_{6.50}$O$_{3.25}$	C$_{11}$H$_{11}$N$_3$O$_4$	C$_9$H$_9$NO$_{3.50}$
	126.11	130.61	249.23	187.17
	Monoclinic	Tetragonal	Triclinic	Triclinic
	$P2_1/n$	$P4_2/n$	$P\bar{1}$	$P\bar{1}$
	100	100	100	100
	12.1144(11)	24.5039(12)	6.687(9)	9.2540(8)
	3.7765(3)	24.5039(12)	7.074(9)	9.5435(9)
	13.1365(12)	3.7849(4)	11.721(16)	10.0539(9)
	90	90	80.61(2)	72.4640(10)
	115.4840(10)	90	87.92(2)	83.730(2)
	90	90	76.02(2)	80.0920(10)
	4	16	2	4
	542.52(8)	2272.6(3)	530.8(12)	832.47(13)
	1.544	1.527	1.559	1.493
	0.126	0.126	0.121	0.117
	5197	21853	6079	8725
	1075	2263	2482	3277
	0.0372, 0.0981	0.0788, 0.1512	0.0920, 0.2295	0.0389, 0.0950
	1.064	1.335	1.103	1.064

	20	21	22	23
	C$_{18}$H$_{18}$N$_4$O$_5$	C$_9$H$_9$NO$_{3.50}$	C$_{21}$H$_{17.67}$N$_{1.67}$O$_3$	C$_{19.50}$H$_{16.50}$N$_{1.50}$O$_3$
	370.36	187.17	341.37	319.84
	Monoclinic	Monoclinic	Triclinic	Triclinic
	$P2_1$	$P2_1/c$	$P\bar{1}$	$P\bar{1}$
	100	100	100	100
	17.056(2)	11.2860(13)	8.0271(16)	7.5553(8)
	5.8142(7)	19.551(2)	16.182(3)	11.6292(13)
	18.163(2)	7.8342(9)	20.306(4)	18.763(2)
	90	90	74.727(3)	88.645(9)
	100.886(2)	108.082(2)	86.151(4)	80.688(9)
	90	90	85.632(4)	76.572(10)
	4	8	6	4
	1768.7(4)	1643.3(3)	2534.1(9)	1582.2(3)
	1.391	1.513	1.342	1.343
	0.104	0.118	0.091	0.091
	18448	16948	26352	21343
	7006	3256	9973	12028
	0.0644, 0.1192	0.0445, 0.1010	0.1260, 0.2205	0.0606, 0.0893
	1.006	1.051	1.142	0.770

24	25	26	27
$C_{24}H_{20}N_2O_5$	$C_{21}H_{20}N_3O_4$	$C_{16}H_{16}N_2O_3$	$C_9H_9NO_{2.50}$
416.42	378.40	284.31	171.17
Triclinic	Triclinic	Monoclinic	Orthorhombic
$P\bar{1}$	$P\bar{1}$	$P2_1/c$	$Pca2_1$
100	298	100	100
7.6809(7)	9.3257(10)	7.4965(7)	10.4873(11)
10.0076(9)	9.5756(10)	18.8462(17)	17.1310(17)
13.4348(12)	24.020(3)	10.1333(9)	8.9842(9)
73.3500(10)	91.162(2)	90	90
82.756(2)	95.450(2)	95.3970(10)	90
84.385(2)	116.545(2)	90	90
2	4	4	8
979.43(15)	1905.4(4)	1425.3(2)	1614.1(3)
1.412	1.319	1.325	1.409
0.100	0.093	0.093	0.104
10078	20031	14492	15984
3773	7513	2816	3186
0.0411, 0.1048	0.0642, 0.1588	0.0415, 0.1084	0.0488, 0.1275
1.059	1.024	1.062	1.060

28a (100K)	28b (298K)	29	30
$C_{17}H_{20}N_4S$	$C_{17}H_{20}N_4S$	$C_{20}H_{24}N_4O_4S$	$C_{29}H_{32}N_4O_{12}S$
312.43	312.43	416.49	660.65
Monoclinic	Monoclinic	Triclinic	Triclinic
$P2_1/c$	$P2_1/c$	$P\bar{1}$	$P\bar{1}$
100	298	298	298
9.903(4)	9.9130(8)	9.1759(9)	8.805(6)
16.3181(15)	16.5329(13)	9.1769(9)	9.634(6)
10.0284(14)	9.9992(8)	13.6079(14)	19.461(12)
90	90	92.146(2)	88.035(11)
98.541(19)	98.0230(10)	94.031(2)	83.349(11)
90	90	115.2640(10)	74.023(11)
4	4	2	2
1602.5(7)	1622.7(2)	1030.81(18)	1576.4(18)
1.295	1.279	1.342	1.392
0.204	0.202	0.191	0.172
5794	16674	10665	16185
2730	3202	4061	6164
0.0353, 0.0876	0.0467, 0.1173	0.0478, 0.1211	0.0972, 0.1964
1.087	1.119	1.033	1.190

31	32	33	34
$C_{24}H_{28}N_5O_{2.50}S$	$C_{33}H_{35}N_4O_3S$	$C_{18.50}H_{25}N_4O_{1.50}S$	$C_{17}H_{22}N_4OS$
458.57	567.71	359.48	330.45
Monoclinic	Triclinic	Monoclinic	Monoclinic
$P2_1/c$	$P\bar{1}$	$C2/c$	$C2/c$
100	100	298	298
12.5118(10)	9.270(4)	24.628(3)	24.549(2)
9.6552(8)	10.539(5)	12.5833(15)	12.5131(11)
19.3403(16)	15.713(7)	15.2002(18)	15.1433(13)
90	102.808(7)	90	90
91.0660(10)	104.176(8)	125.803(2)	125.4670(10)
90	95.930(8)	90	90
4	2	8	8
2336.0(3)	1431.0(11)	3820.5(8)	3788.6(6)
1.304	1.318	1.250	1.159
0.172	0.155	0.186	0.180
23586	14968	19537	19376
4589	5664	3777	3755
0.0480, 0.1079	0.0830, 0.1593	0.0523, 0.1472	0.0500, 0.1412
1.098	1.124	1.052	1.111

35	36	37	38
$C_{18}H_{25}N_4O_{1.50}S$	$C_{17}H_{22}N_4OS$	$C_{21}H_{24}N_4O_4S$	$C_{25}H_{28}N_4O_8S$
353.48	330.45	428.50	544.57
Monoclinic	Monoclinic	Monoclinic	Triclinic
$C2/c$	$C2/c$	$P2_1/n$	$P\bar{1}$
298	298	298	298
24.541(7)	24.850(4)	10.852(5)	8.518(3)
12.459(3)	12.4355(17)	13.748(7)	9.804(4)
15.178(4)	15.128(2)	13.879(7)	16.210(6)
90	90	90	95.956(7)
125.485(4)	125.521(2)	97.856(8)	97.945(7)
90	90	90	107.789(7)
8	8	2	2
3778.8(18)	3804.9(9)	2051.3(17)	1261.2(8)
1.243	1.154	1.387	1.434
0.187	0.179	0.194	0.186
19241	19429	20986	13184
3719	3781	4054	4971
0.0590, 0.1537	0.0691, 0.1697	0.0418, 0.1125	0.0864, 0.1789
1.022	1.134	1.068	1.243

39	40	41	42
$C_{17}H_{20}N_3O_{0.50}$	$C_{17}H_{27}Cl_2N_3O_3$	$C_{20}H_{23}N_3O_4$	$C_{21}H_{23}N_3O_4$
274.36	392.32	369.41	381.42
Monoclinic	Monoclinic	Triclinic	Orthorhombic
$P2_1/c$	$P2_1/c$	$P\bar{1}$	$P2_12_12_1$
298	298	298	298
9.801(3)	8.539(3)	10.3222(16)	8.930(3)
17.308(5)	13.703(4)	10.7865(17)	9.877(3)
9.009(2)	17.468(5)	10.8589(17)	22.497(6)
90	90	111.053(2)	90
106.000(4)	103.311(5)	115.931(2)	90
90	90	99.711(2)	90
4	4	2	4
1469.0(7)	1989.1(10)	935.2(3)	1984.4(10)
1.241	1.310	1.312	1.277
0.077	0.347	0.093	0.090
15057	20269	9393	20643
2896	3964	3686	3949
0.0652, 0.1574	0.0499, 0.1206	0.0565, 0.1223	0.0458, 0.0888
1.060	1.094	1.087	1.015

43	44	45
$C_{21}H_{25}N_3O_5$	$C_{20}H_{24}N_3O_2$	$C_{24}H_{25}N_3O_3$
399.44	338.42	403.47
Monoclinic	Monoclinic	Monoclinic
$C2/c$	$P2_1/c$	$P2_1/c$
298	298	298
25.244(4)	10.631(9)	13.941(8)
18.525(3)	9.315(8)	15.599(9)
8.9052(13)	18.052(15)	9.412(5)
90	90	90
102.753(3)	103.771(13)	99.499(11)
90	90	90
8	4	4
4061.9(10)	1736(3)	2019(2)
1.306	1.295	1.328
0.094	0.085	0.089
20808	8744	20342
3977	3813	3901
0.0791, 0.1917	0.0784, 0.2147	0.1056, 0.3023
1.134	0.869	1.255

ABOUT THE AUTHOR

Ranjit Thakuria, youngest son of Late Girish Chandra Thakuria and Smt. Renu Thakuria, was born in Guwahati, Kamrup District of Assam, India, in 1982. He received his primary education from Dispur Udyachal Prathomik Vidyalay and completed his secondary school education at Don Bosco High School, Panbazar, Guwahati. He then completed his Intermediate education and B. Sc. from B. Barooah College, Guwahati, Assam. After the completion of his M.Sc. (Organic Chemistry as Special Paper) from Gauhati University, Guwahati, he joined School of Chemistry, University of Hyderabad, to pursue PhD in 2006 under the supervision of Prof Ashwini Nangia. He qualified CSIR-UGC-National Eligibility Test for Junior Research Fellowship (JRF) held in June 2005 and was awarded research fellowship by the University Grant Commission (UGC) for 2006-2011 (JRF and SRF).

RESEARCH PUBLICATIONS

1. Guest Control in the Self-Assembly of H-shaped Host to Cyclopentanoid $(5,_4^3)$ Net.
    R. Thakuria, B. Sarma and A. Nangia.
    Cryst. Growth Des., **2008**, 8, 1471–1473.

2. Molecular networks. Design and serendipity.
    B. R. Bhogala, S. K. Chandran, L. S. Reddy, **R. Thakuria** and A. Nangia.
    CrystEngComm, **2008**, 10, 1735–1738.

3. Silver(I) complexes of N-4-halophenyl-N'-4-pyridyl ureas. Isostructurality, urea···nitrate hydrogen bonding, and Ag···halogen interaction.
    S. K. Chandran, **R. Thakuria** and A. Nangia.
    CrystEngComm, **2008**, 10, 1891–1898. (Inside cover art)

4. Supramolecular networks of a H-shaped aromatic phenol host.
    R. Thakuria, B. Sarma and A. Nangia.
    New J. Chem., **2010**, 34, 623–636. (Cover art and included in Top10 most accessed Article)

5. Conformational and Synthon Polymorphism in Furosemide (Lasix).
    N. J. Babu, S. Cherukuvada, **R. Thakuria** and A. Nangia.
    Cryst. Growth Des., **2010**, 10, 1979–1989.

6. Pyrazinamide Polymorphs: Relative Stability and Vibrational Spectroscopy.
    S. Cherukuvada, **R. Thakuria** and A. Nangia.
    Cryst. Growth Des., **2010**, 10, 3931–3941.

7. Highly soluble olanzapinium maleate crystalline salts.
    R. Thakuria and A. Nangia.
    CrystEngComm, **2011**, DOI: 10.1039/C0CE00787K.

8. Crystal structures of Mirtazapine molecular salts.
    B. Sarma, **R. Thakuria**, N. K. Nath and A. Nangia.
    CrystEngComm, **2011**, DOI: 10.1039/C0CE00746C.

9. Cocrystals of Pyrogallol/ Catechol with N-Heterocycle Bases.
    R. Thakuria, S. Cherukuvada and A. Nangia. (Manuscript in preparation)

10. Olanzapine and its highly soluble salts.
    R. Thakuria and A. Nangia. (Manuscript in preparation)

11. Stable and Soluble Amorphous Forms of Olanzapine.
    R. Thakuria, N. J. Babu and A. Nangia.
    Patent application No. 747/CHE/2010.